ISSN 2686-7575 (Online)

ТОНКИЕ ХИМИЧЕСКИЕ ТЕХНОЛОГИИ

Fine Chemical Technologies

- Theoretical Basis of Chemical Technology
- Chemistry and Technology of Organic Substances
- Chemistry and Technology of Medicinal Compounds and Biologically Active Substances
- Biochemistry and Biotechnology
- Synthesis and Processing of Polymers and Polymeric Compositions
- Chemistry and Technology of Inorganic Materials
- Analytical Methods in Chemistry and Chemical Technology
- Mathematical Methods and Information Systems in Chemical Technology

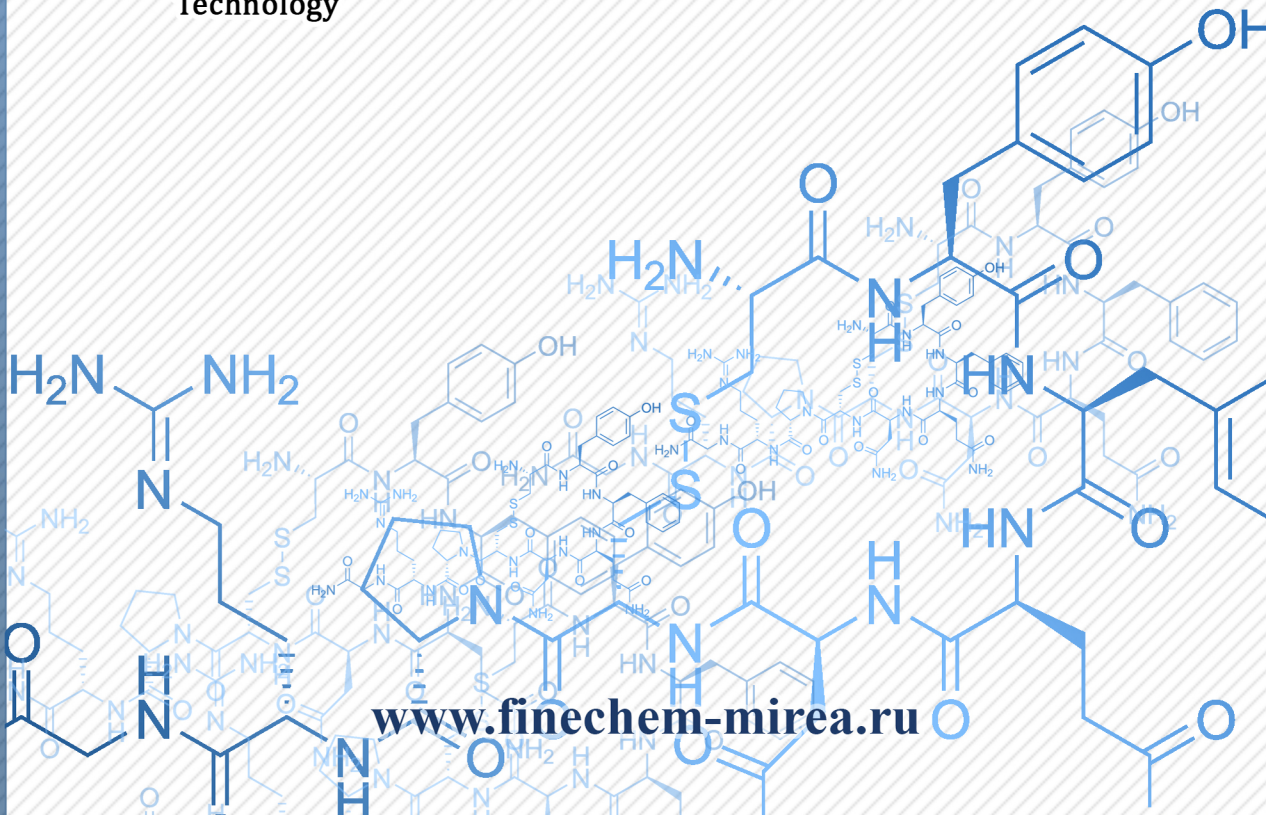

20(6)
2025

www.finechem-mirea.ru

ISSN 2686-7575 (Online)

ТОНКИЕ ХИМИЧЕСКИЕ ТЕХНОЛОГИИ

Fine Chemical Technologies

- Theoretical Basis of Chemical Technology
- Chemistry and Technology of Organic Substances
- Chemistry and Technology of Medicinal Compounds and Biologically Active Substances
- Biochemistry and Biotechnology
- Synthesis and Processing of Polymers and Polymeric Composites
- Chemistry and Technology of Inorganic Materials
- Analytical Methods in Chemistry and Chemical Technology
- Mathematical Methods and Information Systems in Chemical Technology

Tonkie Khimicheskie Tekhnologii = Fine Chemical Technologies.
Vol. 20, No. 6, 2025

Тонкие химические технологии = Fine Chemical Technologies.
Том 20, № 6, 2025

https://doi.org/10.32362/2410-6593-2025-20-6
www.finechem-mirea.ru

https://doi.org/10.32362/2410-6593-2025-20-6
www.finechem-mirea.ru ISSN 2686-7575 (Online)

**Tonkie Khimicheskie Tekhnologii =
Fine Chemical Technologies
2025, Vol. 20, No. 6**

The peer-reviewed scientific and technical journal Fine Chemical Technologies highlights the modern achievements of fundamental and applied research in the field of fine chemical technologies, including the theoretical basis of chemical technology, chemistry and technology of medicinal compounds and biologically active substances, organic substances and inorganic materials, biochemistry and biotechnology, synthesis and processing of polymers and polymeric composites, analytical and mathematical methods and information systems in chemistry and chemical technology.

Founder and Publisher

Federal State Budget
Educational Institution of Higher Education
"MIREA – Russian Technological University"
78, Vernadskogo pr., Moscow, 119454, Russian Federation.
Publication frequency: bimonthly.
The journal was founded in 2006. The name was Vestnik MITHT until 2015 (ISSN 1819-1487).

The journal is included into the List of peer-reviewed science press of the State Commission for Academic Degrees and Titles of the Russian Federation; the Unified State List of Scientific Publications – White List (K1).

The journal is indexed: SCOPUS, DOAJ, Chemical Abstracts, Science Index, RSCI, Ulrich's International Periodicals Directory

86, Vernadskogo pr., Moscow, 119571, Russian Federation.
Phone: +7 (499) 600-80-80 (#31288)
E-mail: *seredina@mirea.ru*

The registration number ПИ № ФС 77-74580 was issued in December 14, 2018 by the Federal Service for Supervision of Communications, Information Technology, and Mass Media of Russia

The subscription index of *Pressa Rossii*: **36924**

Publication date 31.12.2025.

**Тонкие химические технологии =
Fine Chemical Technologies
2025, том 20, № 6**

Научно-технический рецензируемый журнал «Тонкие химические технологии» освещает современные достижения фундаментальных и прикладных исследований в области тонких химических технологий, включая теоретические основы химической технологии, химию и технологию лекарственных препаратов и биологически активных соединений, органических веществ и неорганических материалов, биохимию и биотехнологию, синтез и переработку полимеров и композитов на их основе, аналитические и математические методы и информационные системы в химии и химической технологии.

Учредитель и издатель

федеральное государственное бюджетное
образовательное учреждение высшего образования
«МИРЭА – Российский технологический университет»
119454, РФ, Москва, пр-т Вернадского, д. 78.
Периодичность: один раз в два месяца.
Журнал основан в 2006 году. До 2015 года издавался под названием «Вестник МИТХТ» (ISSN 1819-1487).

Журнал входит в Перечень ведущих рецензируемых научных журналов ВАК РФ, в Единый государственный перечень научных изданий – Белый список (К1).

Индексируется: SCOPUS, DOAJ, Chemical Abstracts, РИНЦ (Science Index), RSCI, Ulrich's International Periodicals Directory

РФ, 119571, Москва, пр. Вернадского, 86, оф. Р-108.
Тел.: +7 (499) 600-80-80 (#31288)
E-mail: *seredina@mirea.ru*

Регистрационный номер и дата принятия решения о регистрации СМИ: ПИ № ФС 77-74580 от 14.12.2018 г. СМИ зарегистрировано Федеральной службой по надзору в сфере связи, информационных технологий и массовых коммуникаций (Роскомнадзор)

Индекс по Объединенному каталогу «Пресса России»: **36924**

Дата опубликования 31.12.2025 г.

EDITORIAL BOARD

РЕДАКЦИОННАЯ КОЛЛЕГИЯ

20(6) 2025 | Tonkie Khimicheskie Tekhnologii
Fine Chemical Technologies

Contents

THEORETICAL BASIS OF CHEMICAL TECHNOLOGY

531 *Boris V. Alekseev, Vladislav Kh. Fedotov, Nikolay I. Kol'tsov*
Solution of the inverse problem for chemical reactions with chaotic dynamics

CHEMISTRY AND TECHNOLOGY OF ORGANIC SUBSTANCES

540 *Olga M. Larina, Iosif I. Lishchiner, Olga V. Malova, Yulia M. Faleeva*
Synthesis of methanol from gaseous products of pyrolysis of sewage sludge

CHEMISTRY AND TECHNOLOGY OF MEDICINAL COMPOUNDS AND BIOLOGICALLY ACTIVE SUBSTANCES

555 *Daria V. Nebesnaia, Ekaterina S. Terendiak, Olga A. Legon'kova, Stanislav A. Kedik, Aleksey V. Panov, Elena S. Zhavoronok*
On the stability of characteristics of cellulose diacetate solutions with an iodine-containing radiopaque substance and solid emboli on their basis

BIOCHEMISTRY AND BIOTECHNOLOGY

565 *Ivan V. Maksin, Darya I. Polyakova, Viktoriia A. Kesareva, Alexander A. Sysuev, Vladislav S. Ivanov, Evgeniia I. Simonova, German A. Khunteev, Yuliya G. Kirillova*
Development of immunochromatographic assay for simultaneous detection of tetracyclines and streptomycin in milk

582 *Ekaterina I. Ryabova, Artem A. Derkaev, Ilias B. Esmagambetov, Mikhail A. Dovgiy, Anton A. Blinov, Roza M. Hossain, Oleg E. Dmitriev, Dmitry S. Polyansky, Anatoly N. Noskov, Dmitry V. Shcheblyakov, Denis Y. Logunov, Alexander L. Gintsburg*
Comparative analysis of three genetic constructs for delivery and expression of a modified single-domain antibody gene in rAAV

SYNTHESIS AND PROCESSING OF POLYMERS AND POLYMERIC COMPOSITES

594 *Boris A. Buravov, Ali Al-Hamzawi, Rashid B. Gadzhiev, Svetlana A. Orlova, Lyubov Yu. Donetskova, Semyon M. Solomakhin, Sergey V. Borisov, Olga S. Fomenko, Stanislav A. Trubachev, Aleksander A. Paletsky, Andrey G. Shmakov, Oleg I. Tuzhikov, Oleg O. Tuzhikov*
Influence of the structure of phosphorus(III)-containing oligoester(meth)acrylates on the physical and mechanical properties, thermal stability, and combustion mechanisms of cured polymers

612 *Ksenia V. Sukhareva, Igor A. Mikhailov, Bekzod B. Khaidarov, Anastasia D. Buluchevskaya, Igor N. Burmistrov*
Surface treatments of nitrile butadiene rubber to enhance wear resistance and mechanical properties

СОДЕРЖАНИЕ

ТЕОРЕТИЧЕСКИЕ ОСНОВЫ ХИМИЧЕСКОЙ ТЕХНОЛОГИИ

531 *Б.В. Алексеев, В.Х. Федотов, Н.И. Кольцов*
Решение обратной задачи для химических реакций с хаотической динамикой

ХИМИЯ И ТЕХНОЛОГИЯ ОРГАНИЧЕСКИХ ВЕЩЕСТВ

540 *О.М. Ларина, И.И. Лищинер, О.В. Малова, Ю.М. Фалеева*
Синтез метанола из газообразных продуктов пиролиза осадка сточных вод

ХИМИЯ И ТЕХНОЛОГИЯ ЛЕКАРСТВЕННЫХ ПРЕПАРАТОВ И БИОЛОГИЧЕСКИ АКТИВНЫХ СОЕДИНЕНИЙ

555 *Д.В. Небесная, Е.С. Терендяк, О.А. Легонькова, С.А. Кедик, А.В. Панов, Е.С. Жаворонок*
О стабильности характеристик растворов диацетата целлюлозы с йодсодержащим рентгеноконтрастным веществом и твердых эмболов на их основе

БИОХИМИЯ И БИОТЕХНОЛОГИЯ

565 *И.В. Максин, Д.И. Полякова, В.А. Кесарева, А.А. Сысуев, В.С. Иванов, Е.И. Симонова, Г.А. Хунтеев, Ю.Г. Кириллова*
Разработка иммунохроматографического анализа для одновременного обнаружения тетрациклинов и стрептомицина в молоке

582 *Е.И. Рябова, А.А. Деркаев, И.Б. Есмагамбетов, М.А. Довгий, А.А. Блинов, Р.М. Хоссаин, О.Е. Дмитриев, Д.С. Полянский, А.Н. Носков, Д.В. Щебляков, Д.Ю. Логунов, А.Л. Гинцбург*
Сравнительный анализ трех генетических конструкций для доставки и экспрессии гена модифицированного однодоменного антитела в составе rAAV

СИНТЕЗ И ПЕРЕРАБОТКА ПОЛИМЕРОВ И КОМПОЗИТОВ НА ИХ ОСНОВЕ

594 *Б.А. Буравов, А. Аль-Хамзави, Р.Б. Гаджиев, С.А. Орлова, Л.Ю. Донецкова, С.М. Соломахин, С.В. Борисов, О.С. Фоменко, С.А. Трубачев, А.А. Палецкий, А.Г. Шмаков, О.И. Тужиков, О.О. Тужиков*
Влияние строения фосфор(III)-содержащих олигоэфир(мет)акрилатов на физико-механические свойства, термическую стабильность и механизмы горения отвержденных полимеров

612 *Ksenia V. Sukhareva, Igor A. Mikhailov, Bekzod B. Khaidarov, Anastasia D. Buluchevskaya, Igor N. Burmistrov*
Surface treatments of nitrile butadiene rubber to enhance wear resistance and mechanical properties

Tonkie Khimicheskie Tekhnologii = Fine Chemical Technologies.
2025;20(6):531–539 ISSN 2686-7575 (Online)

Theoretical basis of chemical technology
Теоретические основы химической технологии

UDC 541.124/128
https://doi.org/10.32362/2410-6593-2025-20-6-531-539
EDN AQQLQV

RESEARCH ARTICLE

Solution of the inverse problem for chemical reactions with chaotic dynamics

Boris V. Alekseev, Vladislav Kh. Fedotov✉, Nikolay I. Kol'tsov
I.N. Ulyanov Chuvash State University, Cheboksary, Chuvash Republic, 428015 Russia
✉ *Corresponding author, e-mail: fvh@inbox.ru*

Abstract

Objectives. To develop and test a method for solving the inverse problem of chemical kinetics for estimating the frequencies of elementary stages of complex chemical reactions occurring in a chaotic regime.

Methods. The method is based on the representation of nonstationary experimental data on reagent concentrations and the rates of their change in the form of a matrix of a particular structure.

Results. The effectiveness of the method is demonstrated by examples of reactions proceeding according to stage schemes similar to the Willamowski–Rossler mechanism, characterized by undamped aperiodic oscillations.

Conclusions. The method allows the frequencies of stages for reactions proceeding according to mechanisms with non-monotonic dynamics of any complexity to be determined with high accuracy.

Keywords

inverse problem of chemical kinetics, chaotic dynamics, nonstationary experimental data, reagent concentrations and rates of their change

Submitted: 05.03.2025
Revised: 05.05.2025
Accepted: 07.11.2025

For citation

Alekseev B.V., Fedotov V.Kh., Kol'tsov N.I. Solution of the inverse problem for chemical reactions with chaotic dynamics. *Tonk. Khim. Tekhnol. = Fine Chem. Technol*. 2025;20(6):531–539. https://doi.org/10.32362/2410-6593-2025-20-6-531-539

НАУЧНАЯ СТАТЬЯ

Решение обратной задачи для химических реакций с хаотической динамикой

Б.В. Алексеев, В.Х. Федотов✉, Н.И. Кольцов

Чувашский государственный университет им. И.Н. Ульянова, Чебоксары, Чувашская Республика, 428015 Россия

✉ *Автор для переписки, e-mail: fvh@inbox.ru*

Аннотация

Цели. Разработка и апробация метода решения обратной задачи химической кинетики по оценке частот элементарных стадий сложных химических реакций, протекающих в хаотическом режиме.

Методы. Метод основан на представлении нестационарных экспериментальных данных о концентрациях реагентов и скоростях их изменения в виде матрицы специальной структуры.

Результаты. Эффективность метода показана на примерах реакций, протекающих по стадийным схемам, аналогичным механизму Вилламовски–Росслера, и характеризующихся незатухающими апериодическими колебаниями.

Выводы. Метод позволяет с высокой точностью определить частоты стадий для реакций, протекающих по механизмам с немонотонной динамикой любой сложности.

Ключевые слова

обратная задача химической кинетики, хаотическая динамика,
нестационарные экспериментальные данные,
концентрации реагентов и скорости их изменения

Поступила: 05.03.2025
Доработана: 05.05.2025
Принята в печать: 07.11.2025

Для цитирования

Алексеев Б.В., Федотов В.Х., Кольцов Н.И. Решение обратной задачи для химических реакций с хаотической динамикой. *Тонкие химические технологии*. 2025;20(6):531–539. https://doi.org/10.32362/2410-6593-2025-20-6-531-539

INTRODUCTION

Currently, there exist a number of methods for solving the inverse problem (IP) of chemical kinetics based on nonstationary data for chemical reactions proceeding in a monotonic mode [1–3]. However, methods for solving the IP for chemical reactions with non-monotonic behavior, such as critical phenomena in particular, have not been studied in practice [4, 5]. It is also known that the IP is incorrect, and its solution is usually ambiguous [6]. Possible approaches to overcoming these difficulties and improving the accuracy of the IP solution were presented in [7–11]. The study [12] considered an IP solution for the Gray–Scott self-oscillating reaction [13] based on experimental amplitude–frequency characteristics. The authors in [14] developed an alternative method for solving the IP for the same reaction and demonstrated that the use of nonstationary values of reagent concentrations and their rates of change allows the uniqueness and accuracy of the solution to be increased.

The earliest examples of chemical reactions whose dynamic models describe chaotic oscillations within the framework of the law of active masses (LAM) were demonstrated by Rossler [15]. Among them, the Willamowski–Rossler mechanism was the simplest [16–18]. In these works, the kinetic parameters of stage diagrams were determined numerically based on the conditions of instability of solutions of ordinary differential equations (ODEs) describing nonstationary models of the corresponding reactions and known criteria of chaos in dynamic systems (Lyapunov exponents, etc.) [19–20].

In this article, we present a method for solving the IP for chemical reactions with unpredictable chaotic dynamics based on data on reagent concentrations and their rates of change.

EXPERIMENTAL

The mechanism of a complex chemical reaction is described by a set of elementary stages

$$\sum b_{+ik}\mathrm{A}_k + \sum a_{+ij}\mathrm{X}_j \leftrightarrow \sum a_{-ij}\mathrm{X}_j + \sum b_{-ik}\mathrm{A}_k, \quad (1)$$

$i = 1, \ldots, s, j = 1, \ldots, n,$

wherein $b_{\pm ik}$, $a_{\pm ij}$ are the stoichiometric coefficients of reagents A_k and X_j, respectively, in the forward

and reverse directions of stage *i*. Let A_k be reagents whose concentrations remain virtually unchanged during the reaction (referred to as non-key, slow reagents in terms of the Bodenstein–Semenov quasi-stationarity principle [21]); X_j are the key reagents whose concentrations change during the reaction (essential reagents in terms of A.M. Zhabotinsky [22]). The dynamics of such a reaction in an isothermal zero-gradient reactor, according to LAM, is described by the ODE system [1]:

$$x'_j = \sum (a_{-ij} - a_{+ij})(w_i \Pi_j x_j^{a+ij} - w_{-i} \Pi_j x_j^{a-ij}),$$
$$j = 1, \ldots, n, \quad (2)$$

wherein $x_j = x_j(t)$ are the concentrations of key reagents x_j (dimensionless, dim.); t is time (s); $x_j(t_0) = x_j^0$ are the initial conditions (i.c.); t_0 is the initial moment of time (s); $w_i = k_i \Pi_k A_k^{b+ik}$, $w_{-i} = k_{-i} \Pi_k A_k^{b-ik}$ are the frequencies of forward and reverse stages, including concentration multipliers of non-key reagents (s^{-1}); k_i, k_{-i} are the constants of stage velocities in the forward and reverse directions (s^{-1}).

In the presence of experimental data on concentrations and rates of change of reagent concentrations, system (2) is a linear system of algebraic equations with respect to stage frequencies, which can be written as

$$v_j = \sum (a_{-ij} - a_{+ij})(w_i r_{ij} - w_{-i} r_{-ij}), j = 1, \ldots, n, \quad (3)$$

wherein v_j are the rates of change in the concentrations of key reagents; r_{ij}, r_{-ij} are the monomials of the stage rates, i.e., the stage rates at single values of the stage frequencies. Dividing the right-hand side of system (3) into monomials and frequencies is convenient, since the numerical values of the monomials are known from the experiment at each time point (they are equal to the product of the concentrations of key reagents), and the values of the frequencies of the stages are the desired parameters of the IP.

System (3) typically includes identical stage velocity monomials with different stage frequency values. Let us combine such monomials (bring similar ones together) and write down system (3) modified in this way in a concise (matrix) form

$$\mathbf{v} = \mathbf{R}\mathbf{w}, \quad (3^*)$$

wherein $\mathbf{R}$ is the matrix of various monomials of velocities (after reduction of similar ones), $\mathbf{w}$ is a vector of stage frequencies.

The best solution to such a system is provided by methods for minimizing the error function $f(\mathbf{w})$ (penalty function), e.g. , in the form of a sum of squared deviations

$$f(\mathbf{w}) = (\mathbf{R}\mathbf{w} - \mathbf{v})^{\mathrm{T}} (\mathbf{R}\mathbf{w} - \mathbf{v}), \quad (4)$$

wherein T is the transpose sign. This solution can be written using the pseudo-inverse matrix $\mathbf{R}^+$ [23]:

$$\mathbf{w} = \mathbf{R}^+ \mathbf{v}. \quad (5)$$

In a special case when the original matrix $\mathbf{R}$ is square and non-degenerate, the pseudo-inverse matrix coincides with the inverse $\mathbf{R}^+ = \mathbf{R}^{-1}$. In the general case, when the number of experimental points is not equal to the number of desired stage frequencies, the matrix $\mathbf{R}$ has an incomplete rank. Then, if the product of the matrices $\mathbf{R}^{\mathrm{T}}\mathbf{R}$ is not degenerate, then

$$\mathbf{R}^+ = (\mathbf{R}^{\mathrm{T}}\mathbf{R})^{-1}\mathbf{R}^{\mathrm{T}}, \quad (6)$$

wherein $\mathbf{R}^{\mathrm{T}}$ is the transposed matrix. If the product $\mathbf{R}^{\mathrm{T}}\mathbf{R}$ has an incomplete rank, then

$$\mathbf{R}^+ = \lim_{\delta \to 0} (\mathbf{R}^{\mathrm{T}}\mathbf{R} + \delta\mathbf{E})^{-1}\mathbf{R}^{\mathrm{T}}, \quad (7)$$

wherein $\mathbf{E}$ is the identity matrix. Calculations performed in computer algebra systems [3, 24] have shown the insufficiency of formula (6) to determine the frequencies of the stages.

For comparison, we also use the penalty function, i.e., the maximum of deviation modules.

$$f(\mathbf{w}) = \max(abs(\mathbf{R}\mathbf{w} - \mathbf{v})). \quad (8)$$

Function (8) is a composition of functions **max** and *abs*, having kinks, and its analysis is more complicated than the analysis of function (4). The minimum of function (8) can be found by dividing the entire space of possible values of the vector $\mathbf{w}$ into regions of smoothness (8), finding the minimum in each of these regions and then selecting the global minimum from these local minima. Obviously, the minimum points of functions (4) and (8) are different, and these minima correspond to different values of the vector $\mathbf{w}$.

RESULTS AND DISCUSSION

Let us apply the method described above to reactions proceeding according to stepwise schemes similar to the Willamowski–Rossler mechanism, characterized by continuous aperiodic (chaotic) oscillations [15–18, 25, 26].

Example 1. Let us consider the homogeneous reaction A + 2B → C + D proceeding according to the scheme [25]:

$$1)\ A + X \leftrightarrow 2X,\ 2)\ B + X + Y \rightarrow 2Y + A,$$
$$3)\ Z + Y \rightarrow D,\ 4)\ A + B \rightarrow Z + C. \quad (1.1)$$

wherein A, B, C, and D are the non-key reagents (can be any); X, Y, and Z are the key reagents. According to this scheme, the reaction $CO + 2NO \rightarrow N_2O + CO_2$ can occur:

$$1)\ CO + CO^* \leftrightarrow 2CO^*,$$
$$2)\ NO + CO^* + NO^* \rightarrow 2NO^* + CO, \quad (1.2)$$
$$3)\ N^* + NO^* \rightarrow N_2O,\ 4)\ CO + NO \rightarrow N^* + CO_2.$$

An unsteady kinetic model of reactions proceeding according to schemes (1.1) and (1.2), under the assumption of quasi-stationarity for non-key reagents, is described by

$$\begin{aligned} x' &= w_1 x - w_{-1} x^2 - w_2 xy, \\ y' &= w_2 xy - w_3 yz, \\ z' &= -w_3 yz + w_4, \end{aligned} \qquad (1.3)$$

wherein w_i, w_{-i} are the frequencies of steps in the forward and reverse directions, including the concentrations of non-key reagents; x, y, and z are the concentrations of key reagents X, Y, and Z. It was shown in [25] that system (1.3) exhibits chaotic oscillations at certain values of the frequencies of stages and current levels (Fig. 1).

The concentrations of key reagents and their rates of change, selected for calculations at certain time points from dependencies $x(t)$, $y(t)$, $z(t)$ (Fig. 1), are shown in Table 1.

Equations (1.3) contain five different monomials of velocities 1, x, x^2, xy, yz. They form a matrix **R** of size $5 \times 3n$, made up of triples of rows $[0, x, -x^2, -xy, 0]$, $[0, 0, 0, xy, -yz]$, and $[1, 0, 0, 0, -yz]$ for reagents X, Y, and Z, respectively, calculated for each experiment. The results of the IP solution for two variants of the penalty function (4) and (8) are given in Table 2.

It can be seen from Table 2 that the errors in determining the frequency of stages by the method described above are small for both methods of selecting the penalty function.

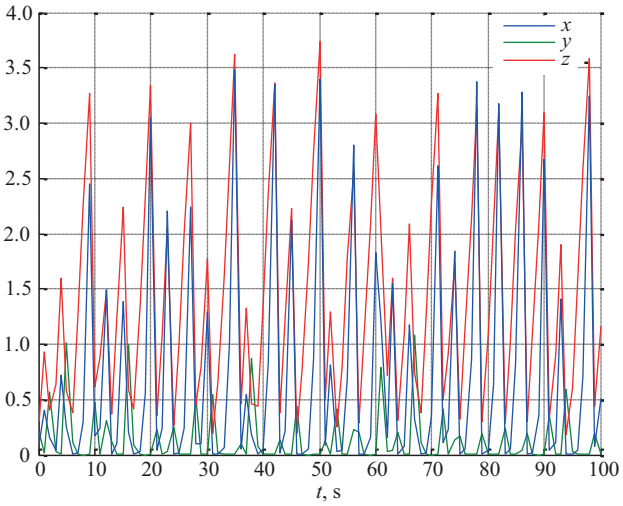

Fig. 1. Dependencies $x(t)$, $y(t)$, $z(t)$ in the reaction A + 2B → C + D described by model (1.3) at $w_1 = 3$, $w_{-1} = 0.75$, $w_2 = 18$, $w_3 = 10$, $w_4 = 1$ s^{-1}, and $x_0 = 0.1$, $y_0 = 0.2$, $z_0 = 0.3$

Table 1. Concentrations of reagents and rates of their change* in the reaction A + 2B → C + D, proceeding according to scheme (1.1) at $w_1 = 3$, $w_{-1} = 0.75$, $w_2 = 18$, $w_3 = 10$, $w_4 = 1$, s^{-1}

t, s	0	5	10	15	20	25
x, a.u.	0.1000	0.2480	0.1663	1.3908	3.0491	0.0127
y, a.u.	0.2000	1.0100	0.4738	0.0000	0.0000	0.0009
z, a.u.	0.3000	0.5827	0.6112	2.2368	3.3339	1.0031
x', s^{-1}	−0.0675	−3.8114	−0.9403	2.7217	2.1732	0.0376
y', s^{-1}	−0.2400	−1.3758	−1.4775	0.0000	0.0006	−0.0088
z', s^{-1}	0.4000	−4.8852	−1.8960	1.0000	0.9991	0.9910

* The rates of change of reagent concentrations x', y', z' are calculated using equations (1.3).

Table 2. Accuracy of the IP solution for reaction (1.1) depending on the penalty function

Penalty function	Stage frequencies	w_1, s^{-1}	w_2, s^{-1}	w_3, s^{-1}	w_4, s^{-1}	w_{-1}, s^{-1}
	The exact value	3.00	18.00	10.00	1.00	0.75
(4)	Estimated value	3.0008	18.0031	9.9998	0.9998	0.7504
	Error rate, %	0.0267	0.0172	0.0020	0.0200	0.0533
(8)	Estimated value	3.0004	18.0029	9.9989	0.9994	0.7503
	Error rate, %	0.0133	0.0161	0.0110	0.0600	0.0400

Example 2. Let us consider the heterogeneous catalytic reaction of $2NO + CO \rightarrow N_2O + CO_2$, occurring on platinum metals according to the step scheme [26]:

$$\begin{aligned} &1)\ CO + Q + QCO \leftrightarrow 2QCO,\\ &2)\ NO + QCO + QN \rightarrow 2QN + CO_2,\\ &3)\ QNO + QN \rightarrow 2Q + N_2O,\ 4)\ NO + Q \rightarrow QNO, \end{aligned} \qquad (2.1)$$

wherein the key reagents are QCO, QN, and QNO are the catalyst surface centers occupied by carbon monoxide and nitrogen, and Q are free catalyst centers. Briefly, without the non-key reagents NO, CO, N_2O, and CO_2, scheme (2.1) takes the form

$$1)\ Q + X \leftrightarrow 2X,\ 2)\ X + Y \rightarrow 2Y,\quad 3)\ Z + Y \rightarrow 2Q,\ 4)\ Q \rightarrow Z, \qquad (2.2)$$

for which the kinetic model (2) can be written as:

$$\begin{aligned} x' &= w_1xq - w_{-1}x^2 - w_2xy,\\ y' &= w_2xy - w_3yz,\\ z' &= -w_3yz + w_4q, \end{aligned} \qquad (2.3)$$

wherein x, y, z, and q are the dimensionless concentrations of key substances QCO = X, QN = Y, QNO = Z and free centers Q on the surface of the catalyst, with $x + y + z + q = 1$ (the law of conservation of the catalyst). It should be noted that the concentrations of key substances and free centers on the surface of the catalyst cannot be measured even by modern physicochemical research methods. It was shown in [26] that the ODE system (2.3) describes chaotic oscillations at certain values of the frequencies of stages and initial conditions (Fig. 2).

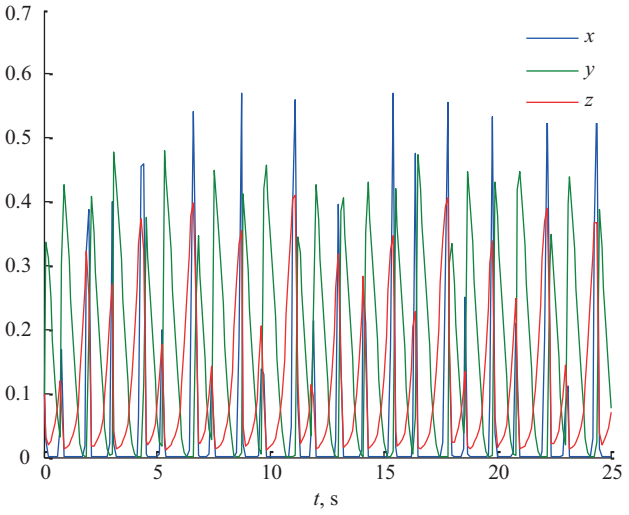

Fig. 2. Dependencies $x(t)$, $y(t)$, $z(t)$ in reaction of interaction of nitrogen and carbon monoxides described by model (2.3) at $w_1 = 50$, $w_2 = 200$, $w_3 = 100$, $w_4 = w_{-1} = 1\ s^{-1}$, $x_0 = y_0 = z_0 = 0.1$

The values of reagent concentrations and their rates of change, selected for calculations at certain time points from dependencies $x(t)$, $y(t)$, $z(t)$ (Fig. 2), are shown in Table 3.

Equations (2.3) contain five different monomials of velocities xq, xy, yz, q, x^2. They form a matrix **R** of size $5 \times 3n$, composed of triples of rows $[xq, -xy, 0, 0, -x^2]$, $[0, xy, -yz, 0, 0]$, and $[0, 0, -yz, q, 0]$ for reagents X, Y, and Z, respectively, calculated for each experiment. The IP solution for penalty functions (4) and (8) are given in Table 4.

Table 3. Concentrations of reagents and rates of their change in the reaction of interaction of nitrogen and carbon monoxides, proceeding according to mechanism (2.1) at $w_1 = 50$, $w_2 = 200$, $w_3 = 100$, $w_4 = w_{-1} = 1\ s^{-1}$

t, s	0	1	2	3	4	5
x, a.u.	0.1000	0.0000	0.3869	0.4011	0.0000	0.0002
y, a.u.	0.1000	0.3701	0.1965	0.0047	0.0044	0.0640
z, a.u.	0.1000	0.0156	0.2543	0.2714	0.1935	0.0787
x', s^{-1}	1.4900	−0.0001	−12.2097	5.9310	0.0018	0.0057
y', s^{-1}	1.0000	−0.5788	10.2050	0.2518	−0.0853	−0.5017
z', s^{-1}	−0.3000	0.0353	−4.8335	0.1940	0.7167	0.3530

Table 4. Dependence of the IP solution accuracy on the choice of the penalty function for the reaction of interaction of nitrogen and carbon monoxides, proceeding according to scheme (2.1)

Penalty function	Stage frequencies	w_1, s^{-1}	w_2, s^{-1}	w_3, s^{-1}	w_4, s^{-1}	w_{-1}, s^{-1}
	The exact value	50.00	200	100	1	1
(4)	Estimated value	49.9728	199.9172	99.9609	1.0020	0.9986
	Error rate, %	0.0544	0.0414	0.0391	0.2000	0.1400
(8)	Estimated value	49.9533	199.9042	99.9130	1.0085	0.9953
	Error rate, %	0.0934	0.0479	0.0870	0.8500	0.4700

It can be seen from Table 4 that the errors in determining the stage frequencies for both variants of penalty functions (4) and (8) are quite small. The found values of the stage frequencies for different penalty functions are almost the same.

CONCLUSIONS

A method for solving the inverse kinetic problem for reactions proceeding by mechanisms with chaotic dynamics is proposed. This method is based on the use of experimentally measured values of reagent concentrations and their rates of change. The proposed approach differs from the previously known methods in the isolation of different stage velocity monomials and the method of forming the experimental data matrix. According to the conducted analysis, the described method makes it possible to accurately determine the frequencies of stages for reactions proceeding through mechanisms with dynamics of any complexity (monotonous, non-monotonous, periodic, and chaotic).

Authors' contributions

B.V. Alekseev—development of methods and algorithms for solving inverse problems, software development, planning and conducting computational experiments, analysis of results.

V.Kh. Fedotov—problem statement, planning and conducting computational experiments, analysis of results, writing the text of the article.

N.I. Kol'tsov—statement of the research goal and objectives, analysis of the obtained results, writing the text of the article.

All authors approved the final version of the article.

The authors declare no conflict of interest.

REFERENCES

1. Ismagilova A.S., Spivak S.I. *Obratnye zadachi khimicheskoi kinetiki* (*Inverse Problems of Chemical Kinetics*). Saarbrucken: Lap Lambert Academic Publ.; 2013, 125 p. (In Russ.). ISBN 978-36593118474. https://www.elibrary.ru/glykiv
2. Yagola A.G., Yanfei V., Stepanova I.EH., Titarenko V.N. *Obratnye zadachi i metody ikh resheniya. Prilozheniya k geofizike* (*Inverse Problems and Methods of their Solution. Applications to Geophysics*). Moscow: Laboratoriya znanii; 2021, 217 p. (In Russ.). ISBN 978-5-93208-555-4
3. Leonov A.S. *Reshenie nekorrektno postavlennykh obratnykh zadach: ocherk teorii, prakticheskie metody i demonstratsii v MATLAB* (*Solution of ill-Posed Inverse Problems: Outline of theory, Practical Methods and Demonstrations in MATLAB*). Moscow: Librokom; 2024, 368 p. (In Russ.). ISBN 978-5-9710-9965-9
4. Pisarenko E.V., Pisarenko V.N. Analysis and simulation of the nonlinear kinetics of reacting chemical systems. *Theor. Found. Chem. Eng*. 2013;47(2):128–135. https://doi.org/10.1134/S004057951302005X
[Original Russian Text: Pisarenko E.V., Pisarenko V.N. Analysis and simulation of the nonlinear kinetics of reacting chemical systems. *Teoreticheskie Osnovy Khimicheskoi Tekhnologii*. 2013;47(2): 173–181 (in Russ.). https://doi.org/10.7868/S0040357113020061]
5. Shatalov M.Y., Fedotov S.I., Shatalov Y.M. New methods of determination of kinetic parameters of the theoretical models from experimental data. *Theor. Found. Chem. Eng*. 2013;47(3): 207–216. https://doi.org/10.1134/S0040579513020097
[Original Russian Text: Shatalov M.Yu., Fedotov S.I., Shatalov Yu.M. New methods of determination of kinetic parameters of the theoretical models from experimental data. *Teoreticheskie Osnovy Khimicheskoi Tekhnologii*. 2013;47(3):260–270 (in Russ.). https://doi.org/10.7868/S0040357113020103]
6. Gorsky V.G. *A prior parameter identifiability analysis of fixed structure models.* In: Letzky E.K. (Ed.). *Design of Experiments and Data Analysis: New Trends and Results*. Moscow: Antal; 1993. P. 92–131.

СПИСОК ЛИТЕРАТУРЫ

1. Исмагилова А.С., Спивак С.И. *Обратные задачи химической кинетики*. Saarbrucken: Lap Lambert Academic Publ.; 2013, 125 с. ISBN 978-36593118474. https://www.elibrary.ru/glykiv
2. Ягола А.Г., Янфей В., Степанова И.Э., Титаренко В.Н. *Обратные задачи и методы их решения. Приложения к геофизике*. М.: Лаборатория знаний; 2021, 217 с. ISBN 978-5-93208-555-4
3. Леонов А.С. *Решение некорректно поставленных обратных задач: очерк теории, практические методы и демонстрации в МАТЛАБ*. М.: Либроком; 2024, 368 с. ISBN 978-5-9710-9965-9
4. Писаренко Е.В., Писаренко В.Н. Анализ и моделирование нелинейной кинетики химических реагирующих систем. *Теор. основы хим. технологии*. 2013;47(2):173–181. https://doi.org/10.7868/S0040357113020061
5. Шаталов М.Ю., Федотов С.И., Шаталов Ю.М. Новый метод определения кинетических параметров теоретических моделей на основе экспериментальных данных. *Теор. основы хим. технологии*. 2013;47(3):260–270. https://doi.org/10.7868/S0040357113020103
6. Gorsky V.G. *A prior parameter identifiability analysis of fixed structure models.* In: Letzky E.K. (Ed.). *Design of Experiments and Data Analysis: New Trends and Results*. Moscow: Antal; 1993. P. 92–131.
7. Федотов В.Х., Кольцов Н.И. Разработка метода решения обратной задачи химической кинетики для каталитических реакций с участием основных веществ в каждой стадии. *Хим. физика*. 2016;35(10):9–15. https://doi.org/10.7868/S0207401X1610006X
8. Кольцов Н.И. Метод решения обратной задачи химической кинетики многостадийных реакций. *Кинетика и катализ*. 2020;61(6):783–788. https://doi.org/10.31857/S0453881120040127
9. Кольцов Н.И. Метод определения констант скоростей стадий химических реакций в закрытом безградиентном реакторе. *Журн. прикладной химии*. 2020;93(10):1474–1481. https://doi.org/10.31857/S0044461820100096

7. Fedotov V.Kh., Kol'tsov N.I. Method of solving the inverse problem of chemical kinetics for catalytic reactions in which each step involves main reactants. *Rus. J. Phys. Chem. B*. 2016;10(5): 753–759. https://doi.org/10.1134/S1990793116050195
[Original Russian Text: Fedotov V.Kh., Kol'tsov N.I. Method of solving the inverse problem of chemical kinetics for catalytic reactions in which each step involves main reactants. *Khimicheskaya Fizika*. 2016;35(10):9–15 (in Russ.). https://doi.org/10.7868/S0207401X1610006X]
8. Kol'tsov N.I. Method for Solving the Inverse Problem of the Chemical Kinetics of Multistage Reactions. *Kinet. Catal*. 2020;61(6):833–838.https://doi.org/10.1134/S0023158420040096
[Original Russian Text: Kol'tsov N.I. Method for Solving the Inverse Problem of the Chemical Kinetics of Multistage Reactions. *Kinetika i Kataliz*. 2020;61(6):783–788 (in Russ.). https://doi.org/10.31857/S0453881120040127]
9. Kol'tsov N.I. Method for Determining the Rate Constants of Chemical Reaction Stages in an Enclosed Gradientless Reactor. *Russ. J. Applied Chem*. 2020;93(10):1544–1552. https://doi.org/10.1134/S1070427220100092
[Original Russian Text: Kol'tsov N.I. Method for Determining the Rate Constants of Chemical Reaction Stages in an Enclosed Gradientless Reactor. *Zhurnal Prikladnoi Khimii*. 2020;93(10):1474–1481 (in Russ.). https://doi.org/10.31857/S0044461820100096]
10. Kol'tsov N.I. Solving the Inverse Problem for Chemical Reactions Occurring in a Plug-Flow Reactor. *Theor. Found. Chem. Eng*. 2021;55(6):1238–1245. https://doi.org/10.1134/S0040579521050237
[Original Russian Text: Kol'tsov N.I. Solving the Inverse Problem for Chemical Reactions Occurring in a Plug-Flow Reactor. *Teoreticheskie Osnovy Khimicheskoi Tekhnologii*. 2021;55(6):772–779 (in Russ.). https://doi.org/10.31857/S0040357121050043]
11. Kol'tsov N.I., Fedotov V.Kh. *Invarianty i obratnye zadachi khimicheskoi kinetiki* (*Invariants and Inverse Problems of Chemical Kinetics*). Cheboksary: Chuvash University Publ.; 2022, 240 p. (In Russ.). ISBN 978-5-7677-3431-3
12. Katsman E.A., Sokolova I.V., Temkin O.N. Solution of reverse kinetic problem for oscillatory reactions. *Theor. Found. Chem. Eng*. 2014;48(2):175–179. https://doi.org/10.1134/S0040579514020067
[Original Russian Text: Katsman E.A., Sokolova I.V., Temkin O.N. Solution of reverse kinetic problem for oscillatory reactions. *Teoreticheskie Osnovy Khimicheskoi Tekhnologii*. 2014;48(2): 190–195 (in Russ.). https://doi.org/10.7868/S0040357114020067]
13. Gray P., Scott S.K. *Chemical Oscillations and Instabilities. Non-linear Chemical Kinetics*. Oxford: Clarendon Press; 1994, 470 p.
14. Alekseev B.V., Fedotov V.Kh., Kol'tsov N.I. Solution of the inverse problem of chemical kinetics for oscillatory reactions. *Theor. Found. Chem. Eng*. 2025. (In press).
15. Rössler O.E. Chaotic behavior in simple reaction system. *Z. Naturfosch*. 1976;A(31):259–264. https://doi.org/10.1515/zna-1976-3-408
16. Willamowski K.D., Rössler O.E. Irregular oscillations in a realistic abstract quadratic mass action system. *Z. Naturforsch*. 1980;35a:317–318. https://doi.org/10.1515/zna-1980-0308
17. Gaspard P. Rössler systems. In: *Encyclopedia of Nonlinear Science*. New York: Routledge; 2005. P. 808–811.
18. Stucki J., Urbanczik R. Entropy Production of the Willamowski-Rossler Oscillator. *Z. Naturforsch*. 2005;60a:599–607. https://doi.org/10.1515/zna-2005-8-907
19. Shuster G. *Determinirovannyi khaos: Vvedenie* (*Deterministic Chaos: An Introduction*): transl. from Engl. Moscow: Mir; 1988, 248 p. (In Russ.). ISBN 5-03-001373-3
10. Кольцов Н.И. Решение обратной задачи для химических реакций, протекающих в реакторе идеального вытеснения. *Теор. основы хим. технологии*. 2021;55(6):772–779. https://doi.org/10.31857/S0040357121050043
11. Кольцов Н.И., Федотов В.Х. *Инварианты и обратные задачи химической кинетики*. Чебоксары: Изд-во Чуваш. ун-та; 2022, 240 с. ISBN 978-5-7677-3431-3
12. Кацман Е.А., Соколова И.В., Темкин О.Н. Решение обратной кинетической задачи для колебательных реакций. *Теор. основы хим. технологии*. 2014;48(2):190–195. https://doi.org/10.7868/S0040357114020067
13. Gray P., Scott S.K. *Chemical Oscillations and Instabilities. Non-linear Chemical Kinetics*. Oxford: Clarendon Press; 1994, 470 p.
14. Алексеев Б.В., Федотов В.Х., Кольцов Н.И. Решение обратной задачи химической кинетики для колебательных реакций. *Теорет. основы хим. технологии*. 2025 (в печати).
15. Rössler O.E. Chaotic behavior in simple reaction system. *Z. Naturfosch*. 1976;A(31):259–264. https://doi.org/10.1515/zna-1976-3-408
16. Willamowski K.D., Rössler O.E. Irregular oscillations in a realistic abstract quadratic mass action system. *Z. Naturforsch*. 1980;35a:317–318. https://doi.org/10.1515/zna-1980-0308
17. Gaspard P. Rössler systems. In: *Encyclopedia of Nonlinear Science*. New York: Routledge; 2005. P. 808–811.
18. Stucki J., Urbanczik R. Entropy Production of the Willamowski-Rossler Oscillator. *Z. Naturforsch*. 2005;60a:599–607. https://doi.org/10.1515/zna-2005-8-907
19. Шустер Г. *Детерминированный хаос: Введение:* пер. с англ. М.: Мир; 1988, 248 с. ISBN 5-03-001373-3
20. Кузнецов С.П. *Динамический хаос*. М.: Физматлит; 2006, 356 с. ISBN 5-94052-100-2
21. Киперман С.Л. *Основы химической кинетики в гетерогенном катализе*. М.: Химия; 1979, 352 с.
22. Жаботинский А.М. *Концентрационные автоколебания*. М.: Наука; 1974, 179 с.
23. Выгодский М.Я. *Справочник по высшей математике*. М.: АСТ; 2019, 703 с. ISBN 978-5-17-117741-6
24. Аладьев В.З. *Системы компьютерной алгебры: Maple: Искусство программирования*. М.: Лаборатория Базовых Знаний; 2006, 792 с. ISBN 5-93208-189-9
25. Кольцов Н.И. Хаотические колебания в простейшей химической реакции. *Известия высших учебных заведений. Химия и хим. технол*. 2018;61(4-5):133–135. https://doi.org/10.6060/tcct.20186104-05.5654
26. Кольцов Н.И, Федотов В.Х. Хаотические колебания в простой гетерогенно-каталитической реакции. *Бутлеровские сообщения*. 2017;50(6):30–33. https://elibrary.ru/zefnpr

20. Kuznetsov S.P. *Dinamicheskii khaos* (*Dynamic Chaos*). Moscow: Fizmatlit; 2006, 356 p. (In Russ.). ISBN 5-94052-100-2
21. Kiperman S.L. *Osnovy khimicheskoi kinetiki v geterogennom katalize* (*Fundamentals of Chemical Kinetics in Heterogeneous Catalysis*). Moscow: Khimiya; 1979, 352 p. (In Russ.).
22. Zhabotinskii A.M. *Kontsentratsionnye avtokolebaniya* (*Concentration Self-Oscillations*). Moscow: Nauka; 1974, 179 p. (In Russ.).
23. Vygodskii M.Ya. *Spravochnik po vysshei matematike* (*Handbook of Higher Mathematics*). Moscow: AST; 2019, 703 p. (In Russ.). ISBN 978-5-17-117741-6
24. Alad'ev V.Z. *Sistemy komp'yuternoi algebry: Maple: Iskusstvo programmirovaniya* (*Computer Algebra Systems: Maple: The Art of Programming*). Moscow: Laboratoriya Bazovykh Znanii; 2006, 792 p. (In Russ.). ISBN 5-93208-189-9
25. Kol'tsov N.I. Chaotic oscillations in the simplest chemical reaction. *ChemChemTech = Izv. Vyssh. Uchebn. Zaved. Khim. Khim. Tekhnol.* 2018;61(4-5):133–135 (in Russ.). https://doi.org/10.6060/tcct.20186104-05.5654
26. Kol'tsov N.I., Fedotov V.Kh. Chaotic oscillations in a simple heterogeneous catalytic reaction. *Butlerovskie soobshcheniya = Butlerov Communications*. 2017;50(6):30–33 (in Russ.). https://elibrary.ru/zefnpr

About the Authors

Boris V. Alekseev, Cand. Sci. (Phys.-Math.), Associate Professor, Department of Physical Chemistry and Macromolecular Compounds, I.N. Ulyanov Chuvash State University (15, Moskovskii pr., Cheboksary, 428015, Russia). E-mail: a402539@yandex.ru. Scopus Author ID 7005563886, ResearcherID GNO-9997-2022, RSCI SPIN-code 7478-3333, https://orcid.org/0000-0003-1971-0806

Vladislav Kh. Fedotov, Cand. Sci. (Chem.), Associate Professor, Department of Physical Chemistry and Macromolecular Compounds, I.N. Ulyanov Chuvash State University (15, Moskovskii pr., Cheboksary, 428015, Russia). E-mail: fvh@inbox.ru. Scopus Author ID 8863837600, ResearcherID B-6529-2017, RSCI SPIN-code 5111-9580, https://orcid.org/0000-0001-8395-6849

Nikolay I. Kol'tsov, Dr. Sci. (Chem.), Professor, Head of the Department of Physical Chemistry and Macromolecular Compounds, I.N. Ulyanov Chuvash State University (15, Moskovskii pr., Cheboksary, 428015, Russia). E-mail: koltsovni@mail.ru. Scopus Author ID 7003771176, ResearcherID O-1354-2017, RSCI SPIN-code 4229-2226, https://orcid.org/0000-0003-2264-1370

Об авторах

Алексеев Борис Васильевич, к.ф.-м.н., доцент кафедры физической химии и высокомолекулярных соединений, ФГБОУ ВО «Чувашский государственный университет имени И.Н. Ульянова» (428015, Россия, г. Чебоксары, Московский пр-т, д. 15). E-mail: a402539@yandex.ru. Scopus Author ID 7005563886, ResearcherID GNO-9997-2022, SPIN-код РИНЦ 7478-3333, https://orcid.org/0000-0003-1971-0806

Федотов Владислав Харитонович, к.х.н., доцент кафедры физической химии и высокомолекулярных соединений, ФГБОУ ВО «Чувашский государственный университет имени И.Н. Ульянова» (428015, Россия, г. Чебоксары, Московский пр-т, д. 15). E-mail: fvh@inbox.ru. Scopus Author ID 8863837600, ResearcherID B-6529-2017, SPIN-код РИНЦ 5111-9580, https://orcid.org/0000-0001-8395-6849

Кольцов Николай Иванович, д.х.н., профессор, заведующий кафедрой физической химии и высокомолекулярных соединений, ФГБОУ ВО «Чувашский государственный университет имени И.Н. Ульянова» (428015, Россия, г. Чебоксары, Московский пр-т, д. 15). E-mail: koltsovni@mail.ru. Scopus Author ID 7003771176, ResearcherID O-1354-2017, SPIN-код РИНЦ 4229-2226, https://orcid.org/0000-0003-2264-1370

Translated from Russian into English by N. Isaeva
Edited for English language and spelling by Dr. David Mossop

Tonkie Khimicheskie Tekhnologii = Fine Chemical Technologies.
2025;20(6):540–554 ISSN 2686-7575 (Online)

UDC 66.092-977;544.473
https://doi.org/10.32362/2410-6593-2025-20-6-540-554
EDN NAQGZO

RESEARCH ARTICLE

Synthesis of methanol from gaseous products of pyrolysis of sewage sludge

Olga M. Larina✉, Iosif I. Lishchiner, Olga V. Malova, Yulia M. Faleeva

Joint Institute for High Temperatures of the Russian Academy of Sciences (JIHT RAS), Moscow, 125412 Russia

✉ *Corresponding author, e-mail: olga.m.larina@ihed.ras.ru*

Abstract

Objectives. To study the influence of compositional variability (different ash and organic matter contents) of sewage sludge on the characteristics of synthesis gas (syngas) and to determine the yield of products in the entire chain of conversion of sewage sludge to methanol through the stage of syngas production by two-stage pyrolysis.

Methods. Syngas was produced by a two-stage pyrolysis method. After heating sewage sludge from 20 to 1000°C in an oxygen-free medium, heterogeneous thermal cracking of the volatile products was carried out in a biochar medium at 1000°C. The syngas was converted to methanol on a CuZnAl catalyst in an isothermal flow heat-pipe reactor at a feedstock feed rate of 600 h^{-1}, an internal reactor pressure of 5 MPa, and temperatures in the catalyst bed of 205, 215, and 225°C. The resultant syngas having a CO_2 content of less than 0.5 vol % and a H_2/CO ratio of 1.8 was used as feedstock for methanol production.

Results. The experimental studies of syngas production from sewage sludge demonstrated the active formation of syngas during two-stage pyrolysis in the temperature range of 140–600°C regardless of the ash content of the sludge. The H_2/CO ratio in the syngas produced by two-stage pyrolysis of sewage sludge was shown to depend on the H/O atomic ratio in the sludge composition. Crude methanol was obtained at maximum yield and purity at a temperature of 225°C in the catalyst bed. The overall conversion of carbon monoxide was 43.6%.

Conclusions. Variability in the composition of sewage sludge significantly influences quantitative parameters to a large extent in terms of the specific volume yield of syngas and insignificantly terms of its composition. No qualitative influence was exerted by the difference in the types of sewage sludge on syngas production. The experimental studies showed that 1 kg of sewage sludge with a relative moisture content up to 5 wt % can produce 1.1 nm^3 of syngas and a further 220 g of pure methanol.

Keywords

sewage sludge, syngas, methanol, two-stage pyrolysis, thermal cracking, catalytic conversion, liquid motor fuels

Submitted: 23.01.2025
Revised: 09.07.2025
Accepted: 10.11.2025

For citation

Larina O.M., Lishchiner I.I., Malova O.V., Faleeva Yu.M. Synthesis of methanol from gaseous products of pyrolysis of sewage sludge. *Tonk. Khim. Tekhnol. = Fine Chem. Technol.* 2025;20(6):540–554. https://doi.org/10.32362/2410-6593-2025-20-6-540-554

НАУЧНАЯ СТАТЬЯ

Синтез метанола из газообразных продуктов пиролиза осадка сточных вод

О.М. Ларина✉, И.И. Лищинер, О.В. Малова, Ю.М. Фалеева

Объединенный институт высоких температур Российской академии наук (ОИВТ РАН), Москва, 125412 Россия

✉ *Автор для переписки, e-mail: olga.m.larina@ihed.ras.ru*

Аннотация

Цели. Исследовать влияние непостоянства состава (различное содержание зольности и органической части) осадка сточных вод (ОСВ) на характеристики синтез-газа, определить выход продуктов во всей цепочке превращений осадка сточных вод в метанол через стадию производства синтез-газа методом двухстадийного пиролиза.

Методы. Синтез-газ был получен методом двухстадийного пиролиза, заключающимся в нагреве ОСВ от 20 до 1000°C в бескислородной среде с последующим термическим гетерогенным крекингом летучих продуктов в среде биоугля при температуре 1000°C. Конверсия синтез-газа в метанол проходила на CuZnAl-катализаторе в проточном изотермическом реакторе на тепловых трубах с объемной скоростью подачи сырья 600 $ч^{-1}$, при давлении внутри реактора 5 МПа, температурах в слое катализатора 205, 215 и 225°C. В качестве сырья для производства метанола был использован синтез-газ с содержанием CO_2 менее 0.5 об. % и отношением H_2/CO, равным 1.8.

Результаты. Результаты экспериментальных исследований процесса получения синтез-газа из ОСВ установили, что независимо от величины зольности осадка, активное образование синтез-газа при двухстадийном пиролизе происходило в интервале температур 140–600°C. Отношение H_2/CO в синтез-газе, произведенным методом двухстадийного пиролиза ОСВ, зависело от атомного отношения H/O в составе осадка. Максимальный выход и чистота метанола-сырца были получены при температуре в слое катализатора равной 225°C. Общая конверсия оксида углерода составила 43.6%.

Выводы. Непостоянство состава ОСВ влияло на количественные показатели в значительной степени по удельному объемному выходу синтез-газа и незначительно по его составу. Качественно на протекание процесса получения синтез-газа различие в видах ОСВ влияния не оказывало. Результаты экспериментальных исследований показали, что из 1 кг ОСВ с относительной влажностью до 5 мас. % может быть произведено 1.1 $нм^3$ синтез-газа и далее 220 г чистого метанола.

Ключевые слова

осадок сточных вод, синтез-газ, метанол, двухстадийный пиролиз, термический крекинг, каталитическая конверсия, жидкие моторные топлива

Поступила: 23.01.2025
Доработана: 09.07.2025
Принята в печать: 10.11.2025

Для цитирования

Ларина О.М., Лищинер И.И., Малова О.В., Фалеева Ю.М. Синтез метанола из газообразных продуктов пиролиза осадка сточных вод. *Тонкие химические технологии*. 2025;20(6):540–554. https://doi.org/10.32362/2410-6593-2025-20-6-540-554

INTRODUCTION

The 2015 Paris Climate Agreement aims to limit global temperature rise to 1.5–2°C above pre-industrial levels [1]. This is to be achieved primarily by reducing greenhouse gas emissions (CH_4 and CO_2), of which Russia, along with China and the USA, is a leading producer [2, 3]. CO_2 emissions can be reduced by partially replacing fossil fuels with carbon-neutral ones, e.g., biomass [4, 5].

In recent years, Russia has been actively developing a Gas-To-Liquid (GTL) technology for producing synthetic liquid hydrocarbon products. The main stages of this technology are the production of synthesis gas (syngas) and its catalytic conversion to motor fuel components [6]. In the classical process, syngas is formed by steam reforming of natural gas [7]. However, for catalytic conversion to synthetic hydrocarbons, it is of no importance how syngas is produced so long as it meets requirements for composition, impurity levels, etc. In the carbon footprint reduction paradigm, biomass can be used to produce syngas using a two-stage pyrolytic conversion method [8, 9]. An alternative to the conventional Fischer–Tropsch process can be a two-stage catalytic synthesis of liquid hydrocarbons in the first stage of which syngas is catalytically converted to methanol, which is then catalytically converted to components of liquid motor fuels [10].

In this paper, sewage sludge is considered as a feedstock for the production of syngas for the subsequent synthesis of liquid hydrocarbons. Over 100 mln m^3

of sewage sludge with an average moisture content of 96% is generated annually in Russia. After dewatering, sewage sludge is transported from wastewater treatment facilities (WWTFs) to sludge piles. This stage can often mark the end of its useful life since its use as a fertilizer in agriculture is limited by the presence of heavy metal ions in its composition [11, 12]. In European countries, more than 20 sewage sludge processing approaches are used, including landfill, use as fertilizer, incineration, pyrolysis, and others [13]. Despite limitations, the primary use of sewage sludge is in agriculture; of the thermal processing methods, incineration is the most widely used [14]. Incineration can significantly reduce sewage sludge volume while generating thermal energy, but this is accompanied by such significant problems as the formation of sulfur oxides [15]. In addition, thermal energy cannot be transferred over long distances. However, if sewage sludge can be converted to some final or intermediate product that can be used, e.g., in the chemical industry, then it is transformed from a liability into an asset.

The aim of the present study is to investigate the effect of variability in the sewage sludge composition on the yield and properties of syngas, as well as to trace the entire chain of conversion of sewage sludge to methanol, an intermediate product of a two-stage catalytic synthesis of liquid hydrocarbons.

MATERIALS AND METHODS

This study examined sewage sludge samples from three different WWTFs in Russia: (1) *Lyubertsy* WWTF (Moscow oblast); (2) *Togliattikauchuk* WWTF (Samara oblast); (3) *Almetyevsk* WWTF (Republic of Tatarstan). The samples consisted of a gray-brown, loose material containing organic fiber impurities (Fig. 1).

Preliminary preparation of feedstock included drying at a temperature of 105°C to reduce the relative humidity to values not exceeding 3–5 wt %. Technical analysis (determination of ash content *A*, volatile matter *VM*, and fixed carbon *FC*) was performed using a NETZSCH STA 2500 Regulus thermogravimetric analyzer (*NETZSCH Group*, Germany). The heating rate of feedstock was 20°C/min. The elemental composition (C, H, N, S) of the samples was determined using a vario MACRO cube elemental analyzer (*Elementar Analysensysteme GmbH*, Germany). The oxygen content (O) was calculated as a residual. The higher calorific value *HCV* was calculated from the elemental composition data. Table 1 presents the results of the technical analysis and elemental analysis of feedstock samples on a dry basis.

Table 1. Characteristics of sewage sludge samples (dry basis)

Parameter	Unit of measure	Sample		
		1	2	3
C	wt %	27.33	14.88	35.91
H		3.60	3.31	5.15
N		3.59	1.76	6.33
S		1.26	0.78	0.86
O		18.34	28.21	24.03
A		45.88	51.06	27.72
FC		9.74	5.70	13.23
VM		44.38	43.24	59.05
HCV	MJ/kg	11.11	6.21	16.12

Conversion of sewage sludge samples into syngas by two-stage pyrolysis was performed in a laboratory setup described previously [16]. The method involved heating the feedstock (sewage sludge) from room temperature 20°C to 1000°C at a rate of 10 deg/min in an oxygen-free medium (pyrolysis). The formed volatile products passed through a thermal cracking zone filled with biochar, a solid residue from the pyrolysis of the same type of sewage sludge that

(1) (2) (3)

Fig. 1. Sewage sludge samples: (1) *Lyubertsy* WWTF, (2) *Togliattikauchuk* WWTF, and (3) *Almetyevsk* WWTF

was present in the pyrolysis zone. The temperature in the cracking zone was maintained at 1000°C throughout the experiment. The volatile components were decomposed by various chemical reactions to form syngas. Biochar was previously obtained by pyrolysis of sewage sludge to 1000°C. The biochar layer height in the cracking zone was identical for all sewage sludge samples and was 10 cm. The relative moisture content of the feedstock samples did not exceed 1%. The syngas composition was determined using a Vario Plus Industrial flow gas analyzer (*MRU*, Germany) after sampling from a gas holder (*NPF Politekhnika*, Russia) in which the syngas was collected during the experiment. The volume was measured using a Shinagawa WS-1A gas meter (*Shinagawa Corporation*, Japan); the specific volume yield was determined as the ratio of the volume of all syngas released from the sewage sludge to the mass of the sample used in the experimental study. The lower calorific value *LCV* of the syngas was calculated using the volume fractions and the calorific value of the combustible gas components under standard conditions (20°C, 101.325 kPa) using the formula

$$LCV = 10^{-2} \cdot (11.78 \cdot [CO] + \\ + 10.05 \cdot [H_2] + 33.367 \cdot [CH_4]), \quad (1)$$

where [CO], [H_2], and [CH_4] are the contents of the respective gases in the mixture, vol %.

Crude methanol was synthesized from syngas in an isothermal catalytic heat-pipe reactor (R-1) [17]. Syngas was fed into the flow-through methanol synthesis reactor at a flow rate of 60 L/h from a cylinder in which a mixture of the desired composition had been previously prepared (Table 2). The volumetric syngas feed rate was 600 h^{-1}. The content of CH_3OH and H_2O in the raw methanol was determined chromatographically using the NetChrom hardware and software system (*NPF META-KHROM*, Russia); the content of dimethyl ether (DME) was measured using a Model 3700 chromatograph (*KHROMATOGRAF*, Russia); the content of trace impurities in methanol was determined chromatographically using a Khromos GKh-1000 chromatograph (at the laboratory of *Khromos*, Dzerzhinsk, Nizhny Novgorod oblast, Russia). The volumetric composition of the syngas at the outlet of the R-1 reactor was measured using an MRU Vario Plus Industrial gas analyzer.

To evaluate the methanol synthesis efficiency, the following metrics were calculated.

1. Overall CO conversion K_1, %:

$$K_1 = \frac{[CO]_{react} \cdot 100}{G \cdot [CO]_{in} \cdot \frac{28}{24.04}} \cdot 100\%, \quad (2)$$

where $[CO]_{react}$ is the mass flow rate of reacted CO, g/h; $[CO]_{in}$ is the CO content of the feedstock, vol %; 28 is the molar mass of CO, g/mol; 24.04 is the molar volume of CO at a temperature of 20°C, L/mol; and G is the volume flow rate of syngas, L/h.

2. Carbon efficiency of CO conversion to methanol, K_2, %:

$$K_2 = \frac{[CH_3OH]_{form} \cdot \frac{12}{32}}{[CO]_{in,m} \cdot \frac{12}{28}} \cdot 100\%, \quad (3)$$

where $[CH_3OH]_{form}$ is the mass of methanol formed, g; $[CO]_{in,m}$ is the mass of the initial carbon monoxide, g; 12 is the molar mass of carbon, g/mol; and 32 is the molar mass of methanol, g/mol.

3. Carbon efficiency of CO conversion to DME, K_3, %:

$$K_3 = \frac{[C_2H_6O]_{form} \cdot \frac{12}{46}}{[CO]_{in,m} \cdot \frac{12}{28}} \cdot 100\%, \quad (4)$$

where $[C_2H_6O]_{form}$ is the mass of DME formed, g.

4. Carbon efficiency of CO conversion to CO_2, K_4, %:

$$K_4 = \frac{[CO_2]_{form} \cdot \frac{12}{44}}{[CO]_{in,m} \cdot \frac{12}{28}} \cdot 100\%, \quad (5)$$

where $[CO_2]_{form}$ is the mass of carbon dioxide formed, g.

Table 2. Composition of syngas fed to methanol production reactor, vol %

CO	H_2	CO_2	N_2	CH_4	Total
34.30	61.95	0.40	2.70	0.65	100

Table 3. Conditions of experimental studies of the synthesis of components of liquid motor fuels from syngas

Parameter	Unit of measure	Reactor R-1
Temperature inside reactor	°C	205, 215, 225
Pressure inside reactor	MPa	5
Volumetric feedstock feed rate	h^{-1}	600
Feedstock	–	Syngas
Catalyst	–	CuO–ZnO/Al_2O_3 metal oxide catalyst (GL-7, *Süd-Chemie*, Germany)
Catalyst properties	–	Loading 100 cm^3, fraction 1.5–2 mL
Catalyst bed height	mm	221

Table 3 presents conditions of experimental studies of the synthesis of methanol from syngas.

RESULTS AND DISCUSSION

Feedstock properties

As a secondary biomass, sewage sludge has characteristics related to its origin. For all types of sewage sludge, the ash content varies from 28 to 57 wt %, the volatile matter content is 38–60 wt %, and the fixed carbon content is 3–11 wt % [15]. The total carbon content of sewage sludge, recalculated on an ash-free basis, is on average approximately 50%, which is comparable to the carbon content of sawdust (53 wt % [18]), and slightly lower than that of lignite (65–70 wt % [18, 19]). This fact allows for a higher calorific value of sewage sludge (on a dry basis) of 22 MJ/kg. In comparison, the corresponding parameter for wood sawdust is in the range of 18–20 MJ/kg; that of rice husks, 15–16 MJ/kg; lignite, 11.8–21.9 MJ/kg [15].

The samples taken for analysis in this study were typical representatives of sewage sludge. Sample 3 stood out from the previously presented ranges in terms of its ash, volatile matter, and fixed carbon contents. In particular, its fixed carbon content *FC* was 2.2% higher than the typical range (Table 1). Among the samples, were included a high-ash sample (51.06 wt %, sample 2) and a sample with an ash content close to the lower limit of the typical range (27.72 wt %, sample 3), indicating different organic matter contents in the samples.

Based on the composition of the syngas, the main elements determining its H_2 and CO contents were carbon, oxygen, and hydrogen. Sample 3 had the highest volatile carbon content (the difference between total *C* and *FC*) at 22.68 wt %, as well as the highest contents of volatile components and hydrogen, the lowest ash content, and a slightly lower oxygen content as compared with sample 2 (Table 1). Therefore, under identical experimental conditions, this sample was expected to produce the maximum syngas volume. In comparison with sample 1, sample 2 contained less volatile carbon (9.18 *vs* 17.59 wt %), but more oxygen (28.21 *vs* 18.34 wt %). Since the contents of volatile components and hydrogen for these two samples were very close (Table 1), at that stage, it was impossible to predict which of samples 1 and 2 would give a higher syngas yield.

Syngas production

Figure 2 shows the dependence of the specific volume yield of syngas and its formation rate (the temperature derivative of the specific volume yield of syngas) on the temperature in the pyrolysis zone for three sewage sludge samples. Syngas production began at a temperature of 140–160°C, which was due to the release of physical moisture from the samples and the subsequent formation of syngas in the cracking zone filled with biochar according to the reaction

$$H_2O + C = H_2 + CO. \quad (6)$$

The intense release of syngas from sample 1 was in the temperature range of 160–600°C; from sample 2 at 150–600°C; from sample 3 at 140–600°C. Since sample 3 had the maximum content of organic matter among the considered sewage sludge, the earlier (lower-temperature) release of syngas from this sample may be associated with the presence of lighter compounds—for example, methanol—in the volatile products [20]. For sample 1, the peak rate of syngas formation was observed at a temperature of 375°C; for sample 2 at 345°C; for sample 3 at 347°C. Thus, regardless of the mineral

matter content of the sewage sludge, the maximum rate of syngas release was in the temperature range of 340–380°C; by the time a temperature of 600°C was reached, the intense release of syngas had ended. It was shown in [21] that, in the composition of the volatile products of pyrolysis of sewage sludge, the mass of pyrolysis liquid consisting of water and organic matter in the temperature range of 200–600°C is four times larger than the mass of the formed incondensable gases. For this reason, the main feedstocks for syngas from the composition of the volatile products of pyrolysis are tars and water. The maximum rates of formation of tars and water are in the temperature ranges of 300–350 and 290–380°C, respectively [21]. Pyrolysis tars contain oxygen-containing compounds (the main ones are acids, ketones, phenols, alcohols, saccharides), aromatic and aliphatic hydrocarbons, and nitrogen-containing compounds (nitriles, pyridines, pyrroles, amines, amides) [22]. All of these are converted to syngas during thermal cracking. The higher the organic matter content of sewage sludge, the higher the mass yields of water and tars, and the higher the specific volume yield of syngas. Sample 3 had the maximum organic matter content, which favored the maximum specific volume yield of syngas among the samples studied. Sample 2 had the maximum ash content, which affected the quantitative characteristics of the syngas (Fig. 2).

Figure 3 shows the results of thermogravimetric analysis (TGA) of sewage sludge samples 1–3 in an inert medium in the temperature range of 150–900°C. The intense release of volatile products from these samples began at 200°C. The end of the range of active mass loss of the samples was at 550 ± 5°C. The two peaks in the rate of mass loss occurring at 290 and 340°C within this temperature range for sample 3 were associated with the decomposition of hemicellulose and cellulose components in the sewage sludge [23]. For sample 1, in the temperature range of hemicellulose decomposition, a shoulder was observed in the range of 294–314°C. This was a combination of several peaks responsible for the decomposition of complex organic compounds with different temperatures of the onset of destruction. The second peak was observed at 344°C, which is within the temperature range of cellulose decomposition [23]. For sample 2, the first peak was observed at 299°C with a shoulder in the range of 329–340°C instead of the second peak. For samples 1 and 2, in the temperature ranges of 394–464°C and 399–419°C, respectively, a shoulder-like structure was also observed on the mass loss rate curve. Due to the overlapping peaks of several reactions, the peak for sample 3 had a shoulder structure over a wide temperature range. Lignin, which is also present in the sludge, is known to actively decompose in this temperature range [24, 25]. Sewage sludge samples were studied by thermogravimetric analysis at different heating rates [26]. According to the presented data, the presence of shoulders on the mass loss rate curve of sewage sludge samples is a typical pattern.

The presence of peaks in the temperature range of 715–750°C for samples 1–3 (Fig. 3) may be due to the decomposition of inorganic carbonates, which are actively formed at temperatures up to 700°C by the interaction of CO_2 from volatile pyrolysis products with CaO from the sewage sludge ash [27, 28]. At temperatures above 700°C, the reverse reaction of $CaCO_3$ decomposition to form CO_2 occurs [29]. Sample 2, which had the maximum ash content, had the highest peak of the mass loss rate in this temperature range.

The TGA results for the sewage sludge samples under study (Fig. 3) correlated well with the results of measurements of specific volume yields and calculations of syngas formation rates for these samples (Fig. 2). The highest syngas formation rate among the studied samples was obtained for sample 3, which exhibited the highest

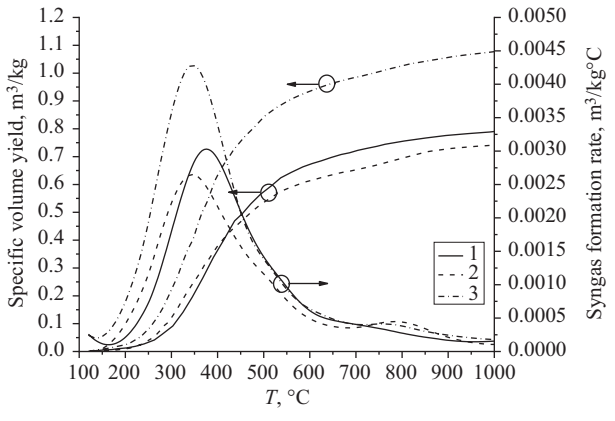

Fig. 2. Specific volume yield and formation rate of syngas from sewage sludge samples 1–3 *vs* temperature in the pyrolysis zone

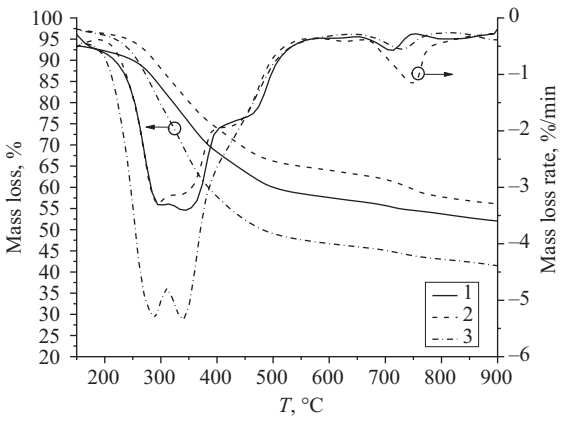

Fig. 3. Results of thermogravimetric analysis of sewage sludge samples 1–3: mass loss (left) and mass loss rate (right)

mass loss rate during thermogravimetric analysis. The data for samples 1 and 2 similarly agreed. The temperature range of intense syngas production for all three samples was 140–600°C, while the range of intense mass loss during thermogravimetric analysis was determined to be 200–550°C. The difference in the earlier onset and later end of the syngas release in comparison with the TGA data was explained by the difference in the masses of the samples used for the two types of analysis (10–20 mg for TGA *vs* 10–15 g for experimental studies), as well as by a small time delay in the determination of the volume yield of syngas in the gas meter in comparison with the measurement of the temperature inside the pyrolysis zone during the experimental study. It is worth noting the increase in the syngas formation rate for samples 2 and 3 at temperatures of 789 and 761°C, respectively (Fig. 2). A fourth peak of the mass loss rate observed in the temperature range of 670–800°C was associated with the formation of CO_2 by the decomposition of inorganic carbonates. During thermal cracking in the presence of carbon, CO_2 was actively converted to CO. It has been shown that H_2 formation actively increases at a sewage sludge pyrolysis temperature above 550°C with the peak occurring at 680°C [21]. Furthermore, throughout the heating of the sewage sludge sample in an oxygen-free medium, the volatile products contained water with one of the peaks of its formation rate at a temperature of 710°C. According to reaction (6), water is converted to syngas by thermal cracking in a charcoal medium. All these circumstances led to the increase in the syngas formation rate for samples 2 and 3 in the temperature range of 760–790°C.

Production of syngas from sewage sludge with an ash content of 22.7% by two-stage pyrolysis was studied [30]. The results were identical to those obtained in the present study: the intense release of syngas continued up to 570°C. The two-stage pyrolysis method was applied to plant biomass [31]. The results showed that the temperature range of intense release of syngas from plant biomass was 200–480°C.

Table 4 presents the main characteristics of the syngas obtained from three types of sewage sludge. The key parameters of the syngas that must be taken into account for its further conversion to liquid products are the H_2/CO ratio and the specific volume yield. For all three sewage sludge samples, the H_2 and CO contents were in the ranges of 57–60 and 37–41 vol %; this indicates the sufficient homogeneity of the syngas composition regardless of the different origin of the sewage sludge and the organic matter content. In addition, the syngas from all three sludge samples had a lower calorific value of 12 MJ/nm^3, a CO_2 content less than 0.5 vol %, and a CH_4 content less than 1 vol %. The organic matter content of sewage sludge determines the specific volume yield of syngas: for sample 3, this metric was maximum, while for sample 2, it was minimum, which correlates with the mineral matter contents of these samples.

Table 4. Characteristics of syngas obtained by two-stage pyrolysis of sewage sludge

Parameter	Unit of measure	Sample		
		1	2	3
Specific volume yield	m^3/kg	0.8	0.7	1.1
H_2	vol %	59.6	57.2	60.9
CO		39.2	41.6	37.9
CO_2		0.4	0.5	0.2
CH_4		0.8	0.7	1.0
H_2/CO ratio	–	1.5	1.4	1.6
LCV	MJ/m^3	11	11	11

The H_2/CO ratio was in the range of 1.4–1.6. The maximum H_2/CO ratio, as well as the maximum H_2 content, was obtained for sample 3. It was assumed and experimentally proven [32] that the H_2/CO ratio in the composition of syngas obtained by two-stage pyrolysis depends on the H/O atomic ratio in the original biomass: the higher the latter ratio, the higher the former. For the sewage sludge samples used in this study, the H/O atomic ratios were 3.1, 1.9, and 3.4, respectively (Table 1). The data in Table 3 show that the H_2/CO ratio was maximum for sample 3 and minimum for sample 2. Based on the obtained experimental data, it can be stated that the assumption [32] is also valid for the sewage sludge studied.

The total content of hydrogen and carbon monoxide in the resulting syngas, as well as their ratio, depends on the type of biomass processed. Two-stage pyrolysis of various samples of primary and secondary biomass was previously studied (Table 5) [30, 32]. Syngas produced from wood biomass (sawdust, not bark) had an H_2/CO ratio close to 1. Syngas obtained by the thermochemical conversion of birch and aspen bark had an H_2/CO ratio of more than 2. The behavior of secondary biomass (chicken litter and sewage sludge) differs during two-stage pyrolysis. Chicken litter has a specific volume yield of syngas and an H_2/CO ratio similar to those of plant biomass (except for bark samples), whereas sewage sludge has a lower specific yield, but a higher H_2/CO ratio (Table 4).

Table 5. Characteristics of syngas obtained by two-stage pyrolysis of various types of biomass

Material	Specific volume yield, m^3/kg	H_2/CO	Reference
Wood sawdust	1.3*	1.1	[32]
Birch bark	1.3*	3.0	[32]
Aspen bark	1.3*	2.1	[32]
Chicken litter	1.2	1.2	[30]

* Specific volume data are presented on a dry ash-free basis.

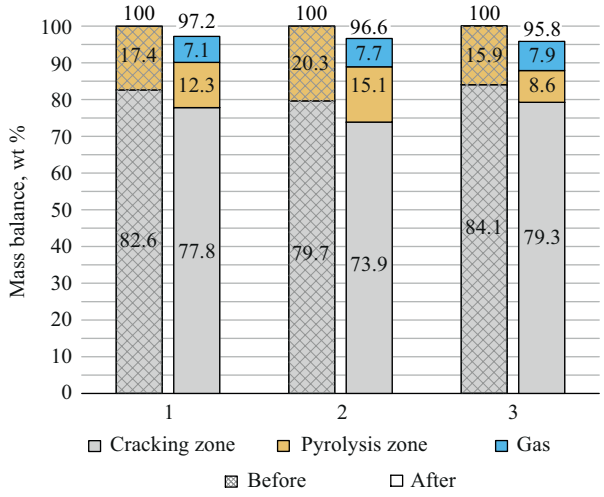

Fig. 4. Mass balance of two-stage pyrolysis of sewage sludge samples 1–3

Figure 4 illustrates the mass balance of two-stage pyrolysis of samples 1–3. For each of the samples, the left column represents the sum of the mass of the test material in the pyrolysis zone and the mass of charcoal in the cracking zone before the experiment. The right column shows the mass distribution of the two-stage pyrolysis products relative to the total mass of the materials before the experiment. The discrepancy in the mass balance is due to the error of the measuring instruments (scales, gas meter, flow gas analyzer), as well as the unaccounted-for mass of pyrolytic carbon deposited on the inner surface of the reactor during the homogeneous cracking of volatile products, which occurs simultaneously with the heterogeneous cracking in the biochar medium in the high-temperature region. However, this discrepancy does not exceed 4.2%. In addition, during the thermal cracking of the volatile products of sewage sludge pyrolysis, nitrogen- and sulfur-containing components are present in the syngas [33]. While this study did not determine nitrogen and sulfur dioxide impurities in the syngas, these factors could also have contributed to the mass balance discrepancy. The resulting syngas contained no liquid fraction, indicating complete conversion of all volatile pyrolysis products to syngas. Thus, unlike conventional methods of syngas tar removal (using cyclones, filters, and scrubbers), two-stage pyrolysis technology preserves the chemical energy contained in the tars, converting it to the calorific value of the syngas.

Methanol synthesis

The error in the volume content of components during the preparation of the gas mixture in the cylinder is 15%. Syngas obtained from sample 3 was used for the preparation of the mixture. Taking into account the error in the component contents, the H_2/CO ratio in the syngas mixture from the cylinder used for methanol synthesis was overestimated at 1.8.

Figure 5 presents the composition of the methanol synthesis products. The mass yield of crude methanol was 9.6, 10.3, and 12.3 g/h at catalyst bed temperatures of 205, 215, and 225°C, respectively.

The syngas leaving the methanol synthesis reactor had lower contents of carbon monoxide and hydrogen,

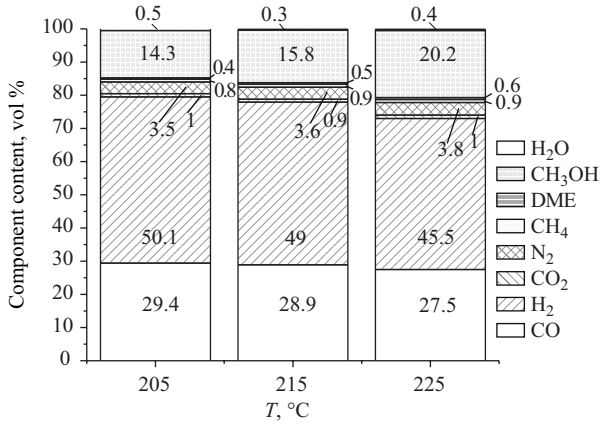

Fig. 5. Composition of methanol synthesis products

which were consumed in the main reaction of methanol synthesis:

$$CO + 2H_2 \rightarrow CH_3OH. \quad (7)$$

The H_2/CO ratios in the gas mixtures also decreased to 1.71, 1.69, and 1.61, respectively, at different catalyst bed temperatures. The carbon dioxide content increased in comparison with that in the feed gas due to the water-gas shift reaction

$$CO + H_2O \rightarrow CO_2 + H_2. \quad (8)$$

Nitrogen and methane were ballast gases and did not participate in the chemical reactions. Therefore, their volume flow rates remained unchanged, but their contents in the effluent increased due to some of the syngas being converted to methanol. This led to an overall decrease in the volume of reaction products. In this case, DME was a byproduct formed by the methanol dehydration reaction

$$2CH_3OH \rightarrow CH_3OCH_3 + H_2O, \quad (9)$$

which reduced the methanol yield. With increasing temperature inside the catalyst bed, the contents of unreacted CO and H_2 decreased and the DME content increased. At the same time, the methanol yield increased. The maximum methanol yield (38.2% of the mass of the synthesis products) was observed at a temperature inside the catalyst bed of 225°C (Fig. 6a). At temperatures of 215 and 225°C, the crude methanol consisted of more than 98.9% pure methanol (Fig. 6b).

Table 6 presents the contents of impurities in the composition of methanol.

Table 6. Microimpurities in methanol, wt %

Component	Temperature in catalyst bed		
	T_1 = 205°C	T_1 = 215°C	T_1 = 225°C
Acetaldehyde	0.20997	0.00457	0.03351
Formic acid	0.04779	0.01956	0.04226
Acetone	0.00073	0.00020	0.00176
Methyl acetate	0.00387	0.00145	0.00120
Ethanol	0.15065	0.08668	0.04937
Propan-1-ol	0.03830	0.02716	0.01452
n-Butanol	0.00583	0.00415	0.00175
Butan-1-ol	0.03662	0.01756	0.01321
Acetic acid	0.00457	0	0
Total	0.50	0.16	0.16

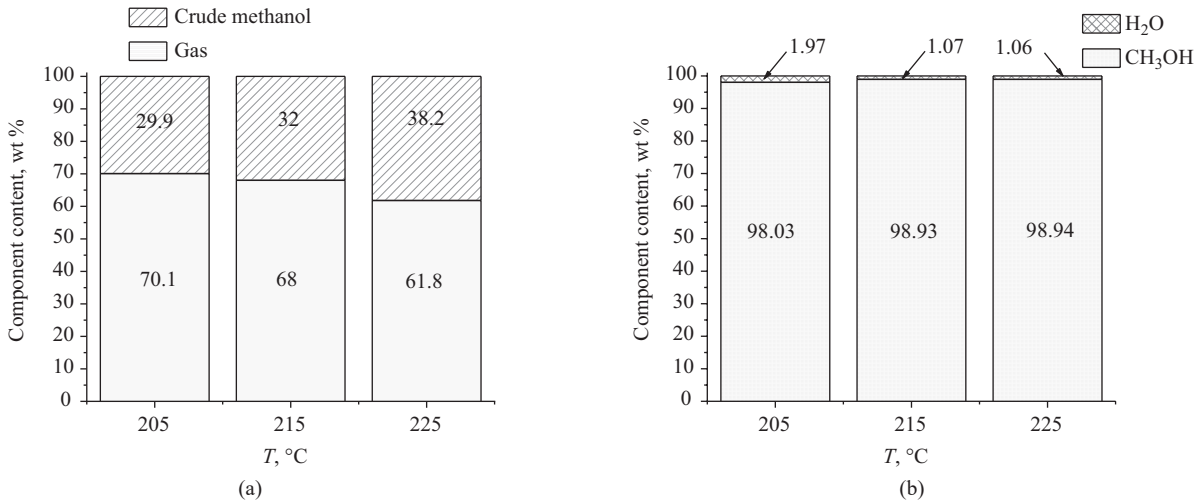

Fig. 6. (a) Mass balance of methanol synthesis and (b) the composition of crude methanol at various temperatures in the catalyst bed

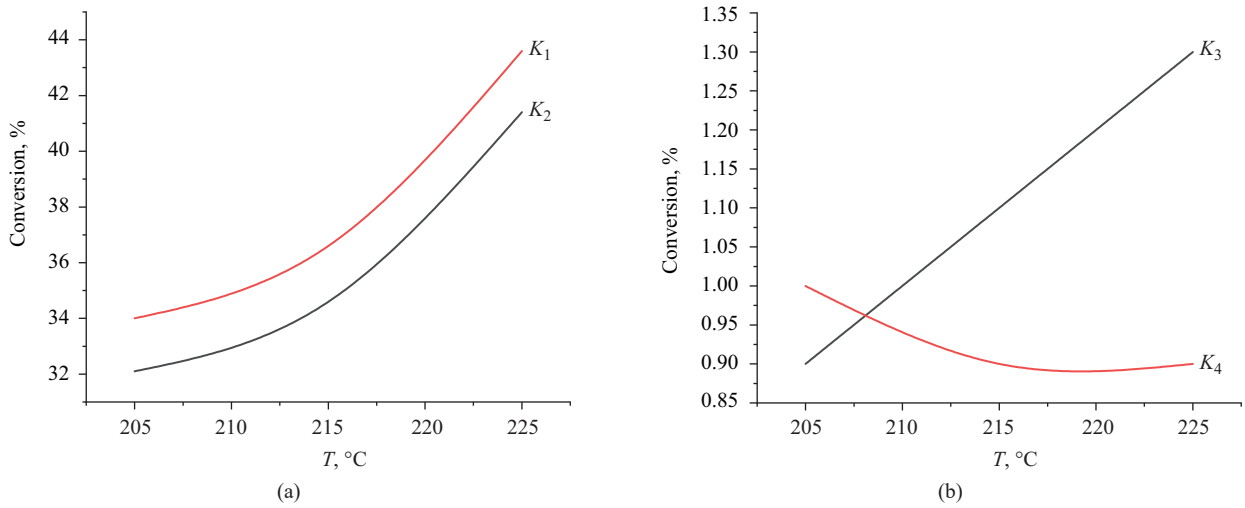

Fig. 7. Dependence of CO conversion on the temperature inside the catalyst bed: (a) K_1 and K_2; (b) K_3 and K_4

The impurity content of methanol decreased with increasing catalyst bed temperature. The water, acetone, formic acid, and ethanol contents of technical methanol were monitored. After reducing the water, formic acid, and ethanol contents, the resulting methanol can be classified as technical grade B methanol in accordance with GOST 2222-95[1].

Figure 7 shows the dependence of the CO conversion on the catalyst bed temperature. With increasing temperature inside the catalyst bed, the conversion of CO to CO_2 decreased, and the conversion of CO to DME and methanol increased. The maximum overall carbon monoxide conversion was 43.6% at a catalyst bed temperature of 225°C. Currently, under industrial conditions, the conversion of syngas to methanol in a single pass does not exceed 20% [34].

The syngas from the cylinder that was used for experimental methanol production studies had a higher H_2/CO ratio than that obtained experimentally from sewage sludge (Tables 2 and 4, respectively). A decrease in the H_2/CO ratio in the syngas led to a decrease in the CO conversion and, consequently, to a decrease in the mass yield of methanol and to an increase in the content of organic impurities [35].

The studies showed that, at a volumetric syngas feed rate of 600 h^{-1}, the maximum methanol yield and maximum CO conversion to methanol were achieved at a catalyst bed temperature of 225°C.

Currently, research is actively being conducted worldwide into methods for producing methanol as an intermediate product for the further synthesis of motor fuels. However, in the context of decarbonization policies, the focus of research has shifted toward the production of biomethanol [36]. Depending on the equipment design, all processes are divided into three groups: high-pressure synthesis on Zn/Cr catalysts (370–420°C, 20–35 MPa), low-pressure synthesis on Zn/Cu/Cr or Zn/Cu/Al catalysts (210–270°C, 5–10 MPa), and synthesis in a gas–liquid–solid three-phase system [34]. In addition, not only experimental studies but also process simulation using various software packages are actively conducted. For example [37], the Aspen Plus software was used to simulate the catalytic conversion of syngas to methanol in a continuous stirred-tank reactor at a temperature of 270°C and a pressure of 40 bar. The simulation results showed that hydrogen recycle to the system provided an increase in methanol production by 50.4% in comparison with the results of the process without H_2 recycle. The conversion of CO, CO_2, and H_2 was 50.4, 99.8, and 100%, respectively. One of the feedstock options for methanol production is syngas mixed from separately produced hydrogen and CO_2 captured from locally available point sources. In this regard, studies are being conducted to assess the role of CO and CO_2 in the methanol synthesis reaction catalyzed by Cu. It has been shown [38] that the rate of methanol synthesis from CO_2 is more than an order of magnitude higher than the rate of synthesis from CO, which helps to substantiate that CO_2 is a direct source of carbon for methanol on a Cu-containing catalyst. The role of CO is to bind water formed during methanol synthesis to form CO_2 via the water-gas shift reaction. Typically, to initiate the reaction of methanol production from syngas, the CO_2 content in the gas mixture must be at least 5 vol %. A method for increasing methanol yield

[1] GOST 2222-95. Interstate Standard. Technical methanol. Specifications. Moscow: Izdatelstvo standartov; 2000, 19 p. (In Russ.).

by creating a cascade of three flow-through catalytic reactors was presented [39]. Syngas unreacted in the first reactor is fed to the second, then to the third. At each stage, crude methanol is collected.

In the present study, the results of which are presented above, the syngas used for conversion to methanol had a CO_2 content of 0.4 vol % (Table 2). The novelty of the obtained results is determined by the apparent lack of publicly available publications on methanol synthesis from syngas at a low CO_2 content (less than 0.5 vol %). The use of sewage sludge as a feedstock for methanol production further underlines the relevance of the research.

CONCLUSIONS

The results of the experimental studies presented in this study confirm that sewage sludge is a suitable feedstock for methanol synthesis. Regardless of the ash content of the sewage sludge, intense syngas production by two-stage pyrolysis began at 140°C and continued until 600°C. The pattern of syngas formation from the sewage sludge samples under study correlated well with the results of their thermogravimetric analysis. With increasing ash content of the samples, the specific volume yield of syngas decreased. The H_2/CO ratio in the syngas obtained by two-stage pyrolysis from the sewage sludge, as well as that obtained from plant biomass, depended on the H_2/O atomic ratio in the sludge. The sample with the lowest H_2/CO atomic ratio yielded syngas with the lowest H_2/CO ratio. The same analogy was observed for the sample with the highest H_2/O atomic ratio. Thus, the heterogeneity of the composition of sewage sludge when processed by two-stage pyrolysis affects only the quantitative characteristics of the syngas and does not influence the actual process.

The maximum yield and purity of crude methanol were achieved at a catalyst bed temperature of 225°C. At this temperature, an overall CO conversion of 43.6% was achieved. After reducing the water, formic acid, and ethanol contents, the resulting methanol can be classified as technical grade B methanol.

Considering the entire chain of conversion of sewage sludge to methanol, 1 kg of sewage sludge can yield 1.1 nm^3 of syngas and then 220 g of pure methanol. The yield of methanol can be increased by creating a cascade of three flow-through catalytic methanol synthesis reactors.

Acknowledgments

This work was supported by the Ministry of Science and Higher Education of the Russian Federation (State Assignment No. 075–00270-24–00).

Authors' contributions

O.M. Larina—processing and analysis of experimental research results on obtaining syngas and its further synthesis into methanol, writing the text of the article.

I.I. Lishchiner—conducting experimental research on converting syngas into methanol, analysis of results.

O.V. Malova—conducting experimental research on converting syngas into methanol, analysis of results.

Yu.M. Faleeva—conducting experimental research on obtaining syngas from sewage sludge.

The authors declare no conflicts of interest.

REFERENCES

1. Pachauri R.K., Meyer L.A. (Eds.). *IPCC, 2014: Climate Change 2014: Synthesis Report. Contribution of Working Groups I, II and III to the Fifth Assessment Report of the Intergovernmental Panel on Climate Change*. Geneva; 2015, 151 p. ISBN 978-92-9169-143-2
2. Filonchyk M., Peterson M.P., Zhang L., Hurynovich V., He Y. Greenhouse gases emissions and global climate change: Examining the influence of CO_2, CH_4, and N_2O. *Sci. Total Environ.* 2024;935:173359. https://doi.org/10.1016/j.scitotenv.2024.173359
3. Braide D., Panaritis C., Patience G., Boffito D.C. Gas to liquids (GTL) microrefinery technologies: A review and perspective on socio-economic implications. *Fuel*. 2024;375:132385. https://doi.org/10.1016/j.fuel.2024.132385
4. Kjärstad J., Johnsson F. The role of biomass to replace fossil fuels in a regional energy system: The case of West Sweden. *Thermal Science*. 2016;20(4):1023–1036. https://doi.org/10.2298/TSCI151216113K

СПИСОК ЛИТЕРАТУРЫ

1. Pachauri R.K., Meyer L.A. (Eds.). *IPCC, 2014: Climate Change 2014: Synthesis Report. Contribution of Working Groups I, II and III to the Fifth Assessment Report of the Intergovernmental Panel on Climate Change*. Geneva; 2015, 151 p. ISBN 978-92-9169-143-2
2. Filonchyk M., Peterson M.P., Zhang L., Hurynovich V., He Y. Greenhouse gases emissions and global climate change: Examining the influence of CO_2, CH_4, and N_2O. *Sci. Total Environ.* 2024;935:173359. https://doi.org/10.1016/j.scitotenv.2024.173359
3. Braide D., Panaritis C., Patience G., Boffito D.C. Gas to liquids (GTL) microrefinery technologies: A review and perspective on socio-economic implications. *Fuel*. 2024;375:132385. https://doi.org/10.1016/j.fuel.2024.132385
4. Kjärstad J., Johnsson F. The role of biomass to replace fossil fuels in a regional energy system: The case of West Sweden. *Thermal Science*. 2016;20(4):1023–1036. https://doi.org/10.2298/TSCI151216113K

5. Yana S., Nizar Irhamni M., Mulyati D. Biomass waste as a renewable energy in developing bio-based economies in Indonesia: A review. *Renewable Sustainable Energy Rev*. 2022;160:112268. https://doi.org/10.1016/j.rser.2022.112268
6. Bazarov B.I., Odilov O.Z., Otabaev N.I. Production of synthetic hydrocarbons from natural gas using GTL technology. *Mekhanika i tekhnologii = Mechanics and Technologies*. 2022;6:122–132 (in Russ.).
7. Mirgayazov I.I., Abdullin A.I. Modern methods of producing synthesis gas and the Fischer-Tropsch process. *Vestnik Kazanskogo tekhnologicheskogo universiteta = Herald of Kazan Technological University*. 2014;9:258–261 (in Russ.).
8. Batenin V.M., Zaichenko V.M., Kosov V.F., *et al*. Pyrolytic conversion of biomass to gaseous fuel. *Dokl. Chem.* 2012;446(1): 196–199. https://doi.org/10.1134/S0012500812090030 [Original Russian Text: Batenin V.M., Zaichenko V.M., Kosov V.F., Sinel'shchikov V.A. Pyrolytic conversion of biomass to gaseous fuel. *Doklady Akademii nauk.* 2012;446(2):179–182 (in Russ.). https://elibrary.ru/pbwfrt]
9. Kosov V., Kosov V., Sinelschikov V., Zaichenko V. *High-Calorific Gas Mixtures Produced from Biomass.* In: Oral A., Bahsi Z., Oze M. (Eds.). *International Congress on Energy Efficiency and Energy Related Materials* (*ENEFM2013*). *Springer Proceedings in Physics*. Cham: Springer; 2014. V. 155. P. 377–383. https://doi.org/10.1007/978-3-319-05521-3_48
10. Kachalov V.V., Lavrenov V.A., Lishchiner I.I., Malova O.V., Tarasov A.L., Zaichenko V.M. Scientific bases of biomass processing into basic component of aviation fuel. *J. Phys.: Conf. Ser.* 2016;774:012136. https://doi.org/10.1088/1742-6596/774/1/012136
11. Valiev V.S., Ivanov D.V., Shagidullin R.R. Methods for urban wastewater sludge disposal (Review). *Rossiiskii zhurnal prikladnoi ehkologii = Russian Journal of Applied Ecology.* 2020;4:52–63 (in Russ.). https://doi.org/10.24411/2411-7374-2020-10034
12. Kominko H., Gorazda K., Wzorek Z. Effect of sewage sludge-based fertilizers on biomass growth and heavy metal accumulation in plants. *J. Environ. Manage.* 2022;305:114417. https://doi.org/10.1016/j.jenvman.2021.114417
13. Chang H., Yuan J., Zhao Y., Bisinella V., Damgaard A., Christensen T.H. Carbon footprints of incineration, pyrolysis, and gasification for sewage sludge treatment. *Resour., Conserv. Recycl.* 2025;212:107939. https://doi.org/10.1016/j.resconrec.2024.107939
14. Kelessidis A., Stasinakis A.S. Comparative study of the methods used for treatment and final disposal of sewage sludge in European countries. *Waste Manage.* 2012;32(6):1186–1195. https://doi.org/10.1016/j.wasman.2012.01.012
15. Syed-Hassan S.S.A., Wang Y., Hu S., Su S., Xiang J. Thermochemical processing of sewage sludge to energy and fuel: Fundamentals, challenges and considerations. *Renewable Sustainable Energy Rev.* 2017;80:888–913. https://doi.org/10.1016/j.rser.2017.05.262
16. Faleeva Y.M., Zaichenko V.M. Two-stage pyrolytic conversion of coffee husk and parchment into synthesis gas. *J. Phys.: Conf. Ser.* 2020;1683(5):052017. https://doi.org/10.1088/1742-6596/1683/5/052017
17. Zagashvili Yu.V., Kuz'min A.M., Imshenetskii V.V., Lishchiner I.I., Malova O.V. Experimental studies of methanol synthesis from nitrogen-ballasted synthesis gas. *Izvestiya Tomskogo politekhnicheskogo universiteta. Inzhiniring georesursov = Bulletin of the Tomsk Polytechnic University. Geo Assets Engineering.* 2021;332(7):140–147 (in Russ.). https://doi.org/10.18799/24131830/2021/7/3272

5. Yana S., Nizar Irhamni M., Mulyati D. Biomass waste as a renewable energy in developing bio-based economies in Indonesia: A review. *Renewable Sustainable Energy Rev*. 2022;160:112268. https://doi.org/10.1016/j.rser.2022.112268

6. Базаров Б.И., Одилов О.З., Отабаев Н.И. Получение синтетических углеводородов из природного газа по технологии GTL. *Механика и технологии*. 2022;6:122–132.
7. Миргаязов И.И., Абдуллин А.И. Современные методы получения синтез-газа и процесс Фишера-Тропша. *Вестник Казанского технологического университета*. 2014;17(9):258–261. https://elibrary.ru/sfmlan
8. Батенин В.М., Зайченко В.М., Косов В.Ф., Синельщиков В.А. Пиролитическая конверсия биомассы в газообразное топливо. *Доклады Академии наук.* 2012;446(2): 179–182. https://elibrary.ru/pbwfrt

9. Kosov V., Kosov V., Sinelschikov V., Zaichenko V. *High-Calorific Gas Mixtures Produced from Biomass.* In: Oral A., Bahsi Z., Oze M. (Eds.). *International Congress on Energy Efficiency and Energy Related Materials* (*ENEFM2013*). *Springer Proceedings in Physics*. Cham: Springer; 2014. V. 155. P 77–383. https://doi.org/10.1007/978-3-319-05521-3_48
10. Kachalov V.V., Lavrenov V.A., Lishchiner I.I., Malova O.V., Tarasov A.L., Zaichenko V.M. Scientific bases of biomass processing into basic component of aviation fuel. *J. Phys.: Conf. Ser.* 2016;774:012136. https://doi.org/10.1088/1742-6596/774/1/012136

11. Валиев В.С., Иванов Д.В., Шагидуллин Р.Р. Способы утилизации осадков городских сточных вод (обзор). *Российский журнал прикладной экологии*. 2020;4:52–63. https://doi.org/10.24411/2411-7374-2020-10034

12. Kominko H., Gorazda K., Wzorek Z. Effect of sewage sludge-based fertilizers on biomass growth and heavy metal accumulation in plants. *J. Environ. Manage.* 2022;305:114417. https://doi.org/10.1016/j.jenvman.2021.114417
13. Chang H., Yuan J., Zhao Y., Bisinella V., Damgaard A., Christensen T.H. Carbon footprints of incineration, pyrolysis, and gasification for sewage sludge treatment. *Resour., Conserv. Recycl.* 2025;212:107939. https://doi.org/10.1016/j.resconrec.2024.107939
14. Kelessidis A., Stasinakis A.S. Comparative study of the methods used for treatment and final disposal of sewage sludge in European countries. *Waste Manage.* 2012;32(6):1186–1195. https://doi.org/10.1016/j.wasman.2012.01.012
15. Syed-Hassan S.S.A., Wang Y., Hu S., Su S., Xiang J. Thermochemical processing of sewage sludge to energy and fuel: Fundamentals, challenges and considerations. *Renewable Sustainable Energy Rev.* 2017;80:888–913. https://doi.org/10.1016/j.rser.2017.05.262
16. Faleeva Y.M., Zaichenko V.M. Two-stage pyrolytic conversion of coffee husk and parchment into synthesis gas. *J. Phys.: Conf. Ser.* 2020;1683(5):052017. https://doi.org/10.1088/1742-6596/1683/5/052017

17. Загашвили Ю.В., Кузьмин А.М., Имшенецкий В.В., Лищинер И.И., Малова О.В. Экспериментальные исследования синтеза метанола из забалластированного азотом синтез-газа. *Известия Томского политехнического университета. Инжиниринг георесурсов.* 2021;332(7):140–147. https://doi.org/10.18799/24131830/2021/7/3272
18. Xu C., Hu S., Xiang J., Zhang L., Sun L., Shuai C., Chen Q., He L., Edreis E.M.A. Interaction and kinetic analysis for coal and biomass co-gasification by TG–FTIR. *Bioresour. Technol.* 2014;154:313–321. https://doi.org/10.1016/j.biortech.2013.11.101
19. He Q., Wan K., Hoadley A., Yeasmin H., Miao Z. TG–GC–MS study of volatile products from Shengli lignite pyrolysis. *Fuel*. 2015;156:121–128. https://doi.org/10.1016/j.fuel.2015.04.043

18. Xu C., Hu S., Xiang J., Zhang L., Sun L., Shuai C., Chen Q., He L., Edreis E.M.A. Interaction and kinetic analysis for coal and biomass co-gasification by TG–FTIR. *Bioresour. Technol.* 2014;154:313–321. https://doi.org/10.1016/j.biortech.2013.11.101
19. He Q., Wan K., Hoadley A., Yeasmin H., Miao Z. TG–GC–MS study of volatile products from Shengli lignite pyrolysis. *Fuel*. 2015;156:121–128. https://doi.org/10.1016/j.fuel.2015.04.043
20. Caballero J.A., Front R., Marcilla A., Conesa J.A. Characterization of sewage sludges by primary and secondary pyrolysis. *J. Anal. Appl. Pyrolysis.* 1997;40-41:433–450. https://doi.org/10.1016/S0165-2370(97)00045-4
21. Nowicki L., Ledakowicz St. Comprehensive characterization of thermal decomposition of sewagesludge by TG–MS. *J. Anal. Appl. Pyrolysis.* 2014;110:220–228. https://doi.org/10.1016/j.jaap.2014.09.004
22. Alvarez J., Lopez G., Amutio M., Artetxe M., Barbarias I., Arregi A., Bilbao J., Olazar M. Characterization of the bio-oil obtained by fast pyrolysis of sewage sludge in a conical spouted bed reactor. *Fuel Process. Technol.* 2016;149: 169–175. https://doi.org/10.1016/j.fuproc.2016.04.015
23. Chen W.-Hs., Wang Ch.-W., Ong Hw.Ch., Show P.L., Hsieh Tz.-Hs. Torrefaction, pyrolysis and two-stage thermodegradation of hemicellulose, cellulose and lignin. *Fuel*. 2019;258:116168. https://doi.org/10.1016/j.fuel.2019.116168
24. Oh D.Yo., Kim D., Choi H., Park K.Yo. Syngas generation from different types of sewage sludge using microwave-assisted pyrolysis with silicon carbide as the absorbent. *Heliyon.* 2023;9(3):e14165. https://doi.org/10.1016/j.heliyon.2023.e14165
25. Quan C., Gao N., Song Q. Pyrolysis of biomass components in a TGA and a fixed-bed reactor: Thermochemical behaviors, kinetics, and product characterization. *J. Anal. Appl. Pyrol*. 2016;121:84–92. https://doi.org/10.1016/j.jaap.2016.07.005
26. Liang W., Feng Yu., Wang K., Wang C., Yang H. Investigation on pyrolysis characteristics and kinetics of sewage sludge with different heat-mass transfer rates. *Fuel*. 2024;372:132192. https://doi.org/10.1016/j.fuel.2024.132192
27. Florin N.H., Maddocks A.R., Wood S., Harris A.T. High-temperature thermal destruction of poultry derived wastes for energy recovery in Australia. *Waste Manage*. 2009;29(4): 1399–1408. https://doi.org/10.1016/j.wasman.2008.10.002
28. Gerasimov G.Y., Khaskhachikh V.V., Sychev G.A., *et al.* Migration Activity of Heavy Metals During Pyrolysis of Dried Sewage Sludge in a Fixed-Bed Reactor. *J. Eng. Phys. Thermophy.* 2023;96:112–119. https://doi.org/10.1007/s10891-023-02667-3 [Original Russian Text: Gerasimov G.Ya., Khaskhachikh V.V., Sychev G.A., Zaichenko V.M. Migration Activity of Heavy Metals During Pyrolysis of Dried Sewage Sludge in a Fixed-Bed Reactor. *Inzhenerno-fizicheskii zhurnal.* 2023;96(1): 114–122 (in Russ.). https://elibrary.ru/uzglct]
29. Larina O.M., Pudova Ya.D. Chicken Litter Pyrolysis and Composition of Gaseous Products Formed. *Solid Fuel Chem.* 2024;58(6):441–451. https://doi.org/10.3103/S0361521924700344
30. Kosov V.F., Lavrenov V.A., Larina O.M., Zaichenko V.M. Use of Two-stage Pyrolysis for Bio-waste Recycling. *Chem. Eng. Transact.* 2016;50:151–156. https://doi.org/10.3303/CET1650026
31. Batenin V.M., Bessmertnykh A.V., Zaichenko V.M., *et al.* Thermal methods of reprocessing wood and peat for power engineering purposes. *Therm. Eng.* 2010;57(11):946–952. https://doi.org/10.1134/S0040601510110066 [Original Russian Text: Batenin V.M., Bessmertnykh A.V., Zaichenko V.M., Kosov V.F., Sinel'shchikov V.A. Thermal methods of reprocessing wood and peat for power engineering purposes. *Teploehnergetika.* 2010;11:36–42 (in Russ.). https://elibrary.ru/nbkpbt]
20. Caballero J.A., Front R., Marcilla A., Conesa J.A. Characterization of sewage sludges by primary and secondary pyrolysis. *J. Anal. Appl. Pyrolysis.* 1997;40-41:433–450. https://doi.org/10.1016/S0165-2370(97)00045-4
21. Nowicki L., Ledakowicz St. Comprehensive characterization of thermal decomposition of sewagesludge by TG–MS. *J. Anal. Appl. Pyrolysis.* 2014;110:220–228. https://doi.org/10.1016/j.jaap.2014.09.004
22. Alvarez J., Lopez G., Amutio M., Artetxe M., Barbarias I., Arregi A., Bilbao J., Olazar M. Characterization of the bio-oil obtained by fast pyrolysis of sewage sludge in a conical spouted bed reactor. *Fuel Process. Technol.* 2016;149: 169–175. https://doi.org/10.1016/j.fuproc.2016.04.015
23. Chen W.-Hs., Wang Ch.-W., Ong Hw.Ch., Show P.L., Hsieh Tz.-Hs. Torrefaction, pyrolysis and two-stage thermodegradation of hemicellulose, cellulose and lignin. *Fuel*. 2019;258:116168. https://doi.org/10.1016/j.fuel.2019.116168
24. Oh D.Yo., Kim D., Choi H., Park K.Yo. Syngas generation from different types of sewage sludge using microwave-assisted pyrolysis with silicon carbide as the absorbent. *Heliyon.* 2023;9(3):e14165. https://doi.org/10.1016/j.heliyon.2023.e14165
25. Quan C., Gao N., Song Q. Pyrolysis of biomass components in a TGA and a fixed-bed reactor: Thermochemical behaviors, kinetics, and product characterization. *J. Anal. Appl. Pyrol*. 2016;121:84–92. https://doi.org/10.1016/j.jaap.2016.07.005
26. Liang W., Feng Yu., Wang K., Wang C., Yang H. Investigation on pyrolysis characteristics and kinetics of sewage sludge with different heat-mass transfer rates. *Fuel*. 2024;372:132192. https://doi.org/10.1016/j.fuel.2024.132192
27. Florin N.H., Maddocks A.R., Wood S., Harris A.T. High-temperature thermal destruction of poultry derived wastes for energy recovery in Australia. *Waste Manage*. 2009;29(4): 1399–1408. https://doi.org/10.1016/j.wasman.2008.10.002
28. Герасимов Г.Я., Хасхачих В.В., Сычев Г.А., Зайченко В.М. Исследование миграционной активности тяжелых металлов при пиролизе высушенного осадка сточных вод в реакторе с неподвижным слоем. *Инженерно-физический журн*. 2023;96(1):114–122. https://elibrary.ru/uzglct
29. Larina O.M., Pudova Ya.D. Chicken Litter Pyrolysis and Composition of Gaseous Products Formed. *Solid Fuel Chem.* 2024;58(6):441–451. https://doi.org/10.3103/S0361521924700344
30. Kosov V.F., Lavrenov V.A., Larina O.M., Zaichenko V.M. Use of Two-stage Pyrolysis for Bio-waste Recycling. *Chem. Eng. Transact*. 2016;50:151–156. https://doi.org/10.3303/CET1650026
31. Батенин В.М., Бессмертных А.В., Зайченко В.М., Косов В.Ф., Синельщиков В.А. Термические методы переработки древесины и торфа в энергетических целях. *Теплоэнергетика*. 2010;11:36–42. https://elibrary.ru/nbkpbt
32. Зайченко В.М., Лавренов В.А., Синельщиков В.А., Фалеева Ю.М. Сравнительный анализ переработки различных видов биомассы в синтез-газ методом двухстадийной пиролитической конверсии. *Химия твердого топлива*. 2022;6:42–50. https://doi.org/10.31857/S0023117722060111
33. Larina O.M., Zaichenko V.M. Thermal cracking in charcoal and ceramics of pyrolysis liquid from sewage sludge. *J. Phys.: Conf. Ser.* 2018;94:012034. https://doi.org/10.1088/1742-6596/946/1/012034
34. Liu G., Hagelin-Weaver H., Welt B. A Concise Review of Catalytic Synthesis of Methanol from Synthesis Gas. *Waste*. 2023;1(1):228–248. https://doi.org/10.3390/waste1010015
35. Лищинер И.И., Малова О.В., Тарасов А.Л., Масленников В.М., Выскубенко Ю.А., Толчинский Л.С., Долинский Ю.Л. Получение метанола из забалластированного азотом синтез-газа. *Катализ в промышленности*. 2010;4:50–55.

32. Zaichenko V.M., Lavrenov V.A., Sinelshchikov V.A., *et al*. Comparative Analysis of the Processing of Various Types of Biomass into Synthesis Gas by Two-Stage Pyrolytic Conversion. *Solid Fuel Chem.* 2022;56(6):448–455. https://doi.org/10.3103/s0361521922060118
[Original Russian Text: Zaichenko V.M., Lavrenov V.A., Sinelshchikov V.A., Faleeva Yu.M. Comparative Analysis of the Processing of Various Types of Biomass into Synthesis Gas by Two-Stage Pyrolytic Conversion. *Khimiya tverdogo topliva.* 2022;6:42–50 (in Russ.). https://doi.org/10.31857/S0023117722060111]
33. Larina O.M., Zaichenko V.M. Thermal cracking in charcoal and ceramics of pyrolysis liquid from sewage sludge. *J. Phys.: Conf. Ser.* 2018;94:012034. https://doi.org/10.1088/1742-6596/946/1/012034
34. Liu G., Hagelin-Weaver H., Welt B. A Concise Review of Catalytic Synthesis of Methanol from Synthesis Gas. *Waste*. 2023;1(1):228–248. https://doi.org/10.3390/waste1010015
35. Lishchiner I.I., Malova O.V., Tarasov A.L., Maslennikov V.M., Vyskubenko Yu.A., Tolchinskii L.S., Dolinskii Yu.L. Methanol producing from synthesis gas ballasted by nitrogen. *Kataliz v promyshlennosti.* 2010;4:50–55 (in Russ.).
36. Kanan S.M., Mohamed Ahm.A., Shabnam A., Habiba Sh. Methanol Production from Bio-syngas. *Comprehensive Methanol Science*. 2025;2:711–724. https://doi.org/10.1016/B978-0-443-15740-0.00008-2
37. Timsina R., Thapa R., Moldestad Br., Eikeland M.S. Methanol Synthesis from Syngas: a Process Simulation. In: *Proceedings of The First SIMS EUROSIM Conference on Modelling and Simulation, SIMS EUROSIM 2021, and 62nd International Conference of Scandinavian Simulation Society*. 2022; 444–449. https://doi.org/10.3384/ecp21185444
38. Nielsen N.D., Jensen A.D., Christensen J.M. The roles of CO and CO_2 in high pressure methanol synthesis over Cu-based catalysts. *J. Catal.* 2021;393:324–334. https://doi.org/10.1016/j.jcat.2020.11.035
39. Meshcheryakov G.V., Komissarov Yu.A., Mishanova V.A. Synthesis of methanol with two tubular reactors and selection of products of synthesis after each reactor. *Bashkirskii khimicheskii zhurnal = Bashkir Chemical Journal.* 2012;19(1):113–115 (in Russ.). https://www.elibrary.ru/oyeyrb

36. Kanan S.M., Mohamed Ahm.A., Shabnam A., Habiba Sh. Methanol Production from Bio-syngas. *Comprehensive Methanol Science*. 2025;2:711–724. https://doi.org/10.1016/B978-0-443-15740-0.00008-2
37. Timsina R., Thapa R., Moldestad Br., Eikeland M.S. Methanol Synthesis from Syngas: a Process Simulation. In: *Proceedings of The First SIMS EUROSIM Conference on Modelling and Simulation, SIMS EUROSIM 2021, and 62nd International Conference of Scandinavian Simulation Society*. 2022;444–449. https://doi.org/10.3384/ecp21185444

38. Nielsen N.D., Jensen A.D., Christensen J.M. The roles of CO and CO_2 in high pressure methanol synthesis over Cu-based catalysts. *J. Catal.* 2021;393:324–334. https://doi.org/10.1016/j.jcat.2020.11.035
39. Мещеряков Г.В., Комиссаров Ю.А., Мишанова В.А. Синтез метанола с двумя трубчатыми реакторами и отбором продуктов синтеза после каждого реактора. *Башкирский химический журнал.* 2012;19(1):113–115. https://www.elibrary.ru/oyeyrb

About the Authors

Olga M. Larina, Cand. Sci. (Eng.), Senior Researcher, Joint Institute for High Temperatures of the Russian Academy of Sciences (JIHT RAS) (13-2, Izhorskaya ul., Moscow, 125412, Russia). E-mail: olga.m.larina@ihed.ras.ru. Scopus Author ID 57190050879, ResearcherID D-3336-2014, https://orcid.org/0000-0003-2023-6806

Iosif Iz. Lishchiner, Cand. Sci. (Chem.), Senior Researcher, Joint Institute for High Temperatures of the Russian Academy of Sciences (JIHT RAS) (13-2, Izhorskaya ul., Moscow, 125412, Russia). E-mail: lii48@bk.ru. Scopus Author ID 6507439331, ResearcherID J-7291-2018, RSCI SPIN-code 6397-8903, https://orcid.org/0000-0002-8437-1532

Olga V. Malova, Cand. Sci. (Chem.), Senior Researcher, Joint Institute for High Temperatures of the Russian Academy of Sciences (JIHT RAS) (13-2, Izhorskaya ul., Moscow, 125412, Russia). E-mail: mov58rus@yandex.ru. Scopus Author ID 57190617511, ResearcherID J-7261-2018, RSCI SPIN-code 5345-4581, https://orcid.org/0000-0001-6081-926X

Yulia M. Faleeva, Researcher, Joint Institute for High Temperatures of the Russian Academy of Sciences (JIHT RAS) (13-2, Izhorskaya ul., Moscow, 125412, Russia). E-mail: faleeva.julia@mail.ru. ResearcherID AAY-2189-2021, SPIN-код РИНЦ 1862-6715, https://orcid.org/0000-0002-7424-5137

Об авторах

Ларина Ольга Михайловна, к.т.н., старший научный сотрудник, ФГБУН «Объединенный институт высоких температур Российской академии наук» (ОИВТ РАН) (125412, Россия, Москва, ул. Ижорская, д. 13, стр. 2). E-mail: olga.m.larina@ihed.ras.ru. Scopus Author ID 57190050879, ResearcherID D-3336-2014, https://orcid.org/0000-0003-2023-6806

Лищинер Иосиф Израилевич, к.х.н., старший научный сотрудник, ФГБУН «Объединенный институт высоких температур Российской академии наук» (ОИВТ РАН) (125412, Россия, Москва, ул. Ижорская, д. 13, стр. 2). E-mail: lii48@bk.ru. Scopus Author ID 6507439331, ResearcherID J-7291-2018, SPIN-код РИНЦ 6397-8903, https://orcid.org/0000-0002-8437-1532

Малова Ольга Васильевна, к.х.н., старший научный сотрудник, ФГБУН «Объединенный институт высоких температур Российской академии наук» (ОИВТ РАН) (125412, Россия, Москва, ул. Ижорская, д. 13, стр. 2). E-mail: mov58rus@yandex.ru. Scopus Author ID 57190617511, ResearcherID J-7261-2018, SPIN-код РИНЦ 5345-4581, https://orcid.org/0000-0001-6081-926X

Фалеева Юлия Михайловна, научный сотрудник, ФГБУН «Объединенный институт высоких температур Российской академии наук» (ОИВТ РАН) (125412, Россия, Москва, ул. Ижорская, д. 13, стр. 2). E-mail: faleeva.julia@mail.ru. ResearcherID AAY-2189-2021, SPIN-код РИНЦ 1862-6715, https://orcid.org/0000-0002-7424-5137

Translated from Russian into English by V. Glyanchenko
Edited for English language and spelling by Thomas A. Beavitt

Tonkie Khimicheskie Tekhnologii = Fine Chemical Technologies.
2025;20(6):555–564
ISSN 2686-7575 (Online)

Chemistry and technology of medicinal compounds
and biologically active substances

Химия и технология лекарственных препаратов
и биологически активных соединений

UDC 543.421/.424;616-073.213;616-073.584
https://doi.org/10.32362/2410-6593-2025-20-6-555-564
EDN OYNKPY

RESEARCH ARTICLE

On the stability of characteristics of cellulose diacetate solutions with an iodine-containing radiopaque substance and solid emboli on their basis

Daria V. Nebesnaia[1], Ekaterina S. Terendiak[1], Olga A. Legon'kova[2], Stanislav A. Kedik[1], Aleksey V. Panov[1], Elena S. Zhavoronok[1,✉]

[1] *MIREA – Russian Technological University (M.V. Lomonosov Institute of Fine Chemical Technologies), Moscow, 119454 Russia*

[2] *A.V. Vishnevsky National Medical Research Center of Surgery, Ministry of Health of the Russian Federation, Moscow, 117997 Russia*

✉ *Corresponding author, e-mail: zhavoronok@mirea.ru*

Abstract

Objectives. Among the materials used for embolization, liquid embolizing agents based on solutions of biocompatible polymers attract particular interest. Such compositions are capable of targeting and reliably occluding a branched vascular network by forming solid emboli directly in the patient's body. The safety and effectiveness of such materials are determined by the stability of the initial composition and the resulting emboli. This article presents a long-term study of the stability of embolizing solutions of a polymer (cellulose diacetate) and a radiopaque additive iohexol in dimethyl sulfoxide, as well as emboli based thereon, in aqueous media.

Methods. The stability of the initial solutions exposed to 60°C for 45 days ("accelerated aging" corresponding to three years of storage at 23 ± 2°C) was studied by rotational viscometry using a *Brookfield* DV2T RV rotary viscometer equipped with a working unit in the form of two coaxial cylinders and by ultraviolet-visible spectrophotometry using a Cary 60 UV-Vis spectrophotometer. The long-term stability of emboli in aqueous media was studied by gel permeation chromatography using a *Gilson* chromatograph (Japan) with refractometric detection and by gas chromatography using an *Agilent* 6890N chromatograph with a DB-5MS column (30 × 0.25 × 0.5 μm), equipped with an *Agilent* 5973 N mass spectrometric detector.

Results. During "accelerated" storage of cellulose diacetate and iohexol solutions in the dark, no changes in the viscosity coefficient (0.268 ± 0.0049 Pa·s at 25°C) and the quantitative content of bound iodine (50.1 ± 1.0 mg/mL) were observed. However, when iohexol solutions in dimethyl sulfoxide were stored under daylight, free iodine was separated in minor quantities. When emboli consisting of cellulose diacetate were stored in an aqueous medium for eight years, the molecular weight of the polymer (60 kDa) remained unchanged. The degradation products of cellulose diacetate, expected in the aqueous extract, were also absent.

Conclusions. The model embolic composition consisting of cellulose diacetate and iohexol in dimethyl sulfoxide is stable when stored in the absence of light. The as-formed solid emboli remain stable for at least eight years when stored in an aqueous environment.

Keywords

embolization, embolic agent, stability, cellulose acetate, iohexol, dimethyl sulfoxide

Submitted: 14.03.2025
Revised: 05.05.2025
Accepted: 11.11.2025

For citation

Nebesnaia D.V., Terendiak E.S., Legon'kova O.A., Kedik S.A., Panov A.V., Zhavoronok E.S. On the stability of characteristics of cellulose diacetate solutions with an iodine-containing radiopaque substance and solid emboli on their basis. *Tonk. Khim. Tekhnol. = Fine Chem. Technol*. 2025;20(6):555–564. https://doi.org/10.32362/2410-6593-2025-20-6-555-564

НАУЧНАЯ СТАТЬЯ

О стабильности характеристик растворов диацетата целлюлозы с йодсодержащим рентгеноконтрастным веществом и твердых эмболов на их основе

Д.В. Небесная[1], Е.С. Терендяк[1], О.А. Легонькова[2], С.А. Кедик[1], А.В. Панов[1], Е.С. Жаворонок[1,✉]

[1] *МИРЭА — Российский технологический университет (Институт тонких химических технологий им. М.В. Ломоносова) Москва, 119454 Россия*

[2] *Национальный медицинский исследовательский центр хирургии им. А.В. Вишневского Минздрава России, Москва, 117997 Россия*

✉ *Автор для переписки, e-mail: zhavoronok@mirea.ru*

Аннотация

Цели. Среди используемых материалов для эмболизации большой интерес представляют жидкие эмболизирующие агенты на основе растворов биологически совместимых полимеров. Такие композиции способны осуществлять надежную преднамеренную окклюзию разветвленной сосудистой сети благодаря формированию твердого эмбола непосредственно в организме пациента. Для обеспечения безопасности и эффективности такого материала важны стабильность исходного состава и итогового эмбола. Целью работы являлось долговременное изучение стабильности эмболизирующих растворов полимера (диацетата целлюлозы) и рентгеноконтрастной добавки йогексола в диметилсульфоксиде, а также эмболов на их основе, выдержанных в водной среде.

Методы. Исследование стабильности исходных растворов, выдерживаемых в течение 45 суток при температуре 60°C («ускоренное старение», соответствующее трем годам хранения при 23 ± 2°C), проводили методом ротационной вискозиметрии на ротационном вискозиметре *Brookfield* DV2T RV с рабочим узлом в виде двух коаксиальных цилиндров и методом спектрофотометрии в ультрафиолетовой и видимой областях спектра при помощи спектрофотометра Cary 60 UV-Vis. Долговременную стабильность эмболов в водных средах исследовали методом гель-проникающей хроматографии на хроматографе *Gilson* (Япония) с рефрактометрическим детектированием и методом газовой хроматографии на хроматографе *Agilent* 6890 N с колонкой DB-5MS (30 × 0.25 × 0.5 мкм), снабженным масс-спектрометрическим детектором *Agilent* 5973 N.

Результаты. Показано, что при «ускоренном» хранении растворов диацетата целлюлозы и йогексола в темноте не наблюдались изменения коэффициента вязкости (0.268 ± 0.0049 Па·с при 25°C) и количественного содержания связанного йода (50.1 ± 1.0 мг/мл). Однако при хранении растворов йогексола в диметилсульфоксиде при естественном освещении отщеплялся свободный йод в малых количествах. При хранении эмболов, состоящих из диацетата целлюлозы, в водной среде в течение восьми лет, молекулярная масса полимера (60 кДа) не изменилась. В вытяжке водной среды также отсутствовали предполагаемые продукты деструкции диацетата целлюлозы.

Выводы. Модельный эмболизирующий состав, состоящий из диацетата целлюлозы и йогексола в диметилсульфоксиде, является стабильным при хранении в отсутствии света. Сформированные твердые эмболы при хранении в водной среде остаются стабильными по крайней мере в течение восьми лет.

Ключевые слова

эмболизация, эмболизирующий агент, стабильность, ацетат целлюлозы, йогексол, диметилсульфоксид

Поступила: 14.03.2025
Доработана: 05.05.2025
Принята в печать: 11.11.2025

Для цитирования

Небесная Д.В., Терендяк Е.С., Легонькова О.А., Кедик С.А., Панов А.В., Жаворонок Е.С. О стабильности характеристик растворов диацетата целлюлозы с йодсодержащим рентгеноконтрастным веществом и твердых эмболов на их основе. *Тонкие химические технологии*. 2025;20(6):555–564. https://doi.org/10.32362/2410-6593-2025-20-6-555-564

INTRODUCTION

Embolization of blood vessels is defined as their targeted blockage by specially injected substrates, referred to as emboli [1, 2]. The objective of this procedure is to obliterate a specified area of arteriovenous discharge without compromising the circulation of normal tissues. Embolic vascular closure can be performed at any level, ranging from large arteries or veins to capillaries [3].

Embolization represents a contemporary trend in the management of a wide range of clinical conditions, including angiodysplasia (congenital vascular abnormalities), aneurysms, varicose veins, etc. Moreover, embolization plays a pivotal role in the treatment of oncological diseases, being an efficacious method of preoperative preparation of patients for subsequent surgical intervention with minimal blood loss [4–7]. Such a procedure is minimally invasive, which is a great advantage. The safety and effectiveness of embolization depend primarily on the surgeon's experience, optimal technical equipment, and, to a lesser extent, on the characteristics of embolizing drugs [8].

Today, there exist various types of embolizing agents [9, 10], including initially solid substrates (gel foam, microparticles, etc.) and structures (spirals, cylinders, occluders), or liquid agents. Among the latter are sclerosing (ethanol, sotradecol, etc.) and polymerizing (cyanoacrylates and other acrylic monomers) substances as well as non-adhesive polymer solutions that are converted into solid emboli already in the patient's body. These agents offer significant advantages due to their capacity to penetrate complex vascular branches, successfully blocking blood vessels in the very center of the vascular lesion without damaging these vessels. As stated in [11], the primary components of such formulations are biologically compatible elements, namely polymer, water-soluble solvent, and radiopaque substances.

The works [12–14] demonstrated the potential of utilizing cellulose acetate—a natural and biologically compatible polymer—as a polymer base for liquid embolizing agents. Its clinical use in the composition of liquid embolizing agents was described, e.g., in [15–17]. Dimethyl sulfoxide, a well-known nonpolar aprotic solvent with anti-inflammatory, antioxidant, and analgesic properties, is widely employed as a solvent for such systems [18, 19]. The radiopaque component is typically composed of a metal powder, most commonly micronized tantalum particles [20, 21], or organic iodine-containing substances, either aliphatic or aromatic in nature [21, 22].

Metal powders ensure effective visualization of the embolus; however, they are an insoluble dispersed phase in a relatively low-viscosity polymer solution. This phase is known to settle readily and is distributed unevenly in the embolizing agent when injected into a blood vessel, resulting in artefacts during subsequent visualization of the embolus in the patient's body [20, 21]. Conversely, iodized aliphatic derivatives demonstrate limited solubility in water and are characterized by a gradual absorption rate into the tissues of living organisms. However, when administered in conjunction with dimethyl sulfoxide, these derivatives exhibit the capacity to liberate free iodine, a process that has been shown to exert deleterious effects on living tissues [23–25]. For comparison, commercially available aromatic iodine derivatives are water-soluble substances, capable of penetrating the extracellular space relatively easily without causing significant complications [26]. In view of that, we employed an iodinated aromatic derivative as a contrasting agent for polymer solutions in dimethyl sulfoxide, a method which provides temporary radiopaque emboli.

When evaluating the efficacy of embolizing pharmaceuticals, the stability of the initial liquid formulation during storage and the behavior of the emboli formed therefrom under conditions analogous to those encountered within a living organism are critical aspects. These parameters determine the shelf life of the liquid embolizing agent and the duration of contact of the hardened embolus with the patient's body. In light of this, our objective was to study the long-term stability of solutions of cellulose diacetate and iohexol in dimethyl sulfoxide, as well as emboli formed on their basis, aged in an aqueous medium.

MATERIALS AND METHODS

The research objects were solutions of Xeniton cellulose diacetate (*Institute of Pharmaceutical Technologies*, Russia) in dimethyl sulfoxide (chemically pure) (*Tula Pharmaceutical Factory*, Russia) with the addition of radiopaque substance 5-[acetyl(2,3-dihydroxypropyl) amino]-*N*,*N*′-bis(2,3-dihydroxypropyl)-2,4,6-triiod-1,3-benzenedicarboxamide (iohexol) (*Zhejiang Haichang Pharmaceutical Co.*, China), CAS 66108-95-0. Modified polyethylene glycol-4000 (up to 4.5 wt %) cellulose diacetate of the Xeniton brand with an average molecular weight of M_n = 60 ± 2 kDa and an average content of acetyl groups of 2.2 ± 0.1 mol/unit was used as a polymer. The structural formulas of the repeating unit of the polymer and the iohexol molecule are shown in Fig. 1.

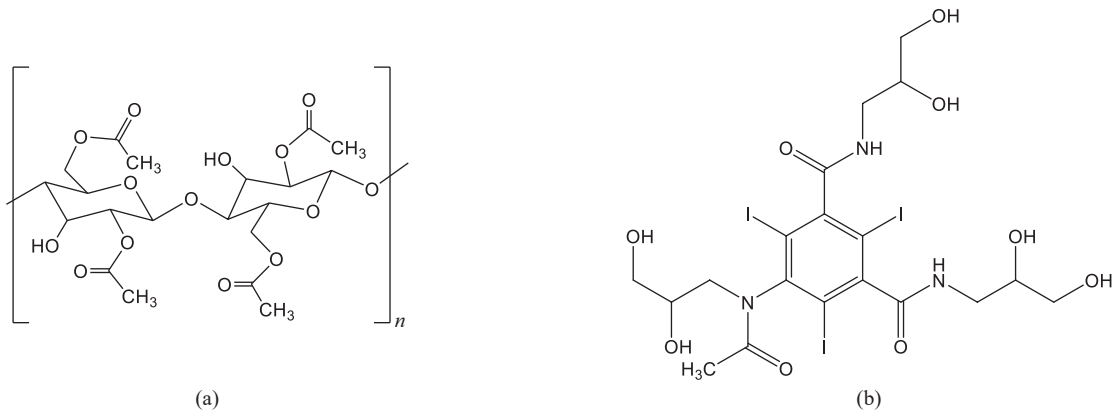

(a) (b)

Fig. 1. Structural formulas of the main components of the studied systems: (a) cellulose diacetate unit; (b) iohexol

The research solutions were prepared by long-term (2–3 days) dissolution of cellulose diacetate in dimethyl sulfoxide at 23 ± 2°C until a homogeneous transparent solution was formed. After that, iohexol was added to the solution upon thorough mixing. The component ratio was polymer/iohexol/dimethyl sulfoxide = 6 : 10 : 84 wt %. The resulting solutions were purged with an inert gas (argon) or left in contact with air, hermetically sealed and kept in a thermostat at 60.0 ± 0.1°C. The solutions were examined (each time a new sample was taken) every 7.5 days for 45 days by rheoviscometry using a Brookfield DV2T RV rotary viscometer (*Brookfield Corporation*, Canada) and ultraviolet–visible (UV–Vis) spectrophotometry using a Cary 60 UV–Vis spectrophotometer (*Agilent Technologies*, USA). In addition, the state of iohexol in solutions kept in the natural diffused sunlight was studied by UV–Vis spectrophotometry.

The as-obtained solutions were used to fabricate emboli models by means of a 1-mL syringe without a needle. The solution was compressed into 20-mL distilled-water buckets, which were obtained via a water distilling apparatus. The exposure time in water was approximately three days, with the water being changed twice. Following a period of three days, the resulting embolus was extracted and, without undergoing desiccation in the atmosphere, was subjected to a process of lyophilization. The resulting dry embolus was crushed, dissolved in tetrahydrofuran (*Merck,* Germany), and examined by gel permeation chromatography. The aqueous medium from the embolus was lyophilized; the resulting dry residue was dissolved in *n*-hexane (*LenReactive*, *Russia*) and studied by gas chromatography with mass spectrometry. Emboli for long-term storage in an aqueous environment (for eight years) were prepared using a similar method, although without the addition of iohexol.

The viscosity characteristics of polymer and iohexol solutions in dimethyl sulfoxide were determined using a Brookfield DV2T RV rotary viscometer equipped with a coaxial cylinder working unit (*Brookfield Corporation*, Canada). The measurements were carried out at a constant temperature of 25.0 ± 0.1°C, maintained by a TC-505MX-230 liquid thermostat (*Brookfield Corporation*, Canada), in the modes of stepwise increase and decrease of the shear rate.

The concentration of bound iodine was determined by UV–Vis spectrophotometry in accordance with the established procedure [23]. Spectra were obtained in quartz cuvettes within the wavelength range of 190–600 nm. Pure dimethyl sulfoxide was utilized as a reference sample. For the purposes of analysis, the initial solutions were subjected to dilution with dimethyl sulfoxide, yielding concentrations of 0.25 mg/mL.

Freeze-dried emboli or aqueous media were obtained using a *Harvest Right* freeze dryer (USA). For the purpose of lyophilization, the samples were subjected to a freezing process followed by drying; the process was executed in accordance with the scheme described in Table 1.

Table 1. Sample lyophilization mode

Stage	1	2	3	4	5	6
Temperature, °C	−40	−20	−5	0	10	20
Vacuum pump on/off	–	+	+	+	+	+
Time, h	2	5	5	10	10	6

The molecular mass characteristics of the emboli polymer were studied by gel permeation chromatography using a *Gilson* chromatograph (Japan) with refractometric detection. The analysis was performed at a temperature of 25°C in tetrahydrofuran with a flow rate of 1.0 mL/min. To separate and identify polymer fractions, an Agilent PLgel 5 μm MIXED B column (separating capacity 500–3000 kDa) was used, which was calibrated according to polystyrene standards with molecular weights of 2940, 10110, 28770, 74800, 230900, and 1390000 g/mol and a polydispersity index of less than 1.12. A solution of embolus lyophilizate in tetrahydrofuran with a polymer concentration of 0.7–10 mg/mL was prepared for analysis.

Gas chromatography experiments were performed using an Agilent 6890N chromatograph (*Agilent Technologies*, USA) with a DB-5MS column (30 × 0.25 × 0.5 μm) equipped with an Agilent 5973 N (gas chromatography–mass spectrometry, GC–MS) mass spectrometric detector. Helium was used as the carrier gas, with a feed rate of 1 mL/min. Injection was carried out at 250°C. A solution of aqueous lyophilizate over an embolus in *n*-hexane with a lyophilizate concentration of 1 mg/mL was prepared for analysis.

RESULTS AND DISCUSSION

At the first stage of analysis, we investigated the stability of the initial solutions of the polymer with iohexol in dimethyl sulfoxide. The control was carried out according to two main indicators—the dynamic viscosity of the solutions and the content of bound iodine in these solutions. It was previously shown that all the studied solutions exhibit Newtonian flow under the conditions studied and can be characterized by a constant coefficient of Newtonian viscosity.

Characteristic dependencies of the Newtonian viscosity coefficient (0.268 ± 0.0049 Pa·s at 25°C) and the bound iodine content (50.1 ± 1.0 mg/mL) are shown in Fig. 2. It can be seen that exposure for at least 45 days at a temperature of 60°C does not lead to changes in these parameters. In other words, the studied solutions of polymer with iohexol in dimethyl sulfoxide are stable under the conditions of exposure to a thermostat (in the dark). The contacting gaseous medium (argon or air) had no effect on the results. According to GPM 1.1.0009.15[1], for climate zone II, this corresponds to three years of storage under natural conditions (25°C at a relative humidity of 60%).

Conversely, our preliminary observations indicated that iohexol solutions in dimethyl sulfoxide exhibit a yellowing tendency in the presence of light over time (a phenomenon not observed when stored in the dark). The investigation focused on the behavior of iohexol solutions in dimethyl sulfoxide, utilizing UV–Vis spectrophotometry (Fig. 3). The study revealed the separation of a minimal amount of iodine during a week-long storage period in natural ambient light. It is possible that iodine is converted into an inorganic form, which can be assessed using inversion voltammetry [27]. Consequently, the storage of embolizing formulations with iohexol should be conducted in a dark environment, avoiding exposure to light.

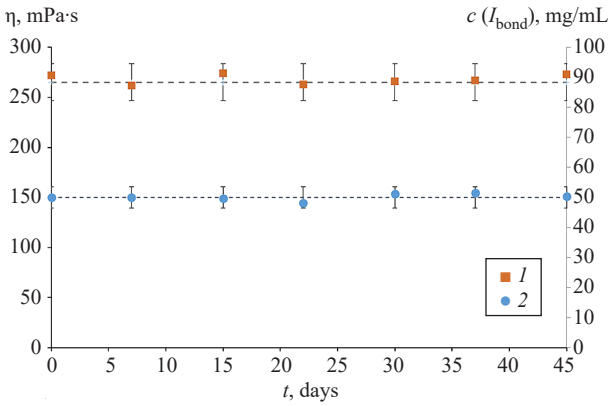

Fig. 2. Dependencies of the dynamic viscosity coefficient η (*1*) and the content of bound iodine *c* (*2*) on exposure duration

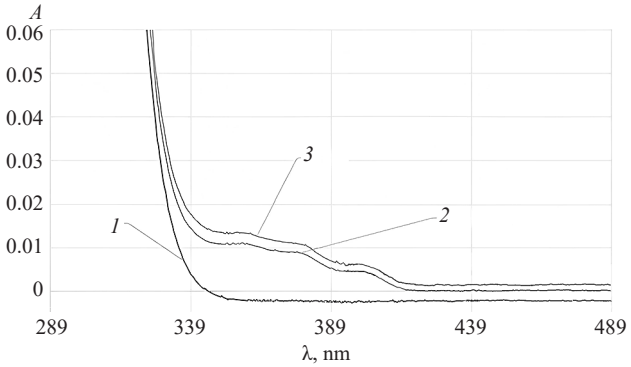

Fig. 3. Typical UV-visible spectra of iohexol solution in dimethyl sulfoxide under storage in the light for 0 (*1*), 6 (*2*), and 24 days (*3*)

At the second stage of the work, we obtained solid emboli from polymer solutions in water and investigated their stability during long-term exposure to an aquatic environment. The differential curves of the molecular weight distribution calculated on the basis of chromatograms are shown in Fig. 4.

[1] GPM 1.1.0009.15. Expiration dates of medicines. The State Pharmacopoeia of the Russian Federation, 13th edition (SP RF XIII). URL: https://pharmacopoeia.regmed.ru/pharmacopoeia/izdanie-13/1/1-1/1-1-9/sroki-godnosti-lekarstvennykh-sredstv/. Accessed September 24, 2025. (In Russ.).

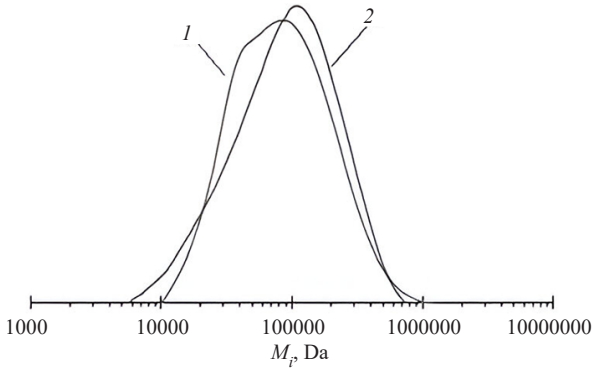

Fig. 4. Characteristic differential molecular weight distribution curves M_i for the original polymer (*1*) and the polymer aged in water for eight years (*2*)

All the distributions obtained are monomodal, which makes it possible to calculate the values of the number-average molecular weight M_n and weight-average molecular weight M_w, as well as the ratio M_w/M_n (Table 2). Figure 4 and Table 2 show that the molecular weight distributions are almost identical, with the average molecular weights and polydispersity coefficients M_w/M_n being close. This finding indicates a negligible degradation of cellulose diacetate in the aquatic environment over a period of eight years

Furthermore, we employed the GC–MS method to analyze the aqueous medium from samples of the same emboli. A typical GC–MS chromatogram is shown in Fig. 5; the analysis of the results using the NIST[2] GC–MS database revealed the presence of 2-pentanone (degree of coincidence 98.0%), dimethyl sulfone (degree of coincidence 92.8%), and glycerin (degree of coincidence 91.2%) in the sample. At the same time, the expected degradation products of the polysaccharide chain were absent. It can be argued with a certain degree of confidence that 2-pentanone and glycerin can be considered as products of thermal degradation of polyethylene glycol, a modifier of cellulose diacetate, and dimethyl sulfone as a product of the transformation of a solvent, dimethyl sulfoxide, from which emboli are formed.

A significant increase in storage time does not lead to fundamental changes in the observed pattern. Thus, it appears safe to conclude that cellulose diacetate exhibits long-term stability (for at least eight years) when exposed to an aqueous medium.

CONCLUSIONS

Our study has addressed the stability of cellulose diacetate and iohexol solutions in dimethyl sulfoxide, which are utilized as liquid embolizing agents. It is shown that these solutions, when stored in the dark, do not change their rheoviscometric characteristics and the content of bound iodine for at least 45 days at 60°C, which corresponds to three years of storage

Table 2. Molecular weight characteristics of the initial polymer and the polymer aged in water for eight years

Sample	M_n*, kDa	M_w*, kDa	M_w/M_n*
Initial polymer	59.5	116.4	1.96
Polymer stored in water for eight years	57.5	124.8	2.17

* Determined from the gel permeation chromatography data.

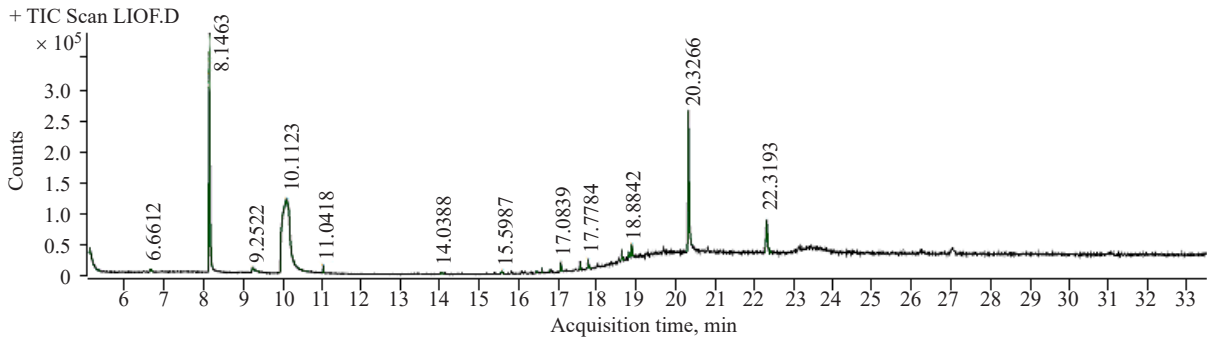

Fig. 5. Characteristic GC–MS chromatogram for a solution of lyophilized aqueous extract from a solid embolus

[2] NIST Chemistry WebBook. URL: https://webbook.nist.gov/chemistry. Accessed September 22, 2025.

under natural conditions. It is demonstrated that the contact of the solution with an inert gas (argon) or air during storage does not fundamentally affect these results. However, in order to avoid yellowing of the composition, it is recommended that the solution be stored in the dark.

The long-term study of the behavior of solid polymer emboli in contact with an aqueous medium has demonstrated that the molecular weight characteristics of the polymer and the composition of the filler fluid remain constant over an eight-year period. This observation suggests the utilization of such emboli as products of prolonged contact with the patient's body (category C).

Acknowledgments

The work was carried out using the equipment of the Center for Collective Use of the MIREA – Russian Technological University and supported by the Ministry of Science and Higher Education of the Russian Federation, Agreement No. 075-15-2021-689 dated 01.09.2021.

Authors' contributions

D.V. Nebesnaia—planning and conducting experimental research, processing the obtained data and discussing the results, preparing the texts of the article.

E.S. Terendiak—planning and conducting experimental research, processing the obtained data and discussing the results, preparing the text of the article.

O.A. Legon'kova—consulting on individual stages of the research, scientific editing of the work.

S.A. Kedik—research concept, scientific editing of the work.

A.V. Panov—consulting at various stages of the research, scientific editing of the work.

E.S. Zhavoronok—research concept and planning, discussion and analysis of the results, preparing the text of the article.

The authors declare no conflicts of interest.

REFERENCES

1. Dan V.N. *Angiodisplazii* (*vrozhdennye poroki razvitiya sosudov*) (*Angiodysplasia* (*Congenital Vascular Malformations*)). Moscow: Verdana; 2008, 200 p. (In Russ.). ISBN 978-5-901439-30-2
2. Chabrot P., Boyer L. *Embolization.* Springer; 2014, 453 p. https://doi.org/10.1007/978-1-4471-5182-1
3. Varghese K., Adhyapak S. *Therapeutic Embolization.* Springer; 2017, 133 p. https://doi.org/10.1007/978-3-319-42494-1
4. Goode J.A., Matson M.B. Embolisation of cancer: what is the evidence? *Cancer Imaging*. 2004;4(2):133–141. https://doi.org/10.1102/1470-7330.2004.0021
5. Alluhaybi A.A., Abdulqader S.B., Altuhayni K., AlTurkstani A., Kabbani A., Ahmad M. Preoperative trans-arterial embolization of a giant scalp congenial hemangioma associated with cardiac failure in a premature newborn. *J. Int. Med. Res*. 2020;48(12):1–7. https://doi.org/10.1177/0300060520977589
6. Potts M.B., Zumofen D.W., Raz E., Nelson P.K., Riina H.A. Curing arteriovenous malformations using embolization. *Neurosurg. Focus.* 2014;37(3);E19. https://doi.org/10.3171/2014.6.FOCUS14228
7. Orron D.E., Bloom A.I., Neeman Z. The role of transcatheter arterial embolization in the management of nonvariceal upper gastrointestinal bleeding. *Gastrointest. Endosc. Clin. North Am*. 2018;28(3):331–349. https://doi.org/10.1016/j.giec.2018.02.006
8. Dan V.N., Sapelkin S.V., Legon'kova O.A., Tsygankov V.N., Varava A.B., Kedik S.A., Zhavoronok E.S., Panov A.V. Materials and methods of arteriovenous malformations endovascular treatment: opportunities and problems. *Voprosy biologicheskoi, meditsinskoi i farmatsevticheskoi khimii = Problems of Biological, Medical and Pharmaceutical Chemistry.* 2016;19(7):3–11 (in Russ.). https://www.elibrary.ru/whpuev

СПИСОК ЛИТЕРАТУРЫ

1. Дан В.Н. *Ангиодисплазии* (*врожденные пороки развития сосудов*). М.: Вердана; 2008, 200 с. ISBN 978-5-901439-30-2
2. Chabrot P., Boyer L. *Embolization.* Springer; 2014, 453 p. https://doi.org/10.1007/978-1-4471-5182-1
3. Varghese K., Adhyapak S. *Therapeutic Embolization.* Springer; 2017, 133 p. https://doi.org/10.1007/978-3-319-42494-1
4. Goode J.A., Matson M.B. Embolisation of cancer: what is the evidence? *Cancer Imaging*. 2004;4(2):133–141. https://doi.org/10.1102/1470-7330.2004.0021
5. Alluhaybi A.A., Abdulqader S.B., Altuhayni K., AlTurkstani A., Kabbani A., Ahmad M. Preoperative trans-arterial embolization of a giant scalp congenial hemangioma associated with cardiac failure in a premature newborn. *J. Int. Med. Res*. 2020;48(12):1–7. https://doi.org/10.1177/0300060520977589
6. Potts M.B., Zumofen D.W., Raz E., Nelson P.K., Riina H.A. Curing arteriovenous malformations using embolization. *Neurosurg. Focus.* 2014;37(3);E19. https://doi.org/10.3171/2014.6.FOCUS14228
7. Orron D.E., Bloom A.I., Neeman Z. The role of transcatheter arterial embolization in the management of nonvariceal upper gastrointestinal bleeding. *Gastrointest. Endosc. Clin. North Am*. 2018;28(3):331–349. https://doi.org/10.1016/j.giec.2018.02.006
8. Дан В.Н., Сапелкин С.В., Легонькова О.А., Цыганков В.Н., Варава А.Б., Кедик С.А., Жаворонок Е.С., Панов А.В. Материалы и методы эндоваскулярного лечения артериовенозных мальформаций: возможности и проблемы. *Вопросы биологической, медицинской и фармацевтической химии.* 2016;19(7):3–11. https://www.elibrary.ru/whpuev
9. Guimaraes M., Lencioni R., Gary P. *Embolization Therapy: Principles and Clinical Applications.* Wolters Kluwer Health; 2014, 816 p.

9. Guimaraes M., Lencioni R., Gary P. *Embolization Therapy: Principles and Clinical Applications.* Wolters Kluwer Health; 2014, 816 p.
10. Hoshino J., Ubara Y., Suwabe T., Sumida K., Hayami N., Mise K., Hiramatsu R., Hasegawa E., Yamanouchi M., Sawa N., Takei R., Takaichi K. Intravascular embolization therapy in patients with enlarged polycystic liver. *Am. J. Kidney Dis.* 2014;63(6):937–944. https://doi.org/10.1053/j.ajkd.2014.01.422
11. Reshetnyak D.V., Zhavoronok E.S., Legon'kova O.A., *et al*. Modern Liquid Embolization Agents Based on Polymers: Composition, Characteristics, and Areas of Application. Review. *Polym. Sci. Ser. D.* 2022;15(1):64–70. https://doi.org/10.1134/S1995421222010154
[Original Russian Text: Reshetnyak D.V., Zhavoronok E.S., Legon'kova O.A., Ogannisyan A.S., Panov A.V., Kedik S.A. Modern liquid embolizing agents based on polymers: composition, properties and application (Review). *Vse materialy. Ehntsiklopedicheskii spravochnik*. 2021;6:3–13 (in Russ.). https://doi.org/10.31044/1994-6260-2021-0-6-3-13]
12. Legon'kova O.A., Dan V.N., Sapelkin S.V., *et al.* Regularities of formation of emboli of liquid polymer solutions in aqueous medium. *Polym. Sci. Ser. D.* 2017;10(1):68–73 (in Russ.). https://doi.org/10.1134/S1995421217010154
[Original Russian Text: Legon'kova O.A., Dan V.N., Sapelkin S.V., Kedik S.A., Zhavoronok E.S., Panov A.V., Asanova L.Yu., Ogarkova P.L., Shilov M.S. Regularities of formation of emboli of liquid polymer solutions in aqueous medium. *Vse materialy. Ehntsiklopedicheskii spravochnik*. 2016;6:9–15 (in Russ.). https://www.elibrary.ru/wfnipv]
13. Legon'kova O.A., Stafford V.V., Ogannisyan A.S., Panov A.V., Zhavoronok E.S., Kedik S.A., Pozyabin S.V., Chupin A.V., Sapelkin S.V., Alekyan B.G. Safety and efficacy assessment of cellulose acetate in modeling of rabbit femoral artery embolization. *Ehndovaskulyarnaya khirurgiya = Russ. J. Endovascular Surgery.* 2021;8(4):398–411 (in Russ.). https://doi.org/10.24183/2409-4080-2021-8-4-398-411
14. Legon'kova O.A., Stafford V.V., Oganissyan A.S., Zhavoronok E.S., Panov A.V., Vinokurova T.I., Kedik S.A. Influence of the nature of radiopaque substances on the behavior of embolizing systems *in vivo*. *Biotekhnologiya = Biotechnology.* 2022;38(3):62–69 (in Russ.). https://doi.org/10.56304/S0234275822030048
15. Tokunaga K., Kinugasa K., Meguro T., Sugiu K., Nakashima H., Mandai Sh., Ohmoto T. Curative treatment of cerebral arteriovenous malformations by embolisation using cellulose acetate polymer followed by surgical resection. *Journal of Clinical Neuroscience*. 2000;7(Suppl. A):1–5. https://doi.org/10.1054/jocn.2000.0700
16. Wright K.C., Greff R.J., Price R.E. Experimental evaluation of cellulose acetate NF and ethylene-vinyl alcohol copolymer for selective arterial embolization. *J. Vascul. Int. Radiol.* 1999;10(9): 1207–1218. https://doi.org/10.1016/S1051-0443(99)70221-6
17. Tokunaga K., Kunigasa K., Kawada S., Nakashima H., Tamiya T., Hirotsune N., Mandai Sh., Ohmoto T. Embolization of cerebral arteriovenous malformations with cellulose acetate polymer: a clinical, radiological, and histological study. *Neurosurgery.* 1999;44(5):981–989. https://doi.org/10.1097/00006123-199905000-00026
18. Brayton C.F. Dimethyl sulfoxide (DMSO): a review. *Cornell Veter*. 1986;76(1):61–90.
19. Madsen B.K., Hilscher M., Zetner D., Rosenberg J. Adverse reactions of dimethyl sulfoxide in humans: a systematic review. *F1000Res*. 2019;7:1746. https://doi.org/10.12688/f1000research.16642.2
10. Hoshino J., Ubara Y., Suwabe T., Sumida K., Hayami N., Mise K., Hiramatsu R., Hasegawa E., Yamanouchi M., Sawa N., Takei R., Takaichi K. Intravascular embolization therapy in patients with enlarged polycystic liver. *Am. J. Kidney Dis.* 2014;63(6):937–944. https://doi.org/10.1053/j.ajkd.2014.01.422
11. Решетняк Д.В., Жаворонок Е.С., Легонькова О.А., Оганнисян А.С., Панов А.В., Кедик С.А. Современные жидкие эмболизирующие агенты на основе полимеров: состав, свойства и области применения. Обзор. *Все материалы. Энциклопедический справочник*. 2021;6:3–13. https://doi.org/10.31044/1994-6260-2021-0-6-3-13
12. Легонькова О.А., Дан В.Н., Сапелкин С.В., Кедик С.А., Жаворонок Е.С., Панов А.В., Асанова Л.Ю., Огаркова П.Л., Шилов М.С. Закономерности формирования эмболов в водной среде из жидких растворов полимеров. *Все материалы. Энциклопедический справочник.* 2016;6:9–15. https://www.elibrary.ru/wfnipv
13. Легонькова О.А., Стаффорд В.В., Оганнисян А.С., Панов А.В., Жаворонок Е.С., Кедик С.А., Позябин С.В., Чупин А.В., Сапелкин С.В., Алекян Б.Г. Оценка безопасности и эффективности ацетата целлюлозы при моделировании эмболизации бедренной артерии кролика. *Эндоваскулярная хирургия.* 2021;8(4):398–411. https://doi.org/10.24183/2409-4080-2021-8-4-398-411
14. Легонькова О.А., Стаффорд В.В., Оганиссян А.С., Жаворонок Е.С., Панов А.В., Винокурова Т.И., Кедик С.А. Влияние природы рентгеноконтрастных веществ на поведение эмболизирующих систем *in vivo*. *Биотехнология.* 2022;37(3):62–69. https://doi.org/10.56304/S0234275822030048
15. Tokunaga K., Kinugasa K., Meguro T., Sugiu K., Nakashima H., Mandai Sh., Ohmoto T. Curative treatment of cerebral arteriovenous malformations by embolisation using cellulose acetate polymer followed by surgical resection. *Journal of Clinical Neuroscience*. 2000;7(Suppl. A):1–5. https://doi.org/10.1054/jocn.2000.0700
16. Wright K.C., Greff R.J., Price R.E. Experimental evaluation of cellulose acetate NF and ethylene-vinyl alcohol copolymer for selective arterial embolization. *J. Vascul. Int. Radiol*. 1999;10(9):1207–1218. https://doi.org/10.1016/S1051-0443(99)70221-6
17. Tokunaga K., Kunigasa K., Kawada S., Nakashima H., Tamiya T., Hirotsune N., Mandai Sh., Ohmoto T. Embolization of cerebral arteriovenous malformations with cellulose acetate polymer: a clinical, radiological, and histological study. *Neurosurgery.* 1999;44(5):981–989. https://doi.org/10.1097/00006123-199905000-00026
18. Brayton C.F. Dimethyl sulfoxide (DMSO): a review. *Cornell Veter*. 1986;76(1):61–90.
19. Madsen B.K., Hilscher M., Zetner D., Rosenberg J. Adverse reactions of dimethyl sulfoxide in humans: a systematic review. *F1000Res*. 2019;7:1746. https://doi.org/10.12688/f1000research.16642.2
20. Lord J., Britton H., Spain S.G., Lewis A.L. Advancements in the development on new liquid embolic agents for use in therapeutic embolization. *J. Mater. Chem. B*. 2020;8(36): 8207–8218. https://doi.org/10.1039/d0tb01576h
21. Hu J., Albadawi H., Chong B.W., Deipolyi A.R., Sheth R.A., Khademhosseini A., Oklu R. Advances in biomaterials and technologies for vascular embolization. *Adv. Mater.* 2019;31(33):e1901071. https://doi.org/10.1002/adma.201901071
22. Tian L., Lu L., Feng J., Melancon M.P. Radiopaque nano and polymeric materials for atherosclerosis imaging, embolization and other catheterization procedures. *Acta Pharm. Sinica B*. 2018;8(3):360–370. https://doi.org/10.1016/j.apsb.2018.03.002

20. Lord J., Britton H., Spain S.G., Lewis A.L. Advancements in the development on new liquid embolic agents for use in therapeutic embolization. *J. Mater. Chem. B*. 2020;8(36): 8207–8218. https://doi.org/10.1039/d0tb01576h
21. Hu J., Albadawi H., Chong B.W., Deipolyi A.R., Sheth R.A., Khademhosseini A., Oklu R. Advances in biomaterials and technologies for vascular embolization. *Adv. Mater.* 2019;31(33):e1901071. https://doi.org/10.1002/adma.201901071
22. Tian L., Lu L., Feng J., Melancon M.P. Radiopaque nano and polymeric materials for atherosclerosis imaging, embolization and other catheterization procedures. *Acta Pharm. Sinica B*. 2018;8(3):360–370. https://doi.org/10.1016/j.apsb.2018.03.002
23. Reshetnyak D.V., Zhavoronok E.S., Legon'kova O.A., *et al*. A Spectrophotometric Study of the Interaction of Aromatic and Aliphatic Iodine-Containing Substances with Dimethyl Sulphoxide. *Polym. Sci. Ser. D.* 2022;15(4):543–548. https://doi.org/10.1134/s1995421222040232
[Original Russian Text: Reshetnyak D.V., Zhavoronok E.S., Legon'kova O.A., Ogannisyan A.S., Panov A.V., Kedik S.A. A Spectrophotometric Study of the Interaction of Aromatic and Aliphatic Iodine-Containing Substances with Dimethyl Sulphoxide. *Klei. Germetiki. Tekhnologii = Adhesives. Sealants. Technologies*. 2022;5:25–31(in Russ.). https://doi.org/10.31044/1813-7008-2022-0-5-25-31]
24. Klyubin V.V., Klyubina K.A., Makovetskaya K.N. A Spectroscopic Method for Determining Free Iodine in Iodinated Fatty-Acid Esters. *Opt. Spectrosc*. 2018;124(1): 53–56. https://doi.org/10.1134/S0030400X18010101
[Original Russian Text: Klyubin V.V., Klyubina K.A., Makovetskaya K.N. A Spectroscopic Method for Determining Free Iodine in Iodinated Fatty-Acid Esters. *Optika i spektroskopiya*. 2018;124(1):56–59 (in Russ.). http://doi.org/10.21883/OS.2018.01.45357.135-17]
25. Giordano M.C., Bazán J.C., Arvia A.J. The interaction of iodine with dimethylsulphoxide in carbon tetrachloride solutions. *J. Inorg. Nuclear Chem.* 1966;28(5):1209–1214. https://doi.org/10.1016/0022-1902(66)80447-5
26. Thomsen H.S., Bellin M.-F., Jakobsen Ja.A., Webb Ju.A.W. Contrast media classification and terminology. In: Thomsen H., Webb Ju. (Eds.). *Contrast Media. Safety Issues and ESUR Guidelines.* Berlin, Heidelberg: Springer-Verlag; 2014. P. 3–11. https://doi.org/10.1007/174_2013_864
27. Nikulin A.V., Martynov L.Yu., Gabaeva R.S., Lazov M.A. Development of a new inversion-voltammetric technique in determining inorganic iodine in *Laminariae thalli* L. for the quality control of raw materials in factory laboratories. *Tonk. Khim. Tekhnol. = Fine Chem. Technol*. 2024;19(4):372–383. https://doi.org/10.32362/2410-6593-2024-19-4-372-383

23. Решетняк Д.В., Жаворонок Е.С., Легонькова О.А., Оганнисян А.С., Панов А.В., Кедик С.А. Спектрофотометрическое исследование взаимодействия ароматических и алифатических йодсодержащих веществ с диметилсульфоксидом. *Клеи. Герметики. Технологии*. 2022;5:25–31. https://doi.org/10.31044/1813-7008-2022-0-5-25-31
24. Клюбин В.В., Клюбина К.А., Маковецкая К.Н. Спектрометрический метод определения несвязанного йода в йодированных эфирах жирных кислот. *Оптика и спектроскопия*. 2018;124(1):56–59. http://dx.doi.org/10.21883/OS.2018.01.45357.135-17
25. Giordano M.C., Bazán J.C., Arvia A.J. The interaction of iodine with dimethylsulphoxide in carbon tetrachloride solutions. *J. Inorg. Nuclear Chem.* 1966;28(5):1209–1214. https://doi.org/10.1016/0022-1902(66)80447-5
26. Thomsen H.S., Bellin M.-F., Jakobsen Ja.A., Webb Ju.A.W. Contrast media classification and terminology. In: Thomsen H., Webb Ju. (Eds.). *Contrast Media. Safety Issues and ESUR Guidelines.* Berlin, Heidelberg: Springer-Verlag; 2014. P. 3–11. https://doi.org/10.1007/174_2013_864
27. Никулин А.В., Мартынов Л.Ю., Габаева Р.С., Лазов М.А. Разработка новой инверсионно-вольтамперометрической методики определения неорганического йода в слоевищах ламинарии (*Laminariae thalli* L.) для контроля качества сырья в условиях заводских лабораторий. *Тонкие химические технологии*. 2024;19(4):372–383. https://doi.org/10.32362/2410-6593-2024-19-4-372-383

About the Authors

Daria V. Nebesnaia, Postgraduate Student, Department of Biotechnology and Industrial Pharmacy, M.V. Lomonosov Institute of Fine Chemical Technologies, MIREA – Russian Technological University (78, Vernadskogo pr., Moscow, 119454, Russia). E-mail: y.darach@yandex.ru. Scopus Author ID 57466621700, RSCI SPIN-code 5958-3911, https://orcid.org/0000-0001-5214-0425

Ekaterina S. Terendiak, Student, M.V. Lomonosov Institute of Fine Chemical Technologies, MIREA – Russian Technological University (78, Vernadskogo pr., Moscow, 119454, Russia). E-mail: ekaterinaterendiak@gmail.com. https://orcid.org/0009-0004-0651-6312

Olga A. Legon'kova, Dr. Sci. (Eng.), Head of the Department of Dressings, Suture and Polymer Materials in Surgery, A.V. Vishnevsky Institute of Surgery, Ministry of Health of Russia (27, Bolshaya Serpukhovskaya ul., Moscow, 117997, Russia). E-mail: oalegonkovapb@yandex.ru. Scopus Author ID 18437207900, RSCI SPIN-code 5042-3281, https://orcid.org/0000-0002-2100-6896

Stanislav A. Kedik, Dr. Sci. (Eng.), Professor, Head of the Department of Biotechnology and Industrial Pharmacy, M.V. Lomonosov Institute of Fine Chemical Technologies, MIREA – Russian Technological University (78, Vernadskogo pr., Moscow, 119454, Russia); General Director, JSC Institute of Pharmaceutical Technologies (of. 1, 21, Skolkovskoe sh., Moscow, 121353, Russia). E-mail: kedik@mirea.ru. Scopus Author ID 7801632547, https://orcid.org/0000-0003-2610-8493

Alexey V. Panov, Can. Sci. (Chem.), Associate Professor, Department of Biotechnology and Industrial Pharmacy, M.V. Lomonosov Institute of Fine Chemical Technologies, MIREA – Russian Technological University (78, Vernadskogo pr., Moscow, 119454, Russia). E-mail: panov@mirea.ru. Scopus Author ID 59339673200, RSCI SPIN-code 5369-3083, https://orcid.org/0000-0002-1603-143X

Elena S. Zhavoronok, Dr. Sci. (Chem.), Associate Professor, Professor, Department of Biotechnology and Industrial Pharmacy, M.V. Lomonosov Institute of Fine Chemical Technologies, MIREA – Russian Technological University (78, Vernadskogo pr., Moscow, 119454, Russia). E-mail: zhavoronok@mirea.ru. Scopus Author ID 7801409746, ResearcherID AAI-1265-2021, H-9420-2013, SPIN-код РИНЦ 4466-0174, https://orcid.org/0000-0002-7235-3361

Об авторах

Небесная Дарья Владимировна, аспирант, кафедра биотехнологии и промышленной фармации, Институт тонких химических технологий им. М.В. Ломоносова, ФГБОУ ВО «МИРЭА – Российский технологический университет» (119454, Россия, Москва, пр-т Вернадского, д. 78). E-mail: y.darach@yandex.ru. Scopus Author ID 57466621700, SPIN-код РИНЦ 5958-3911, https://orcid.org/0000-0001-5214-0425

Терендяк Екатерина Сергеевна, студент, Институт тонких химических технологий им. М.В. Ломоносова, ФГБОУ ВО «МИРЭА – Российский технологический университет» (119454, Россия, Москва, пр-т Вернадского, д. 78). E-mail: ekaterinaterendiak@gmail.com. https://orcid.org/0009-0004-0651-6312

Легонькова Ольга Александровна, д.т.н., заведующая отделом перевязочных, шовных и полимерных материалов в хирургии, ФГБУ «НМИЦ хирургии им. А.В. Вишневского» Минздрава России (117997, Москва, ул. Большая Серпуховская, д. 27). E-mail: oalegonkovapb@yandex.ru. Scopus Author ID 18437207900, SPIN-код РИНЦ 5042-3281, https://orcid.org/0000-0002-2100-6896

Кедик Станислав Анатольевич, д.т.н., профессор, заведующий кафедрой биотехнологии и промышленной фармации, Институт тонких химических технологий им. М.В. Ломоносова, ФГБОУ ВО «МИРЭА – Российский технологический университет» (119454, Россия, Москва, пр-т Вернадского, д. 78); генеральный директор, АО «Институт фармацевтических технологий» (121353, Москва, Сколковское ш., д. 21, оф. 1.). E-mail: kedik@mirea.ru. Scopus Author ID 7801632547, https://orcid.org/0000-0003-2610-8493

Панов Алексей Валерьевич, к.х.н., доцент, кафедра биотехнологии и промышленной фармации, Институт тонких химических технологий им. М.В. Ломоносова, ФГБОУ ВО «МИРЭА – Российский технологический университет» (119454, Россия, Москва, пр-т Вернадского, д. 78). E-mail: panov@mirea.ru. Scopus Author ID 59339673200, SPIN-код РИНЦ 5369-3083, https://orcid.org/0000-0002-1603-143X

Жаворонок Елена Сергеевна, д.х.н., доцент, профессор, кафедра биотехнологии и промышленной фармации, Институт тонких химических технологий им. М.В. Ломоносова, ФГБОУ ВО «МИРЭА – Российский технологический университет» (119454, Россия, Москва, пр-т Вернадского, д. 78). E-mail: zhavoronok@mirea.ru. Scopus Author ID 7801409746, ResearcherID AAI-1265-2021, H-9420-2013, SPIN-код РИНЦ 4466-0174, https://orcid.org/0000-0002-7235-3361

Translated from Russian into English by N. Isaeva
Edited for English language and spelling by Dr. David Mossop

Tonkie Khimicheskie Tekhnologii = Fine Chemical Technologies.
2025;20(6):565–581 ISSN 2686-7575 (Online)

Biochemistry and biotechnology
Биохимия и биотехнология

UDC 577.11
https://doi.org/10.32362/2410-6593-2025-20-6-565-581
EDN SCSQPA

RESEARCH ARTICLE

Development of immunochromatographic assay for simultaneous detection of tetracyclines and streptomycin in milk

Ivan V. Maksin[1,2,✉], Darya I. Polyakova[2,3], Viktoriia A. Kesareva[2,3], Alexander A. Sysuev[1], Vladislav S. Ivanov[2], Evgeniia I. Simonova[2,3], German A. Khunteev[2], Yuliya G. Kirillova[1]

[1] *MIREA – Russian Technological University (Lomonosov Institute of Fine Chemical Technologies), Moscow, 119454 Russia*
[2] *Rapid Bio, Moscow, 121205 Russia*
[3] *Patrice Lumumba Peoples' Friendship University of Russia, Moscow, 117198 Russia*
✉ *Corresponding author, e-mail: maxinivanv@gmail.com*

Abstract

Objectives. To optimize indirect antibody immobilization on gold nanoparticles (GNPs) using anti-species antibodies for enhanced conjugate stability and to develop an immunochromatographic assay (ICA) for antibiotic detection in milk.

Methods. The GNPs were synthesized by reduction of tetrachloroauric acid in the presence of seed particles. The size of GNPs was determined spectrophotometrically according to literature data using a *Thermo Fisher Scientific* Varioskan LUX instrument. Monoclonal mouse antibodies to tetracycline and streptomycin were immobilized on the surface of the GNPs via anti-mouse antibodies. Conjugates of bovine serum albumin with tetracycline and streptomycin were obtained through Mannich reaction and click-reaction, respectively. The coupling ratio was determined by MALDI-TOF mass spectrometry on a *Bruker* RapifleX instrument. Immunoreagents were dispensed onto a nitrocellulose membrane using a *BioDot* ZX1010 dispenser. The assembled multi-membrane composite was cut into test strips using a *KinBio* ZQ4500 guillotine cutter. The test results were interpreted visually and using an *Allsheng* TSR-100 test strip reader.

Results. Following conjugate formation via indirect immobilization using anti-species antibodies, it was necessary to block residual binding sites on the anti-species antibodies in order to enhance solution-phase conjugate stability. As a result of optimizing the concentrations of immunoreagents, an ICA was developed for the simultaneous detection of streptomycin and tetracyclines in milk. The detection limit of the optimized ICA for tetracyclines and streptomycin was 2–7.5 and 25 ng/mL, respectively, for visual result interpretation, and 0.29–2.15 and 1.34 ng/mL, respectively, when using a test strip reader.

Conclusions. It is shown that the stability of the resulting conjugates in solution can be enhanced by blocking the free binding sites of the anti-species antibodies to prevent cross-linking of the nanoparticles caused by anti-species antibody binding.

Keywords

lateral flow immunoassay, antibiotics, rapid test, gold nanoparticles, tetracycline, streptomycin, immobilization

Submitted: 30.04.2025
Revised: 07.08.2025
Accepted: 11.11.2025

For citation

Maksin I.V., Polyakova D.I., Kesareva V.A., Sysuev A.A., Ivanov V.S., Simonova E.I., Khunteev G.A., Kirillova Yu.G. Development of immunochromatographic assay for simultaneous detection of tetracyclines and streptomycin in milk. *Tonk. Khim. Tekhnol. = Fine Chem. Technol*. 2025;20(6):565–581. https://doi.org/10.32362/2410-6593-2025-20-6-565-581

НАУЧНАЯ СТАТЬЯ

Разработка иммунохроматографического анализа для одновременного обнаружения тетрациклинов и стрептомицина в молоке

И.В. Максин[1,2,✉], Д.И. Полякова[2,3], В.А. Кесарева[2,3], А.А. Сысуев[1], В.С. Иванов[2], Е.И. Симонова[2,3], Г.А. Хунтеев[2], Ю.Г. Кириллова[1]

[1] *МИРЭА – Российский технологический университет (Институт тонких химических технологий им. М.В. Ломоносова), Москва, 119454 Россия*

[2] *ООО «Рапид Био», Москва, 121205 Россия*

[3] *Российский университет дружбы народов им. П. Лумумбы, Москва, 117198 Россия*

✉ *Автор для переписки, e-mail: maxinivanv@gmail.com*

Аннотация

Цели. Оптимизация стабильности конъюгатов, полученных методом непрямой иммобилизации специфических антител на наночастицах золота (НЧЗ) при помощи антивидовых антител, и разработка на их основе иммунохроматографического анализа (ИХА) для определения антибиотиков в молоке.

Методы. НЧЗ синтезировали восстановлением золотохлористоводородной кислоты в присутствии зародышей. Размер определяли спектрофотометрически по литературным данным на приборе *Thermo Fisher Scientific* Varioskan LUX. Моноклональные мышиные антитела к тетрациклину и стрептомицину иммобилизовали на поверхности НЧЗ посредством анти-мышиных антител. Конъюгаты бычьего сывороточного альбумина с тетрациклином и стрептомицином получали реакцией Манниха и клик-реакцией соответственно. Степень конъюгации определяли при помощи MALDI-TOF масс-спектрометрии на приборе *Bruker* RapifleX. Иммунореагенты наносили на нитроцеллюлозную мембрану на диспенсере *BioDot* ZX1010. Собранный мультимембранный композит нарезали на тест-полоски на гильотинном резчике *KinBio* ZQ4500. Результаты ИХА интерпретировали визуально, а также при помощи считывателя тест-полосок *Allsheng* TSR-100.

Результаты. После получения конъюгатов посредством непрямой иммобилизации при помощи антивидовых антител необходимо проводить блокировку оставшихся незанятыми сайтов связывания антивидовых антител, чтобы повысить стабильность конъюгатов в растворе. В результате оптимизации концентраций иммунореагентов был разработан ИХА для одновременного обнаружения стрептомицина и тетрациклинов в молоке. Предел обнаружения оптимизированного анализа тетрациклинов и стрептомицина составил 2–7.5 и 25 нг/мл при визуальной интерпретации результатов, 0.29–2.15 и 1.34 нг/мл при использовании считывателя тест-полосок соответственно.

Выводы. Установлено, что блокировка свободных сайтов связывания вторичных антител повышает стабильность полученных конъюгатов антител в растворе, предотвращая кросс-сшивки наночастиц, вызываемые связыванием антивидовых антител.

Ключевые слова

антибиотики, экспресс-тест, наночастицы золота, тетрациклин, стрептомицин, иммобилизация

Поступила: 30.04.2025
Доработана: 07.08.2025
Принята в печать: 11.11.2025

Для цитирования

Максин И.В., Полякова Д.И., Кесарева В.А., Сысуев А.А., Иванов В.С., Симонова Е.И., Хунтеев Г.А., Кириллова Ю.Г. Разработка иммунохроматографического анализа для одновременного обнаружения тетрациклинов и стрептомицина в молоке. *Тонкие химические технологии*. 2025;20(6):565–581. https://doi.org/10.32362/2410-6593-2025-20-6-565-581

INTRODUCTION

Detecting antibiotics in food products is a critical task for ensuring food safety and protecting public health. The uncontrolled use of antibiotics in veterinary medicine leads to their accumulation in animal products, potentially posing a threat to human health due to increased antibiotic resistance in microorganisms and occurrence of allergic reactions.

Highly sensitive and specific physicochemical analysis methods, including high-performance liquid chromatography and mass spectrometry, are effectively used for antibiotic detection. However, due to their reliance on expensive equipment and the expertise of highly qualified specialists [1], these methods are used only in large laboratory centers.

Efficient testing in non-laboratory settings is based on the use of simple and accessible methods such as immunochromatographic assay (ICA). The principle of ICA is based on a highly specific antigen-antibody interaction followed by separation of the resulting immune complex as the fluid moves along a porous membrane. ICA is characterized by its simplicity and rapidity, allowing for a qualitative assessment of the presence or absence of a target compound in a sample without using additional equipment [2].

However, one of the main factors hindering the widespread use of ICA is its relatively low sensitivity [2, 3]. Traditional approaches to increasing ICA sensitivity include the use of high-signal-intensity labels, such as quantum dots [4], signal enhancement by coloring with silver salts [5], analyte concentration using functionalized magnetic nanoparticles [6], and preincubation of the sample with the antibody-label conjugate before adding it to the test strip [7]. In applying these approaches, it is important that the key advantages of the method, i.e., its speed and ease of use, are not sacrificed in the pursuit of a low detection limit.

Orienting specific antibodies on sensor surfaces in order to maximize the exposure of binding sites is a relatively new and promising approach in immunoassay, allowing for a significant reduction in the detection limit of immunosensors. Numerous approaches aimed at targeted immobilization of antibodies have been recently reviewed [3, 8]. For example, the research group led by B.B. Dzantiev has developed a number of highly sensitive test systems [9–11], including those with the simultaneous detection of multiple analytes on a single test strip [12, 13]. Nevertheless, the development of new systems remains relevant and requires an expanded scope of application.

The present work sets out to develop an immunoassay for the simultaneous determination of streptomycin and tetracyclines in raw milk with instrument-free interpretation of the results. To achieve a low detection limit of the ICA, we used secondary antibodies specific to the Fc fragment of mouse immunoglobulin G to immobilize mouse antibodies to tetracycline and streptomycin on the surface of gold nanoparticles (GNPs). We also applied the approach of preincubating the sample with the antibody-label conjugate before adding it to the test strip.

MATERIALS AND METHODS

Materials, reagents and solutions

The following reagents were used: bovine serum albumin (BSA), fraction V5 (*Proliant*, New Zealand), streptomycin sulfate (*PanReac Applichem*, Spain), propynyloxypropionic acid hydrazide, γ-azidobutyric acid oxysuccinimide ester (*Primetech*, Republic of Belarus), aurichlorohydric acid (*Aurat*, Russia), tetracycline hydrochloride (*Biotopped*, China), HEPES ((4-(2-hydroxyethyl)-1-piperazineethanesulfonic acid), sucrose, tris(hydroxymethyl)aminomethane (*Dia-M*, Russia), tris-hydroxypropyltriazolylmethyl-amine (THPTA) (*Lumiprobe*, Russia), guanidine hydrochloride, sodium citrate (*Helicon*, Russia), L-ascorbic acid (*Sigma-Aldrich*, USA), hydroxylamine hydrochloride (*Panreac*, Spain), formaldehyde (*neoFroxx*, Germany). The following state standard samples were used as analytes to determine the detection limit and cross-reactivity: streptomycin sulfate, tetracycline hydrochloride, doxycycline hyclate, chloramphenicol (*VGNKI*, Russia), as well as oxytetracycline hydrochloride (*Thermo Fisher Scientific*, USA), penicillin G sodium salt (*Biotopped*, China), chlortetracycline hydrochloride, cefoperazone sodium salt (*Molekula*, United Kingdom), gentamicin sulfate, kanamycin sulfate (*neoFroxx*, Germany). The remaining reagents used were of Russian manufacture and had a qualification of at least chemically pure. Milk samples with a fat content of 3.2% were purchased from a retail network in Moscow. When preparing standard solutions of antibiotics in milk, the concentrations were calculated based on the pure active substance, taking into account the molecular weight of the corresponding salts. In addition, polyclonal goat antibodies to chicken egg antibodies, polyclonal goat antibodies to mouse antibodies, chicken egg IgY antibodies (*Arista Biologicals*, USA), mouse monoclonal antibodies to tetracycline, and mouse monoclonal antibodies to streptomycin (*Eastmab*, China) were used. Deionized water (Milli-Q®, *Millipore*, USA) was used to prepare solutions, GNP preparations, and conjugates based on them.

Thin-layer chromatography (TLC) was performed on RP-18 F254s reverse-phase aluminum plates (*Merck*, Germany).

SM31-40 adhesive backing (*KinBio*, China), 70CNPH analytical nitrocellulose membrane, FR-1 sample membrane, and AP45 absorbent membrane (*Advanced Microdevices*, India) were used to manufacture ICA strips.

Preparation of BSA–streptomycin (STR) conjugate

Preparation of STR–alkyne conjugate. Streptomycin sulfate (408 mg, 0.56 mmol) and propynyloxypropionic acid hydrazide (30 mg, 0.21 mmol) were added to 0.85 mL of 0.45 M Na_2CO_3 solution. The reaction mixture was incubated for 24 h at 4°C. Reaction completion was monitored by TLC in a methylene chloride/methanol = 40 : 1 system based on the disappearance of the starting material (retention coefficient R_f = 0.3). After elution, the plates were treated with ninhydrin solution and heated for visualization. The STR–alkyne concentration in the solution was assumed to be 0.247 M.

Preparation of BSA–azide conjugate. To a solution of 3.2 mL of BSA with a concentration of 20 mg/mL (0.962 μmol) in 0.1 M sodium bicarbonate, pH 8.5, 0.6 mL of a solution of γ-azidobutyric acid oxysuccinimide ester with a concentration of 6 mg/mL (15.91 μmol) in dimethyl sulfoxide was added. The reaction mixture was then incubated for 24 h at 4°C. The conjugate was purified by dialysis against deionized water. After dialysis, the protein concentration was determined by ultraviolet–visible (UV–Vis) spectrophotometry on a UV5Nano instrument (*Mettler Toledo*, Switzerland). The resulting conjugate was stored at 4°C.

Preparation of BSA–STR conjugate (*copper reducing agent—L-ascorbic acid*). To a solution of 0.5 mL BSA–azide with a concentration of 8.46 mg/mL (0.063 μmol, 1 equiv.), 0.1 mL of a 1 M HEPES solution with pH 7.2 and 13 μL of STR–alkyne (3.211 μmol, 50 equiv.) were added. In a separate test tube, solutions of 6.25 μL of 20 mM $CuSO_4$ (0.125 μmol, 2 equiv.) and 12.5 μL of 50 mM THPTA (0.625 μmol, 10 equiv.) were mixed. Next, the entire volume of the resulting solution was transferred into a mixture of BSA–azide and STR–alkyne. Then 25 μL of 100 mM guanidine chloride (2.5 μmol, 40 equiv.), 25 μL of 100 mM L-ascorbic acid (2.5 μmol, 40 equiv.), and 25 μL of 100 mM NaOH (2.5 μmol, 40 equiv.) were added. The test tube was filled with argon and left under stirring for 24 h. The conjugate was purified by dialysis against 10 mM phosphate-buffered saline (PBS), pH 7.4. This conjugate is referred to hereinafter as BSA–STR.

Preparation of BSA–STR conjugate (*copper reducing agent—hydroxylamine*). To a solution of 0.5 mL BSA–azide with a concentration of 8.46 mg/mL (0.063 μmol, 1 equiv.), 0.1 mL of a 1 M HEPES solution with pH 7.2 and 13 μL of STR–alkyne (3.211 μmol, 50 equiv.) were added. In a separate test tube, solutions of 6.25 μL of 20 mM $CuSO_4$ (0.125 μmol, 2 equiv.) and 12.5 μL of 50 mM THPTA (0.625 μmol, 10 equiv.) were mixed. The entire volume of the resulting solution was transferred into the mixture of BSA–azide and STR–alkyne. Then 50 μL of 100 mM hydroxylamine hydrochloride (5 μmol, 80 equiv.) were added. The test tube was filled with argon and left under stirring for 24 h. The conjugate was purified by dialysis against 10 mM PBS, pH 7.4. After dialysis, the protein concentration was determined by UV–Vis spectrophotometry using a UV5Nano instrument (*Mettler Toledo*, Switzerland). The prepared conjugate was stored at 4°C.

Synthesis of BSA–tetracycline (TET) conjugate

BSA–TET conjugate was prepared using a published method with modifications [14]. 8 mL of a solution of 18.75 mg/mL of BSA, 2 mL of a 3 M sodium acetate solution, and 12 mL of a water solution of 8.3 mg/mL of tetracycline hydrochloride were mixed. Then, 3.75 mL of a 37% formaldehyde solution were added dropwise with stirring. The container was protected from light with foil. The reaction mixture was stirred for 6 h at room temperature (20–22°C). Dialysis was then performed against 10 mM of PBS, pH 7.4.

MALDI-TOF[1] spectrometry

Mass spectrometric analysis was performed in positive ion registration mode on a RapifleX instrument (*Bruker*, Germany) at the Skolkovo Institute of Science and Technology, Advanced Mass Spectrometry Shared Use Center. A solution of HCCA (α-cyano-4-hydroxycinnamic acid) matrix was used for the analysis: a weighed portion of dry HCCA matrix (*Sigma-Aldrich*, USA) was dissolved in 50% aqueous acetonitrile with 0.5% of trifluoroacetic acid with a concentration of 20 mg/mL. Samples (1 μL) were applied on a Ground

[1] Matrix-activated laser desorption/ionization, MALDI is a process in which the analyte is ionized by a laser in the presence of a special matrix. After ionization, the ions are separated by time-of-flight (TOF), allowing the molecule to be identified according to the thus-determined mass-to-charge ratio.

Steel target (*Bruker*, Germany). Following desiccation of the droplet, 1 μL of the matrix was applied over the sample. Crystallization of the sample and matrix occurred at room temperature in a laminar flow hood. Each sample was analyzed in a single technical replicate in positive ion measurement mode. The *m*/*z* measurement error was no more than 500 ppm (up to 35 Da at a mass of 70000 Da). Spectra were visualized using Origin 9.8 (*OriginLab*, USA).

GNP synthesis

GNPs were synthesized according to the procedure [15]. First, a seed solution was prepared. 100 μL of a 5% tetrachloroauric acid solution was added to 50 mL of deionized water while stirring at 700 rpm. The mixture was brought to a boil. Then 1.5 mL of a 1% sodium citrate solution was added, and boiling was continued for 15 min. The prepared seed solution was brought to room temperature prior to use. Then, 1 mL of the resulting GNP seed solution, 0.5 mL of 1% sodium citrate solution, 0.1 mL of 5% tetrachloroauric acid, and 0.25 mL of 0.5% hydroquinone solution were added to 49 mL of deionized water with stirring at 700 rpm. The resulting sol was stored at 4°C for two months.

Test strip preparation

A ZX1010 dispenser (*BioDot*, USA) was used. After applying BSA–STR and BSA–TET conjugates to the test zone of a nitrocellulose membrane, chicken egg immunoglobulins IgY were applied to the control zone. The membrane with the applied reagents was dried in an oven at 45°C for 1 h. The multimembrane composite was cut into 4 mm wide test strips using a ZQ4500 guillotine cutter (*KinBio*, China) and stored at room temperature in a sealed bag with silica gel.

Selection of the optimal pH and protein concentration for sorption on the GNP surface

The selection was performed according to the method described in [16]. The optimal antibody concentration and pH values for the conjugation were determined on the basis of the nanoparticle conjugate stability to the strong electrolyte (10% NaCl solution). The selection was performed using spectrophotometry on a Varioskan LUX instrument (*Thermo Fisher Scientific*, USA). As the nanoparticle sol aggregates, the peak in the solution's absorption spectrum broadens along with a decreased optical density (OD) of the solution at the wavelength of maximum light absorption and increases in the long-wavelength region. Therefore, the degree of aggregation can be measured using the conventional spectral coefficient $K = OD_{536}/OD_{750}$, which reflects the degree of aggregation (aggregation coefficient). As the sol aggregates, the K value will decrease.

Conjugation of antibodies with GNPs

20 μg of polyclonal goat antibodies to mouse immunoglobulins were added to 10 mL of GNP solution adjusted to pH 8. The mixture was incubated for 1 h on an orbital shaker. Then, following the addition of 0.4 mL of 10% BSA solution, the mixture was further incubated for an additional 30 min and centrifuged for 30 min at 5000g. The supernatant was collected and the pellet resuspended in 0.5 mL of 4 mM tris buffer, pH 8, containing 5% of sucrose and 0.1% of BSA. The resulting conjugate was designated as GNP–anti-mouse. A conjugate of GNPs with polyclonal goat antibodies to chicken IgY antibodies was prepared similarly and designated as GNP–anti-IgY. The resulting conjugates were stored at 4°C.

Antibodies to streptomycin or tetracycline were added to the GNP–anti-mouse conjugate, and the mixture was incubated on an orbital shaker. After 10 min, mouse immunoglobulins were added to block the remaining binding sites. The resulting conjugates were designated as GNP–anti-STR and GNP–anti-TET, respectively. The prepared conjugates were stored at 4°C.

Conducting ICA

A solution of the GNP–anti-TET, GNP–anti-STR, and GNP–anti-IgY conjugates was mixed with 200 μL of milk sample in a well of a microtiter plate. The milk was used without prior treatment or dilution. The range of immunoreagent concentrations tested is shown in Table 1. The well was then placed in a preheated 40°C incubator for 5 min. A test strip was then immersed in the well for 5 min. The test strip was removed from the solution along with the sample membrane to stop the reaction. The color intensity of the test strip line was read using a TSR-100 reader (*Allsheng*, China).

Processing ICA results

Origin 9.8 software (*Origin Lab*, USA) was used to analyze the relationship between signal intensity (y) and analyte concentration in the sample (x). A sigmoid function was used to approximate the concentration dependencies:

$$y = (a - b) / [1 + (x / c)^d] + b,$$

where *a* is the maximum signal; *b* is the minimum signal; *c* (or IC_{50}) is the antigen concentration at which the signal decreases by 50% of its range of changes; *d* is the slope of the approximating dependence at point *c*.

The instrumental detection limit was defined as the analyte concentration causing a 10% decrease in the recorded analytical signal [17]. The visual detection limit was defined as the minimum concentration of the analyte at which the intensity of the test line coloring will be weaker than the intensity of the control line coloring or will be comparable.

RESULTS AND DISCUSSION

To achieve the aim of this study, several tasks had to be completed: (1) synthesize streptomycin and tetracycline conjugates with a carrier protein for immobilization on the analytical membrane; (2) optimize the immobilization of specific antibodies to antibiotics on the GNP surface mediated by secondary antibodies; (3) determine the detection limit of the ICA using the obtained immunoreagents.

Synthesis of BSA conjugates with antibiotics

BSA–STR conjugate **1** was obtained using a click reaction (Fig. 1) [18]. BSA was pre-conjugated with the oxysuccinimide ester of γ-azidobutyric acid to obtain BSA–azide conjugate **2**. According to MALDI-TOF mass spectrometry, the conjugation efficiency was 14 azide groups per one BSA molecule. Alkyne adduct **3** was prepared by reacting streptomycin with propynyloxypropionic acid hydrazide to form the corresponding hydrazone **3**. The reactivity of streptomycin with adipic acid dihydrazide has been described previously [19]. This formed the basis for the procedure used in this study.

Sodium L-ascorbate is typically used as a copper reducing agent in the click reaction. It has been reported [18] that the dehydroascorbate oxidation byproduct can interact with protein side chains (primarily arginine). For this reason, it is recommended to add a dehydroascorbate trap ("scavenger") into the reaction mixture, for example, aminoguanidine. To protect the guanidine groups of streptomycin from the undesired reaction, we performed the click reaction using two different copper reducing agents: sodium L-ascorbate with the addition of guanidine as a "scavenger" and hydroxylamine. Conjugation results, according to MALDI-TOF mass spectrometry, were 6.0 and 5.6 hapten molecules per 1 BSA molecule when using sodium L-ascorbate and hydroxylamine, respectively (Fig. 2). In a comparative experiment in the ICA, the conjugates were no different from each other in performance (data not shown). We subsequently used a conjugate obtained by reduction in the presence of hydroxylamine alone.

The BSA–TET conjugate **5** was obtained under standard conditions using the Mannich reaction [14]. The conjugation efficiency was 1 tetracycline molecule per 1 BSA molecule (Fig. 2).

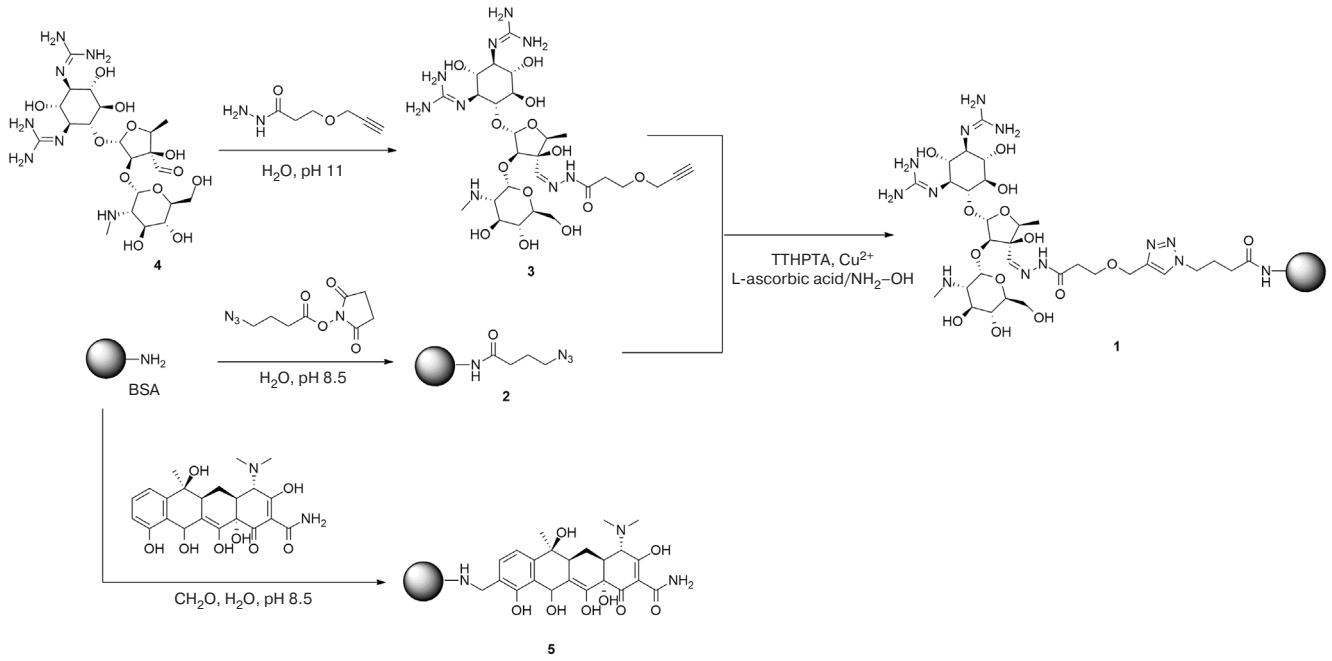

Fig. 1. Scheme of the synthesis of BSA–STR **1** and BSA–TET **5** conjugates

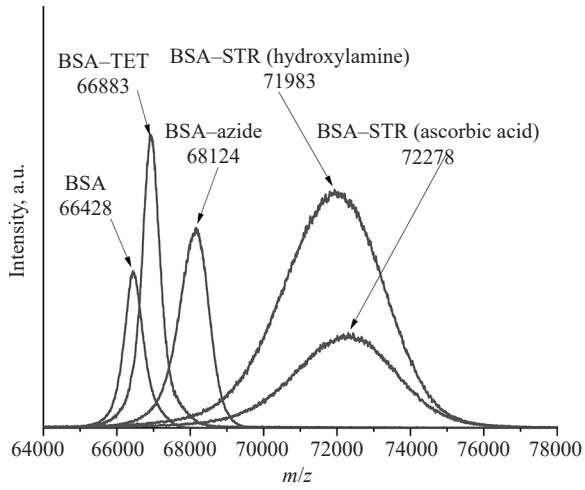

Fig. 2. MALDI-TOF mass spectra of the BSA conjugates

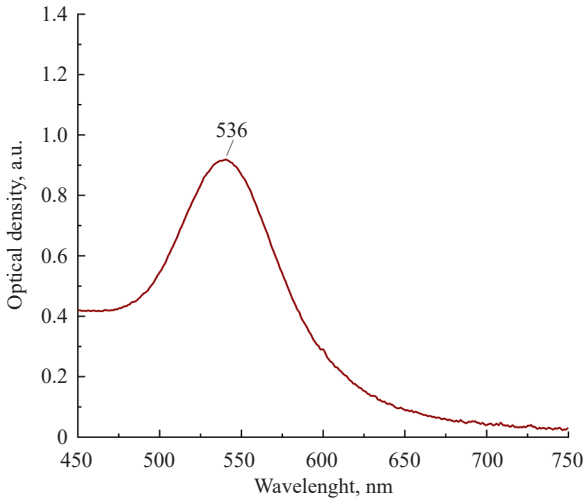

Fig. 3. Light absorption spectrum of the colloidal GNPs

Synthesis of GNPs

According to UV–Vis spectrophotometry data, the wavelength of maximum light absorption of the obtained sol is 536 nm, which corresponds to an average particle size of approximately 55–60 nm (Fig. 3) [20].

Scheme of competitive ICA for the determination of tetracyclines and streptomycin

The ICA strip for tetracycline and streptomycin detection was designed as follows (Fig. 4). BSA–TET, BSA–STR, and chicken egg immunoglobulin IgY conjugates applied to a nitrocellulose membrane formed two test lines (TL) and a control line (CL), respectively, on the assay membrane. After mixing the analytical GNP–anti-TET, GNP–anti-STR conjugates and the control GNP–anti-IgY conjugate with the sample in a microwell immediately before analysis, the mixtures were incubated for 5 min. The time of antibodies interaction with the analyte increases due to the stage of their incubation with the sample. This results in a decrease in the detection limit [7] since providing better kinetic conditions for the formation of the antibody-antigen complex as compared to the traditional ICA format: the reaction in this format is limited by the diffusion of immunoreagents in the porous structures of the test strip membrane [21].

Following immersion of the test strip in the sample mixed with the GNP conjugate, the mixture moves along the test strip coated with the reagents due to capillary action. If there are no analytes in the sample (Fig. 4a), antibodies will bind to the analytes attached to BSA. This will lead to the accumulation of gold particles on the TL and the appearance of a characteristic color. If one or both analytes are present in the sample (Fig. 4b), it (or they) will prevent the binding of the GNP conjugate to the BSA-conjugated analyte on the TL. As a result, the color of the TL will be dim or absent.

Since the assay conditions and milk sample composition can affect the visual interpretation of the result, we considered it necessary to use a control line as a standard for comparing coloring intensity. Therefore, the CL is colored due to the specific binding of the GNP–anti-IgY to chicken egg immunoglobulins IgY. Thus, the coloring intensity will be constant and independent of the fraction of the analyte conjugate retained on the CL.

The assay result is determined by comparing the brightness of the TL and CL. If the TL is brighter than the CL, the result is negative. If the TL is less bright than the CL, or their brightness is comparable, the result is positive. We considered the chosen method of result evaluation to be more acceptable taking into account the subjectivity of visual interpretation. This makes it possible to lower the detection limit of the assay when visually interpreting results, since a result will be considered to be positive not only in case of complete disappearance of the test line (typical for high analyte concentrations), but even in the case of a visible decrease in its intensity for relatively low analyte concentrations.

Conjugation of antibodies to GNPs

Secondary antibodies were conjugated to GNPs by physical adsorption at pH 8 and a concentration of 2 μg/mL. The selected parameters were obtained on the basis of an experiment to select optimal conditions (Fig. 5).

Preliminary experiments with the immobilization of antibodies to streptomycin on GNPs using secondary antibodies showed that the resulting conjugate was unstable. Within 24 h of conjugate preparation,

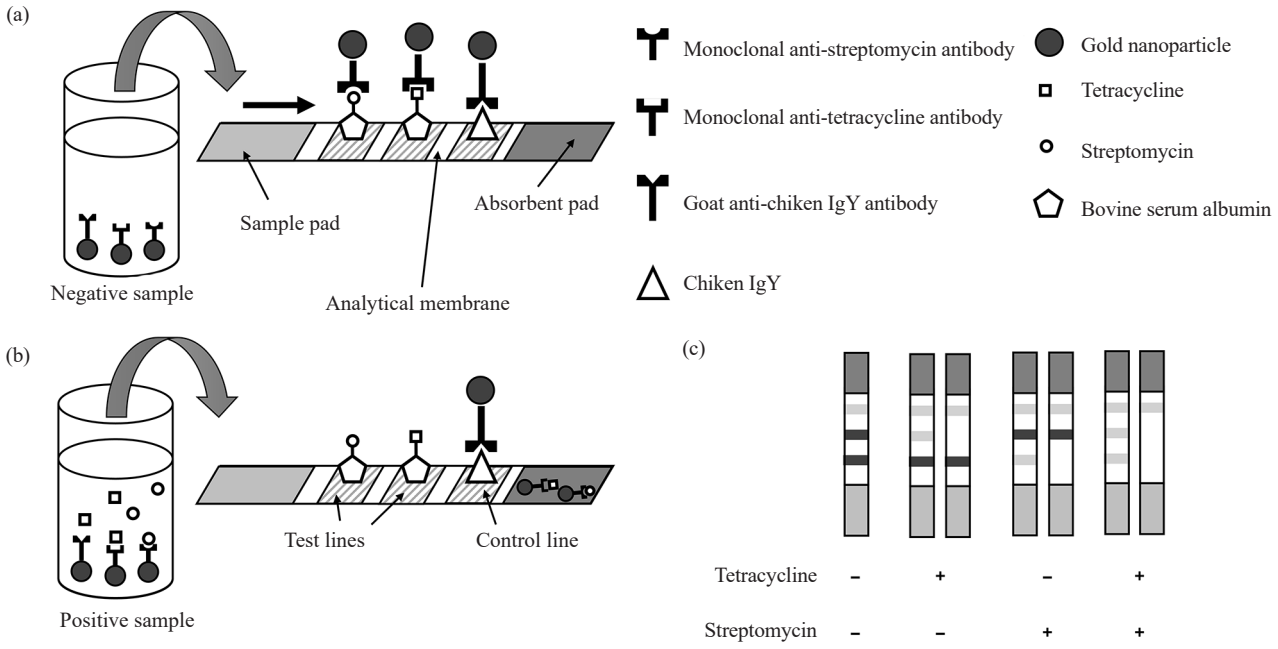

Fig. 4. Schematic diagram of the developed competitive ICA of tetracyclines and streptomycin.
(a) Negative sample; (b) positive sample; (c) result interpretation scheme

a statistically significant loss of activity was observed (Fig. 6, striped column, $p < 0.05$) along with significant aggregation, as evidenced by a decrease in the aggregation coefficient of the conjugate solution. When using two conjugates in the assay (GNP–anti-TET and GNP–anti-STR), an increase in the intensity of tetracycline coloring was observed upon the addition of streptomycin to the sample. We assume that both of these phenomena are due to the formation of nanoparticle aggregates caused by cross-linking via the binding of secondary antibodies carrying both streptomycin and tetracycline antibodies at the same time. As a result, when the sample contains streptomycin, the portion of the resulting polyvalent conjugate that was retained on the streptomycin line may migrate to the tetracycline line.

To prevent aggregation and the formation of polyvalent aggregates, we considered it rational to block unoccupied secondary antibody binding sites by using nonspecific mouse immunoglobulin G. A model experiment without specific antibodies to streptomycin and tetracycline showed that the dependence of aggregation on the amount of mouse

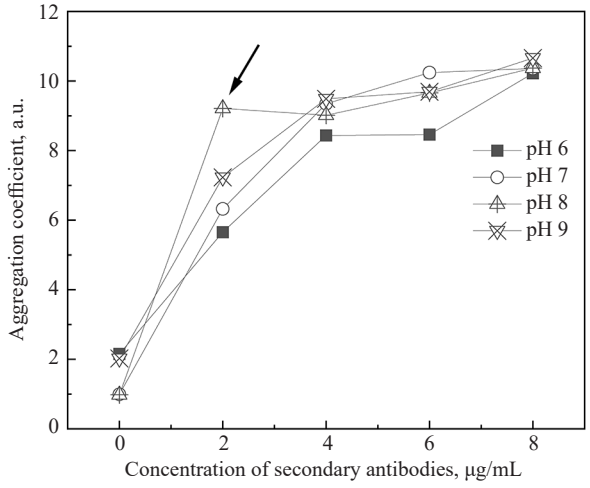

Fig. 5. Selection of optimal conditions for the sorption of antibodies to mouse immunoglobulins. The arrow indicates the selected concentration and pH value

antibodies administered was nonlinear and had a distinct minimum (Fig. 7). An increase in the degree of aggregation was observed in the concentration range of 1–7 μg/mL. This can be explained by the fact that, at low concentrations, the number of secondary antibody binding sites significantly exceeds the number of mouse antibodies, while the mouse antibodies themselves bind adjacent nanoparticles. Starting at a concentration of 9 μg/mL, a stabilizing effect occurred, which can be explained by the fact that the amount of mouse antibodies is now comparable to the number of secondary antibody binding sites to prevent the formation of large aggregates. When a concentration of 20 μg/mL was achieved, some aggregation was still observed ($p < 0.05$), but we considered it acceptable for further use (Fig. 7). The selected concentration was used to synthesize the GNP–anti-TET and GNP–anti-STR conjugates. The GNP–anti-STR conjugate prepared using blocking antibodies at a concentration of 20 μg/mL retained its functionality 24 h after preparation (Fig. 6, grey column). The next stage of work was to select the optimal concentrations of the test system immunoreagents to achieve the lowest detection limit.

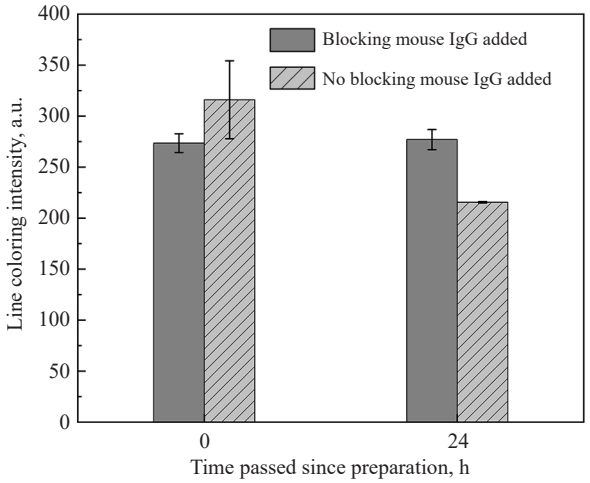

Fig. 6. Activity of the GNP–anti-STR conjugate
in the presence and in the absence of blocking immunoglobulins (20 μg/mL)

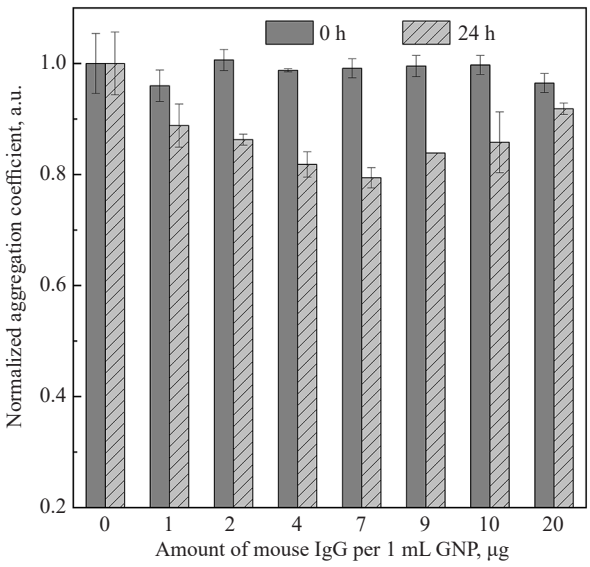

Fig. 7. Selection of the optimal concentration of mouse immunoglobulins for blocking free binding sites of secondary antibodies of the conjugate

Optimization of the detection limit

To achieve a low detection limit, we used well-known methodological approaches [22], which involved selecting the antibody-to-label ratio and immunoreagent concentrations (Table 1). Visual interpretation of the result involves comparing the brightness of the test lines with the control line. Therefore, when selecting the immunoreagent concentration, we aimed to ensure that the brightness of the control line was significantly lower.

The detection limit of the developed assay and a comparison with some previously published studies are presented in Table 2 and Fig. 8. According to the Technical Regulations of the Customs Union "On the Safety of Milk and Dairy Products" (TR CU 033/2013[2]), the maximum permissible concentrations of streptomycin and tetracycline antibiotics are 200 and 10 ng/mL, respectively. The achieved detection limits, which are deemed sufficient for use of the test system in accordance with TR CU 033/2013, are at the same level as previously published studies (Table 2).

Table 1. Selected immunoreagent amounts

Immunoreagent	Studied concentration range	Selected amount
BSA–TET	0.5–2.0 mg/mL	1 mg/mL
BSA–STR	0.1–1.0 mg/mL	0.2 mg/mL
GNP–anti-TET	10–20 μL	20 μL
GNP–anti-STR	10–20 μL	20 μL
GNP–anti-IgY	1–5 μL	3.5 μL
Anti-TET antibody	2–9 μg/mL	4 μg/mL
Anti-STR antibody	2–9 μg/mL	5 μg/mL
Mouse immunoglobulin	0–20 μg/mL	20 μg/mL

Table 2. Comparison of the developed ICA with published methods. Instrumental limit of detection (iLOD), visual limit of detection (vLOD)*

Antibiotic	Detection method	Sample type	iLOD, ng/mL	vLOD, ng/mL	References
Tetracycline	Fluorescence analysis	Water	750	–	[23]
		Buffer	2.86	–	[24]
	High performance liquid chromatography	Milk	21	–	[25]
	Enzyme-linked immunosorbent assay	Milk	IC_{50} = 0.72	–	[26]
	Colorimetric paper-based sensor with signal detection via smartphone imaging	Milk	0.5	–	[27]
	ICA	Human serum	0.4	11	[28]
		Milk	–	0.8	[29]
		Milk	Chlortetracycline		This work
			2.15	7.5	
			Oxytetracycline		
			0.29	2	

[2] Technical Regulations of the Customs Union "On the safety of milk and dairy products" (TR CU 033/2013) (as amended on June 23, 2023) (in Russ.). URL: https://docs.cntd.ru/document/499050562. Accessed June 14, 2025.

Table 2. Continued

Antibiotic	Detection method	Sample type	iLOD, ng/mL	vLOD, ng/mL	References
Tetracycline	ICA	Milk	Doxycycline		This work
			0.78	6	
			Tetracycline		
			1.27	4	
Streptomycin	Surface-enhanced Raman scattering	Milk	$2.13 \cdot 10^{-3}$	–	[30]
	Aggregation-based L-histidine functionalized GNP assay	Milk	0.66	–	[31]
	Electrochemical sensor	Milk	$0.33 \cdot 10^{-3}$	–	[32]
	Resolved fluorescence of nanoparticles in ICA	Milk	1.10 ng/g	–	[33]
	ICA	Milk	0.4	50	[34]
		Milk	1.34	25	This work

* The table does not aim to provide a comprehensive overview and includes only selected examples from the literature.

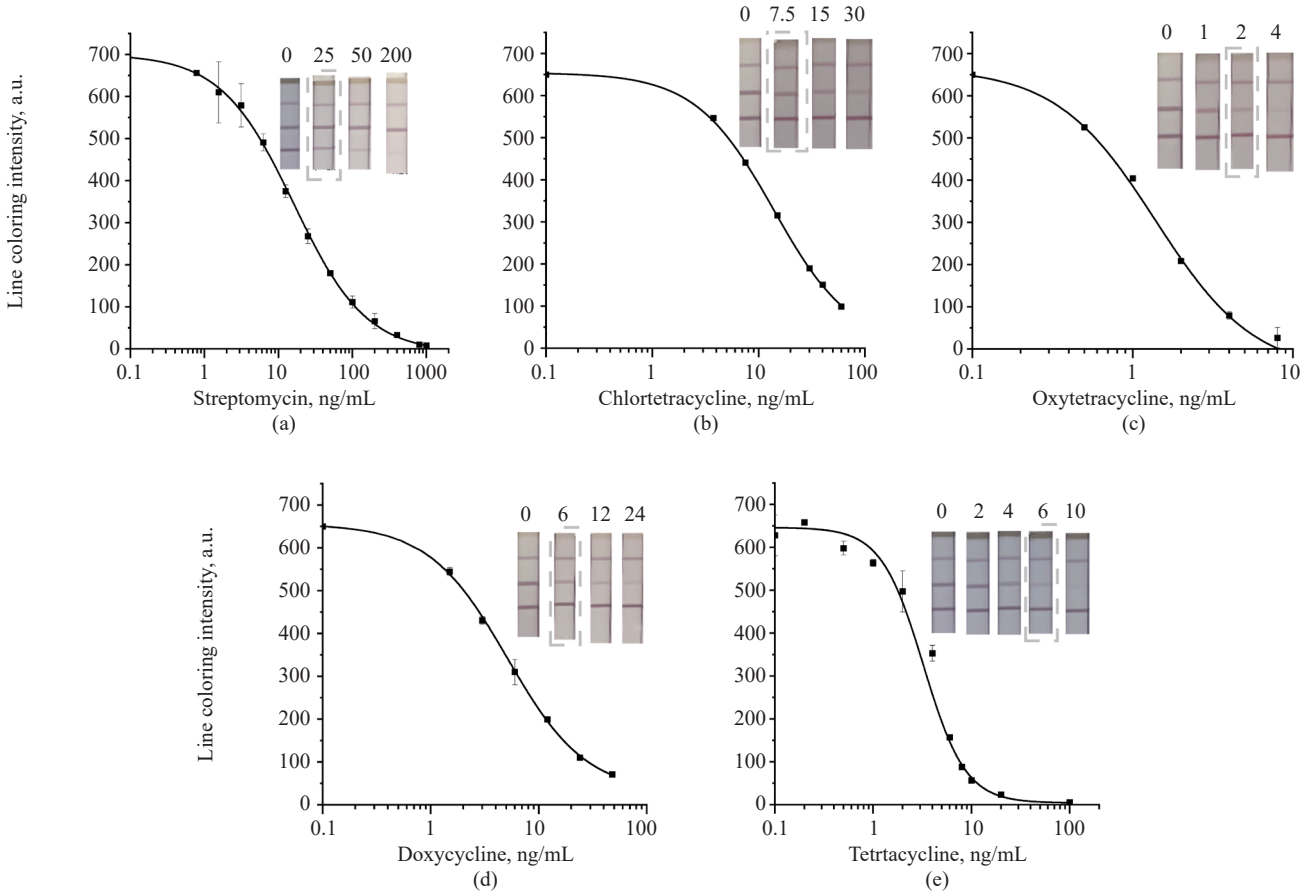

Fig. 8. Calibration curves showing the dependence of the test line color intensity on the concentration of streptomycin and tetracyclines in milk, and photographs of ICA results for the detection of (a) streptomycin, (b) chlortetracycline, (c) oxytetracycline, (d) doxycycline, and (e) tetracycline. The numbers above the photographs indicate the tested concentration of the corresponding analyte

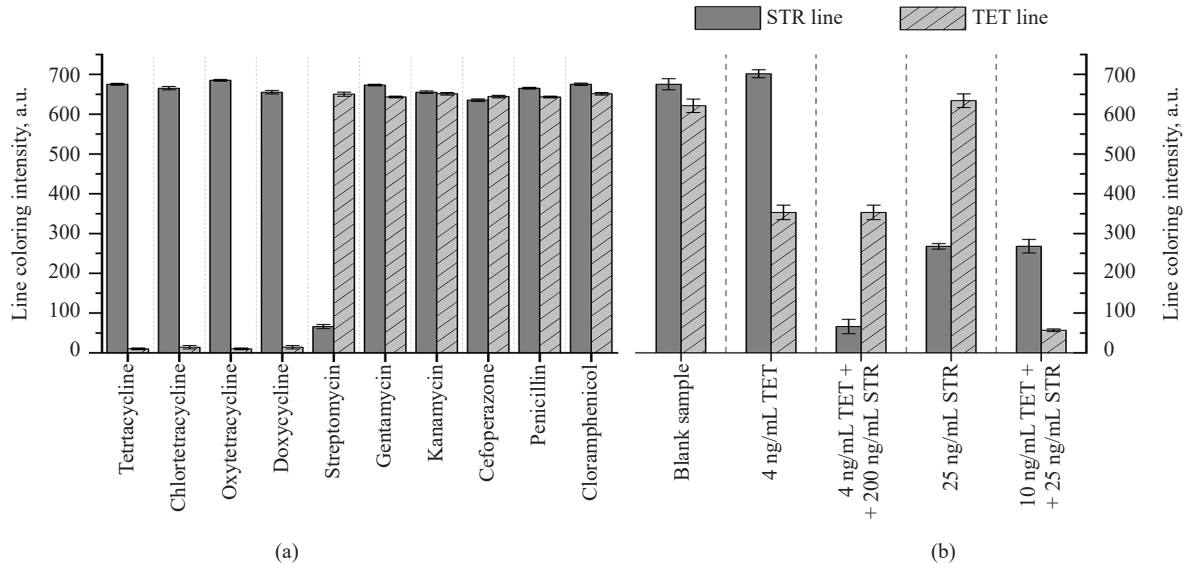

Fig. 9. (a) Assessment of the test system's cross-reactivity; (b) evaluation of the effect on the signal caused by the simultaneous presence of tetracycline and streptomycin in the sample

Additionally, the specificity of the developed assay to other aminoglycosides—gentamicin and kanamycin, as well as penicillin and chloramphenicol—was tested. No statistically significant effect of cross-reagents at a concentration of 1000 ng/mL in milk on the signal was demonstrated (Fig. 9a). The lack of cross-reactivity with aminoglycosides can be explained by the high specificity of antibodies to streptomycin and the more significant differences in the structures of the antibiotics under study. There was also no mutual interference between streptomycin and tetracycline (Fig. 9b).

CONCLUSIONS

A test system for the simultaneous detection of tetracyclines and streptomycin in undiluted milk has been developed. The visual detection limits for streptomycin, chlortetracycline, oxytetracycline, doxycycline, and tetracycline are 25, 7.5, 2, 6, and 4 ng/mL, respectively. By blocking the free centers of secondary antibodies, it becomes possible to improve the stability of the conjugates. The developed test system meets regulatory requirements and can be recommended for practical use in monitoring milk contamination with antibiotics. The methodological approaches used in this study for the simultaneous detection of tetracyclines and streptomycin are suitable for use in the development of a test system for the simultaneous detection of three or four groups of antibiotics.

Acknowledgments

The authors thank Maria Gennadievna Zavialova, a member of the Skoltech Advanced Mass Spectrometry Core Facility at the Skolkovo Institute of Science and Technology. We thank the *Rapid Bio* for providing the materials and equipment for the study.

Authors' contributions

I.V. Maksin—conceptual development of the study, interpretation and graphical presentation of the experimental data, processing results, and writing the text of the article.

D.I. Polyakova—selecting the ICA parameters and processing results.

V.A. Kesareva—selecting the ICA parameters and processing results.

A.A. Sysuev—synthesis of BSA conjugates with streptomycin and tetracycline.

V.S. Ivanov—methodological support for the study and discussion of the results.

E.I. Simonova—conceptual development of the study.

G.A. Khunteev—discussion of the results and conceptual development of the study.

Yu.G. Kirillova—conceptual development of the study, writing the text of the article, and discussion of the results.

Conflict interest declaration

Authors—I.V. Maksin, D.I. Polyakova, V.A. Kesareva, V.S. Ivanov, E.I. Simonova, and G.A. Khunteev—are employees of *Rapid Bio* (Moscow, Russia), a company engaged in the development and production of immunological test systems. This company provided financial support for this study. All authors confirm the absence of other potential conflicts of interest.

REFERENCES

1. Lu N., Chen J., Rao Z., Guo B., Xu Y. Recent Advances of Biosensors for Detection of Multiple Antibiotics. *Biosensors* (*Basel*). 2023;13(9):850. https://doi.org/10.3390/bios13090850
2. Panferov V.G., Safenkova I.V., Zherdev A.V., *et al.* Methods for Increasing Sensitivity of Immunochromatographic Test Systems with Colorimetric Detection (Review). *Appl. Biochem. Microbiol*. 2021;57(2):143–151. https://doi.org/10.1134/S0003683821020113
[Original Russian Text: Panferov V.G., Safenkova I.V., Zherdev A.V., Dzantiev B.B. Methods for Increasing Sensitivity of Immunochromatographic Test Systems with Colorimetric Detection (Review). *Prikladnaya biokhimiya i mikrobiologiya*. 2021;57(2):107–116 (in Russ.). https://doi.org/10.31857/S0555109921020112]
3. Lu Z.Y., Chan Y.H. The importance of antibody orientation for enhancing sensitivity and selectivity in lateral flow immunoassays. *Sens. Diagnost*. 2024;3(10):1613–1634. https://doi.org/10.1039/D4SD00206G
4. Sabzehmeidani M.M., Kazemzad M. Quantum dots based sensitive nanosensors for detection of antibiotics in natural products: A review. *Sci. Total Environ*. 2022;810:151997. https://doi.org/10.1016/j.scitotenv.2021.151997
5. Hendrikson O.D., Zvereva E.A., Zherdev A.V., Dzantiev B.B. Development of approaches for highly sensitive immunochromatographic detection of aquatic toxins in water and food products. *Baltiyskiy morskiy forum = Baltic Maritime Forum*. 2022. V 4. P. 39–49 (in Russ). https://elibrary.ru/dctmph
6. Liu C., Yang L., Zhang W., Li D., Li L., Wang H., Ma Y., Li C. A magnetic nanoparticle-based lateral flow immunochromatography assay for the rapid detection of fluoroquinolones in milk. *Eur. Food Res. Technol*. 2021;247(10):2645–2656. https://doi.org/10.1007/s00217-021-03820-z
7. Gubaidullina M.K., Urusov A.E., Zherdev A.V., *et al.* Immunochromatographic Test Systems using Anti-Species Antibodies–Colloidal Gold Conjugate: Their Features and Benefits on the Example of Ochratoxin A Detection. *Moscow Univ. Chem. Bull*. 2018;73(2):63–68. https://doi.org/10.3103/S0027131418020049
[Original Russian Text: Gubaidullina M.K., Urusov A.E., Zherdev A.V., Chuanlai K., Dzantiev B.B. Immunochromatographic Test Systems using Anti-Species Antibodies–Colloidal Gold Conjugate: Their Features and Benefits on the Example of Ochratoxin A Detection. *Vestnik Moskovskogo universiteta. Seriya 2. Khimiya.* 2018;59(2):144–150 (in Russ.).]
8. Gan S.Y., Tye G.J., Chew A.L., Ng W.K., Lai N.S. Linker-mediated oriented antibody immobilisation strategies for a more efficient immunosensor and diagnostic applications: A review. *Biosens. Bioelectron.: X*.: 2023;14:100379. https://doi.org/10.1016/j.biosx.2023.100379
9. Barshevskaya L.V., Sotnikov D.V., Zherdev A.V., Dzantiev B.B. Modular Set of Reagents in Lateral Flow Immunoassay: Application for Antibiotic Neomycin Detection in Honey. *Biosensors* (*Basel*). 2023;13(5):498. https://doi.org/10.3390/bios13050498

СПИСОК ЛИТЕРАТУРЫ

1. Lu N., Chen J., Rao Z., Guo B., Xu Y. Recent Advances of Biosensors for Detection of Multiple Antibiotics. *Biosensors* (*Basel*). 2023;13(9):850. https://doi.org/10.3390/bios13090850
2. Панфёров В.Г., Сафенкова И.В., Жердев А.В., Дзантиев Б.Б. Способы повышения чувствительности иммунохроматографических тест-систем с колориметрической детекцией (обзор). *Прикладная биохимия и микробиология*. 2021;57(2):107–116. https://doi.org/10.31857/S0555109921020112
3. Lu Z.Y., Chan Y.H. The importance of antibody orientation for enhancing sensitivity and selectivity in lateral flow immunoassays. *Sens. Diagnost*. 2024;3(10):1613–1634. https://doi.org/10.1039/D4SD00206G
4. Sabzehmeidani M.M., Kazemzad M. Quantum dots based sensitive nanosensors for detection of antibiotics in natural products: A review. *Sci. Total Environ*. 2022;810:151997. https://doi.org/10.1016/j.scitotenv.2021.151997
5. Гендриксон О.Д., Зверева Е.А., Жердев А.В., Дзантиев Б.Б. Разработка подходов для высокочувствительной иммунохроматографической детекции акватоксинов в воде и пищевых продуктах. В сб.: *Балтийский морской форум: материалы X Международного морского форума*. 2022. Т. 4. С. 39–49. https://elibrary.ru/dctmph
6. Liu C., Yang L., Zhang W., Li D., Li L., Wang H., Ma Y., Li C. A magnetic nanoparticle-based lateral flow immunochromatography assay for the rapid detection of fluoroquinolones in milk. *Eur. Food Res. Technol*. 2021;247(10):2645–2656. https://doi.org/10.1007/s00217-021-03820-z
7. Губайдуллина М.К., Урусов А.Е., Жердев А.В., Чуанлай К., Дзантиев Б.Б. Иммунохроматографические тест-системы с использованием конъюгата антивидовые антитела-коллоидное золото: особенности и возможности на примере определения охратоксина А. *Вестник Московского университета. Серия 2. Химия*. 2018;59(2):144–150.
8. Gan S.Y., Tye G.J., Chew A.L., Ng W.K., Lai N.S. Linker-mediated oriented antibody immobilisation strategies for a more efficient immunosensor and diagnostic applications: A review. *Biosens. Bioelectron.: X*.: 2023;14:100379. https://doi.org/10.1016/j.biosx.2023.100379
9. Barshevskaya L.V., Sotnikov D.V., Zherdev A.V., Dzantiev B.B. Modular Set of Reagents in Lateral Flow Immunoassay: Application for Antibiotic Neomycin Detection in Honey. *Biosensors* (*Basel*). 2023;13(5):498. https://doi.org/10.3390/bios13050498
10. Barshevskaya L.V., Zvereva E.A., Zherdev A.V., Dzantiev B.B. Highly Sensitive Lateral Flow Immunodetection of the Insecticide Imidacloprid in Fruits and Berries Reached by Indirect Antibody–Label Coupling. *Foods*. 2025;14(1):25. https://doi.org/10.3390/foods14010025
11. Zvereva E.A., Zherdev A.V., Aslamova A.A., Hendrickson O.D., Dzantiev B.B., Eremin S.A. Simple indirect immunochromatographic detection of herbicide 2,4-dichlorophenoxyacetic acid in fresh juices. *J. Food Compos. Analys*. 2025;140:107236. https://doi.org/10.1016/j.jfca.2025.107236

10. Barshevskaya L.V., Zvereva E.A., Zherdev A.V., Dzantiev B.B. Highly Sensitive Lateral Flow Immunodetection of the Insecticide Imidacloprid in Fruits and Berries Reached by Indirect Antibody–Label Coupling. *Foods*. 2025;14(1):25. https://doi.org/10.3390/foods14010025
11. Zvereva E.A., Zherdev A.V., Aslamova A.A., Hendrickson O.D., Dzantiev B.B., Eremin S.A. Simple indirect immunochromatographic detection of herbicide 2,4-dichlorophenoxyacetic acid in fresh juices. *J. Food Compos. Analys*. 2025;140:107236. https://doi.org/10.1016/j.jfca.2025.107236
12. Hendrickson O.D., Zvereva E.A., Zherdev A.V., Godjevargova T., Xu C., Dzantiev B.B. Development of a double immunochromatographic test system for simultaneous determination of lincomycin and tylosin antibiotics in foodstuffs. *Food Chem*. 2020;318:126510. https://doi.org/10.1016/j.foodchem.2020.126510
13. Bartosh A.V., Sotnikov D.V., Hendrickson O.D., Zherdev A.V., Dzantiev B.B. Design of Multiplex Lateral Flow Tests: A Case Study for Simultaneous Detection of Three Antibiotics. *Biosensors* (*Basel*). 2020;10(3):17. https://doi.org/10.3390/bios10030017
14. Huong N.T., Huyen H.T., Phong T.Q. Conjugation of tetracycline with carrier proteins and production of its polyclonal antibody for the development of rapid test. *Vietnam J. Sci. Technol*. 2024;62(1):23–34. https://doi.org/10.15625/2525-2518/17325
15. Kumar D., Mutreja I., Sykes P. Seed mediated synthesis of highly mono-dispersed gold nanoparticles in the presence of hydroquinone. *Nanotechnology*. 2016;27(35):355601. https://doi.org/10.1088/0957-4484/27/35/355601
16. Maksin I.V., Kuandykova A., Luzyanin T.A., *et al*. Increasing the Sensitivity of Immunochromatographic Assay for the Determination of Penicillin in Milk by Oriented Immobilization of Penicillin-Binding Protein on the Colloidal Gold Surface. *J. Anal. Chem*. 2025;80(6):1040–1051. https://doi.org/10.1134/S1061934825700388
[Original Russian Text: Maksin I.V., Kuandykova A., Luzyanin T.A., Ivanov V.S., Kirillova Yu.G., Khunteev G.A. Increasing the Sensitivity of Immunochromatographic Assay for the Determination of Penicillin in Milk by Oriented Immobilization of Penicillin-Binding Protein on the Colloidal Gold Surface. *Zhurnal analiticheskoi khimii*. 2025;80(6):545–557. https://doi.org/10.31857/S0044450225060021]
17. Uhrovčík J. Strategy for determination of LOD and LOQ values – Some basic aspects. *Talanta*. 2014;119:178–180. https://doi.org/10.1016/J.TALANTA.2013.10.061
18. Presolski S.I., Hong V.P., Finn M.G. Copper-Catalyzed Azide–Alkyne Click Chemistry for Bioconjugation. *Curr. Protoc. Chem. Biol*. 2011;3(4):153–162. https://doi.org/10.1002/9780470559277.ch110148
19. Burkin M.A., Gal'vidis I.A., Kononenko G.P. Methods for sanitary surveillance of livestock production. VII. Enzymoimmunoassay of streptomycin. *Sel'skokhozyaistvennaya Biologiya = Agricultural Biology*. 2012;47(6):109–115. https://doi.org/10.15389/agrobiology.2012.6.109eng
20. Bastús N.G., Comenge J., Puntes V. Kinetically controlled seeded growth synthesis of citrate-stabilized gold nanoparticles of up to 200 nm: Size focusing versus Ostwald ripening. *Langmuir*. 2011;27(17):11098–11105. https://doi.org/10.1021/la201938u
12. Hendrickson O.D., Zvereva E.A., Zherdev A.V., Godjevargova T., Xu C., Dzantiev B.B. Development of a double immunochromatographic test system for simultaneous determination of lincomycin and tylosin antibiotics in foodstuffs. *Food Chem*. 2020;318:126510. https://doi.org/10.1016/j.foodchem.2020.126510
13. Bartosh A.V., Sotnikov D.V., Hendrickson O.D., Zherdev A.V., Dzantiev B.B. Design of Multiplex Lateral Flow Tests: A Case Study for Simultaneous Detection of Three Antibiotics. *Biosensors* (*Basel*). 2020;10(3):17. https://doi.org/10.3390/bios10030017
14. Huong N.T., Huyen H.T., Phong T.Q. Conjugation of tetracycline with carrier proteins and production of its polyclonal antibody for the development of rapid test. *Vietnam J. Sci. Technol*. 2024;62(1):23–34. https://doi.org/10.15625/2525-2518/17325
15. Kumar D., Mutreja I., Sykes P. Seed mediated synthesis of highly mono-dispersed gold nanoparticles in the presence of hydroquinone. *Nanotechnology*. 2016;27(35):355601. https://doi.org/10.1088/0957-4484/27/35/355601
16. Максин И.В., Куандыкова А., Лузянин Т.А., Иванов В.С., Кириллова Ю.Г., Хунтеев Г.А. Повышение чувствительности иммунохроматографического анализа для определения пенициллина в молоке за счет ориентированной иммобилизации пенициллин-связывающего белка на поверхности коллоидного золота. *Журн. аналитической химии*. 2025;80(6):545–557. https://doi.org/10.31857/S0044450225060021
17. Uhrovčík J. Strategy for determination of LOD and LOQ values – Some basic aspects. *Talanta*. 2014;119:178–180. https://doi.org/10.1016/J.TALANTA.2013.10.061
18. Presolski S.I., Hong V.P., Finn M.G. Copper-Catalyzed Azide–Alkyne Click Chemistry for Bioconjugation. *Curr. Protoc. Chem. Biol*. 2011;3(4):153–162. https://doi.org/10.1002/9780470559277.ch110148
19. Буркин М.А., Гальвидис И.А., Кононенко Г.П. Методы санитарного контроля животноводческой продукции. Сообщение VII. Иммуноферментный анализ стрептомицина. *Сельскохозяйственная биология*. 2012;47(6):109–115. https://doi.org/10.15389/agrobiology.2012.6.109rus
20. Bastús N.G., Comenge J., Puntes V. Kinetically controlled seeded growth synthesis of citrate-stabilized gold nanoparticles of up to 200 nm: Size focusing versus Ostwald ripening. *Langmuir*. 2011;27(17):11098–11105. https://doi.org/10.1021/la201938u
21. Zherdev A.V., Zvereva E.A., Taranova N.A., Safenkova I.V., Vostrikova N.L., Dzantiev B.B. Immunochromatographic food control tools: New developments and practical prospects. *Theory and Practice of Meat Processing*. 2024;9(4):280–295. https://doi.org/10.21323/2414-438X-2024-9-4-280-295
22. Zvereva E.A., Byzova N.A., Sveshnikov P.G., Zherdev A.V., Dzantiev B.B. Cut-off on demand: adjustment of the threshold level of an immunochromatographic assay for chloramphenicol. *Anal. Methods*. 2015;7(15):6378–6384. https://doi.org/10.1039/c5ay00835b
23. Guo J., Xin J., Wang J., Li Z., Yang J., Yu X., Yan M., Mo J. A high-efficiency and selective fluorescent assay for the detection of tetracyclines. *Sci Rep*. 2024;14(1):22918. https://doi.org/10.1038/s41598-024-74411-7
24. Han L., Fan Y.Z., Qing M., Liu S.G., Yang Y.Z., Li N.B., Luo H.Q. Smartphones and Test Paper-Assisted Ratiometric

21. Zherdev A.V., Zvereva E.A., Taranova N.A., Safenkova I.V., Vostrikova N.L., Dzantiev B.B. Immunochromatographic food control tools: New developments and practical prospects. *Theory and Practice of Meat Processing*. 2024;9(4):280–295. https://doi.org/10.21323/2414-438X-2024-9-4-280-295
22. Zvereva E.A., Byzova N.A., Sveshnikov P.G., Zherdev A.V., Dzantiev B.B. Cut-off on demand: adjustment of the threshold level of an immunochromatographic assay for chloramphenicol. *Anal. Methods*. 2015;7(15):6378–6384. https://doi.org/10.1039/c5ay00835b
23. Guo J., Xin J., Wang J., Li Z., Yang J., Yu X., Yan M., Mo J. A high-efficiency and selective fluorescent assay for the detection of tetracyclines. *Sci Rep*. 2024;14(1):22918. https://doi.org/10.1038/s41598-024-74411-7
24. Han L., Fan Y.Z., Qing M., Liu S.G., Yang Y.Z., Li N.B., Luo H.Q. Smartphones and Test Paper-Assisted Ratiometric Fluorescent Sensors for Semi-Quantitative and Visual Assay of Tetracycline Based on the Target-Induced Synergistic Effect of Antenna Effect and Inner Filter Effect. *ACS Appl. Mater. Interfaces*. 2020;12(41):47099–47107. https://doi.org/10.1021/acsami.0c15482
25. Moudgil P., Bedi J.S., Aulakh R.S., Gill J.P.S., Kumar A. Validation of HPLC Multi-residue Method for Determination of Fluoroquinolones, Tetracycline, Sulphonamides and Chloramphenicol Residues in Bovine Milk. *Food Anal. Methods*. 2019;12(2):338–346. https://doi.org/10.1007/s12161-018-1365-0
26. Chen Y., Kong D., Liu L., Song S., Kuang H., Xu C. Development of an ELISA and Immunochromatographic Assay for Tetracycline, Oxytetracycline, and Chlortetracycline Residues in Milk and Honey Based on the Class-Specific Monoclonal Antibody. *Food Anal. Methods*. 2016;9(4): 905–914. https://doi.org/10.1007/s12161-015-0262-z
27. Wang X., Li J., Jian D., Zhang Y., Shan Y., Wang S., Liu F. Paper-based antibiotic sensor (PAS) relying on colorimetric indirect competitive enzyme-linked immunosorbent assay for quantitative tetracycline and chloramphenicol detection. *Sens. Actuators B: Chem*. 2021;329:129173. https://doi.org/10.1016/j.snb.2020.129173
28. Berlina A.N., Bartosh A.V., Zherdev A.V., Xu C., Dzantiev B.B. Development of Immunochromatographic Assay for Determination of Tetracycline in Human Serum. *Antibiotics*. 2018;7(4):99. https://doi.org/10.3390/antibiotics7040099
29. Tian Y., Bu T., Zhang M., Sun X., Jia P., Wang Q., Liu Y., Bai F., Zhao S., Wang L. Metal-polydopamine framework based lateral flow assay for high sensitive detection of tetracycline in food samples. *Food Chem*. 2021;339:127854. https://doi.org/10.1016/j.foodchem.2020.127854
30. Wang X., Chen C., Waterhouse G.I.N., Qiao X., Xu Z. Ultra-sensitive detection of streptomycin in foods using a novel SERS switch sensor fabricated by AuNRs array and DNA hydrogel embedded with DNAzyme. *Food Chem*. 2022;393:133413. https://doi.org/10.1016/j.foodchem.2022.133413
31. Shinde S.K., Kim D.Y., Saratale R.G., Kadam A.A., Saratale G.D., Syed A., Bahkali A.H., Ghodake G.S. Histidine Functionalized Gold Nanoparticles for Screening Aminoglycosides and Nanomolar Level Detection of Streptomycin in Water, Milk, and Whey. *Chemosensors*. 2021;9(12):358. https://doi.org/10.3390/chemosensors9120358
32. Roushani M., Ghanbari K. An electrochemical aptasensor for streptomycin based on covalent attachment of the aptamer onto a mesoporous silica thin film-coated gold electrode. *Microchim. Acta*. 2019;186(2):115. https://doi.org/10.1007/s00604-018-3191-x
33. Jiang J., Luo P., Liang J., Shen X., Lei H., Li X. A highly sensitive and quantitative time resolved fluorescent microspheres lateral flow immunoassay for streptomycin and dihydrostreptomycin in milk, honey, muscle, liver, and kidney. *Anal. Chim. Acta*. 2022;1192:339360. https://doi.org/10.1016/j.aca.2021.339360
34. Zhou J., Nie W., Chen Y., Yang C., Gong L., Zhang C., Chen Q., He L., Feng X. Quadruplex gold immunochromatogaraphic assay for four families of antibiotic residues in milk. *Food Chem*. 2018;256:304–310. https://doi.org/10.1016/j.foodchem.2018.02.002

32. Roushani M., Ghanbari K. An electrochemical aptasensor for streptomycin based on covalent attachment of the aptamer onto a mesoporous silica thin film-coated gold electrode. *Microchim. Acta*. 2019;186(2):115. https://doi.org/10.1007/s00604-018-3191-x
33. Jiang J., Luo P., Liang J., Shen X., Lei H., Li X. A highly sensitive and quantitative time resolved fluorescent microspheres lateral flow immunoassay for streptomycin and dihydrostreptomycin in milk, honey, muscle, liver, and kidney. *Anal. Chim. Acta*. 2022;1192:339360. https://doi.org/10.1016/j.aca.2021.339360
34. Zhou J., Nie W., Chen Y., Yang C., Gong L., Zhang C., Chen Q., He L., Feng X. Quadruplex gold immunochromatogaraphic assay for four families of antibiotic residues in milk. *Food Chem*. 2018;256:304–310. https://doi.org/10.1016/j.foodchem.2018.02.002

About the Authors

Ivan V. Maksin, Postgraduate Student, Department of Biotechnology and Industrial Pharmacy, M.V. Lomonosov Institute of Fine Chemical Technologies, MIREA – Russian Technological University (78, Vernadskogo pr., Moscow, 119454, Russia); Research Scientist, Rapid Bio, (42/1, Bol'shoi bul., Moscow, 121205, Russia). E-mail: maxinivanv@gmail.com. RSCI SPIN-code 1550-5855, https://orcid.org/0009-0007-9730-1465

Darya I. Polyakova, Student, Institute of Pharmacy and Biotechnology, Patrice Lumumba Peoples' Friendship University of Russia (RUDN University) (6, Miklukho-Maklaya ul., Moscow, 117198, Russia); Laboratory Assistant, Rapid Bio, (42/1, Bol'shoi bul., Moscow, 121205, Russia). E-mail: dpolyakova@drdbiotech.ru. https://orcid.org/0009-0007-8354-6883

Viktoriya A. Kesareva, Student, Institute of Pharmacy and Biotechnology, Patrice Lumumba Peoples' Friendship University of Russia (RUDN University) (6, Miklukho-Maklaya ul., Moscow, 117198, Russia); Laboratory Assistant, Rapid Bio, (42/1, Bol'shoi bul., Moscow, 121205, Russia). E-mail: vkesareva@drdbiotech.ru. https://orcid.org/0000-0001-6544-4057

Alexander A. Sysuev, Assistant, Department of Biotechnology and Industrial Pharmacy, M.V. Lomonosov Institute of Fine Chemical Technologies, MIREA – Russian Technological University (78, Vernadskogo pr., Moscow, 119454, Russia). E-mail: sysuev@mirea.ru. https://orcid.org/0009-0007-8233-4221

Vladislav S. Ivanov, Leading Research Scientist, Rapid Bio, (42/1, Bol'shoi bul., Moscow, 121205, Russia). E-mail: vivanov@drdbiotech.ru. https://orcid.org/0000-0003-1025-2714

Evgeniya I. Simonova, Postgraduate Student, Department of Veterinary Medicine, Agro-Technological Institute, Patrice Lumumba Peoples' Friendship University of Russia (RUDN University) (6, Miklukho-Maklaya ul., Moscow, 117198, Russia); Project Director, Rapid Bio, (42/1, Bol'shoi bul., Moscow, 121205, Russia). E-mail: simonova1999@yandex.ru. Scopus Author ID 57222665772, RSCI SPIN-code 9612-6527, https://orcid.org/0000-0001-7798-3859

German A. Khunteev, Can. Sci. (Med.), Director of Science, Rapid Bio, (42/1, Bol'shoi bul., Moscow, 121205, Russia). E-mail: gk@drdbiotech.ru. Scopus Author ID 7801430884, ResearcherID AAC-4456-2019, RSCI SPIN-code 6573-5340, https://orcid.org/0000-0001-8182-1836

Yulia G. Kirillova, Can. Sci. (Chem.), Associate Professor, Department of Biotechnology and Industrial Pharmacy, M.V. Lomonosov Institute of Fine Chemical Technologies, MIREA – Russian Technological University (78, Vernadskogo pr., Moscow, 119454, Russia). E-mail: dryulets@mail.ru. Scopus Author ID 9332799900, ResearcherID F-5697-2016, RSCI SPIN-code 7949-6038, https://orcid.org/0000-0002-0988-8515

Об авторах

Максин Иван Владимирович, аспирант, кафедра биотехнологии и промышленной фармации, Институт тонких химических технологий им. М.В. Ломоносова, ФГБОУ ВО «МИРЭА – Российский технологический университет» (119454, Россия, Москва, пр-т Вернадского, д. 78); ученый-исследователь, ООО «Рапид Био» (121205, Россия, Москва, Большой бульвар, д. 42, стр. 1). E-mail: maxinivanv@gmail.com. SPIN-код РИНЦ 1550-5855, https://orcid.org/0009-0007-9730-1465

Полякова Дарья Ивановна, студент, Институт фармации и биотехнологии, ФГАОУ ВО «Российский университет дружбы народов имени Патриса Лумумбы» (РУДН) (117198, Россия, Москва, ул. Миклухо-Маклая, д. 6); лаборант, ООО «Рапид Био» (121205, Россия, Москва, Большой бульвар, д. 42, стр. 1). E-mail: dpolyakova@drdbiotech.ru. https://orcid.org/0009-0007-8354-6883

Кесарева Виктория Александровна, студент, Институт фармации и биотехнологии, ФГАОУ ВО «Российский университет дружбы народов имени Патриса Лумумбы» (РУДН) (117198, Россия, Москва, ул. Миклухо-Маклая, д. 6); лаборант, ООО «Рапид Био» (121205, Россия, Москва, Большой бульвар, д. 42, стр. 1). E-mail: vkesareva@drdbiotech.ru. https://orcid.org/0000-0001-6544-4057

Сысуев Александр Анатольевич, ассистент, кафедра биотехнологии и промышленной фармации, Институт тонких химических технологий им. М.В. Ломоносова, ФГБОУ ВО «МИРЭА – Российский технологический университет» (119454, Россия, Москва, пр-т Вернадского, д. 78). E-mail: sysuev@mirea.ru. https://orcid.org/0009-0007-8233-4221

Иванов Владислав Сергеевич, ведущий ученый-исследователь, ООО «Рапид Био» (121205, Россия, Москва, Большой бульвар, д. 42, стр. 1). E-mail: vivanov@drdbiotech.ru. https://orcid.org/0000-0003-1025-2714

Симонова Евгения Игоревна, аспирант, Департамент ветеринарной медицины, Аграрно-технологический институт, ФГАОУ ВО «Российский университет дружбы народов имени Патриса Лумумбы» (РУДН) (117198, Россия, Москва, ул. Миклухо-Маклая, д. 6); директор по проектам, ООО «Рапид Био» (121205, Россия, Москва, Большой бульвар, д. 42, стр. 1). E-mail: simonova1999@yandex.ru. Scopus Author ID 57222665772, SPIN-код РИНЦ 9612-6527, https://orcid.org/0000-0001-7798-3859

Хунтеев Герман Анатольевич, к.м.н., директор по науке, ООО «Рапид Био» (121205, Россия, Москва, Большой бульвар, д. 42, стр. 1). E-mail: gk@drdbiotech.ru. Scopus Author ID 7801430884, ResearcherID AAC-4456-2019, SPIN-код РИНЦ 6573-5340, https://orcid.org/0000-0001-8182-1836

Кириллова Юлия Геннадьевна, к.х.н., доцент, кафедра биотехнологии и промышленной фармации, Институт тонких химических технологий им. М.В. Ломоносова, ФГБОУ ВО «МИРЭА – Российский технологический университет» (119454, Россия, Москва, пр-т Вернадского, д. 78). E-mail: dryulets@mail.ru. Scopus Author ID 9332799900, ResearcherID F-5697-2016, SPIN-код РИНЦ 7949-6038, https://orcid.org/0000-0002-0988-8515

Translated from Russian into English by M. Povorin
Edited for English language and spelling by Thomas A. Beavitt

Tonkie Khimicheskie Tekhnologii = Fine Chemical Technologies.
2025;20(6):582–593
ISSN 2686-7575 (Online)

Biochemistry and biotechnology
Биохимия и биотехнология

UDC 60
https://doi.org/10.32362/2410-6593-2025-20-6-582-593
EDN VKKHOP

RESEARCH ARTICLE

Comparative analysis of three genetic constructs for delivery and expression of a modified single-domain antibody gene in rAAV

Ekaterina I. Ryabova[1], ✉, Artem A. Derkaev[1], Ilias B. Esmagambetov[1], Mikhail A. Dovgiy[1], Anton A. Blinov[1], Roza M. Hossain[1], Oleg E. Dmitriev[1], Dmitry S. Polyansky[2], Anatoly N. Noskov[1], Dmitry V. Shcheblyakov[1], Denis Y. Logunov[1], Alexander L. Gintsburg[1]

[1] *N.F. Gamaleya National Research Center for Epidemiology and Microbiology, Ministry of Health of the Russian Federation, Moscow, 123098 Russia*

[2] *MIREA – Russian Technological University (M.V. Lomonosov Institute of Fine Chemical Technologies), Moscow, 119454 Russia*

✉ *Corresponding author, e-mail: ryabovaei96@gmail.com*

Abstract

Objectives. To obtain and compare the efficiency of three recombinant adeno-associated virus (rAAV) variants expressing the gene of the modified single-domain antibody B11-Fc specific to botulinum toxin type A (BoNT/A): rAAV-DJ-CMV-B11-Fc, rAAV-DJ-CASI-B11-Fc, and scAAV-DJ-CMV-B11-Fc.

Methods. The AAV-DJ Packaging System (*Cell Biolabs*, USA) was used to create target constructs and obtain rAAV. Expression of the B11-Fc antibody gene in the obtained rAAV was assessed *in vitro* (HEK293, CHO-S, and C2C12 cell lines) and *in vivo* (BALB/c mice) using biolayer interferometry. The protective properties of the drugs were investigated on the model of lethal intoxication of mice with BoNT/A.

Results. The rAAV-DJ-CMV-B11-Fc drug demonstrated a high level of B11-Fc antibody production both *in vitro* and *in vivo* without a significant decrease in concentration for at least 6 months. Comparable levels of B11-Fc production were demonstrated by rAAV-DJ-CASI-B11-Fc and scAAV-DJ-CMV-B11-Fc drugs in both *in vitro* and *in vivo* studies, with the exception of C2C12 cells, where rAAV-DJ-CASI-B11-Fc demonstrated the highest efficacy. When investigating the protective activity of the drugs against a lethal dose of BoNT/A, it was found that rAAV-DJ-CASI-B11-Fc possessed more pronounced activity in the first two days following administration as compared to rAAV-DJ-CMV-B11-Fc. However, at later stages, starting from 3 months, the rAAV-DJ-CMV-B11-Fc drug product demonstrated the most pronounced protection against high doses of BoNT/A.

Conclusions. The obtained data show that rAAV-DJ-CASI-B11-Fc should be used for the induction of protection against BoNT/A at early stages (24–48 h) after administration, whereas for protection against the highest doses of BoNT/A in the long term, rAAV-DJ-CMV-B11-Fc should be used. Studies into the specific activity of the drugs at later stages after administration are still ongoing.

Keywords

rAAV, adeno-associated virus, single-domain antibodies, botulism, passive immunization, prophylaxis

Submitted: 03.09.2025
Revised: 23.09.2025
Accepted: 11.11.2025

For citation

Ryabova E.I., Derkaev A.A., Esmagambetov I.B., Dovgiy M.A., Blinov A.A., Hossain R.M., Dmitriev O.E., Polyansky D.S., Noskov A.N., Shcheblyakov D.V., Logunov D.Y., Gintsburg A.L. Comparative analysis of three genetic constructs for delivery and expression of a modified single-domain antibody gene in rAAV. *Tonk. Khim. Tekhnol. = Fine Chem. Technol.* 2025;20(6):582–593. https://doi.org/10.32362/2410-6593-2025-20-6-582-593

НАУЧНАЯ СТАТЬЯ

Сравнительный анализ трех генетических конструкций для доставки и экспрессии гена модифицированного однодоменного антитела в составе rAAV

Е.И. Рябова[1,✉], А.А. Деркаев[1], И.Б. Есмагамбетов[1], М.А. Довгий[1], А.А. Блинов[1], Р.М. Хоссаин[1], О.Е. Дмитриев[1], Д.С. Полянский[2], А.Н. Носков[1], Д.В. Щебляков[1], Д.Ю. Логунов[1], А.Л. Гинцбург[1]

[1] *Национальный исследовательский центр эпидемиологии и микробиологии им. Н.Ф. Гамалеи Министерства Здравоохранения Российской Федерации, Москва, 123098 Россия*

[2] *МИРЭА – Российский технологический университет (Институт тонких химических технологий им. М.В. Ломоносова), Москва, 119454 Россия*

✉ *Автор для переписки, e-mail: ryabovaei96@gmail.com*

Аннотация

Цели. Получить и сравнить эффективность трех вариантов rAAV, экспрессирующих ген модифицированного однодоменного антитела B11-Fc, специфичного к ботулиническому токсину типа A (BoNT/A) — rAAV-DJ-CMV-B11-Fc, rAAV-DJ-CASI-B11-Fc и scAAV-DJ-CMV-B11-Fc.

Методы. Для создания целевых конструкций и получения rAAV использовали систему AAV-DJ Packaging System (*Cell Biolabs*, США). Экспрессию гена антитела B11-Fc в составе полученных rAAV оценивали *in vitro* (клеточные линии HEK293, CHO-S и C2C12) и *in vivo* (мыши линии BALB/c) при помощи биослойной интерферометрии. Защитные свойства препаратов изучали на модели летальной интоксикации мышей BoNT/A.

Результаты. Препарат rAAV-DJ-CMV-B11-Fc показал высокий уровень продукции антитела B11-Fc как *in vitro*, так и *in vivo* без значимого снижения концентрации в течение как минимум 6 месяцев. Препараты rAAV-DJ-CASI-B11-Fc и scAAV-DJ-CMV-B11-Fc показали сравнимый уровень продукции B11-Fc как *in vitro* и *in vivo*, за исключением клеток C2C12, где rAAV-DJ-CASI-B11-Fc показал самую высокую эффективность. При изучении защитной активности препаратов против летальной дозы BoNT/A продемонстрировано, что в первые двое суток rAAV-DJ-CASI-B11-Fc и scAAV-DJ-CMV-B11-Fc обладают более выраженной активностью по сравнению с rAAV-DJ-CMV-B11-Fc. Однако на более поздних сроках, начиная с 3 месяца, препарат rAAV-DJ-CMV-B11-Fc демонстрирует наиболее выраженную защиту против высоких доз BoNT/A.

Выводы. Полученные в ходе исследования данные показывают, что для индукции защиты от BoNT/A на ранних сроках (24–48 ч) после введения следует применять препарат rAAV-DJ-CASI-B11-Fc, тогда как для индукции защиты от максимально высоких доз BoNT/A в долгосрочной перспективе следует использовать rAAV-DJ-CMV-B11-Fc. Исследования специфической активности препаратов на более поздних сроках после введения продолжаются.

Ключевые слова

rAAV, аденоассоциированный вирус, однодоменные антитела, ботулизм, пассивная иммунизация, профилактика

Поступила: 03.09.2025
Доработана: 23.09.2025
Принята в печать: 11.11.2025

Для цитирования

Рябова Е.И., Деркаев А.А., Есмагамбетов И.Б., Довгий М.А., Блинов А.А., Хоссаин Р.М., Дмитриев О.Е., Полянский Д.С., Носков А.Н., Щебляков Д.В., Логунов Д.Ю., Гинцбург А.Л. Сравнительный анализ трех генетических конструкций для доставки и экспрессии гена модифицированного однодоменного антитела в составе rAAV. *Тонкие химические технологии*. 2025;20(6):582–593. https://doi.org/10.32362/2410-6593-2025-20-6-582-593

INTRODUCTION

Recombinant adeno-associated virus (rAAV) vectors are an excellent tool not only for developing gene therapy agents, but also for creating preventive measures against infectious diseases based on passive genetic immunization. This principle is based on the delivery and long-term expression of neutralizing antibody genes specific to a particular pathogen. This approach has proven effective in creating preventive measures for influenza, COVID-19, HIV infection and other diseases [1, 2]. The effectiveness of rAAV-based passive genetic immunization drugs depends significantly on the design of the genetic construct used to ensure the expression of the neutralizing antibody gene.

In a previous study, we obtained an rAAV that provides long-term expression of the gene for the neutralizing modified single-domain antibody B11-Fc[1] (rAAV-B11-Fc). It was experimentally established that a single administration of rAAV-B11-Fc provides complete protection to animals from a lethal dose of botulinum neurotoxin serotype A for at least 120 days [3]. This study is a continuation of the aforementioned article and focuses on selecting the optimal genetic construct for delivering and expressing the B11-Fc antibody gene within an rAAV and developing a prototype candidate drug for genetic passive immunization and botulism prevention.

Thus, the aim of the present study is to obtain and compare the effectiveness of three rAAV constructs expressing the B11-Fc antibody gene, which is specific for botulinum toxin type A (BoNT/A): rAAV-DJ[2]-CMV-B11-Fc, rAAV-DJ-CASI-B11-Fc, and scAAV-DJ-CMV-B11-Fc. For convenience and clarity, rAAV-DJ-CMV-B11-Fc is used to refer to the previously used construct [3] for carrying the gene for the modified B11-Fc single-domain antibody [4] under the control of the CMV promoter (Cytomegalovirus promoter). rAAV-DJ-CASI-B11-Fc is a construct similar in structure but including the CASI[3]-promoter, representing a synthetic hybrid promoter that contains elements from CMV, chicken β-actin, and the UbC (Ubiquitin C) intron, as well as the woodchuck hepatitis virus (WHV) posttranscriptional regulatory element (WPRE), which enhances mRNA stability and expression levels. scAAV-DJ-CMV-B11-Fc is a self-complementary form of the vector expressing the B11-Fc gene under the control of the CMV promoter.

MATERIALS AND METHODS

Obtaining rAAV drugs. The rAAV-DJ-CMV-B11-Fc drug was obtained using plasmids as previously described [3]. The rAAV-DJ-CASI-B11-Fc drug was obtained using pAAV-CASI-B11-Fc, pAAV-DJ-vector (*Cell Biolabs*, USA), and pHelper Vector (*Cell Biolabs*, USA) plasmids. The pAAV-CASI-B11-Fc construct was obtained by synthesizing the CASI promoter sequence along with cloning sites and the WPRE sequence and polyadenylation signal at *Eurogen* (Russia), followed by cloning of the synthesized sequence between the left and right inverted terminal repeats (ITR), with replacing the existing expression cassette. The scAAV-DJ-CMV-B11-Fc drug was obtained using the plasmids pscAAV-CMV-B11-Fc, pAAV-DJ-vector (*Cell Biolabs*, USA), and pHelper Vector (*Cell Biolabs*, USA). The pscAAV-CMV-B11-Fc plasmid was obtained by cloning the B11-Fc gene sequence into the pscAAV-MCS plasmid (*Cell Biolabs*, USA).

To obtain rAAV vectors, the Human Embryonic Kidney 293 (HEK293) cell line (from the cell culture collection of the N.F. Gamaleya National Research Center for Epidemiology and Microbiology of the Ministry of Health of Russia) was used. Cultivation and transfection were performed as previously described under adherent conditions at 37°C and 5% CO_2 [3, 5]. Viral products were purified using affinity chromatography (AC) on the POROS CaptureSelect AAVX Affinity Resin sorbent (*Thermo Fisher Scientific*, USA) according to the manufacturer's instructions. Further purification and buffer exchange were performed using size exclusion chromatography (SEC) on an XK 26/100 column packed with Superdex 200 sorbent (*Cytiva*, USA). Final formulation of the drugs was performed using 100 kDa Amicon Ultra-15 centrifugal concentrators (*Merck*, USA). The quantity and quality of the obtained drugs were studied as described in [5].

The specific activity of rAAV drugs *in vitro*. HEK293 cells, CHO-S (serum-free suspension-adapted Chinese hamster ovary cells) (*Thermo Fisher Scientific*, USA, Cat. No. R80007), and C2C12 (a mouse C3H myoblast cell line) (ATCC® CRL-1772™) were transduced at a dose of 10^5 vg/cell. Culture fluid samples were collected at 96 and 144 h. The concentration of B11-Fc in the culture medium was determined by biolayer interferometry (BLI) using an OctetRED96e System (*Fortebio*, USA) and Anti-Human IgG Fc sensors (*Fortebio*, USA).

[1] B11-Fc is a single-domain antibody modified with a human IgG1 Fc fragment.

[2] rAAV-DJ is recombinant Adeno-Associated Virus (rAAV) with a DJ-type capsid, which is a synthetic (chimeric) serotype created by DNA shuffling from eight different natural AAV serotypes.

[3] CASI-promoter is a synthetic (chimeric) promoter. It consists of the CMV enhancer, the chicken β-actin promoter (CAG), and the UbC enhancer.

Specific activity of rAAV drugs *in vivo*. Female BALB/c inbred mice (6 weeks old, 18–20 g) (Scientific Center for Biomedical Technologies of the Federal Medical Biological Agency of Russia, Andreevka branch) were administered rAAV at a dose of 10^{11} vg/animal intramuscularly. Blood was collected at key time points. The concentration of B11-Fc in serum was determined similarly to the *in vitro* experiment. The protective activity of the drugs against BoNT/A was studied as described in [3, 6]. The study was conducted in a vivarium under standard conditions: polycarbonate cages, stocking density up to 5 animals per cage. Feeding was carried out with complete pelleted feed (*ad libitum*) with access to water. All procedures were performed in accordance with the protocol approved by the local ethics committee of the N.F. Gamaleya National Research Center for Epidemiology and Microbiology (protocol No. 11 dated June 25, 2021).

Statistical analysis. Statistical analysis was performed using GraphPad Prism 9.0 software (*Dotmatics*, USA). Survival was analyzed using the Kaplan–Meier method with the log-rank test. Significance level $p < 0.05$.

RESULTS AND DISCUSSION

Design of genetic constructs and production of rAAV drugs

The desired level, stability, and specificity of tissue expression are determined by *cis*-acting elements of rAAV vectors, including promoters. In this study, we investigated the efficiency of B11-Fc antibody expression within rAAV vectors carrying three different genetic constructs: rAAV-DJ-CMV-B11-Fc, rAAV-DJ-CASI-B11-Fc, and scAAV-DJ-CMV-B11-Fc.

The CMV promoter is widely used due to its high expression in various cells (e.g., human colon carcinoma HCT116, colorectal adenocarcinoma DLD-1, and brain and liver cells) [7]. However, it is subject to epigenetic silencing *in vivo*, particularly in muscle and liver cells, which limits its long-term activity and can trigger an immune response [8–11].

The CASI promoter is a synthetic hybrid type (CMV, β-actin, UBC), whose methylation resistance ensures stable expression. In studies of induced pluripotent stem cells differentiated into retinal pigment epithelium cells (iPSC-RPE) [12], as well as in gene therapy for colorectal cancer using the drug AdC68-cetuximab [13], the CASI promoter demonstrated high and stable expression both *in vivo* and *in vitro* [14]. Thus, according to the literature, the CASI promoter is an effective means for delivering and expressing a transgene in muscle tissue.

Self-complementary adeno-associated virus (scAAV) vectors contain double-stranded DNA, which, according to the literature data, allows for faster and higher levels of transgene expression [15–17]. However, scAAV elicits a more pronounced immune response against the transgene [18, 19]. It should also be noted that the scAAV-DJ-CMV-B11-Fc construct carries the core CMV promoter sequence without an enhancer, as the effective packaging capacity of AAV is limited to approximately 5000 nucleotides; when packaging self-complementary scAAV particles, this capacity is effectively reduced by almost half due to the packaging of both sense and antisense DNA together, which necessitates the shortening of regulatory element sequences in the construct.

Furthermore, all three constructs contain different introns that contribute to increased transgene expression: the human β-globin intron in the pAAV-DJ-CMV-B11-Fc construct, the human ubiquitin C intron in the pAAV-DJ-CASI-B11-Fc construct, and the SV40 small intron in the pscAAV-DJ-CMV-B11-Fc construct. The WPRE located downstream of the transgene in the pAAV-DJ-CASI-B11-Fc construct helps to stabilize mRNA and increase transgene expression.

Thus, we selected the three most promising genetic constructs for delivering and effectively expressing the B11-Fc antibody gene within rAAV. The study used the synthetic serotype rAAV-DJ, which is capable of transducing a wide range of different cells and tissues [10, 20] and which have been previously used for delivering and expressing neutralizing antibody genes [2, 3].

The corresponding plasmid constructs pAAV-DJ-CMV-B11-Fc, pAAV-DJ-CASI-B11-Fc, and pscAAV-DJ-CMV-B11-Fc were used to obtain three rAAV drugs. Schematic diagrams of the genetic constructs are shown in Fig. 1.

The rAAV-DJ-CMV-B11-Fc, rAAV-DJ-CASI-B11-Fc, and scAAV-DJ-CMV-B11-Fc drugs obtained from HEK293 cell culture were purified using affinity and size exclusion chromatography. The quality of the drugs was assessed using SDS-PAGE electrophoresis in polyacrylamide gel, Western blot, and electron microscopy. The rAAV preparation scheme and typical quality control results are presented in Fig. 2.

Comparison of B11-Fc expression in the obtained rAAV drugs *in vitro* and *in vivo*

To assess B11-Fc expression, HEK293, CHO-S, and C2C12 cell lines were transduced with rAAV-DJ-CMV-B11-Fc, rAAV-DJ-CASI-B11-Fc, scAAV-DJ-CMV-B11-Fc, and rAAV-DJ-CMV-EGFP (as a control). The drug was added at a rate of 100000 genomic copies per cell. Culture fluid samples were collected 96 and 144 h after transduction.

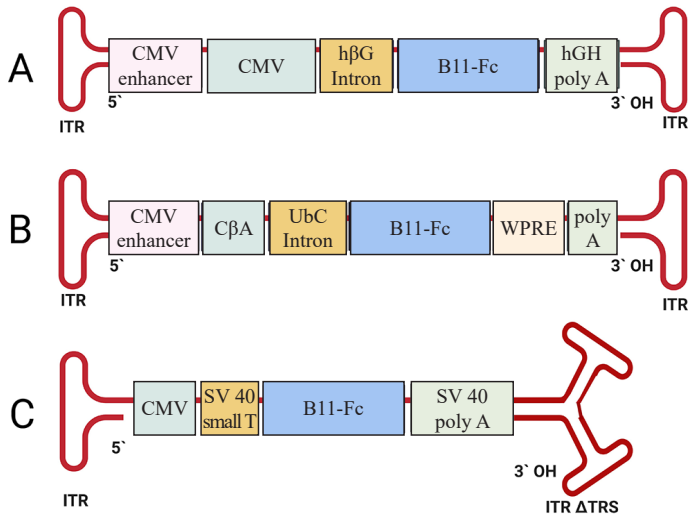

Fig. 1. Schematic representation of the obtained genetic constructs containing the gene of the modified antibody B11-Fc.

A: pAAV-DJ-CMV-B11-Fc scheme, CMV is a sequence of the full-length CMV promoter with enhancer; hβG intron is an intron of the human β-globin gene; B11-Fc is a sequence encoding the antibody B11-Fc; hGH poly A is a polyadenylation signal of human growth hormone; ITR are inverted terminal repeats.

B: pAAV-DJ-CASI-B11-Fc scheme; CASI is a synthetic hybrid promoter containing the CMV enhancer and CβA (chicken β-actin); UbC intron is an intron of ubiquitin C; B11-Fc is a sequence encoding the antibody B11-Fc, fused with the Fc fragment; WPRE is a woodchuck hepatitis virus post-transcriptional regulatory element; poly A is a synthetic polyadenylation signal; ITR are inverted terminal repeats.

C: pscAAV-DJ-CMV-B11-Fc scheme, CMV is a CMV core promoter sequence without enhancer; SV40 small T is a small intron of SV40 virus; B11-Fc is a sequence encoding B11-Fc antibody; SV40 poly A is an SV40 polyadenylation signal; ITR ΔTRS is a modified ITR with nickase site deletion, required for formation of self-complementary structure of vector DNA

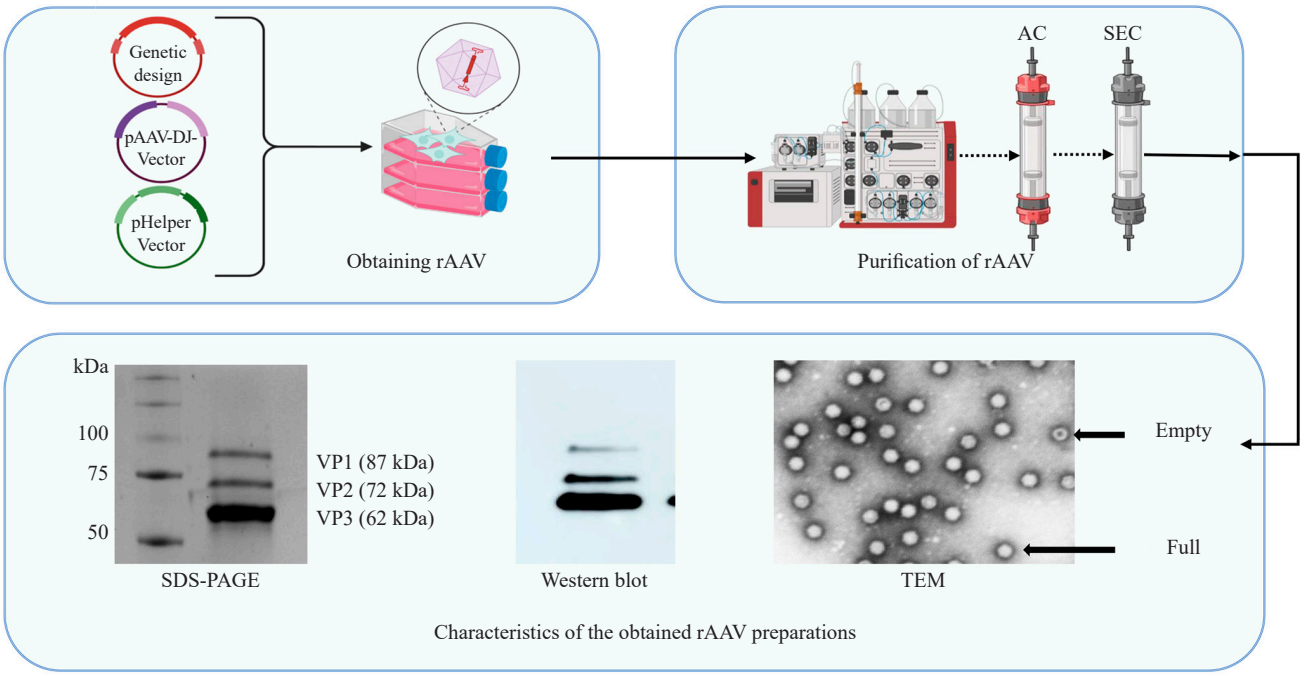

Fig. 2. Brief scheme of the rAAV preparation process. AC is affinity chromatography, SEC is size-exclusion chromatography, SDS-PAGE is polyacrylamide gel electrophoresis, VP1, VP2, VP3 are structural proteins of adeno-associated virus, TEM is transmission electron microscopy

No cytotoxic effect was observed when the drugs were transduced at the selected dose. Analysis using biolayer interferometry (BLI) showed that the production level of B11-Fc depends on the promoter and cell line (Fig. 3a).

The rAAV-DJ-CMV-B11-Fc construct provided high expression in CHO-S cells (up to 69.2 μg/mL by 144 h), while the level was lower in C2C12 cells (6.13 μg/mL at 96 h). The CASI promoter (rAAV-DJ-CASI-B11-Fc) provided stable expression (Fig. 3a), particularly in C2C12 myoblast cells (up to 19.5 μg/mL), which indirectly confirms its effectiveness for muscle tissue. scAAV-DJ-CMV-B11-Fc provided a moderate level of antibody expression in CHO-S and HEK293 cells, but the lowest level in C2C12. However, antibody expression was not shown when transduced with the control vector (rAAV-DJ-CMV-EGFP). Thus, the rAAV-DJ-CMV-B11-Fc drug provides a high level of B11-Fc expression in CHO-S and HEK293 cells, and the rAAV-DJ-CASI-B11 drug provides a high level of expression in C2C12 cells, while the scAAV-DJ-CMV-B11-Fc drug provides a moderate level of expression in CHO-S and HEK293 cells and a low level of expression in C2C12 cells.

The choice of cell lines was based on the fact that, due to the low mitotic activity of muscle tissue, genetic passive immunization drugs based on rAAV are usually administered intramuscularly to ensure long-term antibody production in the body. The less intensely the cells divide, the longer rAAV is able to persist as episomes and express the transgene [12, 16, 17].

Thus, C2C12 myoblast cells were chosen as a model for muscle tissue for the indirect assessment of the effectiveness of the constructs *in vitro*. The HEK293 cell line was used as an alternative model to study the expression level of the obtained rAAV constructs in other cell types, particularly epithelial cells. CHO-S cell line was selected based on its high efficiency for antibody production, including modified single-domain antibodies [6, 21].

During the experiment, it was shown that the rAAV-DJ-CASI-B11-Fc construct had the highest efficiency in myoblast cells, which is consistent with the literature data [14, 18]. At the same time, despite the expectation of higher expression for the scAAV-DJ-CMV-B11-Fc construct due to more efficient transduction, the rAAV-DJ-CMV-B11-Fc construct produced the highest expression in HEK293 and CHO-S cells. Since the scAAV-DJ-CMV-B11-Fc construct provided the lowest level of B11-Fc antibody production, the hypothesis about the advantage of self-complementary rAAV in our experiment was not confirmed; however, this outcome may be due to the absence of an enhancer sequence in the construct.

To assess B11-Fc expression *in vivo*, BALB/c mice were injected with 10^{11} vg of rAAV constructs: rAAV-DJ-CMV-B11-Fc, rAAV-DJ-CASI-B11-Fc, scAAV-DJ-CMV-B11-Fc, as well as a negative control rAAV-DJ-CMV-EGFP (8 animals per group). Serum was collected on days 1, 2, 3, 7, 14, 21, 28, 56, 62, 84, 112, 120, 140, 149, 168, and 184 after injection with various rAAV variants. The dosage of the drugs was chosen based on data from previous studies [3]. B11-Fc expression began within 24 h in all groups. The maximum concentration was observed in the CMV vector group and was more than 250 μg/mL on day 120, with approximately 230 μg/mL maintained up to day 184. The CASI vector provided up to 120 μg/mL (peak on day 56), followed by stabilization at a level of ~80 μg/mL. The concentration of scAAV reached ~75 μg/mL by day 120 and remained stable (Fig. 3b). In the group of animals injected with the control vector (rAAV-DJ-CMV-EGFP), no specific BLI signal was detected (not shown in the graph).

Thus, *in vitro* data from C2C12 cell studies may not fully reflect transgene expression from rAAV following

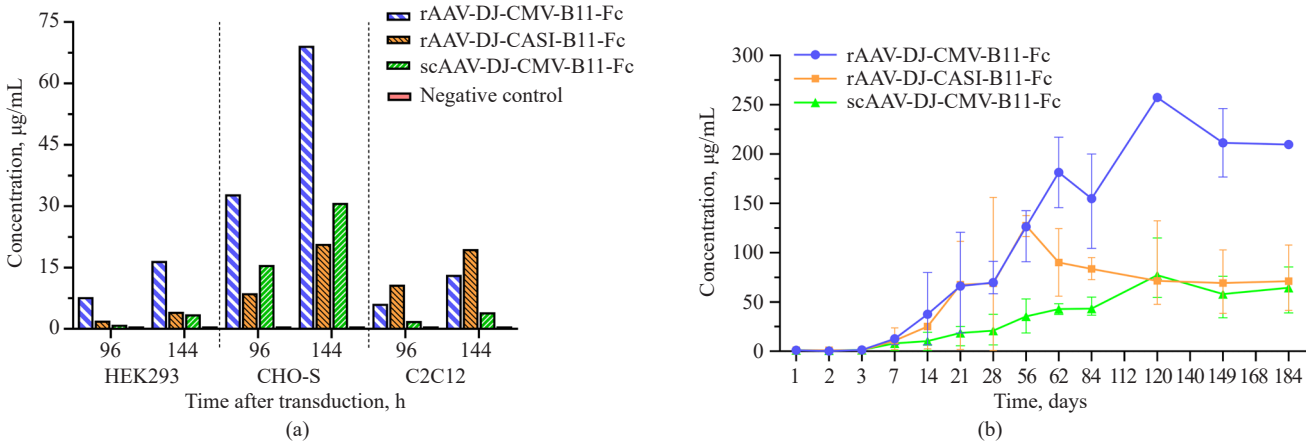

Fig. 3. Concentration of B11-Fc antibodies (μg/mL): (a) in culture fluid after rAAV transduction; (b) in mouse serum, at different time points after rAAV injection

intramuscular administration *in vivo*. However, based on the combined *in vivo* data presented above, a preliminary conclusion can be drawn about the promising nature of the rAAV-DJ-CMV-B11-Fc construct for delivering and expressing the B11-Fc antibody gene.

As a result, all the constructs studied provide a significant level of gene expression and B11-Fc antibody production both *in vitro* and *in vivo*. However, the rAAV-DJ-CMV-B11-Fc construct shows the best results, which correlates with the data on the protective activity of the drugs *in vivo*, described in the next section.

Evaluation of the protective capacity of rAAV-B11-Fc *in vivo*

The experiment evaluated the ability of various rAAV constructs expressing the B11-Fc single-domain antibody to protect mice from BoNT/A toxin. The effectiveness of the therapeutic antibodies was evaluated based on the survival rate of the animals after toxin administration. Mice were injected with 10^{11} vg of rAAV, followed by different doses of BoNT/A toxin administered intraperitoneally at various intervals. The research results are presented in Fig. 4.

Within 24 h, rAAV-DJ-CASI-B11-Fc and scAAV-DJ-CMV-B11-Fc provided 100% survival from 5 and 10 LD_{50}, while rAAV-DJ-CMV-B11-Fc showed ~60% survival. After 48 h, all constructs, including rAAV-DJ-CMV-B11-Fc, provided 100% protection at doses up to 20 LD_{50}, but at 30 LD_{50}, rAAV-DJ-CMV-B11-Fc only protected 80% of the animals. On the 10th day after administration, all drugs provided complete protection at doses up to 150 LD_{50}. After 78 days, the CMV vector maintained 100% protection even at 1000 LD_{50}, while

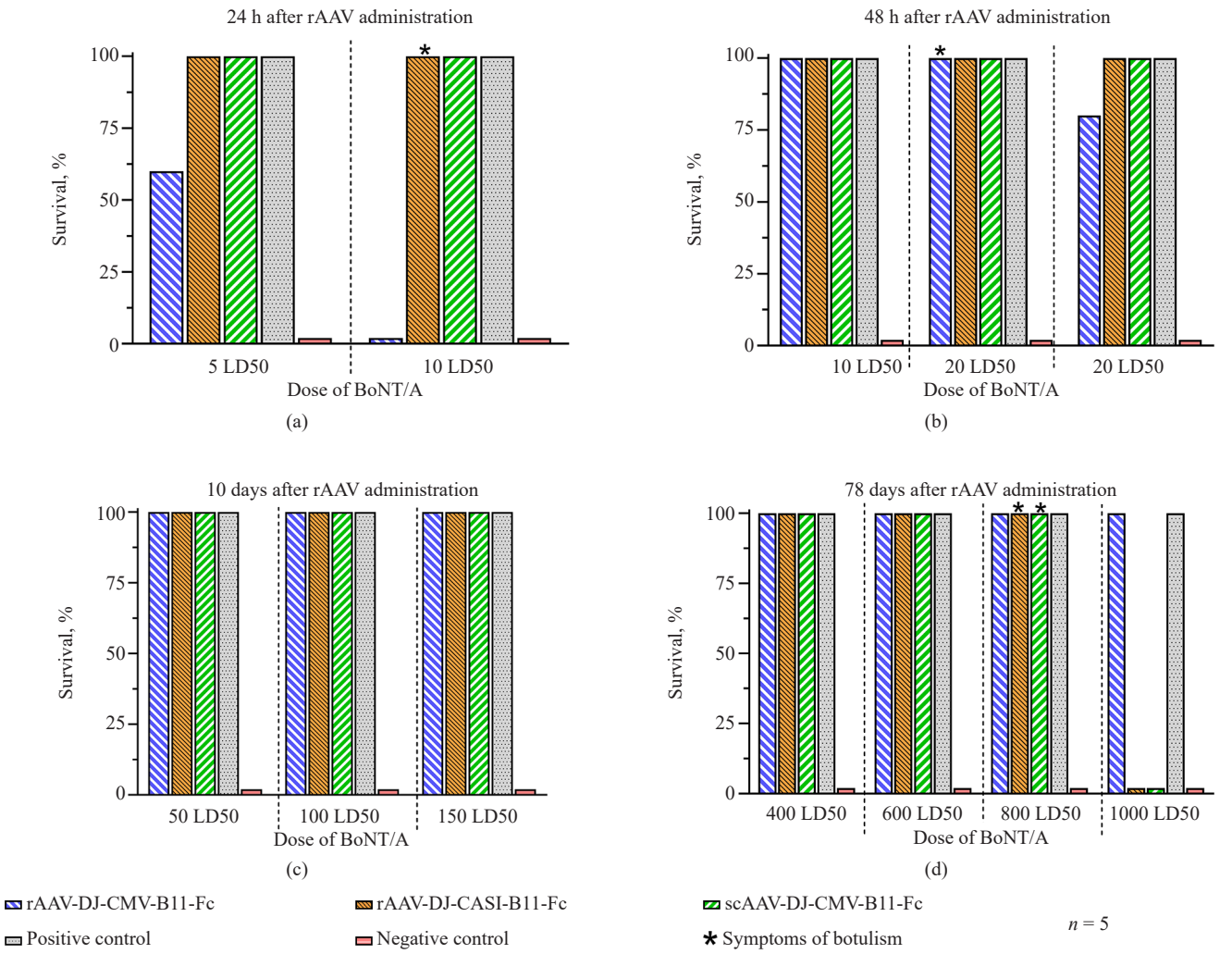

Fig. 4. Protective activity of rAAV drugs expressing neutralizing antibody B11-Fc when different doses of BoNT/A were administered at different times. The survival rate of animals (%) is shown when intoxicated with different doses of BoNT/A (in LD_{50}) 24 h (a), 48 h (b), 10 days (c), and 78 days (d) after rAAV administration. The groups with botulism symptoms are marked with an asterisk (*); the number of animals was $n = 5$ for each group

rAAV-DJ-CASI-B11-Fc and scAAV-DJ-CMV-B11-Fc were only effective against 800 LD_{50}.

Positive controls were animals that received purified B11-Fc intramuscularly at a dose that provided protection against BoNT/A toxin [6]. Administration of the rAAV drugs under study resulted in a pronounced protective effect against intoxication, as evidenced by animal survival and the absence of intoxication signs. At the same time, in the negative control groups (saline administration), there was 100% animal mortality.

The obtained data confirm the possibility of inducing long-lasting protection against BoNT/A with a single intramuscular administration of rAAV drugs expressing the B11-Fc antibody gene. At the same time, it has been shown that rAAV-DJ-CMV-B11-Fc exhibits more pronounced activity against extremely high doses of botulinum toxin starting from 2–3 months after administration. Less encouraging data on the protective activity of rAAV-DJ-CMV-B11-Fc [3] may be due to differences in the drug purification scheme, as described in the previous chapter. In turn, the rAAV-DJ-CASI-B11-Fc and scAAV-DJ-CMV-B11-Fc drugs can potentially be used, among other things, for emergency prophylaxis of botulism, since they provide protection as early as 24 h after administration.

CONCLUSIONS

In this study, a comparative analysis of three rAAV constructs expressing a modified single-domain antibody B11-Fc against botulinum neurotoxin type A (BoNT/A) was conducted.

The obtained data demonstrate that the rAAV vector design (including genome shape and promoter type) has a key influence on transgene expression levels and the duration of the protective effect. The rAAV-CMV-B11-Fc and rAAV-CASI-B11-Fc constructs are promising for long-term passive immunization. The scAAV-CMV-B11-Fc vector can be used in situations requiring early expression and protection in an emergency prophylaxis setting.

Authors' contributions

E.I. Ryabova—performing transfection and expression experiments in HEK293, CHO-S, and C2C12 cell lines; data collection and analysis; writing the manuscript text.

A.A. Derkaev—performing *in vivo* experiments on the botulism model; evaluating protective efficacy; data collection and analysis.

I.B. Esmagambetov—general supervision; revising the manuscript text; approval of the final version of the manuscript for publication.

M.A. Dovgiy—development and cloning of rAAV constructs expressing the B11-Fc single-domain antibody.

A.A. Blinov—analysis of prototypes using Western blot and SDS-PAGE; processing experimental data.

R.M. Hossain—quantitative evaluation of antibody production in culture supernatant; processing experimental data.

O.E. Dmitriev—chromatographic purification of vectors; analysis of drug properties.

D.S. Polyansky—preparation of figures, illustrations, and structural diagrams of constructs; participation in writing and formatting the manuscript.

A.N. Noskov—research concept; isolation and purification of botulinum toxin type A.

D.V. Shcheblyakov—design of the genetic construct expressing the single-domain antibody fused to an Fc fragment; research supervision.

D.Y. Logunov, **A.L. Gintsburg**—research supervision; approval of the final version of the manuscript for publication.

The authors declare no conflicts of interest.

REFERENCES

1. Laursen N.S., Friesen R.H., Zhu X., Jongeneelen M., Blokland S., Vermond J., Van Eijgen A., Tang C., Van Diepen H., Obmolova G., van der Neut Kolfschoten M., *et al.* Universal protection against influenza infection by a multidomain antibody to influenza hemagglutinin. *Science*. 2018;362(6414):598–602. https://doi.org/10.1126/science.aaq0620
2. Esmagambetov I.B., Ryabova E.I., Derkaev A.A., Shcheblyakov D.V., Dolzhikova I.V., Favorskaya I.A., *et al.* rAAV expressing recombinant antibody for emergency prevention and long-term prophylaxis of COVID-19. *Front. Immunol*. 2023;14:1129245. https://doi.org/10.3389/fimmu.2023.1129245
3. Derkaev A.A., Ryabova E.I., Esmagambetov I.B., Shcheblyakov D.V., Godakova S.A., Vinogradova I.D., Noskov A.N., Logunov D.Y., Naroditsky B.S., Gintsburg A.L. rAAV expressing recombinant neutralizing antibody for the botulinum neurotoxin type a prophylaxis. *Front. Microbiol*. 2022;13:960937. https://doi.org/10.3389/fmicb.2022.960937

СПИСОК ЛИТЕРАТУРЫ

1. Laursen N.S., Friesen R.H., Zhu X., Jongeneelen M., Blokland S., Vermond J., Van Eijgen A., Tang C., Van Diepen H., Obmolova G., van der Neut Kolfschoten M., *et al.* Universal protection against influenza infection by a multidomain antibody to influenza hemagglutinin. *Science*. 2018;362(6414):598–602. https://doi.org/10.1126/science.aaq0620
2. Esmagambetov I.B., Ryabova E.I., Derkaev A.A., Shcheblyakov D.V., Dolzhikova I.V., Favorskaya I.A., *et al.* rAAV expressing recombinant antibody for emergency prevention and long-term prophylaxis of COVID-19. *Front. Immunol*. 2023;14:1129245. https://doi.org/10.3389/fimmu.2023.1129245
3. Derkaev A.A., Ryabova E.I., Esmagambetov I.B., Shcheblyakov D.V., Godakova S.A., Vinogradova I.D., Noskov A.N., Logunov D.Y., Naroditsky B.S., Gintsburg A.L. rAAV expressing recombinant neutralizing antibody for the botulinum neurotoxin type a prophylaxis. *Front. Microbiol*. 2022;13:960937. https://doi.org/10.3389/fmicb.2022.960937

4. Godakova S.A., Noskov A.N., Vinogradova I.D., Ugriumova G.A., Solovyev A.I., Esmagambetov I.B., *et al*. Camelid VHHs fused to human fc fragments provide long term protection against botulinum neurotoxin a in mice. *Toxins*. 2019;11(8):464. https://doi.org/10.3390/toxins11080464
5. Ryabova E.I., Derkaev A.A., Esmagambetov I.B., Shcheblyakov D.V., Dovgiy M.A., Byrikhina D.V., Prokofiev V.V., Chemodanova I.P. Comparison of different technologies for producing recombinant adeno-associated virus on a laboratory scale. *BIOpreparaty. Profilaktika, diagnostika, lechenie = BIOpreparations. Prevention, Diagnosis, Treatment*. 2021;21(4):266–278 (in Russ.). https://doi.org/10.30895/2221-996X-2021-21-4-266-278
6. Derkaev A.A., Ryabova E.I., Esmagambetov I.B., Shcheblyakov D.V., Noskov A.N., Vinogradova I.D., Prokofiev V.V., Polyansky D.S., Logunov D.Y., Gintsburg A.L. A modified single-domain antibody candidate for the treatment of botulism caused by botulinum toxin type A. *BIOpreparaty. Profilaktika, diagnostika, lechenie = BIOpreparations. Prevention, Diagnosis, Treatment*. 2025;25(1): 58–70 (in Russ.). https://doi.org/10.30895/2221-996X-2025-591
7. Cabrera A., Edelstein H.I., Glykofrydis F., Love K.S., Palacios S., Tycko J., Zhang M., Lensch S., Shields C.E., Livingston M., Weiss R., *et al*. The sound of silence: Transgene silencing in mammalian cell engineering. *Cell Syst*. 2022;13(12):950–973. https://doi.org/10.1016/j.cels.2022.11.005
8. Xu L., Daly T., Gao C., Flotte T.R., Song S., Byrne B.J., Sands M.S.., Ponder K.P. CMV-β-actin promoter directs higher expression from an adeno-associated viral vector in the liver than the cytomegalovirus or elongation factor 1α promoter and results in therapeutic levels of human factor X in mice. *Human Gene Ther*. 2001;12(5):563–573. https://doi.org/10.1089/104303401300042500
9. Wang L., Bell P., Somanathan S., Wang Q., He Z., Yu H., McMenamin D., Goode T., Calcedo R., Wilson J.M. Comparative study of liver gene transfer with AAV vectors based on natural and engineered AAV capsids. *Mol. Ther*. 2015;23(12):1877–1887. https://doi.org/10.1038/mt.2015.179
10. Choi V.W., McCarty D.M., Samulski R.J. AAV hybrid serotypes: Improved vectors for gene delivery. *Curr. Gene Ther*. 2005;5(3):299–310. https://doi.org/10.2174/1566523054064968
11. Wang D., Tai P.W., Gao G. Adeno-associated virus vector as a platform for gene therapy delivery. *Nature Rev. Drug Discov*. 2019;18(5):358–378. https://doi.org/10.1038/s41573-019-0012-9
12. Brydon E.M., Bronstein R., Buskin A., Lako M., Pierce E.A., Fernandez-Godino R. AAV-mediated gene augmentation therapy restores critical functions in mutant PRPF31$^{+/-}$ iPSC-derived RPE cells. *Mol. Ther. Methods Clin. Develop*. 2019;15:392–402. https://doi.org/10.1016/j.omtm.2019.10.014
13. Xing M., Wang X., Chi Y., Zhou D. Gene therapy for colorectal cancer using adenovirus-mediated full-length antibody, cetuximab. *Oncotarget*. 2016;7(19):28262. https://doi.org/10.18632/oncotarget.8596
14. Hollidge B.S., Carroll H.B., Qian R., Fuller M.L., Giles A.R., Mercer A.C., Danos O., Liu Y., Bruder J.T., Smith J.B. Kinetics and durability of transgene expression after intrastriatal injection of AAV9 vectors. *Front. Neurol*. 2022;13:1051559 https://doi.org/10.3389/fneur.2022.1051559
15. McCarty D.M. Self-complementary AAV vectors; advances and applications. *Mol. Ther*. 2008;16(10):1648–1656. https://doi.org/10.1038/mt.2008.171
16. Yokoi K., Kachi S., Zhang H.S., Gregory P.D., Spratt S.K., Samulski R.J., Campochiaro P.A. Ocular gene transfer with self-complementary AAV vectors. *Investigative Ophthalmology & Visual Science* (*IOVS*). 2007;48(7): 3324–3328. https://doi.org/10.1167/iovs.06-1306

4. Godakova S.A., Noskov A.N., Vinogradova I.D., Ugriumova G.A., Solovyev A.I., Esmagambetov I.B., *et al*. Camelid VHHs fused to human fc fragments provide long term protection against botulinum neurotoxin a in mice. *Toxins*. 2019;11(8):464. https://doi.org/10.3390/toxins11080464
5. Рябова Е.И., Деркаев А.А., Есмагамбетов И.Б., Щебляков Д.В., Довгий М.А., Бырихина Д.В., Прокофьев В.В., Чемоданова И.П. Сравнение различных технологий получения рекомбинантного аденоассоциированного вируса в лабораторном масштабе. *БИОпрепараты. Профилактика, диагностика, лечение*. 2021;21(4):266–278. https://doi.org/10.30895/2221-996X-2021-21-4-266-278
6. Деркаев А.А., Рябова Е.И., Есмагамбетов И.Б., Щебляков Д.В., Носков А.Н., Виноградова И.Д., Прокофьев В.В., Полянский Д.С.., Логунов Д.Ю., Гинцбург А.Л. Кандидатный препарат на основе модифицированных однодоменных антител для терапии ботулизма, вызванного ботулиническим токсином типа А. *БИОпрепараты. Профилактика, диагностика, лечение*. 2025;25(1):58–70. https://doi.org/10.30895/2221-996X-2025-591
7. Cabrera A., Edelstein H.I., Glykofrydis F., Love K.S., Palacios S., Tycko J., Zhang M., Lensch S., Shields C.E., Livingston M., Weiss R., *et al*. The sound of silence: Transgene silencing in mammalian cell engineering. *Cell Syst.* 2022;13(12):950–973. https://doi.org/10.1016/j.cels.2022.11.005
8. Xu L., Daly T., Gao C., Flotte T.R., Song S., Byrne B.J., Sands M.S.., Ponder K.P. CMV-β-actin promoter directs higher expression from an adeno-associated viral vector in the liver than the cytomegalovirus or elongation factor 1α promoter and results in therapeutic levels of human factor X in mice. *Human Gene Ther*. 2001;12(5):563–573. https://doi.org/10.1089/104303401300042500
9. Wang L., Bell P., Somanathan S., Wang Q., He Z., Yu H., McMenamin D., Goode T., Calcedo R., Wilson J.M. Comparative study of liver gene transfer with AAV vectors based on natural and engineered AAV capsids. *Mol. Ther*. 2015;23(12):1877–1887. https://doi.org/10.1038/mt.2015.179
10. Choi V.W., McCarty D.M., Samulski R.J. AAV hybrid serotypes: Improved vectors for gene delivery. *Curr. Gene Ther*. 2005;5(3):299–310. https://doi.org/10.2174/1566523054064968
11. Wang D., Tai P.W., Gao G. Adeno-associated virus vector as a platform for gene therapy delivery. *Nature Rev. Drug Discov*. 2019;18(5):358–378. https://doi.org/10.1038/s41573-019-0012-9
12. Brydon E.M., Bronstein R., Buskin A., Lako M., Pierce E.A., Fernandez-Godino R. AAV-mediated gene augmentation therapy restores critical functions in mutant PRPF31$^{+/-}$ iPSC-derived RPE cells. *Mol. Ther. Methods Clin. Develop*. 2019;15:392–402. https://doi.org/10.1016/j.omtm.2019.10.014
13. Xing M., Wang X., Chi Y., Zhou D. Gene therapy for colorectal cancer using adenovirus-mediated full-length antibody, cetuximab. *Oncotarget*. 2016;7(19):28262. https://doi.org/10.18632/oncotarget.8596
14. Hollidge B.S., Carroll H.B., Qian R., Fuller M.L., Giles A.R., Mercer A.C., Danos O., Liu Y., Bruder J.T., Smith J.B. Kinetics and durability of transgene expression after intrastriatal injection of AAV9 vectors. *Front. Neurol*. 2022;13:1051559. https://doi.org/10.3389/fneur.2022.1051559
15. McCarty D.M. Self-complementary AAV vectors; advances and applications. *Mol. Ther*. 2008;16(10):1648–1656. https://doi.org/10.1038/mt.2008.171
16. Yokoi K., Kachi S., Zhang H.S., Gregory P.D., Spratt S.K., Samulski R.J., Campochiaro P.A. Ocular gene transfer with self-complementary AAV vectors. *Investigative Ophthalmology & Visual Science* (*IOVS*). 2007;48(7): 3324–3328. https://doi.org/10.1167/iovs.06-1306

17. Rincon M.Y., de Vin F., Duqué S.I., Fripont S., Castaldo S.A., Bouhuijzen-Wenger J., Holt M.G. Widespread transduction of astrocytes and neurons in the mouse central nervous system after systemic delivery of a self-complementary AAV-PHP.B vector. *Gene Ther.* 2018;25(2):83–92. https://doi.org/10.1038/s41434-018-0005-z
18. Wu T., Töpfer K.., Lin SW., Li H., Bian A., Zhou X.Y., High K.A., Ertl H.C. Self-complementary AAVs induce more potent transgene product-specific immune responses compared to a single-stranded genome. *Mol. Ther.* 2012;20(3):572–579. https://doi.org/10.1038/mt.2011.280
19. McCarty D.M., Monahan P.E., Samulski R.J. Self-complementary recombinant adeno-associated virus (scAAV) vectors promote efficient transduction independently of DNA synthesis. *Gene Ther*. 2001;8(16):1248–1554. https://doi.org/10.1038/sj.gt.3301514
20. Katada Y., Kobayashi K., Tsubota K., Kurihara T. Evaluation of AAV-DJ vector for retinal gene therapy. *Peer J*. 2019;7:e6317. https://doi.org/10.7717/peerj.6317
21. Polyansky D.S., Ryabova E.I., Derkaev A.A., Starkov N.S., Kashapova I.S., Shcheblyakov D.V., Karpov A.P., Esmagambetov I.B. Development of technology for culturing a cell line producing a single-domain antibody fused with the Fc fragment of human IgG1. *Fine Chem. Technol*. 2024;19(3): 240–257. https://doi.org/10.32362/2410-6593-2024-19-3-240-257

17. Rincon M.Y., de Vin F., Duqué S.I., Fripont S., Castaldo S.A., Bouhuijzen-Wenger J., Holt M.G. Widespread transduction of astrocytes and neurons in the mouse central nervous system after systemic delivery of a self-complementary AAV-PHP.B vector. *Gene Ther.* 2018;25(2):83–92. https://doi.org/10.1038/s41434-018-0005-z
18. Wu T., Töpfer K.., Lin S.W., Li H., Bian A., Zhou X.Y., High K.A., Ertl H.C. Self-complementary AAVs induce more potent transgene product-specific immune responses compared to a single-stranded genome. *Mol. Ther.* 2012;20(3):572–579. https://doi.org/10.1038/mt.2011.280
19. McCarty D.M., Monahan P.E., Samulski R.J. Self-complementary recombinant adeno-associated virus (scAAV) vectors promote efficient transduction independently of DNA synthesis. *Gene Ther*. 2001;8(16):1248–1554. https://doi.org/10.1038/sj.gt.3301514
20. Katada Y., Kobayashi K., Tsubota K., Kurihara T. Evaluation of AAV-DJ vector for retinal gene therapy. *Peer J*. 2019;7:e6317. https://doi.org/10.7717/peerj.6317
21. Полянский Д.С., Рябова Е.И., Деркаев А.А., Старков Н.С., Кашапова И.С., Щебляков Д.В., Карпов А.П., Есмагамбетов И.Б. Разработка технологии культивирования клеточной линии, продуцирующей однодоменное антитело, слитое с Fc-фрагментом IgG1 человека. *Тонкие химические технологии*. 2024;19(3):240–257. https://doi.org/10.32362/2410-6593-2024-19-3-240-257

About the Authors

Ekaterina I. Ryabova, Junior Researcher, Laboratory of Immunobiotechnology, N.F. Gamaleya National Research Center for Epidemiology and Microbiology (The Gamaleya National Center), Ministry of Health of the Russian Federation (18, Gamaleya ul., Moscow, 123098, Russia); Postgraduate Student, K.I. Skryabin Moscow State Academy of Veterinary Medicine and Biotechnology – MVA (23, Akademika Skryabina ul., Moscow, 109472, Russia). E-mail: ryabovaei96@gmail.com. Scopus Author ID 57301278100, ResearcherID AAE-7335-2022, RSCI SPIN-code 6963-1376, https://orcid.org/0000-0002-2687-5185

Artem A. Derkaev, Junior Researcher, Laboratory of Immunobiotechnology, N.F. Gamaleya National Research Center for Epidemiology and Microbiology (The Gamaleya National Center), Ministry of Health of the Russian Federation (18, Gamaleya ul., Moscow, 123098, Russia). E-mail: derkaev.a@yandex.ru. Scopus Author ID 57381507000, ResearcherID AFU-7075-2022, RSCI SPIN-code 9339-9440, https://orcid.org/0000-0003-3776-3856

Ilias B. Esmagambetov, Cand. Sci. (Biol.), Leading Researcher, Head of the Laboratory of Stromal Regulation of Immunity, N.F. Gamaleya National Research Center for Epidemiology and Microbiology (The Gamaleya National Center), Ministry of Health of the Russian Federation (18, Gamaleya ul., Moscow, 123098, Russia). E-mail: iesmagambetov@yandex.ru. Scopus Author ID 56120429700, ResearcherID E-3327-2014, RSCI SPIN-code 8132-2320, https://orcid.org/0000-0002-2063-2449

Mikhail A. Dovgiy, Junior Researcher, Laboratory of Immunobiotechnology, N.F. Gamaleya National Research Center for Epidemiology and Microbiology (The Gamaleya National Center), Ministry of Health of the Russian Federation (18, Gamaleya ul., Moscow, 123098, Russia). E-mail: imhail@yandex.ru. ResearcherID AFV-2114-2022, RSCI SPIN-code 4033-2216, https://orcid.org/0000-0002-0017-7784

Anton A. Blinov, Laboratory Research Assistant, Laboratory of Stromal Regulation of Immunity, N.F. Gamaleya National Research Center for Epidemiology and Microbiology (The Gamaleya National Center), Ministry of Health of the Russian Federation (18, Gamaleya ul., Moscow, 123098, Russia). E-mail: blinow.t@gmail.com. ResearcherID OCL-6033-2025, https://orcid.org/0009-0005-9866-7376

Roza M. Hossain, Junior Researcher, Laboratory of Stromal Regulation of Immunity, N.F. Gamaleya National Research Center for Epidemiology and Microbiology (The Gamaleya National Center), Ministry of Health of the Russian Federation (18, Gamaleya ul., Moscow, 123098, Russia). E-mail: xossain2013@gmail.com. ResearcherID OCL-6134-2025, https://orcid.org/0009-0009-4483-2697

Oleg E. Dmitriev, Leading Engineer**,** Laboratory of Stromal Regulation of Immunity, N.F. Gamaleya National Research Center for Epidemiology and Microbiology (The Gamaleya National Center), Ministry of Health of the Russian Federation (18, Gamaleya ul., Moscow, 123098, Russia). E-mail: d.e.oleg.work@gmail.com. ResearcherID ODJ-2714-2025, https://orcid.org/0000-0003-3709-8358

Dmitry S. Polyansky, Assistant Professor, I.P. Alimarin Department of Analytical Chemistry, M.V. Lomonosov Institute of Fine Chemical Technologies, MIREA – Russian Technological University (78, Vernadskogo pr., Moscow, 119545, Russia). E-mail: polanskiydmitriy15@gmail.com. Scopus Author ID 57890564200, https://orcid.org/0000-0003-0792-7063

Anatoly N. Noskov, Dr. Sci. (Biol.), Leading Researcher**,** Laboratory of Immunobiotechnology, N.F. Gamaleya National Research Center for Epidemiology and Microbiology (The Gamaleya National Center), Ministry of Health of the Russian Federation (18, Gamaleya ul., Moscow, 123098, Russia). E-mail: a_n_noskov@mail.ru. Scopus Author ID 7005685081

Dmitry V. Shcheblyakov, Dr. Sci. (Biol.), Leading Researcher, Head of the Department of Genetics and Molecular Biology of Bacteria, Head of the Laboratory of Immunobiotechnology, N.F. Gamaleya National Research Center for Epidemiology and Microbiology (The Gamaleya National Center), Ministry of Health of the Russian Federation (18, Gamaleya ul., Moscow, 123098, Russia). E-mail: sdmitryv@yahoo.com. Scopus Author ID 35073056900, ResearcherID E-5899-2014, RSCI SPIN-code 6357-2725, https://orcid.org/0000-0002-1289-3411

Denis Y. Logunov, Academician at the Russian Academy of Sciences, Dr. Sci. (Biol.), Deputy Director for Research, N.F. Gamaleya National Research Center for Epidemiology and Microbiology (The Gamaleya National Center), Ministry of Health of the Russian Federation (18, Gamaleya ul., Moscow, 123098, Russia). E-mail: ldy78@yandex.ru. Scopus Author ID 22835557900, ResearcherID E-8300-2014, RSCI SPIN-code 4000-4717, https://orcid.org/0000-0003-4035-6581

Alexander L. Gintsburg, Academician at the Russian Academy of Sciences, Academician at the Russian Academy of Medical Sciences, Dr. Sci. (Biol.), Professor, Director of the N.F. Gamaleya National Research Center for Epidemiology and Microbiology (The Gamaleya National Center), Ministry of Health of the Russian Federation (18, Gamaleya ul., Moscow, 123098, Russia). E-mail: gintsburg@gamaleya.org. Scopus Author ID 7005111491, RSCI SPIN-code 7626-0373, https://orcid.org/0000-0003-1769-5059

Об авторах

Рябова Екатерина Игоревна, младший научный сотрудник, лаборатория иммунобиотехнологии, ФГБУ «Национальный исследовательский центр эпидемиологии и микробиологии имени почетного академика Н.Ф. Гамалеи» Министерства здравоохранения Российской Федерации (123098, Россия, Москва, ул. Гамалеи, д. 18); аспирант, ФГБОУ ВО «Московская государственная академия ветеринарной медицины и биотехнологии – МВА имени К.И. Скрябина» (109472, Россия, Москва, ул. Академика Скрябина, д. 23). E-mail: ryabovaei96@gmail.com. Scopus Author ID 57301278100, ResearcherID AAE-7335-2022, SPIN-код РИНЦ 6963-1376, https://orcid.org/0000-0002-2687-5185

Деркаев Артем Алексеевич, младший научный сотрудник, лаборатория иммунобиотехнологии, ФГБУ «Национальный исследовательский центр эпидемиологии и микробиологии имени почетного академика Н.Ф. Гамалеи» Министерства здравоохранения Российской Федерации (123098, Россия, Москва, ул. Гамалеи, д. 18). E-mail: derkaev.a@yandex.ru. Scopus Author ID 57381507000, ResearcherID AFU-7075-2022, SPIN-код РИНЦ 9339-9440, https://orcid.org/0000-0003-3776-3856

Есмагамбетов Ильяс Булатович, к.б.н., ведущий научный сотрудник, заведующий лабораторией стромальной регуляции иммунитета, ФГБУ «Национальный исследовательский центр эпидемиологии и микробиологии имени почетного академика Н.Ф. Гамалеи» Министерства здравоохранения Российской Федерации (123098, Россия, Москва, ул. Гамалеи, д. 18). E-mail: iesmagambetov@yandex.ru. Scopus Author ID 56120429700, ResearcherID E-3327-2014, SPIN-код РИНЦ 8132-2320, https://orcid.org/0000-0002-2063-2449

Довгий Михаил Андреевич, младший научный сотрудник, лаборатория иммунобиотехнологии, ФГБУ «Национальный исследовательский центр эпидемиологии и микробиологии имени почетного академика Н.Ф. Гамалеи» Министерства здравоохранения Российской Федерации (123098, Россия, Москва, ул. Гамалеи, д. 18). E-mail: imhail@yandex.ru. ResearcherID AFV-2114-2022, SPIN-код РИНЦ 4033-2216, https://orcid.org/0000-0002-0017-7784

Блинов Антон Анатольевич, лаборант исследователь, лаборатория стромальной регуляции иммунитета, ФГБУ «Национальный исследовательский центр эпидемиологии и микробиологии имени почетного академика Н.Ф. Гамалеи» Министерства здравоохранения Российской Федерации (123098, Россия, Москва, ул. Гамалеи, д. 18). E-mail: blinow.t@gmail.com. ResearcherID OCL-6033-2025, https://orcid.org/0009-0005-9866-7376

Хоссаин Роза Махбубовна, младший научный сотрудник, лаборатория стромальной регуляции иммунитета, ФГБУ «Национальный исследовательский центр эпидемиологии и микробиологии имени почетного академика Н.Ф. Гамалеи» Министерства здравоохранения Российской Федерации (123098, Россия, Москва, ул. Гамалеи, д. 18). E-mail: xossain2013@gmail.com. ResearcherID OCL-6134-2025, https://orcid.org/0009-0009-4483-2697

Дмитриев Олег Евгеньевич, ведущий инженер, лаборатория стромальной регуляции иммунитета, ФГБУ «Национальный исследовательский центр эпидемиологии и микробиологии имени почетного академика Н.Ф. Гамалеи» Министерства здравоохранения Российской Федерации (123098, Россия, Москва, ул. Гамалеи, д. 18). E-mail: d.e.oleg.work@gmail.com. ResearcherID ODJ-2714-2025, https://orcid.org/0000-0003-3709-8358

Полянский Дмитрий Сергеевич, ассистент, кафедра аналитической химии им. И.П. Алимарина, Институт тонких химических технологий им. М.В. Ломоносова, ФГБОУ ВО «МИРЭА – Российский технологический университет» (119454, Россия, Москва, пр-т Вернадского, д. 78). E-mail: polanskiydmitriy15@gmail.com. Scopus Author ID 57890564200, https://orcid.org/0000-0003-0792-7063

Носков Анатолий Николаевич, д.б.н., ведущий научный сотрудник**,** лаборатория иммунобиотехнологии, ФГБУ «Национальный исследовательский центр эпидемиологии и микробиологии имени почетного академика Н.Ф. Гамалеи» Министерства здравоохранения Российской Федерации (123098, Россия, Москва, ул. Гамалеи, д. 18). E-mail: a_n_noskov@mail.ru. Scopus Author ID 7005685081

Щебляков Дмитрий Викторович, д.б.н., ведущий научный сотрудник, руководитель отдела генетики и молекулярной биологии бактерий, заведующий лабораторией иммунобиотехнологии, ФГБУ «Национальный исследовательский центр эпидемиологии и микробиологии имени почетного академика Н.Ф. Гамалеи» Министерства здравоохранения Российской Федерации (123098, Россия, Москва, ул. Гамалеи, д. 18). E-mail: sdmitryv@yahoo.com. Scopus Author ID 35073056900, ResearcherID E-5899-2014, SPIN-код РИНЦ 6357-2725, https://orcid.org/0000-0002-1289-3411

Логунов Денис Юрьевич, д.б.н., академик Российской академии наук, заместитель директора по научной работе, ФГБУ «Национальный исследовательский центр эпидемиологии и микробиологии имени почетного академика Н.Ф. Гамалеи» Министерства здравоохранения Российской Федерации (123098, Россия, Москва, ул. Гамалеи, д. 18). E-mail: ldy78@yandex.ru. Scopus Author ID 22835557900, ResearcherID E-8300-2014, SPIN-код РИНЦ 4000-4717, https://orcid.org/0000-0003-4035-6581

Гинцбург Александр Леонидович, академик Российской академии наук, академик Российской академии медицинских наук, д.б.н., профессор, директор ФГБУ «Национальный исследовательский центр эпидемиологии и микробиологии имени почетного академика Н.Ф. Гамалеи» Министерства здравоохранения Российской Федерации (123098, Россия, Москва, ул. Гамалеи, д. 18). E-mail: gintsburg@gamaleya.org. Scopus Author ID 7005111491, SPIN-код РИНЦ 7626-0373, https://orcid.org/0000-0003-1769-5059

Translated from Russian into English by H. Moshkov

Edited for English language and spelling by Thomas A. Beavitt

Tonkie Khimicheskie Tekhnologii = Fine Chemical Technologies.
2025;20(6):594–611 ISSN 2686-7575 (Online)

Synthesis and processing of polymers and polymeric composites
Синтез и переработка полимеров и композитов на их основе

UDC 678.7;678.764.43;678.01;678.85;614.841.41;544.452
https://doi.org/10.32362/2410-6593-2025-20-6-594-611
EDN XIVTBW

RESEARCH ARTICLE

Influence of the structure of phosphorus(III)-containing oligoester(meth)acrylates on the physical and mechanical properties, thermal stability, and combustion mechanisms of cured polymers

Boris A. Buravov[1], Ali Al-Hamzawi[2], Rashid B. Gadzhiev[1], Svetlana A. Orlova[1], Lyubov Yu. Donetskova[1], Semyon M. Solomakhin[1], Sergey V. Borisov[1], Olga S. Fomenko[1], Stanislav A. Trubachev[3], Aleksander A. Paletsky[3], Andrey G. Shmakov[3], Oleg I. Tuzhikov[1], Oleg O. Tuzhikov[1]✉

[1] *Volgograd State Technical University, Volgograd, 400005 Russia*
[2] *Al-Qadisiyah, Al-Diwaniyah, 58002 Iraq*
[3] *Institute of Chemical Kinetics and Combustion, Siberian Branch of the Russian Academy of Sciences, Novosibirsk, 630090 Russia*

✉ *Corresponding author, e-mail: tuzhikovoleg@mail.ru*

Abstract

Objectives. The work sets out to investigate the influence of the structure of spacer in structure of phosphorus(III)-containing oligoester(meth)acrylates on physical and mechanical properties of polymers and their combustibility.

Methods. The physical and mechanical properties of polymers were determined using the following: DMA 242 E Artemis dynamic mechanical analyzer (*NETZSCH*, Germany); universal testing machine for standard tests on materials (*ZwickRoell Group*, Germany); GT-7045-HMH(L) impact test machine (*Gotech Testing Machines, Inc*., Taiwan); Q-1500 D derivatograph of the Paulic–Paulic–Erdey system (thermogravimetry, *IOM*, Hungary); Oxygen Index Module device for determination of burning behavior by plastic flammability testing according to oxygen index (*Concept Equipment*, United Kingdom); GT-7045-HMH(L) device for determination of the Vicat softening temperature (*Gotech Testing Machines, Inc*., Taiwan); SFT-110XW supercritical fluid extractor (*Supercritical Fluid Technologies, Inc*., USA) for supercritical fluid extraction with carbon dioxide.

Results. The influence of the spacer structure in the structure of phosphorus(III)-containing oligoester(meth)acrylates on the dynamic mechanical and physicomechanical properties of polymers was established. Comparative assessment of the impact of the spacer structure on properties of polymers was carried out in terms of their heat stability (thermogravimetric analysis) and combustibility (measurement of limited oxygen index). It is established that polymers having balanced physical and mechanical properties can be obtained by introducing spacer characteristics into the oligomer structure. Polymers obtained on the basis of phosphorus(III)-containing oligoester(meth)acrylates with spacers demonstrate considerable resistance to impact strength tests.

Conclusions. The achieved results testify to the possibility of obtaining polymers on the basis of phosphorus(III)-containing oligoester(meth)acrylates with spacer attributes that possess increased resistance to impact strength and thermal stability tests at an insignificant decrease in their combustibility.

Keywords

spacer, phosphorus-containing polymers, dynamic mechanical analysis, DMA, limited oxygen index, coupled combustion model

Submitted: 24.02.2025
Revised: 14.04.2025
Accepted: 13.11.2025

For citation

Buravov B.A., Al-Hamzawi A., Gadzhiev R.B., Orlova S.A., Donetskova L.Yu., Solomakhin S.M., Borisov S.V., Fomenko O.S., Trubachev S.A., Paletsky A.A., Shmakov A.G., Tuzhikov O.I., Tuzhikov O.O. Influence of the structure of phosphorus(III)-containing oligoester(meth)acrylates on the physical and mechanical properties, thermal stability, and combustion mechanisms of cured polymers. *Tonk. Khim. Tekhnol. = Fine Chem. Technol.* 2025;20(6):594–611. https://doi.org/10.32362/2410-6593-2025-20-6-594-611

НАУЧНАЯ СТАТЬЯ

Влияние строения фосфор(III)-содержащих олигоэфир(мет)акрилатов на физико-механические свойства, термическую стабильность и механизмы горения отвержденных полимеров

Б.А. Буравов[1], А. Аль-Хамзави[2], Р.Б. Гаджиев[1], С.А. Орлова[1], Л.Ю. Донецкова[1], С.М. Соломахин[1], С.В. Борисов[1], О.С. Фоменко[1], С.А. Трубачев[3], А.А. Палецкий[3], А.Г. Шмаков[3], О.И. Тужиков[1], О.О. Тужиков[1]✉

[1] *Волгоградский государственный технический университет, Волгоград, 400005 Россия*

[2] *Университет Аль-Кадисия, Эд-Дивания, 58002 Ирак*

[3] *Институт химической кинетики и горения им. В.В. Воеводского, Сибирское отделение Российской академии наук, Новосибирск, 630090 Россия*

✉ *Автор для переписки, e-mail: tuzhikovoleg@mail.ru*

Аннотация

Цели. Исследование влияния строения спейсера в структуре фосфор(III)-содержащих олигоэфир(мет)акрилатов на физико-механические свойства полимеров и их горючесть.

Методы. Физико-механические свойства полимеров определяли с помощью динамического механического анализатора DMA 242 E Artemis (*NETZSCH*, Германия); универсальной машины для испытаний (*ZwickRoell Group*, Германия); копера GT-7045-HMH(L) (*Gotech Testing Machines, Inc.*, Тайвань); дериватографа Q-1500 D системы Паулик–Паулик–Эрдей (термогравиметрические исследования, *MOM*, Венгрия); установки «Oxygen Index Module» для определения кислородного индекса пластмасс — Fire Testing (*Concept Equipment*, Великобритания), прибора Копер GT-7045-HMH(L) для определения температуры размягчения по Вика (*Gotech Testing Machines, Inc.*, Тайвань); сверхкритического флюидного экстрактора SFT-110XW (*Supercritical Fluid Technologies, Inc.*, США) для флюидной экстракции сверхкритическим диоксидом углерода.

Результаты. Установлено влияние строения спейсера в структуре фосфор(III)-содержащих олигоэфир(мет)акрилатов на динамические механические и физико-механические свойства полимеров. Сделана сопоставительная оценка влияния строения спейсера на свойства полимеров, их термостабильность (проведен термогравиметрический анализ) и горючесть (измерен кислородный индекс). Установлено, что введение спейсера в структуру олигомера приводит к получению полимеров со сбалансированными физико-механическими свойствами. Полимеры на основе фосфор(III)-содержащих олигоэфир(мет)акрилатов со спейсерами обладают значительно большим сопротивлением ударным нагрузкам.

Выводы. Достигнутые результаты свидетельствуют о возможности получения полимеров на основе фосфор(III)-содержащих олигоэфир(мет)акрилатов со спейсером, обладающих повышенным сопротивлением ударным нагрузкам и термостойкостью при незначительном снижении их горючести.

Ключевые слова

спейсер, фосфорсодержащие полимеры, динамический механический анализ, кислородный индекс, сопряженная модель горения

Поступила: 24.02.2025
Доработана: 14.04.2025
Принята в печать: 13.11.2025

Для цитирования

Буравов Б.А., Аль-Хамзави А., Гаджиев Р.Б., Орлова С.А., Донецкова Л.Ю., Соломахин С.М., Борисов С.В., Фоменко О.С., Трубачев С.А., Палецкий А.А., Шмаков А.Г., Тужиков О.И., Тужиков О.О. Влияние строения фосфор(III)-содержащих олигоэфир(мет)акрилатов на физико-механические свойства, термическую стабильность и механизмы горения отвержденных полимеров. *Тонкие химические технологии*. 2025;20(6):594–611. https://doi.org/10.32362/2410-6593-2025-20-6-594-611

INTRODUCTION

A compendium of research into the synthesis of phosphorus-containing acrylates, including the characteristics of their curing and an assessment of the properties of the resulting materials can be found in [1]. Further development of the described direction is presented in the works [2–4]. However, a more recent round of research is associated with establishing the possibility of synthesizing monomers with spacers, which in turn determines the relevance of publishing a series of articles on this topic.

In a previous publication, the results of a study on the synthesis of spatially separated phosphorus-containing oligoester (met)acrylates (a phosphorus-containing polymerizable compound, PPC) were presented along with an evaluation of the effect of the spacer structure on the kinetics of their photo-curing [5].

The materials presented in the present article, which are a continuation of earlier research based on B.A. Buravov's dissertation[1], are devoted to the study of the physical and mechanical properties of cured phosphorus-containing oligomeric(meth)-acrylates with spacers based on trivalent phosphorus. The synthesized monomers are envisaged for use as raw materials for the manufacture of products having reduced flammability by laser stereolithography (LSL) and digital light processing (DLP), as well as 3D printing methods used e.g. in automotive, aviation and railway technology applications. In this connection, it is important to evaluate the effect of the spacer structure on the physicomechanical properties of cured materials in order to predict possible options for the use of end products. Therefore, the effect of the spacer and its structure on the properties of cured polymers was evaluated using the dynamic mechanical analysis (DMA) method.

The present study investigates the temperature variation of the complex dynamic mechanical modulus of phosphorus(III)-based polymers containing oligoester methacrylates. The influence of the spacer structure on the modulus of accumulation of mechanical losses is estimated along with the damping factor of polymers. As a rule, these results on temperature changes in the plastic-elastic properties of the material allow us to get an idea of the structure of the formed polymer and assess the boundary conditions of its application. The establishment of these areas has been facilitated by the implementation of Cole–Cole diagrams, a method that has been instrumental in the analysis of the balanced properties of cured polymers.

EXPERIMENTAL

The properties of polymers were studied using PPCs that differ in terms of their structure, in particular, concerning the presence of a spacer in the structure of the initial monomer. The chemical formulas of compounds PPC-1, PPC-2, and PPC-3 are shown in Fig. 1.

The structure of PPC-4 is similar to that of PPC-2 and PPC-3, but one of the functional ether methacrylate groups has been replaced with an allyl group. The synthesis of PPC-4 was carried out similarly to that of PPC-2 and PPC-3, but in this case, when loading the reagents, one mole of glycidyl methacrylate (GMA) out of the four used in the synthesis of PPC-3 and PPC-4 was replaced with one mole of allyl glycidyl ether [6].

The synthesized compounds are summarized in Fig. 2, which shows the differences in the structure of the compounds, as well as the types of compounds used in the synthesis to form a particular functionality in the product.

Polymer samples used later for testing were obtained in molds by curing PPCs in the presence of 0.5% by weight of the photoinitiator phenyl-bis(2,4,6-trimethylbenzoyl)-phosphine oxide (phenyl-bis(2,4,6-trimethylbenzoyl)-phosphine oxide (BAPO) under the influence of ultraviolet (UV) radiation in the UV Exposure Lab Chamber (*SPDI UV*, USA). Here, the radiation range of the mercury lamp is 200–400 nm, while the power is 62 W/cm^2 at a curing time in the chamber of 25 min. The exposure time of the samples following extraction from the molds is 10 min.

UV-cured polymer samples were subjected to sol–gel analysis by fluid extraction with supercritical carbon dioxide (using a supercritical fluid extractor SFT-110XW, *Supercritical Fluid Technologies, Inc*., USA). The results of the analysis indicate almost complete binding of monomers during polymerization (Table 1). The degree of curing was 100.0, 99.4, 98.0% for PPC-1, PPC-2, and PPC-3, respectively.

Table 1. Sol–gel analysis results

Samples	Gel fraction content, wt %	
	At 18°C	At 40°C
PPC-1	100.0	–
PPC-2	99.4	99.98
PPC-3	98.0	100.00

Note: the ratio of PPC/BAPO = 99.5 : 0.5 wt %. Conditions: pressure is 1300 psi, time is 3 h.

[1] Buravov B.A. Synthesis and properties of polymerization-capable phosphorus-containing oligomers with a spacer in the structure. Cand. Sci. Thesis (Chem.). Volgograd; 2020, 161 p. (In Russ).

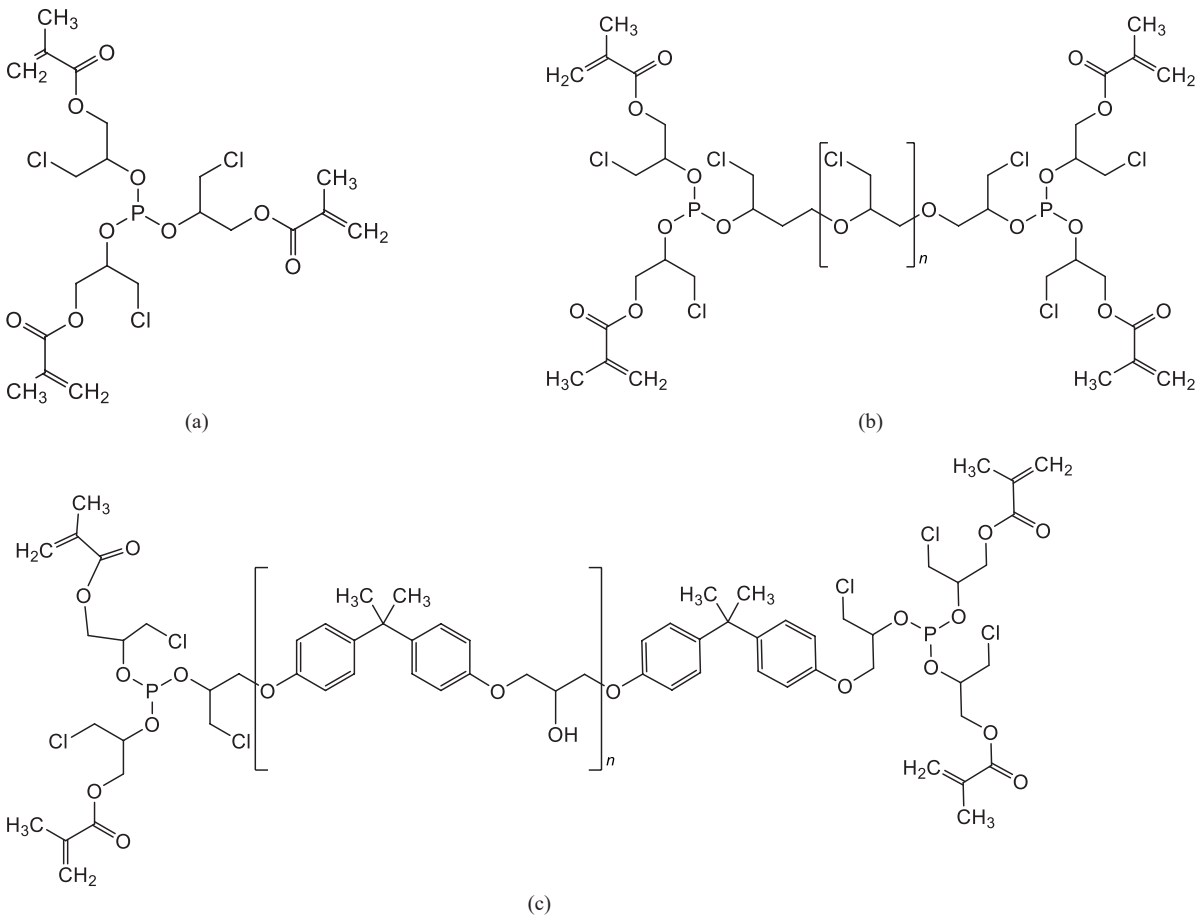

Fig. 1. Structure of (a) PPC-1; (b) PPC-2; (c) PPC-3

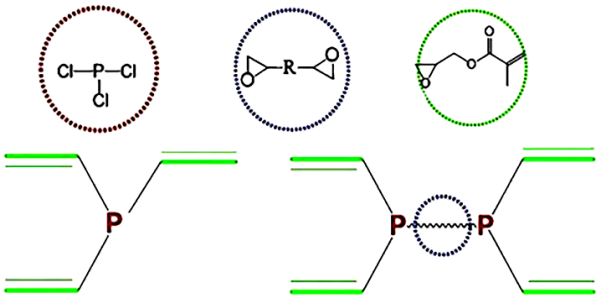

Fig. 2. Generalized structural chemical formulas and the starting reagents for their production: (a) PPC-1, without spacer; (b) PPC-2 and PPC-3, with the different spacer structure

The results of the sol–gel analysis indicate that the presence of spacer in the structure of the initial compound practically does not limit the conversion of the oligomeric methacrylate fragment into a spatially cross-linked material.

The study of the effect of the spacer and its structure on the properties of cured polymers was carried out under dynamic loading in accordance with GOST R 57916-2017[2] using the DMA method on a DMA 242 E Artemis device (*NETZSCH*, Germany) under double-arm bending conditions using the equipment and techniques supplied to the device.

[2] GOST R 57916-2017 (ISO 6721-5:1996). National Standard of the Russian Federation. Plastics. Determination of dynamic mechanical properties. Part 5. Flexural vibration. Non-resonance method. Moscow: Standartinform; 2017 (in Russ.).

RESULTS AND DISCUSSION

Dynamic flexural modulus of elasticity (*E′*)

The dynamic modulus of elasticity (*E′*) is a storage modulus that represents the energy stored in a sample under sinusoidally applied load. According to GOST R 56801-2015[3], the modulus of elasticity, which is proportional to the maximum energy stored during the loading cycle, serves as a measure of the stiffness of a viscoelastic material. The temperature dependence of changes in the stiffness of the studied cured polymers with and without different spacer structures is shown in Fig. 3. The summarized data is presented in Table 2. The analysis of the above data makes it possible to compare the rigidity and degree of structuring of the polymer matrix [7, 8].

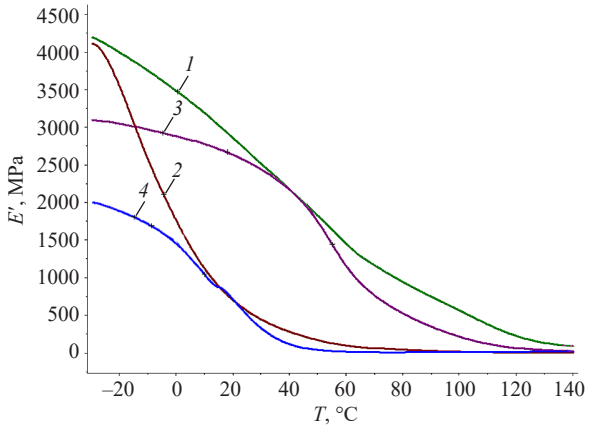

Fig. 3. Temperature dependence of the modulus of elasticity *E′*: (*1*) PPC-1; (*2*) PPC-2; (*3*) PPC-3; (*4*) PPC-4

The elastic modulus of all materials studied has three temperature-dependent areas:

- low-temperature area of the vitreous state;
- temperature area of the transition period, i.e., the area of rapid relaxation processes in the polymer matrix under the influence of applied loads, indicating that the material is in a transitional glassy-viscoelastic state;
- high-temperature area representing a plateau of highly elastic state of the material.

It can be seen from the presented data that the PPC-1 sample having the highest rigidity (*E′* = 4200 MPa*)* at a temperature of −25°C is the one whose monomer does not contain a spacer in the structure. The RPC-2 sample containing an aliphatic spacer (product residue E-181) is characterized by a slightly lower initial hardness value (*E′* = 4120 MPa). The PPC3 polymer, containing an aromatic spacer (ED-20 epoxy residue), has even lower rigidity (*E′* = 3090 MPa). A significantly lower initial stiffness value (*E′* = 2000 MPa) is obtained in the cured product sample (PPC-4) with an aromatic spacer in which one of the four methacrylate groups is replaced by an allylic one. This group, which is characterized by a lower reactivity compared to methacrylates, probably does not fully enter into photopolymerization reactions that act as a defective group, which ultimately leads to a decrease in crosslinking density. The compound PPC-4 (Fig. 4) was additionally synthesized by us under conditions similar to the preparation of PPC-1, PPC-2, and PPC-3 to identify the effect of defect formation in the structure of crosslinked polymers.

Table 2. Results of dynamic mechanical analysis of structured samples

Parameter	PPC-1	PPC-2	PPC-3	PPC-4
E'_{max}, MPa	4200	4120	3090	2000
E'_{min}, MPa	88	12	30	9
$T_{E_{min}}$, °C	140	70	140	120
T_g, °C, E'_{max}	−5	−20	35	0.0
E_a, kJ/mol	283.0	568.8	283.7	203.4

Note: *E′* is the dynamic modulus of elasticity under bending; E'_{max}, E'_{min} is the maximum and minimum value of the dynamic modulus of elasticity under bending; $T_{E_{min}}$ is the temperature at the minimum value of the modulus of elasticity under bending; T_g, °C, E'_{max} is the glass transition temperature determined at the maximum temperature of the dynamic modulus of elasticity; E_a is the activation energy of the viscous flow.

We should note significant differences in the response of material properties to the effect of temperature (Fig. 3). The sample without a spacer (curve *1*) probably has a homogeneous globular supramolecular structure, which determines a monotonous decrease in the value of the dynamic modulus of elasticity in the temperature range from −25 to +114°C. At the same time, the slight inflection in the region of 60°C is probably due to the release of interglobular bonds of the cured material, which differ little in terms of structure and chemical nature of the formed chemical bonds inside the globules.

The introduction of a soft spacer into the structure of the PPC-2 polymer, consisting of an aliphatic low-molecular-weight unit with oxygen in its main chain (Fig. 3, curve *3*), has practically no effect on the initial value of the dynamic modulus of elasticity compared

[3] GOST R 56801-2015 (ISO 6721-1:2011). National Standard of the Russian Federation. Plastics. Determination of dynamic mechanical properties. Part 1. General principles. Moscow: Standartinform; 2016 (in Russ.).

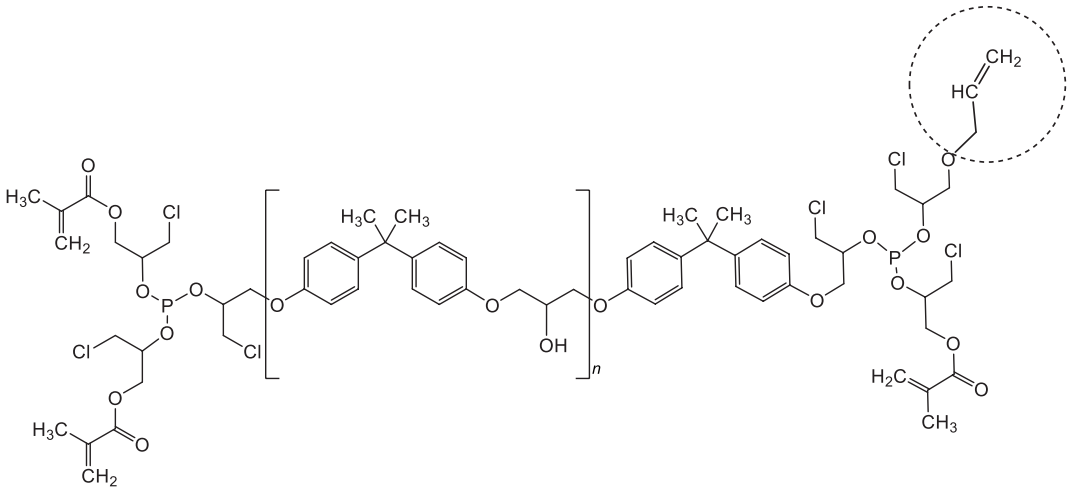

Fig. 4. Structure of PPC-4

with the PPC-1 sample without a spacer (Fig. 3, curve *1*). However, with a relatively small increase in temperature, the soft spacer exerts a plasticizing effect, which manifests itself in a fairly active and significant decrease in the dynamic modulus of elasticity of the PPC-2 sample without any observed transient phenomena [9], as is observed in other samples (PPC-1, PPC-3, PPC-4).

The dependence of the dynamic modulus of elasticity on the temperature of a polymer containing a volumetric hard aromatic spacer (PPC-3), a residue from ED-20 epoxy resin, has a pronounced bend in the range of 40°C (Fig. 3, curve *2*), which can be explained by an increase in the mobility of the globules of the formed matrix of the crosslinked polymer connected to each other an aromatic structure spacer. Accordingly, the E' value of the PPC-3 polymer matrix at temperatures from −25 to +40°C is determined by the combined effect of the spacer structure and the crosslinked globular structure of the polymer. An increased effect of the presence of a spacer above the specified temperature is expressed by a significant decrease in E' compared to the indicator of the PPC-1 polymer without a spacer.

The replacement of one of the four methacrylate fragments with a less reactive allylic fragment (Fig. 4, dotted line) significantly affects the elastic properties of the polymer matrix at low temperatures from −30 to +20°C. This effect, which is determined by a lower conversion of allyl groups during their polymerization, is confirmed by calculations of the crosslinking density shown below (Table 4). The introduction of a less reactive group leads to a decrease in the stiffness of the globules and consequent reduction in the initial values of the modulus of elasticity to 2000 MPa at −25°C, which shifts the transition state characteristic of PPC-3 to 0°C.

This assumption is confirmed by the values of the activation energy E_a of the viscous flow of polymers, which are determined by the results of DMA studies (Table 2). PPC-1 and PPC-3 have almost identical values of activation energies (283.0 and 283.7 kJ/mol, respectively). The increased activation energy of the viscous flow of PPC-2, which is almost twice as high as that of PPC-1 and PPC-3, can probably be explained by the flexibility of the spacer containing articulated oxygen in the main chain and presence of a polar substituent in the side chain [10].

For the PPC-4 polymer, there is a decrease in the activation energy from 283.7 to 203.4 kJ/mol, which indicates a significant decrease in the packing density of the globules of the resulting material. This was confirmed by calculations of the total crosslinking density of cured polymers (Table 4).

Dynamic loss modulus (E'')

The dynamic loss modulus (E'') is the energy dissipated as heat during the test cycle, and is determined by the area under the temperature dependence curve (Fig. 5) [11]. In fact, this is a characteristic of the mechanism of diffuse relaxation.

The investigated temperature dependence of the loss modulus of samples with spacers of different structures contained in the initial products retains the tendency of stiffness changes discussed above. Table 3 summarizes the research results.

The graphical and tabular data show the effect of the spacer in the polymer matrix on the value of the loss modulus and the temperature change of its maximum, which characterize the structural changes of the polymer.

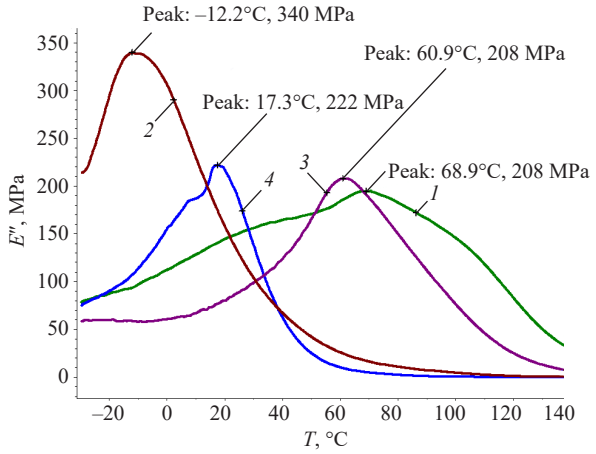

Fig. 5. Temperature dependence of the dynamic loss modulus E'': (*1*) PPC-1; (*2*) PPC-2; (*3*) PPC-3; (*4*) PPC-4

Table 3. Summary data by loss modulus

Parameter	PPC-1	PPC-2	PPC-3	PPC-4
E''_{max}, MPa	195	340	208	222
T_g, °C, E''_{max}	69	−12	60	17

The results obtained indicate that the polymer PPC-1, which does not have a spacer, has minimal dissipation of loading energy, characterized by a high packing density of polymer chains of the methacrylate fragment. Polymers having a volumetric aromatic spacer (PPC-3 and PPC-4) have relatively little difference in E''_{max} value. The presence of an aliphatic spacer in PPC-2 significantly increases the amount of stress energy dissipation during bending (E'' = 340 MPa) at sufficiently low temperatures characterized by a phase transition at lower temperatures (T_g = −12°C), which is probably due to the plasticizing effect of the mobile aliphatic spacer.

It should be noted that the shape of the temperature dependence of the loss modulus of the spacer samples differs significantly from the shape of the temperature dependence of the loss modulus of the comparison sample. The dependence of the loss modulus of PPC-1 has the form of a large halo over a wide temperature range. This behavior of the material can be explained in terms of a set of structures having a wide range of molecular weight distribution of polymer globules, as well as close values of strained interglobular and intraglobular chemical bonds, which are comparable both in terms of nature and strength.

The introduction of a low-reactive allyl group (PPC-4) has a significant effect on the properties of the material. As compared to PPC-3, the temperature of the maximum loss modulus decreases from 60 to 17°C, while the value of E'' increases from 208 to 222 MPa.

Thus, the introduction of spacers into the oligomer structure has a significant effect on the loss modulus. Polymer globules without a spacer have low mobility and consequently reduced tendency to dissipate energy from the applied load, which ultimately should make the material brittle. The presence of an aliphatic spacer, which likely acts as a soft crosslinking between the resulting high-molecular globules, significantly increases the loss modulus due to the plasticizing effect. The presence of a hard aromatic spacer exerts a negligible influence on the value of the indicator, concurrently constraining the temperature range of its maximum. This phenomenon can be elucidated by the diminished values of the molecular mass distribution of interconnected globular structures, which are circumscribed by the size of the monomer molecule.

Damping factor ($tg\delta_f$)

The magnitude of the values of the damping coefficient $tg\delta_f$ (damping factor) is an indicator of the relationship between the formed polymer phases of the material. The interaction, adhesion (penetration) between the phases, including their compatibility, as well as the effect of the curing method of the composite material, can be determined by the temperature dependencies of the indicator, whose maximum is used to determine the temperature (T_g) of the transition of the material to a viscoplastic state [12].

Figure 6 shows the temperature dependencies of the damping coefficient $tg\delta_f$. From the presented data, it can be seen that $tg\delta_f$ takes on large values with increasing temperature to reach a maximum in the region of the phase transition to the viscoelastic state.

It should be noted that $tg\delta_f$ has lower values at temperatures below T_g for all samples, since the segments of the chain of the cured material are not in a labile, but in a sedentary state. As the temperature increases, the chain segments, while maintaining the overall structure, become more mobile, which leads to an increase in the values of the indicator. Thus, the higher the extreme value of $tg\delta_f$, the higher the degree of molecular mobility [12].

Comparing the maximum values of $tg\delta_f$ of the studied samples of cured polymers based on PPC-1 (0.376) and PPC-3 (0.381), it is possible to make an assumption about their almost equal molecular mobility and relatively close values of phase transition temperatures (127 and 114°C, respectively). Considering the structure of the compounds, it can be stated that the aromatic spacer is inactive in polymer structures, which provides them with rigidity by limiting the mobility of globular segments [13].

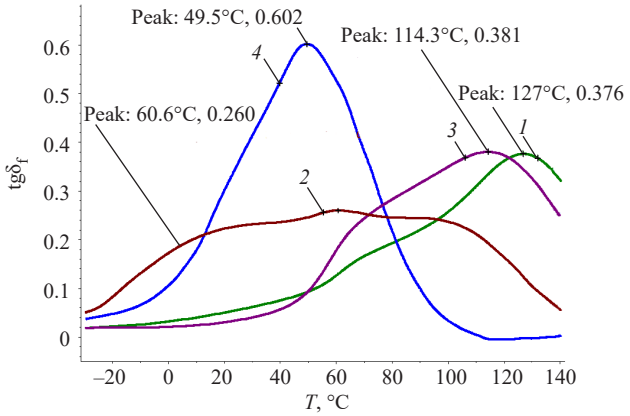

Fig. 6. Temperature dependence of $tg\delta_f$ structured phosphorus-containing oligomers: (*1*) PPC-1; (*2*) PPC-2; (*3*) PPC-3; (*4*) PPC-4

The temperature dependence of the PPC-4 damping coefficient, which is characterized by a lower crosslinking density (Fig. 6), has the maximum indicator value (0.6) compared to the others; this maximum manifests at a temperature of 50°C, which is 77 and 65°C lower than that of the samples PPC-1 and PPC-3, respectively. This may be attributed to the lower density of intra-globular PPC-4 crosslinking.

The crosslinking density [14, 15] was calculated according to the formula (1):

$$v = \frac{E'_r}{3 \cdot R \cdot T_r}, \quad (1)$$

where ν is the crosslinking density, mol/m^3; E'_r is the value of the dynamic modulus of elasticity under bending E' (J) at T_g + 30°C, the index r means the rubbery (elastic) state/area; T_r is the absolute temperature corresponding to T_g + 30°C; R is the universal gas constant, J/(K·mol).

The results of calculating the total crosslinking density are presented in Table 4.

Table 4. Summary data on the damping factor

Parameter	PPC-1	PPC-2	PPC-3	PPC-4
$tg\delta_{f\,max}$,	0.38	0.26	0.38	0.60
T_g, °C, $tg\delta_f$	127	60	114	50
v, mol/m^3	15473	10129	8018	4510

The temperature dependence of the PPC-2 damping coefficient has a rather blurred halo over a wide temperature range (from −30 to +140°C), while it practically does not change at temperatures from 20 to 110°C, having a slightly pronounced maximum at 60°C. This indicates the high viscoplastic properties of the polymer, which should provide high values of impact resistance as confirmed by additional studies (Fig. 7).

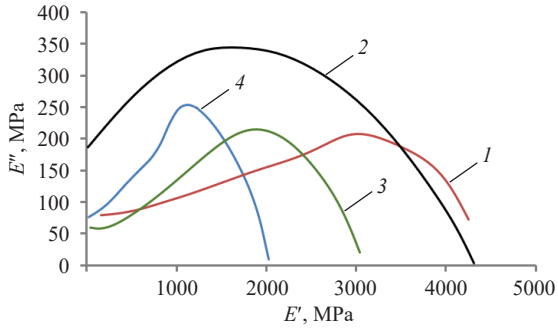

Fig. 7. Cole–Cole diagrams of UV-cured composites: (*1*) PPC-1; (*2*) PPC-2; (*3*) PPC-3; (*4*) PPC-4

The Cole–Cole diagram

Figure 7 shows the Cole–Cole graph, a tool for studying structural changes occurring in crosslinked polymers, which is important when comparing the effect of a spacer on the viscoelastic properties of polymer materials [16] since ultimately determining their physicomechanical properties. The semicircular character of the Cole–Cole graph, which is constructed in coordinates of the change in the loss modulus from the modulus of elasticity, can be used to characterize the degree of balance of the properties of the crosslinked polymer composite [17]. The imperfection of the semicircular shape indicates the structural heterogeneity of the formed material. On the other hand, the proximity of the shape of the dependence to the ideal sector of the circle indicates the balance of the structures composing the polymer matrix [14] over a wide temperature range. The summarized data is given in Table 5.

From the presented graphical data, it can be seen that the shape of the dependence of the loss modulus on the elastic modulus of a polymer containing no spacer is far from the shape of the ideal sector of a circle, whose maximum is shifted to the region of large values of the elastic modulus (Fig. 7, curve *1*). The introduction of a spacer of different structures brings the Cole–Cole diagram to a more perfect form (curves *2* and *3*), shifting the maximum of the loss modulus to the region of lower values of the elastic modulus close to its average value. Since the diagram characterizes the interaction of the structures of the formed crosslinked polymer, the introduction of a spacer can be concluded to leads to the formation of a more perfect structure [18] and consequent improvement in physicomechanical properties, including resistance to shock loads. This assumption

was confirmed by further comparative tests of the studied materials (see below).

Table 5. Summary data obtained from the Cole–Cole diagram

Parameter	PPC-1	PPC-2	PPC-3	PPC-4
E''_{max} (Cole–Cole), MPa	206	344	214	252
E' at E''_{max} (Cole–Cole), MPa	3056	1612	1943	1125
$\frac{1}{2}E'_{max}$, MPa	2100	2060	1545	1000

The replacement of one methacrylate group with an allyl group that is relatively less reactive to polymerization under the studied conditions [19] leads to a significant change in the Cole–Cole diagram (Fig. 7, curve *4*) and a decrease in characteristic parameters (Table 5). The shape of curve *4* deviates towards a less perfect one compared to the analogues of PPC-2 and PPC-3 (curves *2* and *3*), while the maximum loss modulus decreases and shifts to the region of lower values of the modulus of elasticity. This indicates an increase in the defect structure of the formed polymer matrix of the crosslinked material when a less reactive allyl group is introduced into the oligomer.

Summarizing the above and comparing the results of the DMA studies, we can conclude that the elastic properties of cured polymers are significantly affected by the introduction of a spacer into the oligomer structure. While the introduction of an aliphatic spacer leads to the formation of a material with increased elastic properties without changing the modulus of elasticity at low temperatures, it also provides greater globular mobility of the cured material. The introduction of an aromatic spacer leads to a decrease in the modulus of elasticity at relatively low temperatures, while maintaining the rigidity of the cured polymer at higher temperatures. In both cases, a more balanced structure of the cured polymer is formed.

The incorporation of low-reactive functional groups has been demonstrated to exert a substantial influence on the supramolecular structure of the material, consequently affecting the physicomechanical properties of the formed crosslinked matrix of the cured polymer.

The findings suggest that the incorporation of spacers within the structures of cured compounds facilitates the intentional fabrication of materials having predetermined viscoelastic properties, which is a process of particular significance for brittle phosphorus-containing materials.

Impact of spacer composition and morphology on a polymer material's physicomechanical properties, its heat, and fire resistance

In order to compare the results of DMA with the physicomechanical properties of polymers obtained in the presence of initiators of UV-cured materials based on PPC-1, PPC-2 and PPC-3, their strength under static bending, resistance to shock loads, heat resistance and fire resistance were investigated. In addition, decomposition models of PPC1, PPC-2, and PPC-3 and kinetic parameters of the ongoing macrostage reactions were obtained. The results of the conducted studies are shown in Figs. 8–10 and Tables 6–10.

Impact strength test results

The study of the effect of a spacer in the structure of oligomers on the impact resistance of polymers based on them was carried out using the incised iodine method in accordance with GOST 19109-2017 (ISO 180:2000)[4]. The obtained values of impact strength (Fig. 8) are fully consistent with the results of the conducted DMA studies.

It can be seen from the presented data that the cured polymer containing a soft aliphatic spacer (PPC-2) is characterized by higher values of impact resistance than the sample containing a hard spacer comprising the remainder of the ED-20 epoxy resin (PPC-3), which is probably due to the greater dissipation of impact energy by the moving part of the spacer.

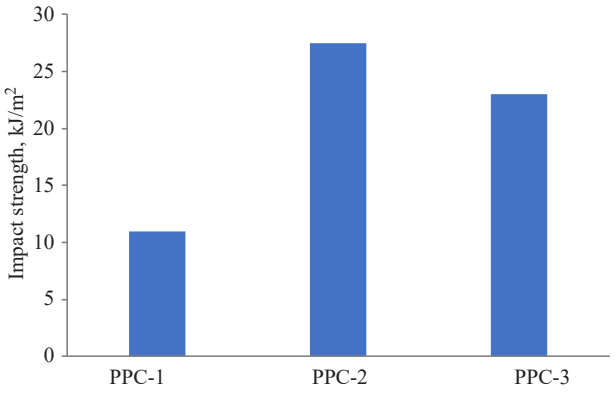

Fig. 8. Impact strength PPC1, PPC-2, and PPC-3

The introduction of spacers into the structure of oligomers is shown to increase the impact strength of cured polymers by 2.5–3 times, with the soft spacer having a more significant effect. This fact is in

[4] GOST 19109-2017 (ISO 180:2000). Interstate Standard. Plastics. Method for determination of Izod impact strength. Moscow: Standartinform; 2018 (in Russ.).

good agreement with the results of the DMA studies presented above.

The values of the modulus of elasticity determined in the study of the resistance of materials to static bending showed compliance with the DMA studies (Table 6) subject to consideration of the compliance of the temperature of the physicomechanical tests.

Table 6. Resistance to bending stress

Parameter	PPC-1	PPC-2	PPC-3
E, GPa	2.57	0.49	1.92
dl at fracture, %	2.6	8.4	2.4
$F_{break.}$, MPa	60	29.5	40.5

Note: *E* is Young's modulus; *dl* is elongation at fracture, %; F_{break} is breaking load, MPa.

RRS-1, which is characterized by a maximum value of Young's modulus *E* at bending (2.57 GPa), collapses with significantly greater applied forces (60 MPa) at the lowest deflection value (2.6%). The introduction of a soft spacer (PPC-2) leads to a decrease in the Young's modulus to 0.45 GPa (more than 5.5 times), a decrease in destructive loading to 29.5 MPa; at the same time, deflection increases by more than 3 times (8.4%) during fracture. The introduction of a hard spacer into the structure of the material (PPC-3) is accompanied by a decrease in its Young's modulus to 1.92 GPa with a 30% decrease in fracture stress and increased deflection values (3.4%).

The results confirm that the plastic properties of cured materials can be significantly enhanced by the introduction of spacers. Thermoplastic properties of polymers determined by the Vicat method according to GOST 15088-2014[5] (Table 7) also indicate an increase in the viscoplastic properties of cured samples containing a spacer in the oligomer structure. Increasing the load does not significantly change the softening temperature of PPC-1, while a decrease in softening temperatures is observed with increasing load for samples with a spacer (PPC-2 and PPC-3).

The results obtained indicate that the introduction of a spacer into the oligomer structure makes it possible to obtain a polymer material with enhanced viscoplastic properties, which is not typical for phosphorus-containing polymer materials and usually restricts their use in compounds.

Table 7. Vicat softening temperature

Test conditions	PPC-1	PPC-2	PPC-3
	Softening point, °C		
Load 10H	231	242 (0.5 mm)*	243
Load 50H	228	170	121

* Immersion of the indenter 0.5 mm into the sample at a temperature of 242°C.

Thermal stability

Considering that phosphorus-containing oligoester methacrylates should have a reduced flammability, it is of interest to evaluate the effect of the spacer on the thermal stability and flammability of polymers.

The thermal stability of the cured samples was evaluated using a Paulic–Paulic–Erdey derivatograph Q–1500 D (*IOM*, Hungary). The research results are shown in Fig. 9 and in Table 8. It can be seen that the samples differ in terms of heat resistance, the dynamics of the destruction process, and the amount of coke residue at 400°C. The presence of an aliphatic spacer in the PPC-2 sample slightly reduces the temperature of the beginning of decomposition of the material (~140°C) compared with PPC-1 (~145°C). The increased temperature of the onset of decomposition to ~190°C caused by the introduction of an aromatic spacer into the structure of the oligomer (PPC-3) indicates an increase in its heat resistance.

It is noted that the thermal degradation of PPC-1 and PPC-2 polymers proceeds by similar mechanisms. This is evidenced by similar dynamic processes occurring in the first stages of the destruction of materials, with the initiation of the process at temperatures of 140–150°C. A similar stage for the PPC-3 sample begins only at 160°C. In this case, the peak of the maximum decay occurs at 320°C, whereas for samples of PPC-1 and PPC-2 it occurs at 260°C. The observed fact indicates an increase in the thermal stability of the polymer when an aromatic spacer is introduced into it.

[5] GOST 15088-2014. Interstate Standard. Plastics. Thermoplastic materials. Determination of Vicat softening temperature (VST). Moscow: Standartinform; 2014 (in Russ.).

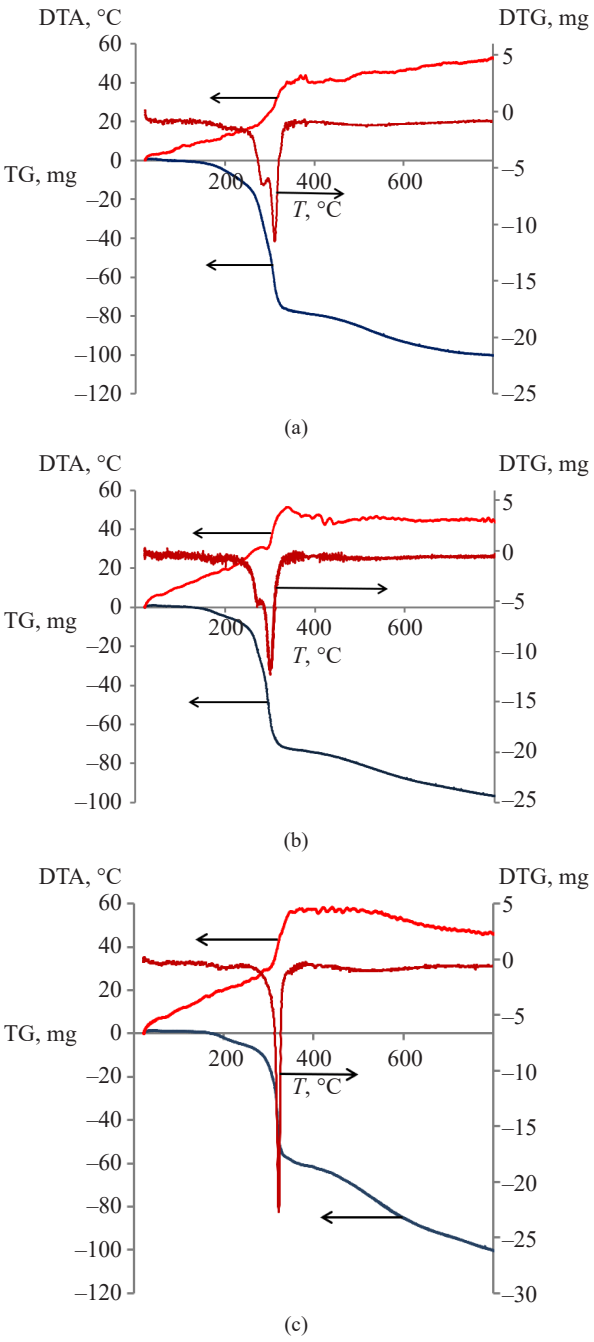

Fig. 9. Derivatograms of cured materials: (a) PPC-1; (b) PPC-2; (c) PPC-3. Heating rate 10°C/min. DTA — differential thermal analysis, °C; TG — thermogravimetry, mg; DTG — derivative thermogravimetry, mg/min

Table 8. Results of derivatographic studies

Samples	$T_{initial}$, °C	T_5, °C	T_{10}, °C	T_{50}, °C	Coke at 400°C, wt %
PPC-1	150	200	236	305	29
PPC-2	140	207	248	300	34
PPC-3	190	249	289	330	44

Note: $T_{initial}$ is the temperature of the beginning of destruction; T_5 is the temperature of 5% mass loss; T_{10} is the temperature of 10% mass loss; T_{50} is the temperature of 50% mass loss.

Table 9. Scheme of the polymer degradation model of PPC-1, PPC-2, PPC-3 and kinetic parameters of the proceeding reactions of macrostages

Reaction	A, 1/s	E_a, kJ/mol	n	Comment	Range T, °C
PPC-1					
RPC-1 → a-liquid	–	–	–	Phase change	~140–300
a-liquid → 0.84 b-liquid + gas	$6 \cdot 10^{12}$	156	0.32	Pyrolysis and evaporation	215–290
b-liquid → 0.29 c-liquid + gas	$1 \cdot 10^{13}$	168	0.42	Pyrolysis and evaporation	240–325
c-liquid → 0.1 a-char + gas	$1 \cdot 10^{2}$	75	1.1	Degradation	330–685
PPC-2					
PPC-2 → 0.98 a-liquid + gas	$5 \cdot 10^{6}$	77.7	2.96	Phase change	120–300
a-liquid → 0.82 b-liquid + gas	$1 \cdot 10^{13}$	155	0.3	Pyrolysis and evaporation	217–275
b-liquid → 0.23 c-liquid + gas	$1 \cdot 10^{15}$	186	0.65	Pyrolysis and evaporation	250–315
c-liquid → 0.1 char + gas	–	–	–	Degradation	~400–600
PPC-3					
PPC3 → a-liquid	–	–	–	Phase change	~150–250
a-liquid → 0.44 a-char + gas	$5 \cdot 10^{8}$	124	0.03	Evaporation	250–325
a-char → 0.1 b-char + gas	$8.6 \cdot 10^{4}$	115	2.89	Degradation	430–700

It should be noted that the thermal degradation of the PPC-3 polymer, which is characterized by a single stage without the formation of intermediate intermediates, probably occurs due to a more thermostable aromatic spacer. The greater heat resistance of PPC-3 is also evidenced by the amount of coke residue formed at a temperature of 400°C and amounting to 44% of the initial mass. For samples PPC-1 and PPC-2, this indicator corresponds to 29 and 34 wt %, respectively.

The study of thermal decomposition processes of PPC1, PPC-2, and PPC-3 at temperatures up to 800°C was carried out according to thermogravimetric analysis using the Reaxfire/gpyro program (2023)[6] within the framework of a decomposition model followed by the release of decomposition products into the gas phase (evaporation/sublimation). The scheme of the PPF decomposition model and the kinetic parameters of the ongoing macrostage reactions are presented in Table 9. The model considered four (for PPC-1 and PPC-2) and three (for PPC-3) sequential reactions (macrostades) of thermal decomposition of a pseudocomponent (in Table 9 they are designated a-, b-, c-liquid) along with the formation of new unidentified pseudocomponents. In this model, liquid can be understood as the solid state of a pseudocomponent that is consumed without

6 Generalized model of pyrolysis of combustible solids. URL: https://github.com/reaxfire/gpyro. Accessed July 07, 2024.

forming a liquid layer (sublimation). Figure 10 shows the nature of the main peaks of the reaction rates of the second and third stages of the decomposition of PPC, comprising an acute peak and a sharp front of the termination of the reaction.

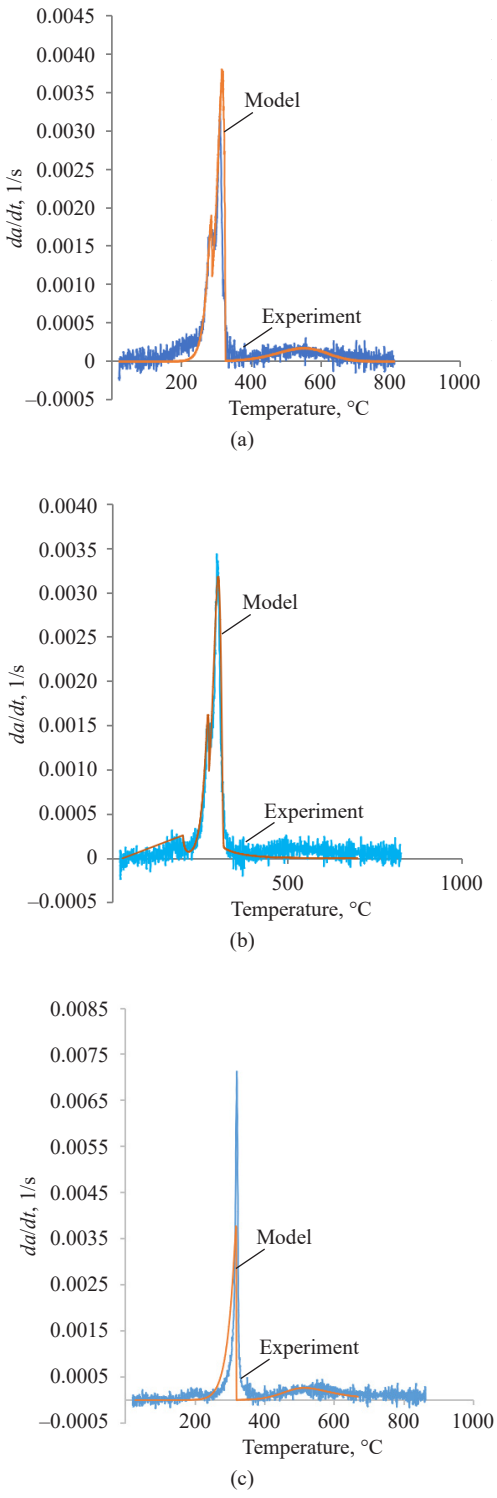

Fig. 10. Comparison of experimental data and simulation of thermal degradation kinetics:
(a) PPC-1; (b) PPC-2; (c) PPC-3

The simulation results satisfactorily describe the experimental data presented in Fig. 10. The reaction rate is represented as:

$$\frac{da}{dt} = k \cdot (1-a)^n, \quad (2)$$

where a is the fraction of the product formed; n is the reaction order; the reaction rate constant k is represented in Arrhenius equation $k = A \cdot \exp\left(-E_a / RT\right)$ (A is the preexponent, E_a is the activation energy of the reaction).

From formula (2), it can be seen that weakly concentration-dependent reactions occur when the reaction index is fractional (n = 0–1). An example is the thermal decomposition of minerals [20]. At n = 0, evaporation occurs, while at n = 1, a reaction involving one component occurs. When n > 1, reactions involving several components occur, as is often observed during the thermal decomposition of polymers [21]. Kinetic parameters for the first stage of decomposition of PPC-1 and PPC-3, which proceed at a low rate, have not been determined. The first stage, according to the proposed model, is associated with a change in the phase of matter and a small gas output (mass loss). It can be assumed that the first stage is associated with the transition of the polymer from a solid state to a softened one, in which the process of surface destruction of the interglobular region takes place. In the case of PPC-1 and PPC-2, the second and third stages are characterized by significant weight loss (60 wt %). In the framework of the proposed model, this is most likely due to the decomposition of the polymer and the formation of a monomer (for example, methyl methacrylate), which enters the gas phase without decomposition (evaporation) and involving partial decomposition of the spacer. This assumption is based on the low values of the reaction index for PPC-1 and PPC-2 (0.32–0.65). In the case of PPC-3 in the second stage, n = 0.03 is very close to zero, i.e., the main process of mass loss is evaporation.

The obtained kinetic data can be used to create a combustion model for the samples studied.

Determination of the flammability of cured phosphorus(III)-containing polymers

The thermal decomposition curves PPC-1 and PPC-2 (Fig. 10), showing the release of combustible products into the gas phase and the process of flame propagation, are close to each other and thus should not affect the values of the limiting oxygen index (LOI). However, with approximately the same phosphorus content, the chlorine content in PPC-1, which is a halogen and acts as a flame retardant, is significantly higher (1.45 times) than in PPC-2, which reduces the LOI for PPC-2 from 28 to 24 units. The amount of phosphorus and chlorine in the PPC-2 and PPC-3 polymers is very close, but the

Table 10. Results of flammability studies of photocured polymers

System components		Wt %		LOI, %
		P	Cl	
PPC-1	BAPO (0.5%)	5.5	18.7	28.0
PPC-2	BAPO (0.5%)	5.7	12.9	24.0
PPC-3	BAPO (0.5%)	5.2	11.8	27.0

LOI of PPC-3 is 3 units higher than that of PPC-2, which can be explained by the higher thermal stability of the aromatic spacer in PPC-3 (the maximum decomposition temperature of PPC-3 is 20°C higher than that of PPC-2) and smaller quantity of gases released (the remaining gases are larger at 400°C).

The flammability of crosslinked polymers was assessed by the LOI determination method (GOST 21793-76[7]). The results are presented in Table 10.

It can be seen from the presented data that the polymer without a spacer has the maximum LOI value. Samples with spacers have slightly lower LOI values.

Thus, it was found that the introduction of a spacer into the oligomer structure has a significant effect on the course of thermal degradation of cured polymers. The introduction of an aromatic spacer into the oligomer structure significantly increases the thermal stability of polymers. The presence of an aliphatic spacer in the structure of the oligomer reduces the temperature of the beginning of decomposition of the material, but leads to an increase in the coke residue in the end compared with the PPC-1 polymer.

CONCLUSIONS

It has been established by DMA that the introduction of an aliphatic spacer is accompanied by a decrease in the glass transition temperature of polymers from −5 to −20°C, the introduction of an aromatic spacer increases the glass transition temperature of the polymer to 35°C. The aliphatic spacer reduces the transition temperature to the viscoelastic state by 67°C, and the aromatic state by 13°C. The impact strength of the samples with spacers in the structure is 2.5–3 times higher than the impact strength of the reference sample without a spacer. Polymers with an aliphatic spacer have the most balanced properties, as confirmed by the Cole–Cole diagrams.

Derivatographic studies have established that the aliphatic spacer in the PPC structure increases the temperature of loss of 5% of the mass by 7°C, while the aromatic space leads to a corresponding loss by 49°C, as well as increasing the coke residue from 29 to 34 and 44 wt %, respectively. The LOI of polymers containing an aromatic spacer is 27, while that of the aliphatic spacer is 24.

Thus, it has been established that the introduction of spacers into the structure of phosphorus-containing polymerizable oligomers makes it possible to obtain polymers with reduced flammability and enhanced viscoelastic characteristics providing high resistance to shock loads.

Acknowledments

The work was financially supported by the Russian Science Foundation (project No. 25-29-00161) using the equipment of the Center for Collective Use at the Volgograd State Technical University.

Authors' contributions

B.A. Buravov—experimental data processing, writing the text of the article.

A. Al-Hamzawi—consultation on experimental procedures.

R.B. Gadzhiev—literature analysis, formalization of the reference list.

S.A. Orlova—literature analysis, formalization of the reference list.

L.Yu. Donetskova—experiment execution, data analysis, data processing.

S.M. Solomakhin—experiment execution, data analysis, data processing.

S.V. Borisov—consultation on rheological properties of binders.

O.S. Fomenko—translation of the abstract into English.

S.A. Trubachev—experiment execution, data analysis, data processing.

A.A. Paletsky—experiment execution, data analysis, data processing.

A.G. Shmakov—experiment execution, data analysis, data processing.

O.I. Tuzhikov—consultation on chemistry of phosphorus-containing compounds, as well as planning, methodology, and implementation of research.

O.O. Tuzhikov—research idea, consultation on experimental procedures, writing the text of the article.

The authors declare no conflicts of interest.

[7] GOST 21796-76. State Standard of the USSR. Plastics. Method for determination of the Oxygen Index. Moscow: Izdatelstvo standartov; 1976 (in Russ.).

REFERENCES

1. Tuzhikov O.I., Khokhlova T.V., Bondarenko S.N., Zotov S.B., Tuzhikov O.O., Rakhmangulova N.I. *Ehlastomery i plastiki s ponizhennoi goryuchest'yu* (*Elastomers and Plastics with Reduced Flammability*). Volgograd: Politekhnik; 2005, 214 p. (In Russ.).
2. Tuzhikov O.I., Khokhlova T.V., Bondarenko S.N., *et al.* Modification of epoxy-4,4′-isopropylidenediphenol resins with phosphorylated methacrylates for preparing compounds of the interpenetrating polymer network type. *Russ. J. Appl. Chem.* 2009;82(11):2034–2040. https://doi.org/10.1134/S107042720911024X
[Original Russian Text: Tuzhikov O.I., Khokhlova T.V., Bondarenko S.N., Dkhaibe M., Orlova S.A. Modification of epoxy-4,4′-isopropylidenediphenol resins with phosphorylated methacrylates for preparing compounds of the interpenetrating polymer network type. *Zhurnal prikladnoi khimii.* 2009;82(11):1887–1893 (in Russ.). https://www.elibrary.ru/tagrwk]
3. Bakhtina G.D., Kochnov A.B., Novakov I.A. Composition effect of copolymers unsaturated oligomers with phosphorus- and chlorine-containing methacrylate on their properties. *Izvestiya VolGGTU = Izvestia VSTU*. 2016;4(183):84–87 (in Russ.). https://www.elibrary.ru/vxlfez
4. Bakhtina G.D., Kochnov A.B., Borisov S.V., Novakov I.A. Properties of methyl methacrylate copolymers with phosphorus-chlorine and silicon-containing methacrylates. *Plasticheskie Massy*. 2018;(9-10):3–6 (in Russ.). https://doi.org/10.35164/0554-2901-2018-9-10-3-6
5. Buravov B.A., Al-Khamzawi A., Bochkarev E.S., Grichishkina N.Kh., Borisov S.V., Sidorenko N.V., Tuzhikov O.I., Tuzhikov O.O. Synthesis of new photo-cured phosphorus-containing oligoestermethacrylates with a spacer in the structure. *Fine Chem. Technol*. 2022;17(5):410–426. https://doi.org/10.32362/2410-6593-2022-17-5-410-426
6. Tuzhikov O.I., Tuzhikov O.O., Buravov B.A., Bochkaryov E.S., Khokhlova T.V., Sidorenko N.V. Use of oligoether acrylate of ((((1-(4-(2-(4-(3-(4-(2-(4-(2-((((1-(аллилокси)-3-halogenopropan-2-yl)oxy)((1-halogen-3-(methylacryloyioxy)propan-2-yl)-oxy)phosphin)oxy)-3-halogenpropoxy)phenyl)propan-2-yl)phenoxy)-2-hydroxypropoxy)phenyl)propan-2-yl)-phenoxy)-3-halogenopropan-2-yl)oxy)phosphin diiyl)bis(oxy))-bis(3-halogenopropane-2,1-diiyl)bis(2-methylacrylate) as a monomer for producing thermo- and heat-resistant polymers with low inflammability: RF Pat. 2712119. Publ. 24.01.2020.
7. Venkategowda T., Manjunatha L.H., Anilkumar P.R. Dynamic mechanical behavior of natural fibers reinforced polymer matrix composites–A review. *Materials Today: Proceedings*. 2022;54(Part 2):395–401. https://doi.org/10.1016/j.matpr.2021.09.465
8. Dias E., Chalse H., Mutha S., *et al*. Review on synthetic/natural fibers polymer composite filled with nanoclay and their mechanical performance. *Materials Today: Proceedings*. 2023; 77(Part 3):916–925. https://doi.org/10.1016/j.matpr.2022.12.059
9. Boyd R.H., Smith G.D. *Polymer Dynamics and Relaxation*. Cambridge University Press; 2010, 266 p. ISBN 978-0521152914
10. Askadskii A.A., Matveev Yu.I. *Khimicheskoe stroenie i fizicheskie svoistva polimerov* (*Chemical Structure and Physical Properties of Polymers*). Moscow: Khimiya; 1983, 248 p. (in Russ.).
11. Jeyaraman J., Jesuretnam B.R., Ramar K. Effect of stacking sequence on dynamic mechanical properties of Indian almond – Kenaf fiber reinforced hybrid composites. *J. Nat. Fibers*. 2022; 19(12):4381–4392. https://doi.org/10.1080/15440478.2020.1858219

СПИСОК ЛИТЕРАТУРЫ

1. Тужиков О.И., Хохлова Т.В., Бондаренко С.Н., Зотов С.Б., Тужиков О.О., Рахмангулова Н.И. *Эластомеры и пластики с пониженной горючестью*. Волгоград: РПК «Политехник»; 2005, 214 с.
2. Тужиков О.И., Хохлова Т.В., Бондаренко С.Н., Дхайбе М., Орлова С.А. Модификация эпоксидиановых смол фосфорсодержащими метакрилатами для получения компаундов типа взаимопроникающих полимерных сеток. *Журн. прикладной химии*. 2009;82(11):1887–1893. https://www.elibrary.ru/tagrwk
3. Бахтина Г.Д., Кочнов А.Б., Новаков И.А. Влияние состава сополимеров ненасыщенных олигомеров с фосфорхлорсодержащим метакрилатом на их свойства. *Известия ВолгГТУ*. 2016;4(183):84–87. https://www.elibrary.ru/vxlfez
4. Бахтина Г.Д., Кочнов А.Б., Борисов С.В., Новаков И.А. Свойства сополимеров метилметакрилата с фосфорхлор- и кремнийсодержащими метакрилатами. *Пластические массы*. 2018;(9-10):3–6. https://doi.org/10.35164/0554-2901-2018-9-10-3-6
5. Буравов Б.А., Аль-Хамзави А., Бочкарев Е.С., Гричишкина Н.Х., Борисов С.В., Сидоренко Н.В., Тужиков О.И., Тужиков О.О. Синтез новых фотоотверждаемых фосфорсодержащих олигоэфирметакрилатов со спейсером в структуре. *Fine Chem. Technol.* 2022;17(5):410–426. https://doi.org/10.32362/2410-6593-2022-17-5-410-426
6. Тужиков О.И., Тужиков О.О., Буравов Б.А., Бочкарёв Е.С., Хохлова Т.В., Сидоренко Н.В. Применение олигоэфиракрилата ((((1-(4-(2-(4-(3-(4-(2-(4-(2-((((1-(allyloxy)-3-галогенпропан-2-ил)окси) ((1-галоген-3-метакрилоилокси)-пропан-2-ил)окси)фосфин)окси)-3-галогенпропокси)-фенил)пропан-2-ил)фенокси)-2-гидроксипропокси)фенил)пропан-2-ил)фенокси)-3-галогенпропан-2-ил)окси)-фосфиндиил)бис(окси))бис(3-галогенпропан-2,1-диил)-бис(2-метилакрилат) в качестве мономера для получения термо- и теплостойких полимеров с пониженной горючестью: пат. 2712119 РФ. Заявка № 2019126210; заявл. 20.08.2019; опубл. 24.01.2020. Бюл. № 3.
7. Venkategowda T., Manjunatha L.H., Anilkumar P.R. Dynamic mechanical behavior of natural fibers reinforced polymer matrix composites–A review. *Materials Today: Proceedings*. 2022; 54(Part 2):395–401. https://doi.org/10.1016/j.matpr.2021.09.465
8. Dias E., Chalse H., Mutha S., *et al*. Review on synthetic/natural fibers polymer composite filled with nanoclay and their mechanical performance. *Materials Today: Proceedings*. 2023;77(Part 3):916–925. https://doi.org/10.1016/j.matpr.2022.12.059
9. Boyd R.H., Smith G.D. *Polymer Dynamics and Relaxation*. Cambridge University Press; 2010, 266 p. ISBN 978-0521152914
10. Аскадский А.А., Матвеев Ю.И. *Химическое строение и физические свойства полимеров*. М.: Химия; 1983, 248 с.
11. Jeyaraman J., Jesuretnam B.R., Ramar K. Effect of stacking sequence on dynamic mechanical properties of Indian almond – Kenaf fiber reinforced hybrid composites. *J. Nat. Fibers*. 2022;19(12):4381–4392. https://doi.org/10.1080/15440478.2020.1858219
12. Huang J., Zhou J., Liu M. Interphase in polymer nanocomposites. *JACS Au*. 2022;2(2):280–291. https://doi.org/10.1021/jacsau.1c00430
13. Van Krevelen D.W., te Nijenhuis K. *Properties of Polymers: Their Correlation with Chemical Structure: their Numerical Estimation and Prediction from Additive Group Contributions*: 4th edition. Elsevier; 2009, 1764 p.

12. Huang J., Zhou J., Liu M. Interphase in polymer nanocomposites. *JACS Au*. 2022;2(2):280–291. https://doi.org/10.1021/jacsau.1c00430
13. Van Krevelen D.W., te Nijenhuis K. *Properties of Polymers: Their Correlation with Chemical Structure: their Numerical Estimation and Prediction from Additive Group Contributions*: 4th edition. Elsevier; 2009, 1764 p.
14. Shao Z.-B., Zhang M.-X., Li Y., *et al*. A novel multi-functional polymeric curing agent: Synthesis, characterization, and its epoxy resin with simultaneous excellent flame retardance and transparency. *Chem. Eng. J*. 2018;345:471–482. https://doi.org/10.1016/j.cej.2018.03.142
15. Luo Q., Sun Y., Biao Y., *et al.* Synthesis of a novel DPPA-containing benzoxazine to flame-retard epoxy resin with maintained thermal properties. *Polymer. Adv. Technol*. 2019;30(8):1989–1995. https://doi.org/10.1002/pat.4631
16. Ben Abdallah A., Kallel A., Hassine T., *et al*. Modeling of viscoelastic behavior of a shape memory polymer blend. *J. Appl. Polymer Sci.* 2022;139(13):51859. https://doi.org/10.1002/app.51859
17. Singh J.K., Rout A.K. Thermal stability and dynamic mechanical analysis of nano-biofillers blended hybrid composites reinforced by cellulosic *Borassus flabellifer* L. fiber. *Int. J. Polymer Anal. Character*. 2023;28(6):552–563. https://doi.org/10.1080/1023666X.2023.2251792
18. Jayakumar A., Jacob J., Parameswaranpillai J., Hameed N., Krishnasamy S. *Polymer Crystallization: Methods, Characterization, and Applications*. Wiley; 2023, 384 p. ISBN 978-3527350810
19. Moad G., Solomon D.H. *The Chemistry of Radical Polymerization*. Elsevier; 2005, 666 p. ISBN 978-0080442860
20. Coats A.W., Redfern J.P. Kinetic Parameters from Thermogravimetric Data. *Nature.* 1964;201:68–69. https://doi.org/10.1038/201068a0
21. Korobeinichev O.P., Paletsky A.A., Gonchikzhapov M.B., Glaznev R.K., Gerasimov I.E., Naganovsky Y.K., *et al*. Kinetics of thermal decomposition of PMMA at different heating rates and in a wide temperature range. *Thermochim. Acta*. 2019;671:17–25. https://doi.org/10.1016/j.tca.2018.10.019

14. Shao Z.-B., Zhang M.-X., Li Y., *et al*. A novel multi-functional polymeric curing agent: Synthesis, characterization, and its epoxy resin with simultaneous excellent flame retardance and transparency. *Chem. Eng. J*. 2018;345:471–482. https://doi.org/10.1016/j.cej.2018.03.142
15. Luo Q., Sun Y., Biao Y., *et al.* Synthesis of a novel DPPA-containing benzoxazine to flame-retard epoxy resin with maintained thermal properties. *Polymer. Adv. Technol*. 2019;30(8):1989–1995. https://doi.org/10.1002/pat.4631
16. Ben Abdallah A., Kallel A., Hassine T., *et al*. Modeling of viscoelastic behavior of a shape memory polymer blend. *J. Appl. Polymer Sci.* 2022;139(13):51859. https://doi.org/10.1002/app.51859
17. Singh J.K., Rout A.K. Thermal stability and dynamic mechanical analysis of nano-biofillers blended hybrid composites reinforced by cellulosic *Borassus flabellifer* L. fiber. *Int. J. Polymer Anal. Character*. 2023;28(6):552–563. https://doi.org/10.1080/1023666X.2023.2251792
18. Jayakumar A., Jacob J., Parameswaranpillai J., Hameed N., Krishnasamy S. *Polymer Crystallization: Methods, Characterization, and Applications*. Wiley; 2023, 384 p. ISBN 978-3527350810
19. Moad G., Solomon D.H. *The Chemistry of Radical Polymerization*. Elsevier; 2005, 666 p. ISBN 978-0080442860
20. Coats A.W., Redfern J.P. Kinetic Parameters from Thermogravimetric Data. *Nature.* 1964;201:68–69. https://doi.org/10.1038/201068a0
21. Korobeinichev O.P., Paletsky A.A., Gonchikzhapov M.B., Glaznev R.K., Gerasimov I.E., Naganovsky Y.K., *et al*. Kinetics of thermal decomposition of PMMA at different heating rates and in a wide temperature range. *Thermochim. Acta*. 2019;671:17–25. https://doi.org/10.1016/j.tca.2018.10.019

About the Authors

Boris A. Buravov, Cand. Sci. (Chem.), Associate Professor, Department of General and Inorganic Chemistry; Senior Researcher, Laboratory of Polymer, Composite and Hybrid Functional Materials, Volgograd State Technical University (28, pr. im. V.I. Lenina, Volgograd, 400005, Russia). E-mail: byravov@ya.ru. Scopus Author ID 57972246000, ResearcherID AAH-5810-2021, RSCI SPIN-code 6730-5763, https://orcid.org/0000-0001-9039-571X

Ali Al-Hamzawi, Lecturer, Department of Chemical Technology, Technical Faculty, Al-Qadisiyah University (Al-Qadisiyah, Al-Diwaniyah, 58002, Iraq). E-mail: ali.alhamzawi80@gmail.com. Scopus Author ID 52902445200, ResearcherID M-2885-2017, RSCI SPIN-code 2551-0018, https://orcid.org/0000-0003-4491-494X

Rashid B. Gadzhiev, Senior lecturer, Department of General and Inorganic Chemistry, Volgograd State Technical University (28, pr. im. V.I. Lenina, Volgograd, 400005, Russia). E-mail: rbgadgiev@mail.ru RSCI SPIN-code 3100-9652, https://orcid.org/0000-0003-2658-7682

Svetlana A. Orlova, Cand. Sci. (Eng.), Associate Professor, Department of General and Inorganic Chemistry, Volgograd State Technical University (28, pr. im. V.I. Lenina, Volgograd, 400005, Russia). E-mail: osa5538@yandex.ru. ResearcherID MCY-1139-2025, RSCI SPIN-code 1410-0323, https://orcid.org/0009-0008-3078-1115

Lyubov Yu. Donetskova, Postgraduate Student, Assistant, Department of General and Inorganic Chemistry, Volgograd State Technical University (28, pr. im. V.I. Lenina, Volgograd, 400005, Russia). E-mail: lovedonetskova@mail.ru. Scopus Author ID 58849621700, ResearcherID KII-1406-2024, RSCI SPIN-code 8843-1727, https://orcid.org/0009-0008-8085-5071

Semyon M. Solomakhin, Postgraduate Student, Engineer, Department of General and Inorganic Chemistry, Volgograd State Technical University (28, pr. im. V.I. Lenina, Volgograd, 400005, Russia). E-mail: solomakhin-sim@mail.ru. Scopus Author ID 59412397400, ResearcherID AFG-4109-2022, RSCI SPIN-code 3085-4660, https://orcid.org/0009-0007-5040-3683

Sergey V. Borisov, Cand. Sci. (Eng.), Associate Professor, Department of Chemistry and Processing Technology of Elastomers; Senior Researcher, Laboratory of Polymer, Composite and Hybrid Functional Materials, Volgograd State Technical University (28, pr. im. V.I. Lenina, Volgograd, 400005, Russia). E-mail: borisov.volgograd@yandex.ru. Scopus Author ID 57193435253, ResearcherID AAF-1221-2021, RSCI SPIN-code 4774-4238, https://orcid.org/0000-0003-4400-0822

Olga S. Fomenko, Cand. Sci. (Philol.), Associate Professor, Department of Foreign Languages, Volgograd State Technical University (28, pr. im. V.I. Lenina, Volgograd, 400005, Russia). E-mail: folgase@gmail.com. RSCI SPIN-code 1083-3264, https://orcid.org/0009-0009-1633-0518

Stanislav A. Trubachev, Cand. Sci. (Phys.-Math.), Assistant Professor, Department of General Physics, Faculty of Physics, Novosibirsk State University (1, Pirogova ul., Novosibirsk, 630090, Russia); Senior Researcher, Laboratory of Kinetics and Combustion, Voevodsky Institute of Chemical Kinetics and Combustion, Siberian Branch of the Russian Academy of Sciences (3, Institutskaya ul., Novosibirsk, 630090, Russia). E-mail: trubachev@kinetics.nsc.ru. Scopus Author ID 57198490232, ResearcherID T-3224-2019, RSCI SPIN-code 8567-1930, https://orcid.org/0000-0001-7923-8318

Aleksander A. Paletsky, Dr. Sci. (Phys.-Math.), Senior Researcher, Laboratory of Kinetics and Combustion, Voevodsky Institute of Chemical Kinetics and Combustion, Siberian Branch of the Russian Academy of Sciences (3, Institutskaya ul., Novosibirsk, 630090, Russia). E-mail: paletsky@kinetics.nsc.ru. Scopus Author ID 6602774865, ResearcherID B-1171-2014, RSCI SPIN-code 3047-5032, https://orcid.org/0000-0003-2715-8484

Andrey G. Shmakov, Dr. Sci. (Chem.), Assistant Professor, Department of Chemical and Biological Physics, Faculty of Physics, Novosibirsk State University (1, Pirogova ul., Novosibirsk, 630090, Russia); Head of the Laboratory of Kinetics and Combustion, Voevodsky Institute of Chemical Kinetics and Combustion, Siberian Branch of the Russian Academy of Sciences (3, Institutskaya ul., Novosibirsk, 630090, Russia). E-mail: shmakov@kinetics.nsc.ru. Scopus Author ID 7006640724, ResearcherID A-9996-2014, RSCI SPIN-code 5968-6120, https://orcid.org/0000-0001-6810-7638

Oleg I. Tuzhikov, Dr. Sci. (Chem.), Professor, Department of Technology of Macromolecular and Fibrous Materials, Volgograd State Technical University (28, pr. im. V.I. Lenina, Volgograd, 400005, Russia). E-mail: tuzhikov_oi@vstu.ru. Scopus Author ID 6507272270, RSCI SPIN-code 7255-0330, https://orcid.org/0000-0003-1893-2861

Oleg O. Tuzhikov, Dr. Sci. (Eng.), Associate Professor, Head of the Department of General and Inorganic Chemistry, Volgograd State Technical University (28, pr. im. V.I. Lenina, Volgograd, 400005, Russia). E-mail: tuzhikovoleg@mail.ru. Scopus Author ID 12645529200, RSCI SPIN-code 8142-5915, https://orcid.org/0000-0001-6316-8896

Об авторах

Буравов Борис Андреевич, к.х.н., доцент, кафедра общей и неорганической химии; старший научный сотрудник, лаборатория полимерных, композитных и гибридных функциональных материалов, ФГБОУ ВО «Волгоградский государственный технический университет» (400005, Россия, Волгоград, пр-т им. В.И. Ленина, д. 28). E-mail: byravov@ya.ru. Scopus Author ID 57972246000, ResearcherID AAH-5810-2021, SPIN-код РИНЦ 6730-5763, https://orcid.org/0000-0001-9039-571X

Аль-Хамзави Али, преподаватель, кафедра химической технологии, технический факультет, Университет Аль-Кадисия (58002, Ирак, г. Эд-Дивания, район Аль-Джамаа, Сунния). E-mail: ali.alhamzawi80@gmail.com. Scopus Author ID 52902445200, ResearcherID M-2885-2017, SPIN-код РИНЦ 2551-0018, https://orcid.org/0000-0003-4491-494X

Гаджиев Рашид Бахман-оглы, старший преподаватель, кафедра общей и неорганической химии, ФГБОУ ВО «Волгоградский государственный технический университет» (400005, Россия, Волгоград, пр-т им. В.И. Ленина, д. 28). E-mail: rbgadgiev@mail.ru. SPIN-код РИНЦ 3100-9652, https://orcid.org/0000-0003-2658-7682

Орлова Светлана Авасхановна, к.т.н., доцент кафедры общей и неорганической химии, ФГБОУ ВО «Волгоградский государственный технический университет» (400005, Россия, Волгоград, пр-т им. В.И. Ленина, д. 28). E-mail: osa5538@yandex.ru. ResearcherID MCY-1139-2025, SPIN-код РИНЦ 1410-0323, https://orcid.org/0009-0008-3078-1115

Донецкова Любовь Юрьевна, аспирант, ассистент, кафедра общей и неорганической химии, ФГБОУ ВО «Волгоградский государственный технический университет» (400005, Россия, Волгоград, пр-т им. В.И. Ленина, д. 28). E-mail: lovedonetskova@mail.ru. Scopus Author ID 58849621700, ResearcherID KII-1406-2024, SPIN-код РИНЦ 8843-1727, https://orcid.org/0009-0008-8085-5071

Соломахин Семён Михайлович, аспирант, инженер, кафедра общей и неорганической химии, ФГБОУ ВО «Волгоградский государственный технический университет» (400005, Россия, Волгоград, пр-т им. В.И. Ленина, д. 28). E-mail: solomakhin-sim@mail.ru. Scopus Author ID 59412397400, ResearcherID AFG-4109-2022, SPIN-код РИНЦ 3085-4660, https://orcid.org/0009-0007-5040-3683

Борисов Сергей Владимирович, к.т.н., доцент, кафедра химии и технологии переработки эластомеров; старший научный сотрудник, лаборатория полимерных, композитных и гибридных функциональных материалов, ФГБОУ ВО «Волгоградский государственный технический университет» (400005, Россия, Волгоград, пр-т им. В.И. Ленина, д. 28). E-mail: borisov.volgograd@yandex.ru. Scopus Author ID 57193435253, Researcher ID AAF-1221-2021, SPIN-код РИНЦ 4774-4238, https://orcid.org/0000-0003-4400-0822

Фоменко Ольга Сергеевна, к.ф.н., доцент кафедры иностранных языков, ФГБОУ ВО «Волгоградский государственный технический университет» (400005, Россия, Волгоград, пр-т им. В.И. Ленина, д. 28). E-mail: folgase@gmail.com. SPIN-код РИНЦ 1083-3264, https://orcid.org/0009-0009-1633-0518

Трубачев Станислав Альбертович, к.ф.-м.н., старший преподаватель, кафедра общей физики, физический факультет, ФГАОУ ВО «Новосибирский национальный исследовательский государственный университет» (НГУ) (630090, Россия, Новосибирск, ул. Пирогова, д. 1); научный сотрудник, лаборатория кинетики процессов горения, ФГБУН «Институт химической кинетики и горения им. В.В. Воеводского Сибирского отделения Российской академии наук» (630090, Россия, Новосибирск, ул. Институтская, д. 3). E-mail: trubachev@kinetics.nsc.ru. Scopus Author ID 57198490232, ResearcherID T-3224-2019, SPIN-код РИНЦ 8567-1930, https://orcid.org/0000-0001-7923-8318

Палецкий Александр Анатольевич, д.ф.-м.н., ведущий научный сотрудник, лаборатория кинетики процессов горения, ФГБУН «Институт химической кинетики и горения им. В.В. Воеводского Сибирского отделения Российской академии наук» (630090, Россия, Новосибирск, ул. Институтская, д. 3). E-mail: paletsky@kinetics.nsc.ru. Scopus Author ID 6602774865, ResearcherID B-1171-2014, SPIN-код РИНЦ 3047-5032, https://orcid.org/0000-0003-2715-8484

Шмаков Андрей Геннадьевич, д.х.н., старший преподаватель, кафедра химической и биологической физики, физический факультет, ФГАОУ ВО «Новосибирский национальный исследовательский государственный университет» (НГУ) (630090, Россия, Новосибирск, ул. Пирогова, д. 1); заведующий лабораторией кинетики процессов горения, ФГБУН «Институт химической кинетики и горения им. В.В. Воеводского Сибирского отделения Российской академии наук» (630090, Россия, Новосибирск, ул. Институтская, д. 3). E-mail: shmakov@kinetics.nsc.ru. Scopus Author ID 7006640724, ResearcherID A-9996-2014, SPIN-код РИНЦ 5968-6120, https://orcid.org/0000-0001-6810-7638

Тужиков Олег Иванович, д.х.н., профессор, кафедра технологии высокомолекулярных и волокнистых материалов, ФГБОУ ВО «Волгоградский государственный технический университет» (400005, Россия, Волгоград, пр-т им. В.И. Ленина, д. 28). E-mail: tuzhikov_oi@vstu.ru. Scopus Author ID 6507272270, SPIN-код РИНЦ 7255-0330, https://orcid.org/0000-0003-1893-2861

Тужиков Олег Олегович, д.т.н., доцент, заведующий кафедрой общей и неорганической химии, ФГБОУ ВО «Волгоградский государственный технический университет» (400005, Россия, Волгоград, пр-т им. В.И. Ленина, д. 28). E-mail: tuzhikovoleg@mail.ru. Scopus Author ID 12645529200, SPIN-код РИНЦ 8142-5915, https://orcid.org/0000-0001-6316-8896

Translated from Russian into English by N. Isaeva
Edited for English language and spelling by Thomas A. Beavitt

Tonkie Khimicheskie Tekhnologii = Fine Chemical Technologies.
2025;20(6):612–621 ISSN 2686-7575 (Online)

Synthesis and processing of polymers and polymeric composites
Синтез и переработка полимеров и композитов на их основе

UDC 678.762.2
https://doi.org/10.32362/2410-6593-2025-20-6-612-621
EDN YIHUJZ

RESEARCH ARTICLE

Surface treatments of nitrile butadiene rubber to enhance wear resistance and mechanical properties

Ksenia V. Sukhareva[1,2], Igor A. Mikhailov[1,2], Bekzod B. Khaidarov[3], Anastasia D. Buluchevskaya[1,✉], Igor N. Burmistrov[3]

[1] *Higher School of Engineering "New Materials and Technologies," Plekhanov Russian University of Economics, Moscow, 109992 Russia*
[2] *Emanuel Institute of Biochemical Physics, Russian Academy of Sciences, Moscow, 119991 Russia*
[3] *National University of Science and Technology "MISIS," Moscow, 119049 Russia*
✉ *Corresponding author, e-mail: buluchevskaya.ad@rea.ru*

Abstract

Objectives. The aim of this work is to investigate rapid surface treatment methods of nitrile butadiene rubber (NBR) using an elastomer composition based on fluoropolymer FKM-32 and fluoroplastic F32L. The article presents new methods for enhancing the mechanical and wear properties of NBR by applying surface coatings.

Methods. Abrasion tests were conducted using an MI-2 tribometer; determination of the tensile strength properties of the samples was performed using a DVT GP UG 5 universal testing machine (*Devotrans*, Turkey). Hardness was ascertained using a Shore A type durometer. Samples were cut out on a pneumatic punching press GT-7016-AR (*GOTECH Testing Machines Inc*., Istanbul, Turkey). Microstructure and elemental composition studies were carried out using a Vega 3 scanning electron microscope (*TESCAN*, Brno, Czech Republic) equipped with an X-Act (*Oxford Instruments*, High Wycombe, United Kingdom) energy-dispersive analysis attachment.

Results. The immersion of NBR in a 10% solution of poly(vinylidene fluoride-co-chlorotrifluoroethylene) (fluoroplast F32L) in 1,1,2-trifluoro-1,2,2-trichloroethane was found to result in the formation of a uniform fluoropolymer-based coating on the rubber surface. This coating results in a decrease in the abrasion value from 0.046 to 0.005 m^3/TJ, corresponding to an increase in abrasion resistance. Furthermore, for rubbers coated by immersion in the fluoroplastic solution, the modulus at 100% and 300% strain increases by 86% and 44%, respectively, while the tensile strength increases by 20%, and the hardness increases by 9 units compared to the as-obtained NBR.

Conclusions. Regardless of pre-soaking in methyl ethyl ketone, the wear resistance of the synthetic rubber is not increased by surface treatment with elastomeric composition based on fluororubber FKM-32 grade followed by thermostating. However, surface-modification of NBR using the M3 method demonstrates better tribological performance and mechanical performance than the untreated sample. A complex of enhanced properties of surface-modified NBR-M3 can be effected by the presence of halogen atoms on the surface layer of the rubber sample.

Keywords

nitrile-butadiene rubber, fluoropolymer, fluoroplastic, wear resistance, mechanical properties

Submitted: 28.01.2025
Revised: 19.06.2025
Accepted: 12.11.2025

For citation

Sukhareva K.V., Mikhailov I.A., Khaidarov B.B., Buluchevskaya A.D., Burmistrov I.N. Surface treatments of nitrile butadiene rubber to enhance wear resistance and mechanical properties. *Tonk. Khim. Tekhnol. = Fine Chem. Technol*. 2025;20(6):612–621. https://doi.org/10.32362/2410-6593-2025-20-6-612-621

НАУЧНАЯ СТАТЬЯ

Обработка поверхности бутадиен-нитрильного каучука для повышения износостойкости и механических свойств

К.В. Сухарева[1,2], И.А. Михайлов[1,2], Б.Б. Хайдаров[3], А.Д. Булучевская[1,✉], И.Н. Бурмистров[3]

[1] *Высшая инженерная школа «Новые материалы и технологии», РЭУ им. Г.В. Плеханова, Москва, 109992 Россия*
[2] *Институт биохимической физики им. Н.М. Эмануэля, Российская академия наук, Москва, 119991 Россия*
[3] *Национальный исследовательский технологический университет «МИСиС», Москва, 119049 Россия*
✉ *Автор для переписки, e-mail: buluchevskaya.ad@rea.ru*

Аннотация

Цели. Разработать новые методы повышения механических и износостойких свойств бутадиен-нитрильных каучуков (nitrile butadiene rubber, NBR) путем нанесения поверхностных покрытий и исследовать методы быстрой обработки поверхности NBR с использованием эластомерной композиции на основе фторполимера ФКМ-32 и фторопласта F32L.

Методы. Испытания на истирание проводили с помощью трибометра МИ-2, определение прочностных свойств образцов — с помощью универсальной испытательной машины DVT GP UG 5 (*Devotrans*, Турция), твердость — с помощью твердомера типа Шор А. Образцы были вырезаны на пневматическом штамповочном прессе GT-7016-AR (*GOTECH Testing Machines Inc.*, Стамбул, Турция). Исследование микроструктуры и элементного состава проводили с помощью сканирующего электронного микроскопа Vega 3 (*TESCAN*, Брно, Чехия), оснащенного энергодисперсионной аналитической приставкой X-Act (*Oxford Instruments*, Хай-Вайкомб, Великобритания).

Результаты. Установлено, что погружение NBR в 10%-ный раствор поливинилиденфторида-трифторхлорэтилена (фторопласта F32L) в 1,1,2-трифтор-1,2,2-трихлорэтане приводит к образованию на поверхности резины равномерного покрытия на основе фторполимера и вызывает снижение величины абразивного износа (истираемость) с 0.046 до 0.005 м^3/ТДж, что соответствует существенному повышению абразивной стойкости NBR. Для каучуков, покрытых погружением во фторопластовый раствор, модуль упругости при 100 и 300%-ных деформациях увеличивается на 86 и 44% соответственно, в то время как прочность на растяжение увеличивается на 20%, а твердость увеличивается на 9 единиц по сравнению с полученным NBR.

Выводы. Обработка поверхности NBR эластомерным составом на основе фторкаучука марки ФКМ-32 с последующим термостатированием не позволяет снизить износостойкость резины независимо от предварительного замачивания в метилэтилкетоне. Модифицированный по поверхности NBR (методом М3) показывает лучшие трибологические и механические характеристики, чем необработанный образец. Наличие атомов галогенов на поверхностном слое образца отвечает за комплекс повышенных свойств поверхностно-модифицированного NBR-M3.

Ключевые слова

бутадиен-нитрильный каучук, фторполимер, фторопласт, износостойкость, механические свойства

Поступила: 28.01.2025
Доработана: 19.06.2025
Принята в печать: 12.11.2025

Для цитирования

Sukhareva K.V., Mikhailov I.A., Khaidarov B.B., Buluchevskaya A.D., Burmistrov I.N. Surface treatments of nitrile butadiene rubber to enhance wear resistance and mechanical properties. *Тонкие химические технологии*. 2025;20(6):612–621. https://doi.org/10.32362/2410-6593-2025-20-6-612-621

INTRODUCTION

In order to achieve the desired surface characteristics of rubber materials, various techniques have been developed. Of particular importance is surface modification, which can significantly change the material's friction characteristics, permeability, thermal stability, and mechanical properties. Methods used for surface modification purposes include those aimed at improving wear resistance and mechanical properties of rubber materials. These include surface irradiation [1], laser manipulation [2], corona discharge [3], plasma treatment including [4], photochemical modifications [5], and surface etching with an oxidation solution such as concentrated sulfuric acid and zirconium phosphate [6–8], as well as magnetron-sputtering [9, 10]. However, the mentioned technologies are typically complex and expensive. Therefore, the aim of the present

work is to explore a cost-effective and efficient approach to improving the tribological characteristics of rubber materials.

Surface halogenation effects are achieved on vulcanized rubber through chemical treatment using free halogen in organic solutions or the gaseous phase, and/or inorganic and organic halogenating agents. The foundation for priority research on polymer halogenation processes, including chlorination and fluorination of rubber surfaces, was established by studies conducted as far back as the 1960s. Significant contributions to the development of halogen-based modification of elastomers were made by researchers such as A.A. Dontsov [11], V.S. Yurovsky [12], Z.N. Nudelman [13–15], I.A. Tutorsky [16], and others. One method described involves chlorinating the surface of SBR using an organic liquid (1,3,5-trichloro-1,3,5-triazinane-2,4,6-trione, TCICA) in ethyl acetate [17]. Surface modification methods of rubber with halogen-containing compounds also include surface treatment using aqueous chlorinating agents, such as HCl-acidified sodium hypochlorite solution in both aqueous and ethanol solutions [18], and organic chlorine salt (sodium dichloro-isocyanurate) [19]. Here, poly(vinylidene fluoride-co-chlorotrifluoroethylene) (PVDF-CTFE) powder was used as a friction-modifying additive for rubber matrices. The study [20] describes a developed approach to obtaining neoprene- and silicone-based elastomers with a low coefficient of friction. The described rubbers were characterized by low physical and frictional properties due to poor compatibility of PVDF-CTFE powder. Recycled poly(vinylidene fluoride-co-chlorotrifluoroethylene) (r-PVDF-CTFE) was employed to prepare nitrile rubber (NBR)/r-PVDF-CTFE composites, characterized by increase in modulus at 300% and 27.8% and decrease in swelling index. Direct fluorination by F_2 has been employed to fluorinate a broad range of polymer materials, improving the hydrophilicity, surface tension, friction coefficient, and scratch resistance of rubber materials by attaching fluorine elements onto the rubber surface, forming –CF, $–CF_2$, or $–CF_3$ groups [21–26]. Direct fluorination can also lead to an increase in the crosslinking density of the fluoroelastomer film on the rubber surface. By increasing the contact angle it is possible to reduce wettability and surface tension while improving chemical resistance and adhesive properties of polymers. Direct fluorination can also be used to reduce the wear properties of rubbers over the course of repeated abrasion [27]. However, one of the main disadvantages of these methods is the high aggressiveness of the halogenation reagent, high labor input, undesirable presence of toxic byproducts, and complex technical design of the production process.

The present work sets out to enhance the wear resistance of synthetic rubber through surface modification with a fluoropolymer-containing solution treatment. The developed technology is characterized by a reduction in production stages through the treatment of the rubber surface with a fluorine-containing compound, as well as the exclusion of aggressive fluorine-containing modifiers from the formulation.

MATERIALS AND METHODS

Materials. NBR (BNKS-18 grade, *KZSK*, Krasnoyarsk, Russia) was used as a basic raw material. Synthetic butadiene-nitrile rubber is a copolymer of acrylic acid nitrile (17–20%) and 1,3-butadiene produced by emulsion polymerization at a temperature of 32°C. The main NBR characteristics and those of the rubber formulated based on NBR are presented in Tables 1 and 2.

Table 1. Properties of BNKS-18

Parameter	Value
Appearance	From light-yellow to dark-brown color
Mooney viscosity	40–70
Mass fraction of acrylonitrile, %	17–20
Glass transition temperature (T_g), °C	–47 ... –50
Density, kg/m³	943

Table 2. Formulation of studied samples in parts per hundred (phr) of rubber

Materials	Compound, phr
Nitrile butadiene rubber (BNKS-18)	100
Zink oxide	3
Sulfur	1.50
Stearic acid	1
Carbon black (P-324)	40
N-tert-butyl-benzothiazole sulfonamide	0.70
Total	146.20

The rubber mixes were prepared according to ASTM D 3184[1] using a two-roll mill at a temperature of 50°C. The vulcanization of rubber blends was conducted

[1] ASTM D 3184. Standard Test Methods for Rubber-Evaluation of NR (Natural Rubber) (Reapproved 2001).

at 170°C for 15 min. Table 2 sets out the parameters of the formulation used.

Fluoropolymer (FKM-32 grade, *HaloPolymer*, Kirovo-Chepetsk, Russia) is a copolymer of vinylidene fluoride and chlorotrifluoroethylene. Fluoroelastomers such as FKM-32 are distinguished by their ability to co-vulcanize with NBR due to the presence of active functional groups in their structure. This enables the formation of an integrated coating layer that is chemically and physically bonded to the rubber substrate, resulting in a unified material with enhanced surface mechanical properties. Unlike rigid polymer coatings, FKM-32 is characterized by significant elasticity. This elasticity allows the protective layer to maintain its integrity under repeated bending, stretching, and other mechanical stresses. FKM-32 is compatible with specific vulcanizing agents, such as *p*-quinone dioxime derivatives, which create crosslinks within the coating that not only enhance its mechanical strength, but also promote the formation of strong adhesive bonds with the rubber surface, improving the coating's resistance to delamination and mechanical damage. The main properties of the fluoropolymer are as presented in Table 3.

Table 3. Properties of FKM-32

Parameter	Value
Appearance	White crumb with individual semitransparent particles of the product
Mooney viscosity MB (4–4) 160°C	70–95
Thermal stability (mass loss at 270°C), wt %, no more than	0.15
T_g, °C	–17
F content, wt %	54–55
Cl content, wt %	14–16

This polymer was used in combination with the vulcanizing agent (quinol ester of *p*-quinone dioxime) and the dithiophosphate accelerator for application onto the surface of NBR rubber. The quinol ester of *p*-quinone dioxime (trade name EH-1 *Minkar*, Russia) appears in the form of a powder having a light-yellow to dark-yellow color. The *p*-quinone dioxime derivative was used as a curing agent for fluoroelastomers (FKM) due to its effective promotion of the formation of a crosslinked structure, which enhances the adhesion of the coating to the substrate and improves its mechanical strength. EH-1 acts not only as a vulcanizing agent but also as an adhesion promoter for the coating to NBR, owing to its chemical reactivity and ability to form strong bonds with the substrate surface. The dithiophosphate accelerator (trade name Kvalaks C1, *NPP Kvalitet*, Moscow, Russia) is a transparent liquid ranging from yellow to brown in color with a zinc mass fraction of 8.8% and a kinematic viscosity at 100°C of not less than 6 cSt. The final formulation of the composition based on fluoropolymer is presented in Table 4. Quinol ether was chosen as the vulcanizing agent, which is capable of structuring halogen-containing—in our case, fluorine-containing—rubbers. Accelerator and the vulcanizing agent dissolve well in methyl ethyl ketone (MEK).

Table 4. Formulation of the composition based on fluoropolymer (FKM-32)

Materials	Compound, phr
Fluoropolymer (FKM-32)	100
Dithiophosphate accelerator	2
The quinol ester of *p*-quinone dioxime	6

The elastomeric composition of this formulation (Table 4) is prepared as a 10% solution in methyl ethyl ketone. Rubbers based on NBR have a high ability to swell in MEK, which in turn facilitates the penetration of fluoropolymer into the rubber sample structure for the purpose of creating a surface-modified layer of NBR rubber.

Poly(vinylidene fluoride-co-chlorotrifluoroethylene) (fluoroplast grade F32L, *HaloPolymer*, Kirovo-Chepetsk, Russia), representing a copolymer of trifluorochloroethylene and vinylidene fluoride, is a chemically resistant polymer that dissolves well in ketones, complex esters, Freon-113, and tetrahydrofuran. Fluoroplasts, including grade F-32L, are characterized by an extremely low coefficient of friction against steel, which allows for a significant reduction in the surface friction of rubber coated with such materials. As a result, the wear resistance and durability of rubber products operating under conditions of friction, sliding, and abrasive stress are greatly improved. The copolymer based on vinylidene fluoride and chlorotrifluoroethylene exhibits excellent chemical resistance to aggressive environments, oils, solvents, and chemical agents. This material may be applied as a surface coating to create a protective barrier that prevents the penetration of aggressive substances into the rubber bulk, thereby preserving its original performance characteristics. Fluoroplast F-32L also features relatively high hardness, resulting in the formation of a rigid and wear-resistant surface layer on the rubber. This protects the softer NBR substrate from damage during contact with hard abrasive

surfaces, preserving its mechanical properties and extending the service life of the product. Being soluble in a number of organic solvents (e.g., 1,1,2-trifluoro-1,2,2-trichloroethane), fluoroplast F-32L can penetrate into the rubber surface during application due to partial swelling of the elastomer. After solvent evaporation, a uniform, thin, and mechanically strong coating is formed, which is firmly bonded to the substrate at the molecular level, thus ensuring high resistance to delamination and mechanical stress. The main properties of the fluoropolymer are as presented in Table 5.

Table 5. Properties of fluoroplast F-32L

Parameter	Value
Appearance	Coarse-grained powder of white or slightly yellowish color
Density, kg/m^3	1920–1950
Thermal stability (mass loss at 270°C 5h), wt %, no more than	0.1–1.0
T_g, °C	30
Coefficient of friction on steel	0.04
Brinell hardness, MPa	29–39

As a solvent for the fluoroplastic, 1,1,2-trifluoro-1,2,2-trichloroethane (CFC-113) was used. This compound is highly volatile and is classified as a low hazard (hazard class 4), meaning it does not necessitate specific protective measures for personnel due to its low toxicity. These attributes make it suitable for this application.

Modification. Various approaches have been proposed for improving the surface properties of NBR-based rubbers through the application of functional coatings. In the present study, samples of NBR rubber were prepared as dumbbell-shaped specimens (for tensile testing) and square-shaped specimens (for abrasion tests) were subjected to different types of surface treatments. The specific surface treatment methods applied to the rubber samples are summarized in Table 6. According to these methods, the developed compositions are intended to form a uniform coating on the rubber surface, which creates a stable surface layer after drying and thermal exposure. This coating is likely to reduce wear rates and the friction coefficient by reinforcing the surface without altering the bulk structure of the vulcanizate.

Table 6. Specific surface treatment methods

Modification type	Description of the modification method
M1	An elastomer composition of the following content: FKM-32, quinol ester of *p*-quinone dioxime and dithiophosphate accelerator (10 wt % solution in MEK) were applied to the rubber surface using a brush (T = 25 ± 0.5°C). The total number of applied layers was 4, with 24 h of drying time between layers. The sample with the dried coating was thermostated at a temperature of 150°C for 10 min.
M2	Pretreatment of NBR rubber was conducted by immersing in MEK for 10 min. An elastomer composition of the following content: FKM-32, quinol ester of *p*-quinone dioxime and dithiophosphate accelerator (10 wt % solution in MEK) were applied to the rubber surface using a brush (T = 25 ± 0.5°C). The total number of applied layers was 4, with 24 h of drying time between layers. The sample with the dried coating was thermostated at a temperature of 150°C for 10 min.
M3	Samples of NBR were immersed in a 10% solution of fluoroplast F32L in 1,1,2-trifluoro1,2,2-trichloroethane and kept for 6 h (T = 25 ± 0.5°C), after which they were dried to a constant weight.

Experimental methods. The abrasion tests were conducted using an MI-2 tribometer, designed for assessing rubber wear, according to the method for determining abrasion resistance under sliding against rigidly fixed abrasive particles according to GOST 426-77[2]. The abrasion resistance was calculated under a load of 26 N and a disk sliding rate of 40.0 rpm, with the test samples securely fixed in a holder. An abrasion disc made of stainless steel grade 25 (SS) and chrome nickel steel (CrNi) served as the abrasion surface. Volume abrasion was assessed every five minutes by weighing the samples and calculating the subsequent mass loss. The samples for the wear resistance test, with a wearing surface in the form of a square (each side measuring 20 mm), were equipped with tabs of 4 mm width and 3 mm height for attachment to the holder frame. Based on the experimental data, the following indicators were calculated.

The volume loss of the rubber (ΔV) in cm for the two tested samples is calculated using Eq. (1):

$$\Delta V = \frac{m_1 - m_2}{\rho}, \quad (1)$$

[2] GOST 426-77. Interstate Standard. Rubber. Method for determination of abrasion resistance under slipping. Moscow: IPK Izdatelstvo standartov; 1977.

where m_1 is the mass of the two samples before the test in kg, m_2 is the mass of the two samples after the test in kg; ρ is the density of the rubber in kg/m^3.

The abrasion resistance (α) in cm^3/kW·h is calculated using Eq. (2):

$$\alpha = \frac{\Delta V}{A} \times \frac{1}{K}. \quad (2)$$

The formula for converting abrasion values from cm^3/kW·h to m^3/TJ is as follows:

$$\text{Abrasion (m}^3\text{/TJ)} = \\ = [\text{Abrasion (cm}^3\text{/kW·h)} \cdot 10^{-6}]/(3.6 \cdot 10^{-3}), \quad (3)$$

where 1 cm^3 = 10^{-6} m^3, 1 kW·h = $3.6 \cdot 10^6$ J = $= 3.6 \cdot 10^{-3}$ TJ.

Abrasion resistance was calculated as loss in weight after 200 and 3000 abrasion cycles.

Determination of the tensile strength properties of the samples was performed using a DVT GP UG 5 universal testing machine (*Devotrans*, Turkey) in accordance with the ISO 37:2024 Standard[3], at a testing rate of 100 mm/min. Samples were cut out on a pneumatic punching press GT-7016-AR (*GOTECH Testing Machines Inc*., Istanbul, Turkey). Each data point was corroborated with five measurements. Hardness was ascertained using a Shore A type durometer, adhering to the testing method outlined in the ASTM D2240-2015 (R 2021) Standard[4]. Shore hardness tests were carried out on specimens with a thickness of 6 mm.

The study of the microstructure and elemental composition of modified NBR rubber was carried out using a Vega 3 scanning electron microscope (*TESCAN*, Brno, Czech Republic) equipped with an X-Act (*Oxford Instruments*, High Wycombe, United Kingdom) energy-dispersive analysis attachment.

RESULTS AND DISCUSSION

The abrasion test was employed to evaluate changes in abrasion resistance and the average friction coefficient of both the as-received and surface-treated NBR samples (Table 7).

Analysis of the performance of samples modified using methods M1 and M2 confirms that their abrasion resistance and friction behavior remains comparable to those of the unmodified (as-received) rubber. Pretreatment involving soaking in MEK had a negligible effect on the efficiency of surface treatment.

When chrome-plated steel was used as the counterbody material, a decrease in wear resistance was observed along with an increase in the friction coefficient, indicating less favorable tribological performance. The limited effectiveness of the M1 and M2 methods may be explained by insufficient interfacial bonding between the NBR surface and the applied fluoroelastomer layer, likely due to the inherently low adhesion of the fluoroelastomer to the rubber substrate.

In contrast, the sample modified via the M3 method demonstrated a significant (nearly two orders of decimal

Table 7. Friction coefficient and abrasion of as-received and modified rubbers

Grinding metal	Rubber	Abrasion, m^3/TJ		Friction coefficient	
		Abrasion cycles			
		200	3000	200	3000
SS*	as-received NBR	0.046	0.043	0.92	0.90
CrNi**	as-received NBR	0.032	0.027	0.93	0.89
SS	NBR-M1	0.048	–	0.95	–
CrNi	NBR-M1	0.027	–	1.55	–
SS	NBR-M2	0.045	–	0.80	–
CrNi	NBR-M2	0.028	–	1.41	–
SS	NBR-M3	0.0005	0.0004	0.50	0.49
CrNi	NBR-M3	0.0004	0.0003	0.47	0.45

* SS is stainless steel grade 25;

** CrNi is chromium-nickel steel.

[3] ISO 37:2024. Rubber, vulcanized or thermoplastic—Determination of tensile stress-strain properties.

[4] ASTM D2240-2015 (R 2021). Standard test method for rubber property. Durometer hardness.

magnitude) improvement in abrasion resistance, decreasing from 0.046 m^3/TJ for the as-received NBR to just 0.005 m^3/TJ. This enhancement is attributed to the formation of a uniform fluoropolymer-based surface coating as a result of immersion in a fluoroplast F32L solution.

The application of the fluoropolymer coating also led to a marked reduction in the initial friction coefficient against metal substrates. This effect is primarily associated with a decrease in adhesive interaction at the sliding interface, which is a well-known characteristic of perfluorinated polymer surfaces. The deposited surface layer exhibits properties similar to those of highly fluorinated polymers, which are distinguished by their extremely low surface energy and exceptional anti-adhesive performance. Fluoropolymers, including the one used in this study, typically demonstrate ultra-low friction coefficients (as low as 0.05 against steel).

The influence of each surface treatment method on the mechanical properties of NBR according to collected and analyzed mechanical test data is summarized in Table 8.

Table 8. Mechanical properties of the initial and modified rubbers

Properties	As-received NBR	NBR-M1	NBR-M2	NBR-M3
Tensile modulus at 100%, MPa	2.05	2.68	3.03	3.82
Tensile modulus at 300%, MPa	6.83	8.29	8.50	9.87
Tensile strength, MPa	10.17	10.81	10.61	12.29
Elongation at break, %	580	530	490	490
Relative residual elongation, %	9	12	9	6
Hardness (Shore A), a.u.	57	61	63	68

As shown in Table 8, the mechanical properties of surface-treated NBR—including tensile modulus at 100% and 300% strain, as well as tensile strength and hardness—show improvements compared to the as-received NBR. For samples modified using methods M1 and M2, the tensile strength remains comparable to that of the unmodified rubber, indicating that the bulk integrity of the elastomeric matrix is preserved. Notably, the hardness of NBR-M1 and NBR-M2 samples increased by 4 and 6 Shore A units, respectively. This change can be attributed to the formation of a stiffer surface layer due to the application of the fluoroelastomer-based composition. However, this increase in hardness is superficial in nature and not associated with a measurable increase in cross-link density: no experimental data (e.g., swelling tests or NMR-based analysis) confirm changes in the network structure of the vulcanizate. For the M3-treated rubber samples, which were immersed in a fluoroplast solution, the modulus at 100% and 300% strain increased by 86% and 44%, respectively; the tensile strength improved by 20%; and the hardness rose by 9 Shore A units compared to the as-received NBR. These findings are in line with previous studies suggesting that increases in hardness correlate with higher values of elastic modulus.

The observed hardness enhancement—particularly in the NBR-M3 sample—is due to the presence of a rigid fluoroplastic surface coating, which reduces the indentation depth during Shore A hardness measurements. This effect, which is mechanical rather than chemical, does not reflect an actual increase in cross-link density within the rubber bulk. Accordingly, the abrasion disc penetrates less deeply into the harder surface layer, which contributes to improved wear resistance. Moreover, it is well known that the friction coefficient of harder rubber is generally lower than that of softer rubber when sliding against rough surfaces [28]. Therefore, the observed decrease in friction for M3-modified samples is consistent with the formation of a rigid, low-energy fluoropolymer surface layer.

The depth and uniformity of the applied surface coating in the M3-modified NBR were evaluated using Scanning Electron Microscopy combined with Energy Dispersive X-ray Spectroscopy (SEM-EDX), as shown in Figs. 1 and 2.

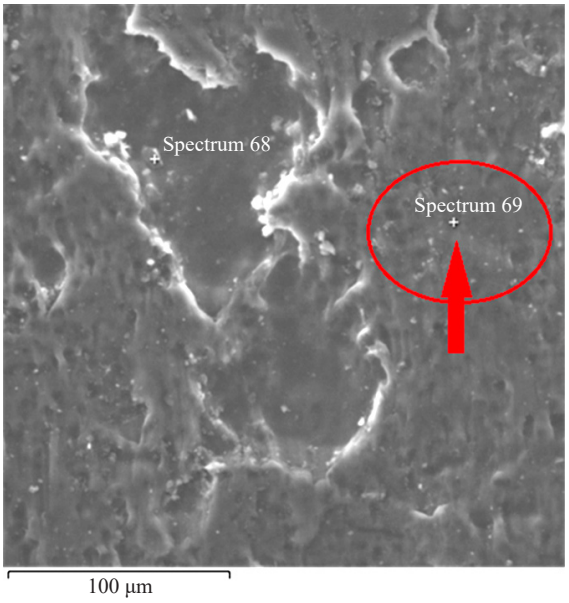

Fig. 1. SEM micrographs of NBR rubber after M3 modification (NBR-M3)

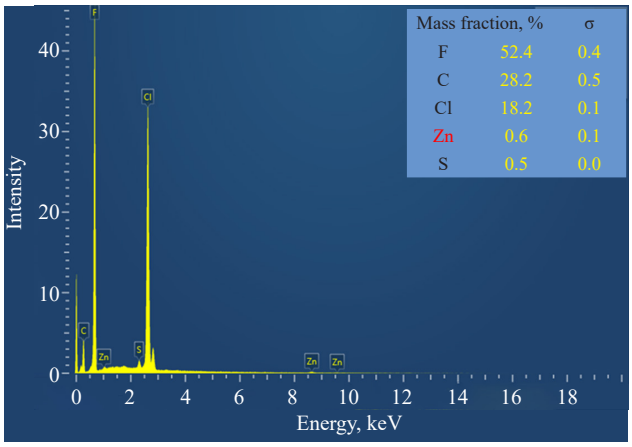

Fig. 2. Energy dispersive X-ray analysis (EDX) spectrum of NBR-M3

The EDX spectrum of the NBR rubber surface after immersion in 1,1,2-trifluoro-1,2,2-trichlorethane was used for quantitative elemental analysis (Figs. 1 and 2). The analysis confirmed the presence of fluorine (52.4 ± 0.4 at. %) and chlorine (18.2 ± 0.1 at. %) in the surface layer of the polymer. Moreover, pointwise EDX measurements indicated a uniform distribution of these halogen elements across the surface, suggesting that the applied fluoropolymer coating is continuous and well-adhered (Fig. 2).

CONCLUSIONS

In this work, new methods of enhancing the surface properties of NBR rubber through fluoropolymer-based coatings are proposed and evaluated. The study considered three surface treatment approaches. Methods M1 and M2 involved applying an elastomeric composition based on FKM-32 and a vulcanizing agent to the rubber surface, with method M2 additionally including a pre-swelling step in MEK for 10 min to facilitate deeper penetration of the composition into the rubber matrix. Method M3 consisted of immersing the rubber samples in a 10% solution of fluoroplast F32L in 1,1,2-trifluoro-1,2,2-trichloroethane for 6 h, resulting in the formation of a rigid surface layer.

Experimental results showed that, regardless of the use of pre-swelling in solvent, methods M1 and M2 had limited influence on improving wear resistance or reducing friction. This limited performance is likely related to insufficient adhesion of the applied elastomeric layer to the NBR substrate. In contrast, surface treatment via method M3 led to a substantial enhancement in both tribological and mechanical properties, including a significant reduction in the friction coefficient and wear rate, as well as increases in modulus and hardness. The improved performance of M3-treated samples is attributed to the presence of a continuous fluoropolymer coating, which modifies the surface characteristics without affecting the bulk rubber structure.

As confirmed by SEM-EDX analysis after drying and washing, the presence of fluorine and chlorine atoms in the surface layer indicates that the applied coating remains intact and is responsible for the observed improvements in performance.

Acknowledgments

The authors thank the Center of Shared Usage "New Materials and Technologies" of Emanuel Institute of Biochemical Physics and Joint Research Center of Plekhanov Russian University of Economics for providing the necessary equipment.

Authors' contributions

K.V. Sukhareva—research concept, experimental work, processing experimental data, writing original draft.

I.A. Mikhailov—research concept, writing original draft, processing experimental data.

B.B. Khaidarov—correction of the research concept, processing experimental data.

A.D. Buluchevskaya—experimental work and editing.

I.N. Burmistrov—correction of the research concept.

The authors declare no competing interests.

REFERENCES

1. Ning K., Lu J., Xie P., Hu J., Huang J., Sheng K. Study on Surface Modification of Silicone Rubber for Composite Insulator by Electron Beam Irradiation. *Nucl Instrum Methods Phys Res B*. 2021;499:7–16. https://doi.org/10.1016/j.nimb.2021.04.019
2. Song J., Vancso G.J. Effects of Flame Treatment on the Interfacial Energy of Polyethylene Assessed by Contact Mechanics. *Langmuir*. 2008;24:4845–4852. https://doi.org/10.1021/la7035532
3. Romero-Sánchez M.D., Pastor-Blas M.M., Martín-Martínez J.M., Zhdan P.A. Watts J.F. Surface Modifications of a Vulcanized Rubber Using Corona Discharge and Ultraviolet Radiation Treatments. *J Mater Sci*. 2001;36:5789–5799. https://doi.org/10.1023/A:1012999820592
4. Martínez L., Álvarez L., Huttel Y., Méndez J., Román E., Vanhulsel A., Verheyde B., Jacobs R. Surface Analysis of NBR and HNBR Elastomers Modified with Different Plasma Treatments. *Vacuum*. 2007;81:1489–1492. https://doi.org/10.1016/j.vacuum.2007.04.025

5. Kavc T., Kern W., Ebel M.F., Svagera R., Pölt P. Surface Modification of Polyethylene by Photochemical Introduction of Sulfonic Acid Groups. *Chemistry of Materials*. 2000;12:1053–1059. https://doi.org/10.1021/cm991158p
6. Nuzaimah M., Sapuan S.M., Nadlene R., Jawaid M. Effect of Surface Treatment on the Performance of Polyester Composite Filled with Waste Glove Rubber Crumbs. *Waste and Biomass Valorization*. 2020;12(2). https://doi.org/10.1007/s12649-020-01008-2
7. Lu X., Wang J., Cai S., Niu B., He Q., He X. Improving Thermo-oxidative Stability and Mediums Resistance of Nitrile Rubber via Surface Superhydrophobic Modification. *J. Appl. Polym. Sci*. 2022;139(17). https://doi.org/10.1002/app.52016
8. Yang Q., Chen S., Gao S., Wan S., He X. Improving Thermal-oxidative Stability of Nitrile Butadiene Rubber Composites by Surface Modification of Zirconium Phosphate. *Polym. Compos*. 2023;44:505–514. https://doi.org/10.1002/pc.27113
9. Wu Y.M., Liu J.Q., Cao H.T., Wu Z.Y., Wang Q., Ma Y.P., Jiang H., Wen F., Pei Y.T. On the Adhesion and Wear Resistance of DLC Films Deposited on Nitrile Butadiene Rubber: A Ti-C Interlayer. *Diam Relat Mater*. 2020;101. https://doi.org/10.1016/j.diamond.2019.107563
10. Zhou Z., Han Y., Qian J. Improving Mechanical and Tribological Behaviors of GLC Films on NBR under Water Lubrication by Doping Ti and N. *Coatings*. 2022;12. https://doi.org/10.3390/coatings12070937
11. Nudelman Z.N., Dontsov A.A., Novitskaya S.P. *Ftorelastomery* (*Fluoroelastomers*). Moscow: Khimiya; 1988. 240 p. (In Russ.).
12. Dontsov A.A., Lozovik G.Ya., Novitskaya S.P. *Khlorirovannye polimery* (*Chlorinated Polymers*). Moscow: Khimiya; 1979. 232 p. (In Russ.).
13. Tutorsky I.A., Potapov E.E., Shvarts A.G. *Khimicheskaya modifikatsiya elastomerov* (*Chemical Modification of Elastomers*). Moscow: Khimiya; 1993. 304 p. (In Russ.).
14. Nudelman Z.N. *Ftorkauchuki: osnovy, pererabotka, primenenie* (*Fluororubbers: Fundamentals, Processing, Application*). Moscow: PIF RIAS; 2007. 383 p. (In Russ.).
15. Nudelman Z.N., Galil-ogly F.A., Novikov A.S. *Ftorkauchuki i reziny na ikh osnove* (*Fluororubbers and Rubbers Based on Them*). Moscow: Khimiya; 1966. 234 p. (In Russ.).
16. Adov M.V., Zuev A.V., Pichkhidze S.Ya., Yurovsky V.S. Application of Fine Rubber Powder Based on Chloroprene Rubber in the Formulation of Rubber Compounds Based on This Rubber. *Kauchuk i rezina*. 2010;4:25–27 (in Russ.).
17. Pastor-Blas M.M., Martín-Martínez J.M. Different Surface Modifications Produced by Oxygen Plasma and Halogenation Treatments on a Vulcanized Rubber. *J. Adhes. Sci. Technol*. 2002;16:409–428. https://doi.org/10.1163/156856102760067190
18. Abbott S.G., Brewis D.M., Manley N.E., Mathieson I., Oliver N.E. Solvent-Free Bonding of Shoe-Soling Materials. *Int. J. Adhes.* 2003;23:225–230. https://doi.org/10.1016/S0143-7496(03)00025-3
19. Daniel P., Thian H.Ng., Heam K.T., Roger L., Matt J.C. The effects of chlorination, thickness, and moisture on glove donning efficiency. *Ergonomics*. 2021;64(3). https://doi.org/10.1080/00140139.2021.1907452
20. Khan M.S., Heinrich G. PTFE-Based Rubber Composites for Tribological Applications. *Advanced Rubber Composites*. 2010:249–310. https://doi.org/10.1007/12_2010_98
21. Belov N.A., Alentiev A.Y., Bogdanova Y.G., Vdovichenko A.Y., Pashkevich D.S. Direct Fluorination as Method of Improvement of Operational Properties of Polymeric Materials. *Polymers* (*Basel*). 2020;12. https://doi.org/10.3390/polym12122836
22. Qiang G., Changou P., Pengwei X., Mingliang P., Peng L. Fluorination of nitrile-butadiene rubber without gelation via radical graft polymerization in presence of chain transfer agent. *European Polymer Journal.* 2021;151. https://doi.org/10.1016/j.eurpolymj.2021.110442
23. Gao J., Dai Y., Wang X., Huang J., Yao J., Yang J., Liu X. Effects of Different Fluorination Routes on Aramid Fiber Surface Structures and Interlaminar Shear Strength of Its Composites. *Appl Surf Sci.* 2013;270:627–633. https://doi.org/10.1016/j.apsusc.2013.01.099
24. Qiang G., Changou P., Siwei Sh., Pengwei X., Mingliang P., Peng L. Facile fluorination of nitrile-butadiene rubber via olefin cross metathesis. *Polymer*. 2021;217. https://doi.org/10.1016/j.polymer.2021.123455
25. Yang X., Yang C., Nie M. Industrial Preparation of Self-Lubricating Polyurethane via Direct Fluorination with Gaseous Fluorine. *ACS Omega*. 2022;7:28388–28395. https://doi.org/10.1021/acsomega.2c03019
26. Belov N.A., Pashkevich D.S., Alentiev A.Y., Tressaud A. Effect of Direct Fluorination on the Transport Properties and Swelling of Polymeric Materials: A Review. *Membranes.* 2021;11(9). https://doi.org/10.3390/membranes11090713
27. Kharitonov A.P. Direct Fluorination of Polymers – From Fundamental Research to Industrial Applications. *Prog Org Coat.* 2008;61:192–204. https://doi.org/10.1016/j.porgcoat.2007.09.027
28. Mostafa A., Abouel-Kasem A., Bayoumi M.R., El-Sebaie M.G. Insight into the Effect of CB Loading on Tension, Compression, Hardness and Abrasion Properties of SBR and NBR Filled Compounds. *Mater Des.* 2009;30: 1785–1791. https://doi.org/10.1016/j.matdes.2008.07.037

About the Authors

Ksenia V. Sukhareva, Cand. Sci. (Chem.), Associate Professor, Head of the Basic Department of the Industry of Quality, Higher Engineering School "New Materials and Technologies," Plekhanov Russian University of Economics (36, Stremyannyi per., Moscow, 115054, Russia); Leading Researcher, Laboratory of Physical Chemistry of Compositions of Synthetic and Natural Polymers, N.M. Emanuel Institute of Biochemical Physics, Russian Academy of Sciences (4, Kosygina ul., Moscow, 119334, Russia). E-mail: sukhareva.kv@rea.ru. Scopus Author ID 57191042974, RSCI SPIN-code 1883-8039, https://orcid.org/0000-0002-0282-7015

Igor A. Mikhailov, Cand. Sci. (Chem.), Director of the Joint Research Center, Plekhanov Russian University of Economics (36, Stremyannyi per., Moscow, 115054, Russia); Laboratory of Physical Chemistry of Compositions of Synthetic and Natural Polymers, N.M. Emanuel Institute of Biochemical Physics, Russian Academy of Sciences (4, Kosygina ul., Moscow, 119334, Russia). E-mail: mikhaylov.ia@rea.ru. Scopus Author ID 57199507317, ResearcherID M-7163-2016, RSCI SPIN-code 4251-3129, https://orcid.org/0000-0003-1196-7973

Bekzod B. Khaidarov, Cand. Sci. (Eng.), Associate Professor; Department of Functional Nanosystems and High-Temperature Materials, National University of Science and Technology "MISIS" (4, Leninskii pr., Moscow, 119049, Russia). E-mail: b.haydarov@misis.ru. Scopus Author ID 57223169688, RSCI SPIN-code 7832-0765, https://orcid.org/0000-0003-2769-7437

Anastasia D. Buluchevskaya, Assistant, Basic Department of Chemistry of Innovative Materials and Technologies, Higher Engineering School "New Materials and Technologies", Plekhanov Russian University of Economics (36, Stremyannyi per., Moscow, 115054, Russia). E-mail: buluchevskaya.ad@rea.ru. RSCI SPIN-code 7486-8251, https://orcid.org/0009-0006-1486-037X

Igor N. Burmistrov, Dr. Sci. (Eng.), Leading Engineer of the Scientific Project, Department of Functional Nanosystems and High-Temperature Materials, National University of Science and Technology "MISIS" (4, Leninskii pr., Moscow, 119049, Russia). E-mail: burmistrov.in@misis.ru. Scopus Author ID 55042347200, ResearcherID A-8212-2014, RSCI SPIN-code 1353-0401, https://orcid.org/0000-0003-0776-2465

Об авторах

Сухарева Ксения Валерьевна, к.х.н., доцент, заведующая базовой кафедрой индустрии качества, Высшая инженерная школа «Новые материалы и технологии», ФГБОУ ВО «Российский экономический университет имени Г.В. Плеханова» (115054, Россия, Москва, Стремянный переулок, д. 36); ведущий научный сотрудник, лаборатория физико-химии композиций синтетических и природных полимеров, ФГБУН Институт биохимической физики им. Н.М. Эмануэля Российской академии наук (199334, Россия, Москва, ул. Косыгина, д. 4). E-mail: sukhareva.kv@rea.ru. Scopus Author ID 57191042974, SPIN-код РИНЦ 1883-8039, https://orcid.org/0000-0002-0282-7015

Михайлов Игорь Анатольевич, к.х.н., директор Центра коллективного пользования, ФГБОУ ВО «Российский экономический университет имени Г.В. Плеханова» (115054, Россия, Москва, Стремянный переулок, д. 36); лаборатория физико-химии композиций синтетических и природных полимеров, ФГБУН Институт биохимической физики им. Н.М. Эмануэля Российской академии наук (199334, Россия, Москва, ул. Косыгина, д. 4). E-mail: mikhaylov.ia@rea.ru. Scopus Author ID 57199507317, ResearcherID M-7163-2016, SPIN-код РИНЦ 4251-3129, https://orcid.org/0000-0003-1196-7973

Хайдаров Бекзод Бахтиёрович, к.т.н., доцент, кафедра функциональных наносистем и высокотемпературных материалов, ФГАОУ ВО «Национальный исследовательский технологический университет «МИСИС» (НИТУ МИСИС) (119049, Россия, Москва, Ленинский пр-т, д. 4, стр. 1). E-mail: b.haydarov@misis.ru. Scopus Author ID 57223169688, SPIN-код РИНЦ 7832-0765, https://orcid.org/0000-0003-2769-7437

Булучевская Анастасия Дмитриевна, ассистент, базовая кафедра химии инновационных материалов и технологий, Высшая инженерная школа «Новые материалы и технологии», ФГБОУ ВО «Российский экономический университет имени Г.В. Плеханова» (115054, Россия, Москва, Стремянный переулок, д. 36). E-mail: buluchevskaya.ad@rea.ru. SPIN-код РИНЦ 7486-8251, https://orcid.org/0009-0006-1486-037X

Бурмистров Игорь Николаевич, д.т.н., ведущий инженер научного проекта, кафедра функциональных наносистем и высокотемпературных материалов, ФГАОУ ВО «Национальный исследовательский технологический университет «МИСИС» (НИТУ МИСИС) (119049, Россия, Москва, Ленинский пр-т, д. 4, стр. 1). E-mail: burmistrov.in@misis.ru. Scopus Author ID 55042347200, ResearcherID A-8212-2014, SPIN-код РИНЦ 1353-0401, https://orcid.org/0000-0003-0776-2465

The text was submitted by the authors in English and edited for English language and spelling by Thomas A. Beavitt

MIREA – Russian Technological University
78, Vernadskogo pr., Moscow, 119454, Russian Federation.
Publication date *December 31, 2025.*
Not for sale

МИРЭА – Российский технологический университет
119454, РФ, Москва, пр-т Вернадского, д. 78.
Дата опубликования *31.12.2025 г.*
Не для продажи

www.finechem-mirea.ru